1-1-2013

A role for microRNA-29a mediating ER stress-induced apoptosis in neuronal cells in the mouse central nervous system.

Katie Nolan
Royal College of Surgeons in Ireland

RCSI

ROYAL COLLEGE OF SURGEONS IN IRELAND

COLÁISTE RÍOGA NA MÁINLEÁ IN ÉIRINN

A role for microRNA-29a mediating ER stress-induced apoptosis in neuronal cells in the mouse central nervous system

Katie Nolan, BSc Hons

A thesis submitted to the Royal College of Surgeons in Ireland
in fulfilment of the requirements for the higher degree of
Doctor of Philosophy

August 2013

Supervisors: Prof. Jochen H. M. Prehn
Dr. Caoimhín G. Concannon

I declare that this thesis, which I submit to RCSI for examination in consideration of the award of a higher degree PhD is my own personal effort. Where any of the content presented is the result of input or data from a related collaborative research programme this is duly acknowledged in the text such that it is possible to ascertain how much of the work is my own. I have not already obtained a degree in RCSI or elsewhere on the basis of this work. Furthermore, I took reasonable care to ensure that the work is original, and, to the best of my knowledge, does not breach copyright law, and has not been taken from other sources except where such work has been cited and acknowledged within the text.

Signed Katie Dolan

RCSI Student Number 091099178

Date 14/11/13.

TABLE OF CONTENTS

LIST OF FIGURES

CHAPTER 1

CHAPTER 2

CHAPTER 3

CHAPTER 4

CHAPTER 5

LIST OF TABLES

CHAPTER 1

CHAPTER 2

SUMMARY

A role for microRNA-29a mediating ER stress-induced apoptosis in neuronal cells in the mouse central nervous system

Disturbances in the folding of proteins within the endoplasmic reticulum (ER) lead to the accumulation of mis-folded and aggregated proteins and the activation of the ER stress response and has been implicated in neurodegenerative diseases such as amyotrophic lateral sclerosis. MicroRNAs are small ribonucleic acids which can modulate the expression of proteins post-translationally and in recent years have been implicated in major disease pathologies. The miR-29 family, of which miR-29a is a member, has been implicated in cancer and neurodegeneration through its effects on apoptosis.

Firstly we investigated the role of miR-29a and its proposed target MCL-1 during ER stress-induced apoptosis. We show that miR-29a is significantly upregulated compared to other miRNAs following ER stress-induced apoptosis in primary cortical neurons. Increased miR-29a expression coincided with a decrease in MCL-1 protein expression. Contrasting this we identified a neuroprotective role for miR-29a antagomir in cortical neurons during ER stress. miR-29a knockdown was shown to increase *Mcl-1* mRNA and we hypothesised that this could be mediating the cytoproptective effect. We identified the importance of MCL-1 in mediating ER stress-induced apoptosis, identifying protection of cortical neurons overexpressing MCL-1 during tunicamycin-induced ER stress. Furthermore we showed loss of MCL-1 sensitised cortical neurons to ER stress-induced cell death and demonstrated a cytoprotective role for MCL-1 in cortical neurons. In addition, cortical neurons were shown to be protected against tunicamycin-induced ER stress in the absence of PUMA or BAX, however we could not abrogate apoptosis and suggest that other mediators of apoptosis compensate for loss of members of the BCL-2

family. Indeed, MCL-1 overexpression was shown to decrease LC3II protein levels suggesting a further level of regulation within cortical neurons involving other apoptosis-mediating pathways such as autophagy.

Having identified miR-29a as upregulated in the central nervous system (CNS) of C57 BL/6 mice, and reduced expression of *Mcl-1* in the same CNS tissue, we confirmed miR-29a expression in lumbar spinal cord from SOD1 transgenic mice. While we could localise miR-29a expression to motoneurons in the lumbar spinal cord, miR-29a knockdown in an $SOD1^{G93A}$ mouse model of ALS did not reduce motor dysfunction nor significantly increase lifespan.

ACKNOWLEDGEMENTS

Firstly I would like to thank my supervisors: Prof. Jochen Prehn for giving me the opportunity to work on this project, for guiding me through my career and for all the invaluable advice and support he has given me during my time in RCSI. A special thank you to Dr. Caoimhin Concannon for answering every stupid question, for all his advice and time spent correcting numerous reports and abstracts. I would have been lost without your guidance and I am ever-so grateful.

I would like to say a huge thank you to Bea and Ujval who taught me the ropes when I first started and always had time for a cup of tea and a chat ☺

Special thanks must go to all the members of the department who have made my time in RCSI so memorable and who I have laughed with continuously! Thank you for all your help and support and friendship, Karen, Gary, Megan, Mollie, Ross Mc, Ross G, Franziska, Linda, Sinead, Claire, James, Guillaume, Eugenia, Cai, ...

I would like to thank all my friends at home for still loving me after all the missed events in the last year. They have been there for me through everything. I am so humbled to have their friendship and I am so proud of every single one of them: Katie, Hannah, Conor, Jessie, Mark, Gavin, Sarah, Andrew, Emily, Sinead, Shane....

To my Aunt Mary and Uncle Willie, who have been inspirations and have been like a second family to me all of my life, your support and encouragement is much appreciated. And to my Uncle Donal, without whom I might never have come this far; your love of life and unending interest is an inspiration. To my cousin Catherine, without whom I would not have set out on this path and my cousin David who helped

me along the way. A special thank you is due to Dorothy for your keen eye and sound advice in proofing this thesis.

To my wonderful boyfriend Matthew; you are the light of my life and my best friend. You have supported me through all the bad time and good and have made me feel like the luckiest person in the world.

A huge thank you and my endless gratitude to my parents, Pat and Aideen, for everything they have done for me. They are a constant source of support and love and help me feel that anything is possible. I could not have made it to this point without their care and encouragement and all the cups of tea ☺. To my brother James, you still can't have my room when I move out but you always cheer me up when im feeling rotten! Hopefully I can return the favour in the next few years!

To all the mice, and especially Seymore, who made this work possible.

And to Orla, a constant source of inspiration and a tireless fighter who gets the most out of life.

ABBREVIATIONS

AD Alzheimers disease

ALS Amyotrophic lateral sclerosis

ANOVA analysis of variance

ATF4 Activating transcription factor 4

ATF6 Activating transcription factor 6

BAK BCL-2 homologous antagonist/killer

BAX BCL-2 associated X

BCL-2 B-cell lymphoma 2

BCL-2 B-cell lymphoma 2

BID BH3 interacting-domain death agonist

BIM BCL-2 like protein 11

CHOP C/EBP homologous protein

CNS central nervous system

DIG dioxygenin

DISC Death-induced silencing complex

DIV Days *in vitro*

eIF2α eukaryotic initiation factor 2 alpha

ER Endoplasmic Reticulum

ERAD ER-associated degradation

FADD Fas-associated via death domain

GRP78 Glucose regulated protein 78kDa

HD Huntingtons disease

HSP90 Heat shock protein 90

ICV intracerebroventricular

IRE1 Inositol-requiring enzyme 1

IRES Internal ribosome entry site

LC3 Protein light chain 3

MCL-1 Myeloid cell leukemia sequence 1

MEF mouse embryonic fibroblast

MOI multiplicity of infection

MOMP mitochondrial outer membrane permeabilisation

mRNA messenger RNA

mTOR Mammalian target of rapamycin

NOXA Phorbal-11-myristate-13-acetate-induced protein 1

PBS Phosphate buffered saline

PCR polymerase chain reaction

PD Parkinsons disease

PERK Pancreatic ER kinase (PKR)-like ER kinase

PND Post natal day

PUMA p53 upregulated mediator of apoptosis

qPCR Quantitative PCR

RNA ribonucleic acid

shRNA small hairpin RNA

SOD1 Superoxide dismutase 1

TNF Tumour necrosis factor

TRADD TNFR1-associated death domain

Tuni Tunicamycin

UPR Unfolded protein response

CHAPTER 1

General Introduction

1.1 ER stress

The endoplasmic reticulum (ER) is a cell organelle that acts as the main site of synthesis, folding and transport of secreted proteins (Lindholm *et al.*, 2006). The correct and efficient functioning of the ER is imperative for normal cellular function. ER stress occurs due to an accumulation and aggregation of misfolded proteins which are consequently toxic to cells (Szegezdi *et al.*, 2006, Schroder and Kaufman, 2005). Such errors in the protein folding capacity of the ER can be brought about by changes in Ca^{2+} concentration and/or the presence of mutated proteins. Due to the wide reaching effects of ER stress throughout an organism and the fate of cells that do not recover, it is not surprising that ER stress has been implicated in many disease pathologies ranging from diabetes mellitus and various types of cancer to many neurodegenerative diseases (Roussel *et al.*, 2013, Lin *et al.*, 2008). In cases of ER stress, the ER implements the unfolded protein response.

1.1.1 Unfolded protein response (UPR)

The UPR is a collection of signalling pathways that act to (1) increase expression of ER chaperones, (2) increase degradation of misfolded proteins and (3) inhibit further protein synthesis (Lindholm *et al.*, 2006). ER chaperones are proteins located in the ER lumen that facilitate folding of secreted proteins into their native confirmations before being transported out of the ER (Nishikawa *et al.*, 2005). Upon misfolded protein accumulation, three transmembrane receptors (pancreatic ER kinase (PKR)-like ER kinase (PERK), activating transcription factor 6 (ATF6) and inositol-requiring enzyme 1(IRE1)) are activated by dissociation of the ER chaperone GRP78 (Walter and Ron, 2011). Downstream signaling through the UPR leads to upregulation of

proteins involved in protein folding and induction of apoptotic cell death.

IRE1 and ATF6 are both responsible for increased gene expression during the UPR while PERK is credited with translational repression of messenger RNA (mRNA) targets (Harding *et al.*, 2000). PERK receptors are homodimers that dimerise and auto-phosphorylate upon activation. Activated PERK phosphorylates eukaryotic initiation factor 2 (eIF2α) inhibiting its function and resulting in inhibition of cap-dependent protein translation (Schroder and Kaufman, 2005). Inhibition of eIF2α allows for eIF2α-independent translation of activating transcription factor 4 (ATF4), a transcription factor that upregulates expression of genes required for ER homeostasis and also CHOP (Oyadomari and Mori, 2004). CHOP is a transcription factor highly implicated in ER stress-induced apoptosis. Cap-dependent translation requires the interaction between eIF4G subunit of the eIF cap binding complex and the 5' cap which induces translation through incorporation with the translation pre-initiation complex (Thakor and Holcik, 2012). Cap-independent protein translation occurs through an internal ribosome entry site (IRES), present on some cellular RNA. During cellular stress, some mRNA can undergo cap-independent protein translation through an IRES, independent of eIF2α phosphorylation (Yamasaki and Anderson, 2008). The IRES can recruit the ribosome and initiate translation. This mechanism has been identified in a variety of proteins involved in apoptosis (Stoneley and Willis, 2004). IRE1 forms oligomers upon activation and this activation leads to splicing of X-box binding protein 1 (XBP1) mRNA (Szegezdi *et al.*, 2006). Spliced XBP1 is a stable, active transcription factor that induces expression of chaperone proteins that mediate ER stress recovery. ATF6 is cleaved in the Golgi apparatus following dissociation from GRP78 and the active ATF6 translocates to the nucleus where it induces genes for chaperones glucose regulated proteins 78 kDa (GRP78) and GRP94 and transcription factors XBP1 and CHOP (Lee *et al.*, 2002). GRP78 is a

highly expressed ER resident chaperone and a member of the heat-shock protein (Hsp70) family (Lee, 2005). GRP78 induction is indicative of ER stress and can occur due to physiological stress or be chemically induced through thapsigargin or tunicamycin treatment in an ATF6 directed manner. GRP94 is a molecular chaperone that works in tandem with GRP78 in the ER to assist in protein folding (Ramakrishnan *et al.*, 1997). GRP94 is a paralog of heat-shock protein 90 (Hsp90) and unlike the transient attachment that GRP78 forms with nascent proteins, GRP94 forms a more stable attachment to assist further in the protein folding. GRP94 has also been implicated in immunogenesis with the observation that it can elicit anti-tumour immune responses through an in-built antigenic peptide-binding function (Nicchitta *et al.*, 2004).

1.1.2 ER-associated degradation (ERAD) and alleviation of ER stress

The UPR also aims to reduce ER stress by removing misfolded proteins. Prolonged ER stress can lead to activation of the ERAD pathway which can remove misfolded proteins through proteasomal degradation (Needham and Brodsky, 2013). Protein quality control in the ER lumen is assessed by molecular chaperones including calnexin and calreticulin which identify immature proteins through recognition of unpaired cysteine residues and immature glycans (Vembar and Brodsky, 2008). Calnexin and calreticulin can then retain these proteins to assist their maturation. However if the proteins are terminally misfolded, they are extracted by ER degradation enhancing alpha-mannosidase-like (EDEM) and ER mannosidase I and targeted for degradation (Meusser *et al.*, 2005). Misfolded proteins are retranslocated from the ER lumen to the cytoplasm. It is thought that this occurs through Sec61, a gated channel which is involved in the initial translocation of proteins into the ER lumen, facilitated by the

cytosolic chaperone AAA-ATPases p97 and by RPT4 (Rabinovich *et al.*, 2002, Lipson *et al.*, 2008). DERLIN-1 and the ubiquitin ligase HRD1 have been shown to form a transmembrane pore that functions to facilitate degradation of misfolded proteins (Ye *et al.*, 2005). Furthermore, dislocation of misfolded proteins requires ubiquitination of the substrates through interaction with a ubiquitin ligase which attaches a chain of ubiqutin molecules to cytoplasmically exposed lysine residues in an enzymatic cascade (Jarosch *et al.*, 2002). Dislocation is directed further by a ubiquitin binding complex Cdc48p which extracts proteins in an ATP-dependent manner. Once present in the cytoplasm, the ubiquitinated proteins are recognised by the 19S capping complexes of the 26S proteasome, which direct both its transport into the proteasome and its digestion. Loss of function mutations in ERAD components resulting in misfolded protein accumulation is seen in Parkinson's disease while premature degradation of mutant cystic fibrosis transmembrane receptor (CFTR) through ERAD has been implicated in the pathology of cystic fibrosis (Meusser *et al.*, 2005).

1.2 Cell death

1.2.1 Types of cell death

Cell death occurs in all types of cells and at all stages of development. Cell death is important both as a regulatory mechanism to maintain cellular homeostasis and during development and growth of an organism (Miura, 2011). Apoptosis or programmed cell death is the main regulatory mechanism of cell death and involves organised cellular breakdown and removal by phagocytes (Peng *et al.*, 2013). Apoptosis is intrinisic to development and maintaining homeostasis. Dysregulation of apoptosis is a hallmark of many cancers and neurodegenerative diseases such as Alzheimers disease (AD) (Mattson, 2000) and amyotrophic lateral sclerosis (ALS) (Sathasivam *et al.*, 2001). Neuronal loss in these neurodegenerative diseases is initiated through activation of caspases (Martin, 2010). Neuronal cells can be rendered resistant to apoptosis through genetic deletion of BCL-2-associated X protein (BAX) and BCL-2 homologous antagonist killer (BAK) (Lindsten *et al.*, 2003). Necrosis is unorganised cell lysis following a fatal insult to the cell that depletes adenosine tri-phosphate (ATP) and destroys the plasma membrane and cell structure (Moriwaki and Chan, 2013). Necrosis is characterised morphologically by mitochondrial and cellular swelling and cell lysis. Evidence of necrotic cell death has been described following glutamate-induced excitotoxicity (Portera-Cailliau *et al.*, 1997) and in cases of ischemia (Martin *et al.*, 1998). For most disease paradigms there is an overlap between both apoptosis and necrosis. Indeed programmed necrosis, termed necroptosis, has been identified that followed a regulated cell death programme mediated by RIP kinase 1 and 3 (Kaczmarek *et al.*, 2013, Moriwaki and Chan, 2013). Autophagy plays a role in cell recycling and maintains homeostasis through degrading aggregated/misfolded proteins (Chaabane *et al.*, 2013). While

autophagy mostly acts to support cell survival (Yu *et al.*, 2004), studies have shown that in the absence of apoptosis, necrosis can be mediated by caspases, the downstream mediators of apoptosis (Edinger and Thompson, 2004). Furthermore autophagy has been shown to promote necrosis in *bax*$^{-/-}$ *bak*$^{-/-}$ deficient mouse embryonic fibroblast (MEF) cells undergoing ER stress (Ullman *et al.*, 2008). These cells cannot undergo apoptotic cell death following an ER stress insult and increased cell death was seen in these cells following autophagy saturation. Mitochondrial disregulation has also been shown to induce cell death through apoptosis and necrosis, demonstrating a shared regulatory network between both mechanisms (Nieminen, 2003). Apoptosis, necrosis and autophagy have all been implicated in many different forms of disease. Interplay between each mechanism has also elucidated pathways of importance for cellular homeostasis (Edinger and Thompson, 2004).

1.2.2 Apoptosis

Apoptosis is an active form of cell death and is characterised morphologically by chromatin condensation and plasma membrane blebbing (Lodish, 2008). It allows the removal of damaged or mutated cells that have compromised function without harming the organism itself such as in necrosis. Apoptosis can be induced when the toxic insult on a cell exceeds autophagic recycling capacity. Cellular apoptosis occurs in all cell types and is necessary to maintain homeostasis (Elmore, 2007). Programmed cell death is important for normal cellular turnover and efficient functioning of the immune system. Neuronal apoptosis has been shown to be particularly important at embryonic level for shaping functional brain development (Yuan and Yankner, 2000). Excessive neuronal apoptosis is the major pathology in motor system disorders such as Parkinson's disease, Huntington's disease and ALS. In these conditions, oxidative stress,

glutamate excitotoxicity and changes in apoptosis mediator expression have been attributed to disease pathology (Mattson, 2000).

There are two main pathways that initiate apoptosis: the extrinsic and the intrinsic pathways (Fig. 1.1).

1.2.2.1 Extrinsic Pathway

The extrinsic pathway is activated following a cellular insult originating at the cell membrane and is mediated by death receptors of the tumour necrosis factor (TNF) receptor super family on the cell membrane (Wang and El-Deiry, 2003). Death receptor stimulation by specific ligands leads to formation of a death-induced silencing complex (DISC) composed of Fas-associated via death domain (FADD) and/or TNFR1-associated death domain protein (TRADD) that binds receptors and causes trimerisation and activation (Tait and Green, 2010). These adapter molecules mediate activation of cysteinyl aspartate protease 8 (caspase 8), the initiator caspase, which in turn cleaves and activates caspase 3 and caspase 7, the effector caspases, to induce apoptosis. Caspases are cysteine-aspartic acid proteases that cleave their target substrate on the terminal asp residue of a tetrapeptide motif (McIlwain *et al.*, 2013). In type I cells, activation of executioner caspases by caspase 8 is sufficient to induce apoptosis. In type II cells, apoptosis is induced through crosstalk between the intrinsic and extrinsic apoptosis pathways. Crosstalk between the extrinsic and intrinsic pathway can occur through caspase 8-mediated cleavage and subsequent activation of the BH3-only proapoptotic BH3 interacting-domain death agonist (BID) to induce MOMP (Li *et al.*, 2002).

1.2.2.2 Intrinsic Pathway

The intrinsic cell death pathway is also known as the B-cell lymphoma 2 (BCL-2) regulated or mitochondrial pathway (Kuwana and Newmeyer, 2003). This pathway is activated internally by cellular stress such as viral infections, DNA damage, ER stress and growth factor deprivation. Execution of the caspase-dependent mitochondrial apoptosis pathway is dependent on the proapoptotic members BAX and BAK which induce MOMP following activation by proapoptotic BH3-only members of the BCL-2 regulatory family (Kroemer and Martin, 2005). Antiapoptotic members of the BCL-2 family can interact with and sequester BH3-only proteins and prevent BAX/BAK activation and MOMP (Danial, 2007). MOMP allows release of apoptogenic molecules cytochrome c and DIABLO (SMAC) from the mitochondrial intermembrane space. Release of these molecules induces a caspase cascade (Brenner and Mak, 2009). Cytochrome c complexes with apoptosis protease activating factor 1 (APAF-1) monomers which undergo a conformational change and oligomerise to form the caspase activation platform termed the apoptosome. The apoptosome acts to activate caspase 9 which in turn cleaves and activates effector caspase 3 and caspase 7 and leads to downstream apoptosis (Youle and Strasser, 2008). Cells which lack cytochrome c have been shown to have reduced caspase 3 activation and were resistant to a variety of stress inducing agents (Li *et al.*, 2000). Second mitochondria-derived activator of caspase (SMAC/DIABLO) neutralises the inhibitor of apoptosis proteins (IAP) family of caspase inhibitory proteins (Srinivasula *et al.*, 2001). It is thought that SMAC/DIABLO displace x-linked inhibitor of apoptosis protein (XIAP) from caspase-9 and prevents apoptosome repression.

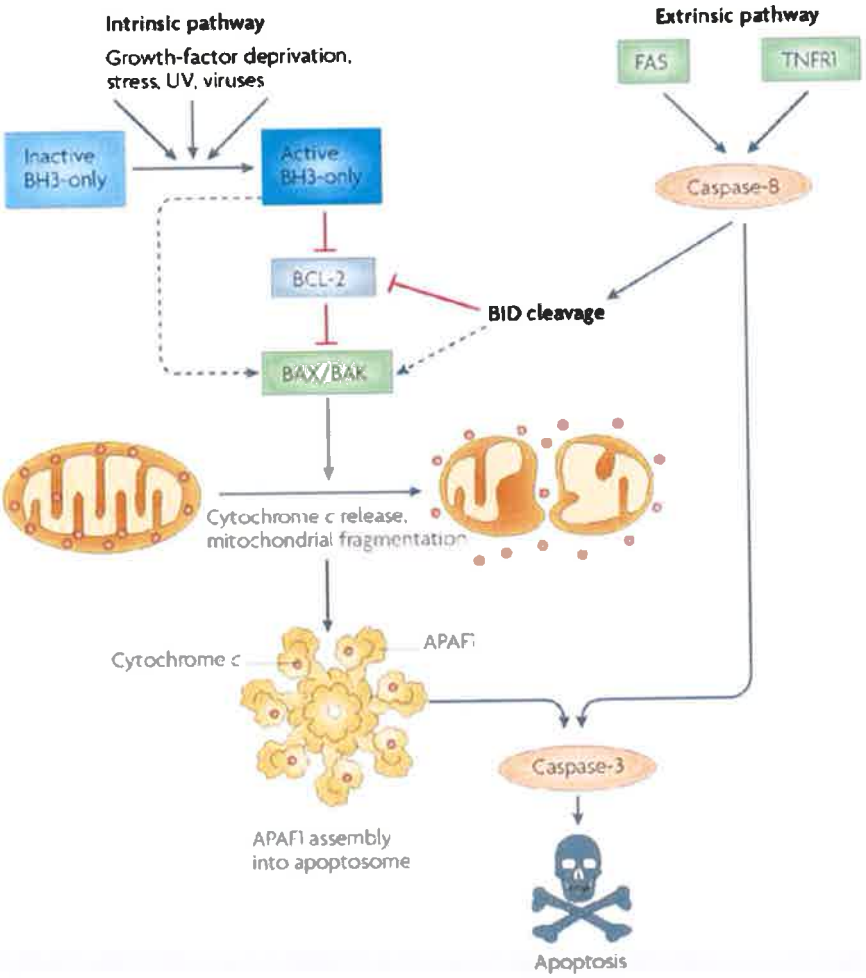

Figure 1.1: Intrinsic and extrinsic pathways of apoptosis. The intrinsic apoptotic pathway, also termed the mitochondrial-mediated pathway, is activated internally in response to cellular stress. Activation of BH3-only proapoptotic proteins leads to mitochondrial membrane permeabilisation by BAX/BAK dimerisation and release of cytochrome c. Cytochrome c forms an apoptosome complex with Apaf-1 which leads to activation of caspase 3 and cell death. The extrinsic pathway is mediated by death receptors and is activated by the ligand binding to the receptor. This recruits caspase 8 and leads to activation of executioner caspase 3. Image adapted from Youle, R.J and Strasser, A. 2008. The BCL-2 protein family: opposing activities that mediate cell death. Nature Reviews. 9:47-59

1.2.3 A role for autophagy

Autophagy is a degradative pathway in the cell involved in maintaining cellular homeostasis (Kroemer and Levine, 2008). Autophagy degrades proteins and cell organelles through trafficking to lysosomes. Lysosomes contain nucleases, proteases and phosphatases that degrade polymers and release their monomeric subunits for further degradation in proteasomes in the cytosol (Lodish, 2008). Autophagy serves a bioenergetic function by upregulating intracellular nutrients and energy generation through recycling of cellular components in times of starvation or when bioenergetic demand is high (Kroemer and Levine, 2008). Autophagy also serves a "house-keeping" role by removing aggregated proteins or misfolded proteins that cause ER stress (Kundu and Thompson, 2008). In this respect, autophagy can be seen to serve either pro-survival roles by maintaining cellular homeostasis or pro-apoptotic roles by assisting the cell death response.

Autophagy can be initiated through de-repression of the inhibitor of autophagy mammalian target of rapamycin (mTOR) Ser/Thr kinase (Nazio *et al.*, 2013). This de-repression allows association of ATG13 (Autophagy specific gene) with ATG1 and stimulation of its catalytic activity. This effect can be mimicked by rapamycin treatment *in vitro*. Autophagosome formation then proceeds through vesicle nucleation and elongation (Maiuri *et al.*, 2007). Vesicle nucleation involves formation of a multicomplex incorporating BECLIN-1 and generation of phosphatidylinositol-3-phosphate (PtdIns3P). Vesicle elongation involves conjugation of ATG12 to ATG5 and conjugation of phosphatidylethanolamine (PE) to LC3-1/ATG8 which leads to conversion of LC3-I to LC3-II. LC3-II is a marker of autophagy as it corresponds to autophagosome formation. Autophagosomes undergo further maturation to autolysosomes through fusion with lysosomes which leads to degradation of autophagic vacuoles.

Due to the major role that autophagic cell death plays in cellular homeostasis, it has been implicated in a protective role in many neurodegenerative disorders including AD and Huntington's disease (Kundu and Thompson, 2008). Current work has demonstrated the importance of autophagy modulation in neurodegeneration in both mTOR-dependent and mTOR–independent pathways (Sarkar and Rubinsztein, 2008, Pei and Hugon, 2008). Due to the intracellular recycling nature of autophagy, it has been considered of therapeutic importance for diseases characterised by accumulation of misfolded proteins (proteinopathies) such as AD or Huntington's disease. The modified neuronal autophagy inducer, phenoxazine, was shown to be neuroprotective in a neuronal Huntington's disease model and decreased aggregated protein concentration in an mTOR-independent manner (Tsvetkov *et al.*, 2010). It is not yet known whether cell death occurs with autophagy or by autophagy (Kroemer and Levine, 2008), with autophagy often being induced as part of the cell death response (Kundu and Thompson, 2008). However, inhibition of autophagy has been shown to induce apoptosis in a caspase-dependent manner (Boya *et al.*, 2005). Furthermore work has implicated BECLIN-1, the mammalian homolog of yeast ATG6, in crosstalk mechanisms between autophagy and apoptosis (Kang *et al.*, 2011). It was recently demonstrated that caspase-mediated cleavage of BECLIN-1 generated two fragments and abolished BECLIN-1 autophagy induction (Wirawan *et al.*, 2010). This inhibition of autophagy-induced release of pro-apoptotic proteins and induced mitochondrial apoptosis. Interestingly the C-terminal fragment of BECLIN-1 acquires an apoptotic role through amplification of mitochondrial mediated apoptosis. BECLIN-1 has previously been shown to interact with members of the BCL-2 family, including myeloid cell leukemia sequence 1 (MCL-1). This presents a further pathway of crosstalk between autophagy and apoptosis (Erlich *et al.*, 2007).

1.2.4 BCL-2 family and its role in apoptosis

B-cell lymphoma 2 (BCL-2) is a family of regulatory proteins that contains both pro- and anti-apoptotic members (Youle and Strasser, 2008). BCL-2 family proteins play an important role in regulation of apoptosis, tumorigenesis and cellular responses to anti-cancer therapy. The family consists of 6 anti-apoptotic genes (BCL-2, BCL-xl, MCL-1, BCL-w, BFL-1, BCL-RAMBO and BCL-B), 3 pro-apoptotic genes (BAX, BAK and BOK) and several BH3-only proteins that are pro-apoptotic interacting proteins that can act as upstream agonists or antagonists (BID, BIM, PUMA, BAD, NOXA, HRK, BIK, BMF, BCL-G and Spike) (Yip and Reed, 2008) (Fig. 1.2). BCL-2 family pro-survival members are multidomain proteins which typically contain BH1, BH2, BH3 and BH4 domains that form a hydrophobic pocket capable of binding a BH3 domain and contributing to the anti-apoptotic function (Aouacheria *et al.*, 2013). Pro-apoptotic members BAX, BAK and BOK are also multidomain proteins which contain BH regions 1-3 capable of binding BH3 other regions. Pro-apoptotic BH3-only proteins share homology with the other members of the BCL-2 family only through their short BH3 motif. Since many pro-apoptotic members contain a BH3 domain alone, this suggests that the BH3 domain is necessary for pro-apoptotic function (Bingle *et al.*, 2000).

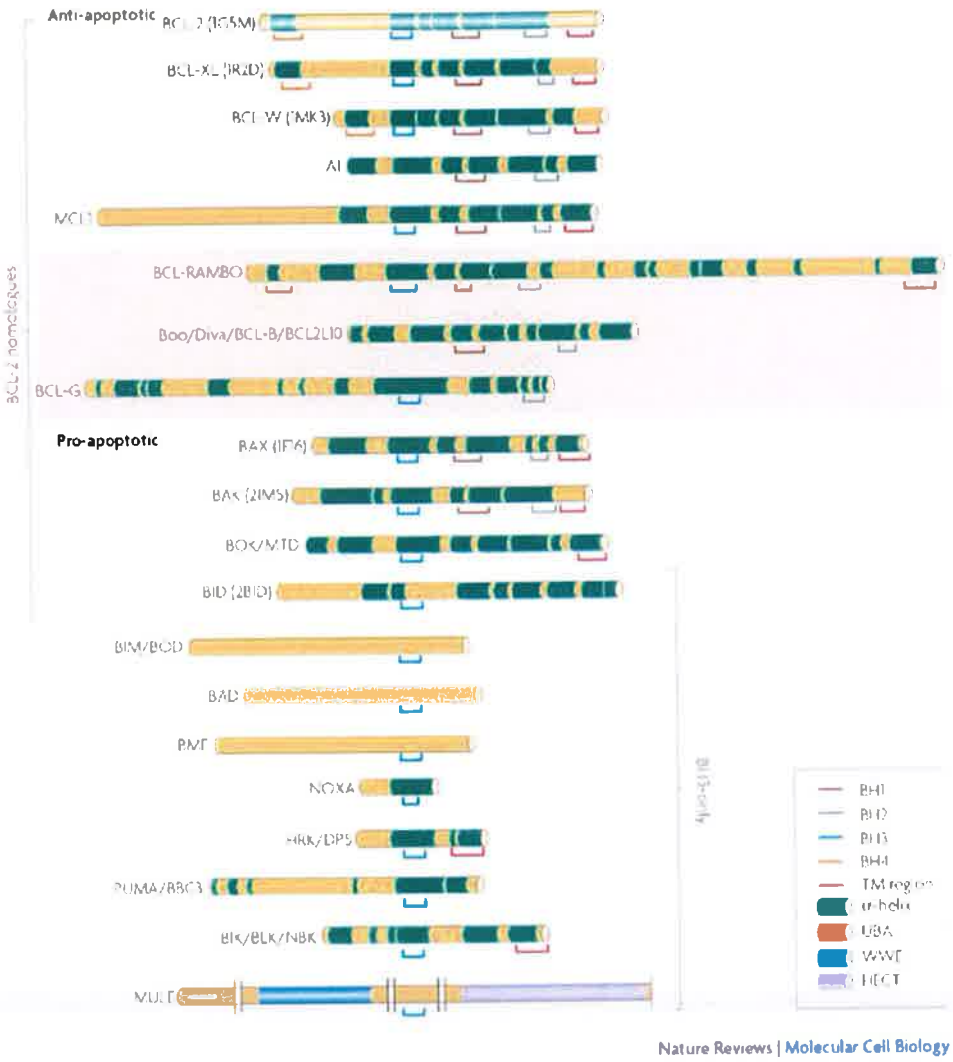

Figure 1.2: The core multi-BH domain BCL-family members. BCL-2 family members classified based on sequence homology. The anti-apoptotic BCL-2 family members typically consist of 4 BH domains (BH1-4). Pro-apoptotic BCL-2 family members contain three domains (BH1-3) while the BH-3 only members contain only BH3 domain. Image taken from Youle, R.J and Strasser, A. 2008. The BCL-2 protein family: opposing activities that mediate cell death. Nature Reviews. 9:47-59

BH3-only proteins regulate activity of both pro- and anti-apoptotic proteins by binding via their BH3 domains (Chipuk and Green, 2008). BCL-2-like protein 11 (BIM), BH3 interacting- domain death agonist (BID) and pro-apoptotic p53 upregulated mediator of apoptosis (PUMA) have been found to bind all anti-apoptotic BCL-2 members while BCL-2-associated death promoter (BAD) and phorbol-12-myristate-13-acetate-induced protein 1 (NOXA) can only bind specific anti-apoptotic members. Anti-apoptotic family members reside in the mitochondria of cells and act to prevent MOMP caused by pro-apoptotic members BAX and BAK. BH3-only members de-repress BAX and BAK by binding to and inhibiting anti-apoptotic BCL-2 members or can act to activate pro-apoptotic multidomain proteins that carry out MOMP. Cheng *et al.* found that BH3-only protein-derived mitochondrial apoptosis, induced through expression of truncated BID (tBID), BIM and NOXA, was completely attenuated in BAX/BAK double knockout mouse lymphocyte cells while apoptosis could occur in downstream effector knockouts (APAF-1, caspase-9 or caspase-3) through a caspase-independent pathway (Cheng *et al.*, 2001). The study also used BCL-2 and BCL-xL mutations to confirm that BCL-2 and BCL-xL were primarily involved in BH3-only protein sequestration and prevention of BAX, BAK activation. BID, BIM and PUMA have been shown to be direct activators of BAX/BAK dependent cell death (Ren *et al.*, 2010). Developmental defects seen in BAX-deficient and BAK-deficient mice were shown to be present in BID, BIM and PUMA triple knockout mice with both types demonstrating cessation of caspase-mediated apoptosis. This work demonstrates the influence the BH3-only proteins have over cell death decisions.

1.2.5 Pro-apoptotic BH3-only proteins

BH3-only members of the BCL-2 family including BIM, BID, PUMA, NOXA and BAD contain a single BH3 domain which can bind to and sequester or abrogate the function of anti-apoptotic members of the BCL-2 family (Zong *et al.*, 2001). While they cannot initiate apoptosis alone, their activity ensures activation of pro-apoptotic BAX and BAK and apoptosis initiation. There are two proposed models for BH3-only protein-mediated apoptosis (Kuwana *et al.*, 2005). The direct model favours BH3-only protein-mediated direct interaction with BAX/BAK and BAX/BAK activation. This model is supported by the structural similarity of BAX to BCL-2 pro-survival proteins and aided by work establishing an interaction between the BID and PUMA BH3 domain and the N-terminal of BAX (Cartron *et al.*, 2004). The indirect model proposes that BH3-only proteins activate BAX/BAK through binding and sequestering of BCL-2 pro-survival proteins (Willis and Adams, 2005). There is increasing evidence to support both theories and it is likely to be context dependent but the role for the BH3-only proteins in activating apoptosis is undeniable.

1.2.6 MCL-1

MCL-1 is an anti-apoptotic member of the BCL-2 family which was first identified as an early induced gene in the myeloid cell line (Zhuang and Brady, 2006). MCL-1 is an early response gene that is associated with rapid induction and turnover (Yang *et al.*, 1996, Kozopas *et al.*, 1993) and has been identified in numerous human cells and tissues. MCL-1 knockout mice undergo embryonic lethality due to failure of implantation which suggests a role for MCL-1 in embryonic development (Yang *et al.*, 1996).

MCL-1 demonstrates sequence homology to BCL-2 in the carboxyl portion but lacks a BH4 domain present in both BCL-2 and BCL-xL (Herrant *et al.*, 2004). Unlike other BCL-2 homologs, MCL-1 contains a PEST (proline, glutamic acid, serine and threonine) domain in its N-terminal (Mei *et al.*, 2005). PEST sequences have been found in proteins with short half-lives and have been associated with directing degradation (Rogers *et al.*, 1986). MCL-1 is localised to the outer mitochondrial membrane (Akgul, 2009). It functions to interact with and sequester the pro-apoptotic BCL-2 member BAK on the outer mitochondrial membrane which in turn prevents mitochondrial permeabilisation and cytochrome c release from the mitochondria. The BH3-only protein NOXA has been shown to mediate the release of MCL-1 from the pro-apoptotic BAK (Gelinas and White, 2005). This action leads to initiation of apoptosis with targeting of MCL-1 to the proteasome for degradation. Work by Willis *et al.* found that in healthy cells BAK was associated with MCL-1 and BCL-xL, both anti-apoptotic BCL-2 family members, and required release from both members to initiate apoptosis (Willis *et al.*, 2005).

MCL-1 is regulated post transcriptionally with *Mcl-1* mRNA having two splice variants (Herrant *et al.*, 2004). MCL-L is a full length variant that contains a BH1-BH3 domain, BCL-2 homology domains, which allows interaction with BCL-2 family members and confers an anti-apoptotic function. MCL-S is a short variant that is responsible for pro-apoptotic actions of MCL-1 due to the presence of a BH3 domain. Both forms have been identified in human tissues (Oyadomari and Mori., 2004). The expression of MCL-1 can be regulated by MULE (MCL-1 ubiquitin ligase E3) which binds to MCL-1 through its BH3 domain and targets it for proteasomal degradation (Zhong *et al.*, 2005). MULE has demonstrated the capacity to compete with BAK through its similar BH3 domain which could disrupt the MCL-1/BAK complex and initiate apoptosis. TRIM-17, an E3 ubiquitin–ligase, has been shown to be necessary for targeting MCL-1 for degradation in a cerebellar granular neuron model (Magiera *et al.*, 2013). Overexpression of TRIM-17

increased MCL-1 phosphorylation and ubiquitination and resulted in proteasome-dependent decrease in MCL-1 protein levels and initiated neuronal death. MCL-1 has also been shown to be regulated at the protein level by PERK-mediated eIF2α (Fritsch *et al.*, 2007). Phosphorylation of eIF2α prevents protein translation during ER stress in an effort to alleviate further stress. Phosphorylated eIF2α was shown to mediate down-regulation of MCL-1 protein levels in a variety of cells and this was shown to drive ER stress-induced apoptosis.

MCL-1 has also been shown to interact with pro-apoptotic BIM (Opferman *et al.*, 2003). BIM activates BAX/BAK and thus the mitochondrial apoptosis pathway by binding to the MCL-1 binding pocket. MCL-1 can be further regulated by caspase cleavage of two aspartic acid residues, ASP127 and ASP157 within the pest domain and the c-terminal fragment that results from cleavage promotes cell death (Michels, J. 2004 oncogene). Work by Herrant *et al.* found that caspase-cleaved MCL-1 associated with pro-apoptotic BIM with greater affinity than MCL-1 wild-type but failed to exert an anti-apoptotic effect on BIM in HeLa cells (Herrant *et al.*, 2004). Caspase-8 cleavage of MCL-1 has also been suggested in a novel crosstalk pathway between the tumour necrosis factor-related apoptosis-inducing ligand (TRAIL) death receptor pathway and the mitochondrial apoptosis pathway (Han *et al.*, 2006). They demonstrated that caspase-8 and caspase-3-mediated degradation of MCL-1 generated free BIM which can act downstream to initiate apoptosis. This work provides a novel link between the extrinsic and intrinsic apoptotic pathways mediated by MCL-1.

Although pro-apoptotic proteins can mediate MCL-1 expression, protein expression can be mediated further by small RNA molecules, microRNAs, that bind to the *Mcl-1* mRNA in the cell and prevent its translation. MicroRNAs are abundant in cells and have a wide variety of functional targets including MCL-1. TargetScan and miRBase databases identified 181 and 176 miRNAs respectively targeting

MCL-1, including the miR-29 family and the miR-193 family (Lam *et al.*, 2010). Experiments *in silico* identified MCL-1 as a target of the miR-29 family (Mott *et al.*, 2007). Subsequent work by (Steele *et al.*, 2010) found that an upregulation of miR-29b by c-myc promoter binding protein (MBP-1) in prostate cancer cells repressed MCL-1 thus affecting tumour growth. Work in this lab previously identified MCL-1 as a target of miR-29a through array screening. In cancer, miR-133b was shown to target the 3'UTR of MCL-1 directly in adenocarcinoma cells (Crawford *et al.*, 2009) while in gastric cancer, miR-512-5p activation was shown to suppress MCL-1 expression and induced apoptosis of gastric cancer cells (Saito *et al.*, 2009).

While overexpression of MCL-1 has been implicated in many cancers, a decreased expression of MCL-1 can play a role in inappropriate cell death. Research conducted by Arbour *et al.* indicated that MCL-1 played a role in regulating neuronal survival following injury (Arbour *et al.*, 2008). Neurons were sensitised to apoptosis following DNA damage with MCL-1 loss and MCL-1 degradation was shown to be necessary for neuronal death. Furthermore, MCL-1 was also shown to be required for neuronal development with loss of MCL-1 in neuronal progenitors resulting in increased apoptosis. A role for MCL-1 has also been shown in mediating implantation and embryo development *in utero* (Rinkenberger *et al.*, 2000). In addition, MCL-1 has been shown to be important for determining cortical neuron cell fate (Germain *et al.*, 2011). *Mcl-1* gene deletion in cortical neurons from the forebrain of adult mice has demonstrated massive cortical apoptosis. Furthermore MCL-1 knockout cortical neurons were shown to undergo enhanced autophagy following stress induction. Removal of autophagy mediator BECLIN-1 or activation of BAX could push cortical neurons to undergo apoptosis. This work demonstrates the importance of MCL-1 in protecting cortical neurons and mediating apoptosis in the adult central nervous system (CNS).

1.2.7 ER stress-mediated apoptosis

Pro-apoptotic members of the BCL-2 family have been shown to be upregulated under conditions of ER stress in various cell types and this leads to BAK/BAX activation and activation of pro-apoptotic caspases which induce cell death (Szegezdi *et al.*, 2006). Work by Reimertz *et al.* identified PUMA, a BH3-only member of the BCL-2 family, as upregulated in SHSY5Y neuroblastoma cells undergoing tunicamycin-induced ER stress in neuroblastoma cells. Their work provided evidence that demonstrated that PUMA upregulation was p53 independent during ER stress. Western blot analysis of PUMA protein levels showed increased PUMA protein levels in tunicamycin-treated SHSY5Y neuroblastoma cells while increased PUMA expression was seen in p53-deficient human SAOS-2 osteosarcoma cells treated with tunicamycin. Furthermore western blot analysis of tunicamycin-treated SHSY5Y cells did not demonstrate increased expression of p53. Immunofluorescence analysis of pro-apoptotic BAX activation confirmed mitochondrial apoptosis pathway activation in SHSY5Y neuroblastoma cells undergoing ER stress following either tunicamycin or thapsigargan treatment. This mitochondrial apoptosis activation coincided with induction of PUMA translation (Reimertz *et al.*, 2003). This work was further supported by experiments in p53-null cortical neurons which showed increased PUMA protein expression when treated with ER stressors tunicamycin and thapsigargin compared to untreated controls (Fricker *et al.*, 2010). Furthermore work by (Galehdar *et al.*, 2010) demonstrated that p53-independent PUMA upregulation in cortical neurons undergoing ER stress was mediated by ATF4 (activating transcription factor 4) through induction of CHOP expression. They suggest that CHOP, a transcription factor induced during ER stress, binds the PUMA promoter and mediates its expression. Through ChIP and PCR analysis they found enhanced binding of ATF4 to the CHOP promoter during tunicamycin and

thapsigargin-induced ER stress which coincided with reductions in PUMA induction in ATF4-deficient cortical neurons under the same ER stress conditions. They also found CHOP knockdown markedly reduced PUMA mRNA induction under induced ER stress.

While Reimertz *et al.* found that PUMA-deficient Hct116 cells had significantly reduced ER stress-induced apoptosis (Reimertz *et al.*, 2003), Puthalakath *et al.* found that *bim-/-* MCF7 cells also had significantly reduced ER stress-induced apoptosis following thapsigargin treatment. BIM was shown to stimulate ER stress-induced apoptosis by two fundamental mechanisms across a wide range of cell types. Firstly, ER stress increased dephosphorylation of BIM by protein phosphates 2A which prevents ubiquitination and degradation of phosphorylated BIM in the proteasome. Secondly, ER stress increased BIM protein expression through C/EBP homologous protein- CCAAT-enhancer-binding protein alpha (CHOP-C/EBPα) mediated transcriptional activation. Luciferase assays identified CHOP as binding a regulatory site on the BIM gene during ER stress and increasing expression of BIM protein (Puthalakath *et al.*, 2007). BIM, a BH3-only pro-apoptotic BCL-2 family member, along with PUMA and NOXA, has been implicated in regulation of ER stress-induced apoptosis (Li *et al.*, 2006). While both studies reported significantly reduced apoptotic levels, neither found complete cessation of apoptosis. Maintenance of apoptosis could occur through activation of alternative BH3 only proteins or through degradation of antiapoptotic BCL-2 family members e.g. MCL-1.

One study by Du *et al.* found that, in the absence of the direct BAK/BAX activators, BID and BIM, other BH3-only proteins such as NOXA, PUMA and BMF exhibited activation of BAK/BAX and subsequent apoptosis (Du *et al.*, 2011). Pore-formation assays showed that both BMF and PUMA removed BCL-xL inhibition of BAX activation with PUMA-mediated activation enhanced in the presence of MCL-1 inhibition. Furthermore work by Tuffy *et al.* found PUMA to be a main

mediator of mitochondrial apoptosis following proteasome inhibition. Following proteasome inhibition, increased caspase-3 activity and reduced cytochrome c immunofluorescence in the mitochondria of neurons indicated activation of mitochondrial apoptosis which coincided with increased BIM and PUMA mRNA and proteins levels (Tuffy *et al.*, 2010). This study also found siRNA-mediated knockdown of BAX in both WT and *puma*$^{-/-}$ cortical neuron treated with a cytotoxic agent to be protective compared to scrambled control treated cells indicating a major role for both BAX and PUMA in mitochondrial apoptosis in cortical neurons.

1.2.8 ER stress and neurodegeneration

ER stress has been implicated in the pathogenesis of many neurodegenerative disorders e.g. ALS (Nawa *et al.*, 2008, Zhao and Ackerman, 2006). The presence of the mutant superoxide dismutase 1 (mSOD1) gene causes aggregation of misfolded mSOD1 protein and subsequent ER stress in ALS. Previous work has shown the effect of ER stress in relation to SOD1 mutation in familial ALS (Kieran *et al.*, 2007). Following identification of PUMA as a key mediator in ER stress-induced apoptosis, the study found PUMA upregulation in the motor neurons of SOD1 mutant mice with corresponding PUMA-deficient motor neurons demonstrating protection from ER stress-induced apoptosis. Increased GRP78 and CHOP expression were also identified in early disease onset in SOD1 mice indicating increased ER stress. A corresponding study by Ilieva *et al.* looked at the role of ER stress in sporadic ALS. They hypothesised that ER stress arising from oxidative stress contributed to sporadic ALS. They found increased ER chaperone expression and increased phosphorylation of the translation initiation factor eIF2α in spinal cord samples from patients with sporadic ALS (Ilieva *et al.*, 2007). Increased ER stress has been implicated in the pathology of both sporadic and familial AD following detection of both increased ER chaperone induction and UPR activity

(Song *et al.*, 2008). β-amyloid is the main mis-folded polypeptide and a major pathophysiology of AD. β-amyloid accumulation has been shown to increase ER stress and cause cytotoxicity through a caspase-12 dependent manner. In familial AD, presenilin dysfunction causes release of calcium into the cytoplasm which increases ER stress (Lin *et al.*, 2008). Activation of the UPR in neurons of AD brains has indicated a role for ER stress in AD pathophysiology (Salminen et al., 2009a). Costa *et al.* utilising mitochondrial depleted rho cells, found that crosstalk between the ER- and mitochondrial-mediated apoptotic cell death in cells treated with β-amyloid peptide, the main constituent of amyloid plaques in AD (Costa *et al.*, 2010). Cells, with (rho+) or without functional mitochondria (rho0) that were stressed with thapsigargin or brefeldin A and subsequently treated with β-amyloid peptide, demonstrated increased ER stress mediator expression and increased caspase activity however ER stress-induced apoptosis only occurred in rho+ cells . It was concluded that apoptotic cell death could not occur without functional mitochondria even in the presence of enhanced ER stress. ER stress has been implicated in other proteinopaties such as Parkinson's Disease (PD) (Omura *et al.*, 2013) and HD (Vidal *et al.*, 2011). Following ischemic or seizure-induced neuronal injury, increased ER stress can lead to neuronal apoptosis (Ward *et al.*, 2004). ER stress following ischemic injury in rat hippocampal neurons has also been shown to lead to increased expression of BH3-only protein PUMA with increased downstream apoptosis (Reimertz *et al.*, 2003).

1.3 MicroRNAs

MicroRNAs (miRNAs) are a family of endogenous, small ribonucleic acids (RNAs) which are 19-22 nucleotides in length (Baulcombe, 2002). miRNAs are negative regulators of gene transcription at the post-transcriptional level. miRNAs act to prevent the translation of messenger RNAs (mRNAs) to protein and to promote mRNA degradation. miRNAs function in mammalian cells by binding to the 3'UTR of the mRNA target strand with imperfect complementarity and it is this imperfect base pairing that drives translational repression and mRNA sequestration (Esau and Monia, 2007). While small interfering RNA (siRNA) and plant miRNAs have been shown to bind to target mRNA with perfect complimentarity and induce endonucleolytic cleavage by the RNA-induced silencing complex (RISC), the imperfect binding nature of mammalian miRNAs to their 3'UTR target site ensures that they cause translational repression or mRNA degradation without endonucleolytic cleavage (Soifer *et al.*, 2007). miRBASE, a miRNA database, identified 2578 mature human miRNAs and 1908 mature mouse miRNAs to date. Ribosome profiling carried out by Guo *et al.* indicated that decreased protein expression following miRNA regulation is a consequence of mRNA degradation (>84%) compared with decreased protein translation alone (Guo *et al.*, 2010). Approximately 30% of all protein-coding genes can be regulated by miRNAs in a whole cell (Filipowicz *et al.*, 2008).

Mammalian miRNAs are formed through multiple processing events in the cell (Winter *et al.*, 2009). Mature miRNAS start out as longer primary transcripts called pri-miRNAs which are hairpin structures, polyadenylated and 5'-7-methylguanosine capped by polymerase II transcription (Fig. 1.3). In the nucleus the pri-miRNA is processed by the RNase II enzyme DROSHA and its double stranded RNA binding partner DiGeorge syndrome critical region gene 8 (DGCR8) / partner of

DROSHA (PASHA) into a pre-miRNA (Lee *et al.*, 2003). DROSHA cleaves 11 base pairs from the hairpin base, the site of the single-stranded RNA double-stranded RNA junction. This 60 nt pre-miRNA is then exported out of the nucleus by EXPORTIN 5 and into the cytoplasm. A second processing step occurs in the cytoplasm when the endoribonuclease DICER and its binding partner TAR RNA binding protein (TRBP) cleaves the pre-miRNA into a double stranded duplex in which one strand is the processed miRNA and the other strand is its compliment (Chendrimada *et al.*, 2005). The miRNA duplex is then processed in the RISC. Orientation and cleavage depends on the differences in thermodynamic stability at the 5' end of the mature miRNA and allows for degradation of the unused compliment strand (Krol *et al.*, 2004). Recently published work identified the "seed region" at the 5' end of mammalian miRNAs as the key determinant in miRNA target specificity (Friedman *et al.*, 2009). Identification of conserved sites 6-8 nucleotides in length that matched the miRNA seed region of interest demonstrated high target predictability. Furthermore, mathematical modeling of miRNA interactions has shown that the efficacy of miRNA-mediated silencing of a given target is reliant upon the relative stability of the miRNA 5' terminal and of the seed region also (Hibio *et al.*, 2012, Esau and Monia, 2007). miRNAs with a strong silencing effect were shown to have an unstable 5' terminal duplex, hypothesized to allow easier incorporation of the mRNA into the RISC complex and a stable seed-target duplex to direct the posttranscriptional repression.The miRNA in the RISC complex can then guide translational repression of target mRNA through the activity of the RISC effector argonaute proteins (AGO) (Esau and Monia, 2007).

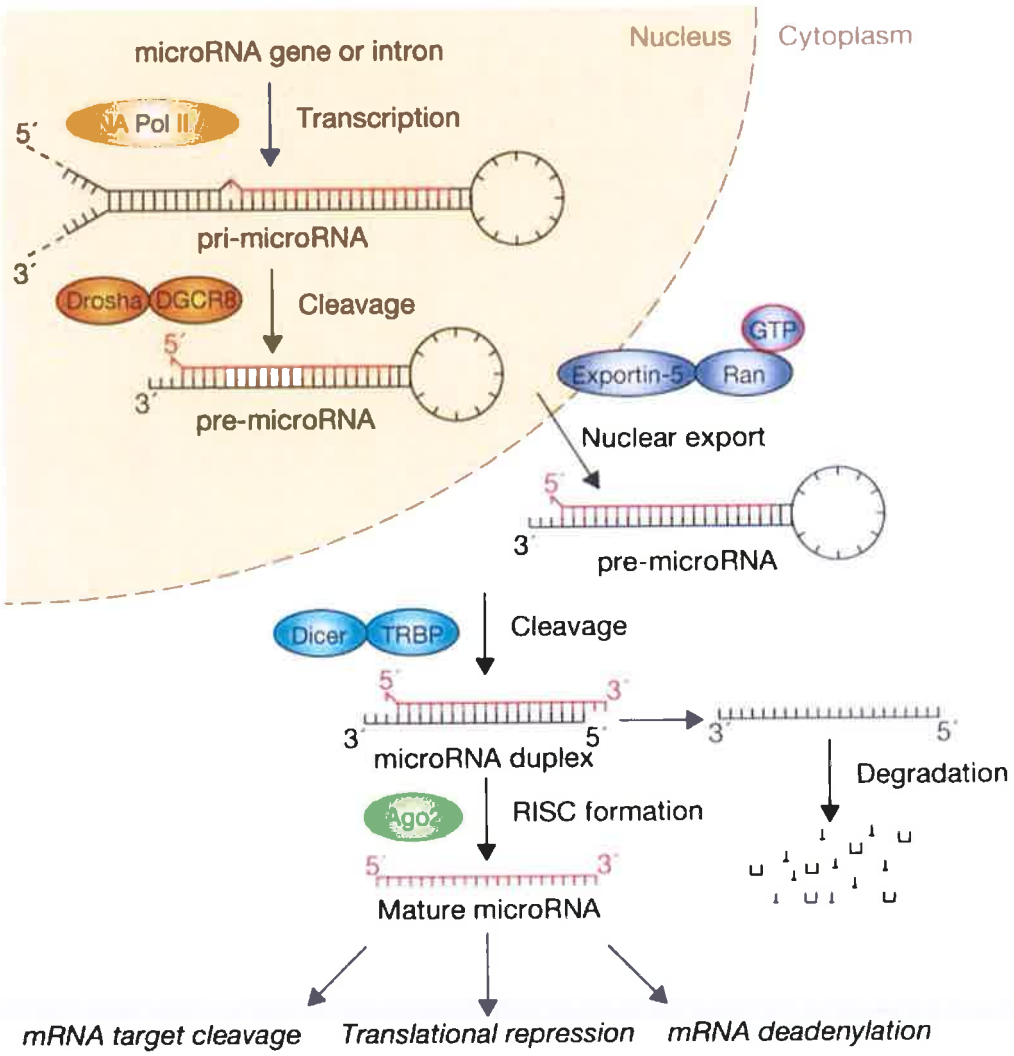

Figure 1.3: MicroRNA processing in the cell. Mature miRNAs are processed from primary hairpin transcripts (pri-miRNA) by RNase II enzyme DROSHA in the nucleus. The resulting pre-miRNA is exported from the nucleus, into the cytoplasm where it is processed further by DICER/TRBP into a double stranded microRNA duplex. The RISC complex cleaves the microRNA duplex to form the mature microRNA which can guide translational repression of target mRNA. Image taken from Winter, J., Jung, S., Keller, S. Gregory, R.I. and Diederichs, S. 2009. Many roads to maturity: microRNA biogenesis pathways and their regulation. Nature Cell Biology, 11(3):228-234.

1.3.1 Roles in disease and dysfunction

Due in part to the variety, abundance and assorted nature of mammalian miRNAs and due to their ability to individually regulate numerous target mRNAs, a huge number of microRNAs have been implicated in various forms of cancer and neurodegenerative diseases (Kloosterman and Plasterk, 2006). Through interactions with their various targets, miRNAS have been shown to play roles in determining differentiation, proliferation and apoptosis, therefore deregulation of miRNAs could have huge ramifications for these systems. Identification of deregulated miRNAs in various forms of cancer has lead to the discovery of both oncogenic roles and tumour suppressor functions of miRNAs. miR-15-miR16 neighbouring miRNAs were first shown to be deleted or down-regulated in chronic lymphocytic leukemia (CLL), suggesting a tumour suppressor role for this group (Calin *et al.*, 2002). Overexpression of miRNA cluster miR-17-92, also known as oncomir-1, has proven to have an oncogenic effect in human B cell lymphomas (Olive *et al.*, 2010). The human miR-17-92 is located on chromosome 13q31.3 which is a region consistently amplified in hematopoietic tumours. Overexpression of this oncomir has demonstrated remarkable tumour potential in multiple mouse models. MiRNA deregulation has also been abundantly published in relation to neurodegeneration. Many miRNAs are located in the CNS and, due to the sensitivity of post-mitotic neurons to stresses, can have devastating effects on pathways within the CNS. Indeed experiments in which DICER activity was lost demonstrated widespread effects (Kim *et al.*, 2007). Loss of DICER in dopaminagic neurons resulted in cell death in the substantia nigra and mouse phenotypes characteristic of Parkinson's disease. Deletion of DICER in the hippocampus resulted in modifications to dendritic spine branching. Furthermore, deletion in purkinje cells resulted in cell death and degeneration of the cerebellum (Davis *et al.*, 2008). Targeting of DICER highlights the importance of miRNAs in maintaining cellular homeostasis in the CNS.

However disregulation of individual miRNAs can have widespread effects.

1.3.2 miRNAs and ER stress

The role miRNAs play in affecting protein translation also suggests a role for miRNA deregulation in propagating ER stress in the CNS which is a hallmark of many neurodegenerative diseases including AD and ALS. miRNA has been shown to both regulate and be regulated by the ER stress UPR machinery. The PERK branch of the UPR pathways has been shown to drive expression of miR-30c-2-3p in cells undergoing tunicamycin-induced ER stress (Byrd *et al.*, 2012). Overexpression of miR-30c-2-3p was shown by luciferase assay to target XBP1, a transcription factor that boosts cell survival following ER stress, and enhances cell death. Conversely, antagomir regulation of miR-30c-2-3p increased XBP1 expression and promoted cell survival. The IRE1α branch of the UPR has also been shown to target miRNAs for degradation (Upton *et al.*, 2012). IRE1α was shown to down-regulate miRNAs miR-17, -34a, -96 and -125b by targeting sites similar to excision sites on XBP1. Downregulation of these miRNAS was shown to de-repress caspase-2 translation and activation which increased cell death in wildtype MEFs undergoing brefeldin A-induced ER stress. MicroRNAs have also been shown to affect expression of downstream targets of the UPR signaling pathways which in turn leads to direct modulation of ER stress and cell death. An example of this is miR-211 which has been shown to be induced by the PERK pathway following tunicamycin-induced cell death (Chitnis *et al.*, 2012). The expression of miR-211 was also shown to require eIF2α phosphorylation and ATF4 induction under control of PERK. Downstream of PERK and ATF4, miR-211 has been shown to attenuate expression of pro-apototic CHOP under conditions of ER stress and allowed the cell to restore cellular homeostasis.

1.3.3 miRNA therapeutics

Due to the vast abundance of miRNAs in all cells and tissues of the human body and due to the wide range of targets, miRNA-based therapeutics have been a topic of much discussion in the last few years. Mechanisms of miRNA expression alteration *in vitro* and *in vivo* include transfection with gene knockout, pri-miRNA, pre-miRNA, mature miRNA, antagomir, small interfering RNA (siRNA) and short hairpin RNA (shRNA) for the miRNA target of interest (van Rooij, 2011). Antisense oligonucleotides or antagomirs are single stranded RNA molecules that can bind their target sequence with perfect complimentarity. It is this perfect complimentarity that allows repression of target translation or target degradation through recruitment of RNase H (Broderick and Zamore, 2011). Antagomirs have a partial phosphorothioate backbone and a 2'-O-methoxyethyl group modification that increases the stability of the RNA (Krutzfeldt *et al.*, 2005). Modifications to further enhance antagomir efficacy include cholesterol conjugation to promote uptake in the cells through association with lipoproteins and, in the case of locked nucleic acids, a type of bi-cyclic RNA analogue; the furanose ring in the RNA backbone is locked in an RNA mimicking N-type (C3'-endo) conformation by the introduction of a methylene bridge between the 2' oxygen and the 4' carbon (Stenvang *et al.*, 2012). The C3'-endo conformation that is held in place by the methylene bridge favours RNA:RNA and DNA:RNA helices and thus increases specificity of the probes. Locked nucleic acid (LNA) probes have high stability and high binding ability which allows for the use of short probes. LNA modified antagomirs to Let7f and miR-1 were shown in a model of ischemic stroke in middle-aged female rats to provide neuroprotection for up to 4 hours following the ischemic insult (Selvamani *et al.*, 2012). Both miR-1 and Let7f target insulin-like growth factor-1 (IGF-1) in the brain and diminish IGF-1 neuroprotective role following cerebral ischemia. Antagonisation of these miRNAs gives a prime example of the therapeutic potential of

modulating miRNAs. Recent work in the Prehn lab using LNA antagomirs specific to miR-134, identified the important role of the brain-specific miR-134 in epilepsy (Jimenez-Mateos *et al.*, 2012). An *in vivo* model of miR-134 during status epilepticus demonstrated that silencing miR-134 using antagomir technology affected hippocampal spine morphology specifically targeting CA3 pyrimidial neuron spine density in the hippocampus and this resulted in mice with resistance to seizures and to the subsequent hippocampal injury. miR-134 was shown to directly target LIM kinase-1 (LimK-1) mRNA, a mediator of β-actin and spine morphology, as a mechanism of action

1.3.4 miR-29, a miR of ER stress

miR-29 family member dysregulation has been implicated in Alzheimer's disease through regulation of β-amyloid cleavage enzyme (BACE1) which can affect β-amyloid overproduction (Hebert *et al.*, 2008). miR-29a and miR-29b have been shown in luciferase assays to interact directly with the 3' UTR of BACE1. miR-29b and miR-29a has also been shown to be down-regulated in patients with Huntington's disease (HD) (Johnson *et al.*, 2008). Previous studies indicate that miR-29 family members, namely miR-29b, negatively regulate *Mcl-1* mRNA expression which can result in increased cell death (Mott *et al.*, 2007). Previous work in this lab had identified miR-29a as upregulated in neuroblastoma cells under conditions of tunicamycin-induced stress. Real time qPCR using Taqman low density array analysis of SHSY5Y neuroblastoma cells treated with 3 μM tunicamycin for up to 12 hr identified a range of miRNAs with altered expression. Thirteen differentially expressed miRNAs were identified as of interest (Table 1.1). GRP78 and CHOP mRNA levels confirmed the presence of ER stress. Target analysis of these miRNAS identified MCL-1, an anti-apoptotic member of the BCL-2 family, as a target of miR-29a. The integral role that MCL-1 plays in maintaining cell survival across all cell types and preventing mitochondrial apoptosis and autophagy-induced

cell death made miR-29a an interesting prospect for control and modulation of ER stress-induced cell death.

Table 1.1: Taqman low density array of 667 differentially expressed microRNAs from SHSY5y neuroblastoma cells undergoing ER stress identified 13 miRNAs that were upregulated. (Work completed by Dr. Isabella Bray, Molecular and Cellular Therapeutics, RCSI).

miRNA	4 h RQ	8 h RQ	12 h RQ
hsa-miR-22	0.306	1.663	2.5155
hsa-miR-29a	1.254	1.712	1.701
hsa-miR-106b	1.171	1.589	1.941
hsa-miR-135b	1.239	1.372	2.016
hsa-miR-148a	1.451	2.762	4.069
hsa-miR-189	0.899	3.183	4.041
hsa-miR-193a	2.291	1.897	0.338
hsa-miR-376a	2.089	1.217	1.163
hsa-miR-378	1.199	1.384	1.906
hsa-miR-424	0.306	1.663	2.516
hsa-miR-545	1.240	1.329	2.419
hsa-miR-594	1.746	1.456	1.057
hsa-miR-642	3.379	6.011	6.420

Further work in the Prehn lab prior to the commencement of this research study confirmed that miR-29a targeted the 3' UTR of MCL-1 through luciferase assay in SHSY5Y cells undergoing tunicamycin-induced cell death (Unpublished work completed by Dr. Caoimhín G. Concannon, Dept. of Physiology and Medical Physics, RCSI).

1.3.5 miR-29 family

miR-29a is member of the miR-29 family of microRNAs which contains miR-29a, b and c (Amodio *et al.*, 2012). In humans the members of the miR-29 family are found on two separate loci on different chromosomes: miR-29b1 and miR-29a on Chromosome 7 at position q32.3 and miR-29b2 and miR-29c on chromosome 1 at position q32.2. miR29b-1 and miR29b-2 are both upstream of miR29a and miR29c respectively. The mature sequences of the members of the miR-29 family are highly conserved in humans, mice and rat. All three members have identical seed region sequences, located at nucleotides 2 to 7 of all microRNAs, and thus have many overlapping targets (Kriegel *et al.*, 2012). Although all members are transcribed on two polycistronic transcripts, the expression patterns of each member can be different in different cell models due to post-transcriptional regulation. Work in HeLa cells, in which miR-29 is abundant, identified the importance of post-transcriptional modification on the miR-29 family (Hwang *et al.*, 2007). Northern blot identified miR-29a as highly expressed in all cell-cycle phases while miR-29b was only highly expressed in mitotic phases. Furthermore miR-29a was found to be localized primarily to the cytoplasm with minor nuclear presence while miR-29b was nuclear enriched. The study attributed nuclear localization to the miR-29b 3' terminal motif (AGUGUU). Mutation studies in this region prevented effective delivery of exogenous miR-29b to the nucleus. miR-29c has been shown to be nuclear-enriched in breast cancer cells (Chen *et al.*, 2012). These differences in localization may also effect the pathways and the interactions that these miRNAs undergo in various cell types and can account for the wide ranging effects of the miR-29 family whether it be regulating extracellular matrix proteins such as collagen and laminin γ1 (Sengupta *et al.*, 2008) or by affecting cell proliferation and death in disease models (Amodio *et al.*, 2012) .

1.3.6 miR-29a

miR-29a has the 22bp sequence:

4-acugauuucuuuugguguucag-26

Studies suggest that miR-29a could be of therapeutic benefit in many disease pathologies. Studies using miR-29a pre-miRNAs and antagomirs showed that miR-29a conferred an apoptotic effect through targeting of MCL-1 in cancer cells (Mott *et al.*, 2007) (Fig. 1.4). Further work in this area suggested a role for NF-kB-mediated repression of miR-29 and subsequent increased MCL-1 expression (Mott *et al.*, 2010). NF-kB can promote cell survival through increasing expression of pro-survival BCL-2 family members including MCL-1. They identified multiple NF-kB binding sites on the miR-29a promoter site and induced miR-29a down-regulation with activation of NF-kB Work by Park *et al.* found that, from a range of miRNAs, miR-29a increased p53 protein levels in HeLa cells and showed enhanced apoptosis and reduced cell viability in a range of cells in a p53 dependent manner (Park *et al.*, 2009). Concurrently (Ye *et al.*, 2010) showed that miR-29a inhibition had an anti-apoptotic effect in myocardial cells that had undergone ischemic reperfusion.

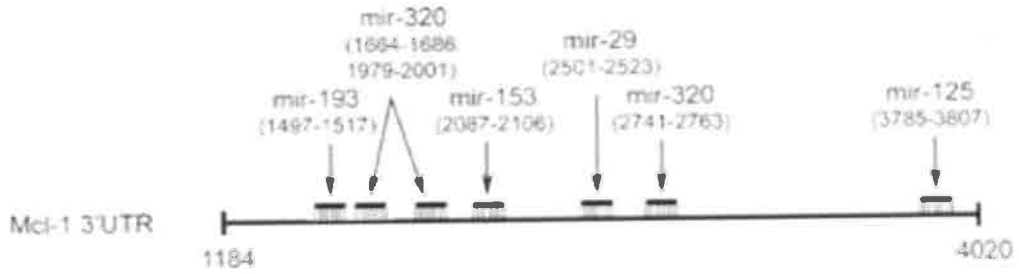

Figure 1.4: Proposed miRNA target sites on the 3' UTR of *Mcl-1* messenger RNA. Independent searches using Miranda and Pictar target prediction programs identified miRNA predicted binding sites within the 3' UTR of MCL-1. Image adapted from "miR-29 regulates MCL-1 protein expression and apoptosis" Image adapted from Mott, J.L., Kobayashi, S., Bronk, S.F. and Gores, G.J. 2007. miR-29 regulates MCL-1 protein expression and apoptotsis. Oncogene. 26:6133-40.

Investigations of miR-29a in disease models and from patient samples found a diverse range of both expression and function. miR-29a was shown to be substantially upregulated in tissue samples from ALS brain frontal cortex and decreased in samples from AD brain compared with neurological controls (Shioya *et al.*, 2010). Previously miR-206, a skeletal muscle specific miRNA was shown to play a role in ALS through targeting of histone deacetylase4 (HDAC4) (Williams *et al.*, 2009). Recent work has confirmed that both miR-29 and miR-206 both target the 3'UTR of HDAC4 in a myogenic cell line (Winbanks *et al.*, 2011). Increased expression of one or both miRNAs repressed translation of HDAC4. While it was beyond the scope of the paper, this result suggests a role for miR-29 in ALS through control of HDAC4.

1.4 Amyotrophic Lateral Sclerosis

ALS is a progressive, fatal neurodegenerative disorder that results in motor neuron loss in both the brain and spinal cord (Leigh and Ray-Chaudhuri, 1994). Upper and lower motoneurons are affected and degeneration of motoneurons results in widespread paralysis and death. ALS is the most prevalent of a group of heterogenous motoneuron disorders including progressive muscular atrophy and bulbar palsy. Onset typically occurs in mid-life with risk increasing by an order of magnitude after 60 years of age (Cleveland and Rothstein, 2001). Average life expectancy is 1-5 years from onset. There is no cure at present and treatments are very limited (Acevedo-Arozena *et al.*, 2011). ALS can be subdivided into both familial ALS and sporadic ALS. Sporadic ALS accounts for approx. 90% of cases and there is no known causative factor or genetic link in these cases (Schymick *et al.*, 2007). Neurodegeneration in ALS is the result of a culmination of cytotoxic processes including glutamate excitotoxicity, oxidative stress, mitochondrial dysfunction, axonal transport defects, pro-inflammatory non-neuronal cells and ER stress due to formation of toxic inclusions (Cheah *et al.*, 2010). Familial ALS (fALS) accounts for approximately 5% of all ALS cases and is thought to be autosomal dominant (Byrne *et al.*, 2011). While both forms are characteristically similar, with hallmarks of disease progression including muscle weakness, atrophy, spasticity and motoneuron loss, they are mechanistically different (Cleveland and Rothstein, 2001). Approximately 20% of all fALS (2-3% of all ALS cases) cases are caused by mutations in the cytoplasmic Cu/Zn superoxide dismutase 1 (SOD1) gene (Rosen *et al.*, 1993, Bruijn *et al.*, 1998). SOD1 protein catalyses the dismutation of superoxide anion radicals which are an error of oxidative phosphorylation in mitochondria. Dismutation leads to formation of water and hydrogen peroxide. Mutations in both wildtype and mutant SOD1 are thought to affect fALS through a toxic gain of function

mechanism; however this is not fully understood yet. One hypothesis is that enzymatic activity of SOD1 causes aberrant oxidative stress leading to neurotoxicity. Another hypothesis proposes that mutant SOD1 forms harmful aggregates in motoneurons and astrocytes and induces an ER stress dependent cell death (Pasinelli and Brown, 2006). Several other genes are thought to be causative in ALS including mutant FUS (fused in sarcoma) and TDP43 (TAR DNA binding protein 43) but these are to a lesser extent than SOD1 (Liscic *et al.*, 2008, Gitcho *et al.*, 2008). While SOD accounts for 20% of fALS, TDP43 and FUS mutations account for 3 – 5% (Lagier-Tourenne and Cleveland, 2009). Recently, mutations in chromosome 9 open reading frame 72 (C9ORF72) have been identified in both frontotemporal dementia (FTD) and ALS and provide a genetic link between both diseases (Cruts *et al.*, 2013). The mutation in intron 1 of C9ORF72 results in an expansion of a G4C2 hexanucleotide repeat and has been shown to be twice as common as SOD1 and three times as common as TDP43 and FUS in fALS (Renton *et al.*, 2011). As mutations in the C9ORF72 gene are the most common mutation in fALS it makes for a desirable experimental paradigm and could lead to progress in early diagnosis and further disease understanding.

The three most common therapies for patients include noninvasive ventilation (NIV), percutaneous endoscopic gastronomy (PEG) and the drug riluzole (Miller *et al.*, 2009b). Riluzole, a 2-aminobenzothiazole, manufactured under the name Rilutek, is the only established drug therapeutic for ALS without tracheostomy and prolongs survival by 2-3 months in only a subset of patients (Miller *et al.*, 2009a). While the mechanisms by which riluzole acts are not fully understood, it has been shown to affect glutamate excitotoxicity by interrupting glutamate transmission and blocking calcium channels which mediate glutamate release, sodium channel blockade and further reductions in excitability of neurons and inhibition of phosphorylation of neurofilaments which impairs axonal transport in neurons (Cheah *et al.*, 2010).

1.4.1 A role for ER stress in ALS pathogenesis

Post-mitotic cells such as neurons are particularly vulnerable to ER stress-induced apoptosis (Marder and Goaillard, 2006). Mutant SOD1 has been shown to have reduced stability and to form aggregates due to increased rate of unfolding. These ubiquitin-positive inclusions have been found intracellularly in both motoneurons and astrocytes of the spinal cord (Kikuchi *et al.*, 2006). SOD1 mutant mice have increased ER stress in spinal cord neurons due to misfolded mutant SOD1 accumulating in the ER (Kieran *et al.*, 2007, Kanekura *et al.*, 2009). This aggregation of mutant SOD 1 was shown to be age and region specific in $SOD1^{G93A}$ transgenic mice and the mutant $SOD1^{G93A}$ was localized to the ER where it was shown to interact with GRP78 and activation of ATF6 in affected spinal cord (Kikuchi *et al.*, 2006) Work by Nishitoh *et al.* found that mutant SOD1 interacts with Derlin-1, a component of ERAD and triggers ER stress through dysfunction of ERAD (Nishitoh *et al.*, 2008). Due to the specific age-related manifestation of fALS in SOD1 mice, Saxena *et al.* provide evidence that, while all motoneurons may be susceptible to ER stress, individual motoneurons fall into select groups within SOD1 mice, differing in how they respond to stress and these subgroups may be responsible for the defined disease pathologies. They identified 3 subgroups, those that were vulnerable to ER stress, (vul), those that were resistant to ER stress (res) and those that were slow to respond (s). The vulnerability of some neurons to early ER stress presented as early manifestations of disease in the mice while more resistant neurons accounted for late manifestations of disease (Saxena *et al.*, 2009). Deletion of BAX and BAK in a $SOD1^{G93A}$ mouse model prevented neuron loss, symptom onset and prolonged life by 2 weeks compared to wildtype SOD1 mice (Reyes *et al.*, 2010). Protection of motoneuron viability in the absence of Bax and Bak supports a role for the mitochondrial apoptotic pathway, a main mediator downstream of ER stress, in the pathogenesis of ALS. A role for caspase activation has also been

demonstrated in SOD1 mutants (Kostic *et al.*, 1997, Rosen, 1993). SOD1 mediates toxicity of motoneurons through prolonged activation of the inflammatory caspase, caspase-1, early in disease onset while subsequent and concomitant activation of caspase-3 further along in disease progression activates astrocyte and motoneuron cell death through loss of motor axons. Overexpression of anti-apoptotic BCL-2, whose mRNA expression is decreased in spinal cord motoneurons in ALS patient samples, in $SOD1^{G93A}$ mice delayed disease onset in these mice by approx. 4 weeks and reduced motoneuron loss in the anterior horn of the spinal cord (Kostic *et al.*, 1997) (Kostic *et al.*, 1997). Staining for c-jun and ubiquitin in age matched spinal cord showed reduced staining for these markers of cell death in the SOD1 mutant mice overexpressing BCL-2. Although the SOD1 mutant BCL-2 overexpressing mice lived longer, the period of disease remained the same for control and BCL-2 overexpressing mice. Further work by the same lab found that overexpression of BCL-2 could also delay caspase-1 and caspase-3 activation in SOD1 mutant spinal cord and thus delay disease onset. However, this did not block eventual decline and SOD1-mediated death (Vukosavic *et al.*, 2000). Salubrinal, an ER stress inhibitor that dephosphorylates eIF2α, has been shown to protect motoneuron in SOD1 transgenic mice following intra-peritoneal injection (Saxena *et al.*, 2009). Daily administration of salubrinal was shown to alleviate muscle weakness and increase life span by approx. 30 days. This work demonstrated the cytotoxicity of ER stress in motoneurons with SOD1 mutations.

Motoneuron death is thought to start with dysfunction in the motoneuron but requires further propagation by non-neuronal cells to induced motoneuron death. Accumulation of mutant SOD1 and induction of ER stress in the neuron is thought to act like a switch in surrounding astrocytes and microglia (Appel *et al.*, 2011). Inactive microglia support surrounding neurons by acting as anti-inflammatory mediators and supporting neuroprotection. However increased stress activates microglia through neurotoxic inter-cell signaling and promotes

microglial-mediated release of reactive oxygen species and pro-inflammatory cytokines. The added insult to motoneurons induces cell death typically seen in fALS. Further evidence of a role for other cells in mediating ALS disease progression comes from a study using SOD1 mutant mice where the SOD1 is flanked by LOX sites and can be deleted through cross breeding with mice expressing Cre recombinase under the motoneuron-specific Islet-1 promoter (Boillee et al., 2006a). SOD1 mutant mice that did not express the SOD1 mutant protein in motoneurons were shown to have delayed disease onset and progression, with overall survival extended by 64 days. Therefore other cells must be affected by the mutant protein. Mice with deleted mutant SOD1 specifically in the microglia, expression of Cre recombinase under microglia-specific CD11b promoter, had markedly reduced rates of disease progression even when motoneurons were expressing SOD1. No changes were seen in microglia or astrocyte activation. This suggests a role for non neuronal cell types in driving the later stages of ALS disease progression following the initial motoneuron insult. Indeed in astrocytes the presence of mutant SOD1 has been shown to further aggravate motoneuron loss and contribute to disease progression (Julien, 2007).

1.4.2 Roles for miRNAs

Due to their abundance and wide-ranging targets, miRNAs have been investigated as possible therapeutic strategies in combating many diseases including ALS (Junn and Mouradian, 2012). Defects in RNA metabolism have been involved in the pathogenesis of ALS with miRNA-mediated post-transcriptional gene regulation controlling the development and function of neurons (Haramati *et al.*, 2010). MicroRNA-206 has been shown to slow disease progression in ALS mouse models by sensing neuronal injury and regenerating neuromuscular synapses (Williams *et al.*, 2009). miR-206 is a skeletal muscle-specific miRNA that is upregulated in mouse models of ALS and enriched in slow twitch muscles in these mice. miR-206 knockout in $SOD1^{G93A}$ mice have accelerated atrophy of skeletal muscles, accelerated disease progression and shorter survival time compared to wildtype $SOD1^{G93A}$ mice. They show that miR-206 functions to regenerate neuromuscular synapses through translational repression of HDAC4. MiR-29a was identified as upregulated in frontal cortex samples from ALS patients. However this result could not be fully validated due to inter-individual variability (Shioya *et al.*, 2010). A study of spleen-expressed miRNAs identified overlap between inflammatory-mediated miRNAs in mouse and human peripheral monocytes during ALS disease progression (Butovsky *et al.*, 2012). Mouse monocytes were shown to be recruited to the spinal cord during disease progression where they increased neuronal loss and aggravated disease pathology. Identification of regulated miRNAs, including miR-29a and miR-376a, that modulate this inflammatory response serves as a biomarker for disease progression and indicates a possible role for miRNA therapeutics in mediating neuron loss in ALS. Although currently there are very few ALS-specific miRNAs identified, the wide ranging pathologies of ALS ensure that a significant role for microRNAs in ALS is not far away.

1.4.3 SOD1 mouse model paradigm

Eleven missense mutations in SOD1 were first reported to be linked to fALS and account for 20% of fALS cases (Rosen, 1993). SOD1 mutant mice have proved invaluable in the effort to understand ALS and the $SOD1^{G93A}$ transgenic mouse is considered the experimental paradigm for fALS as its rate of motor neuron loss and degeneration is comparable to human ALS (Ludolph *et al.*, 2007). It is also an excellent mouse model of ALS that displays all the histopathological characteristics observed in both sporadic and familial ALS. $SOD1^{G93A}$ mice carry a mutation for glycine to alanine at residue 93 on chromosome 12 (Gurney *et al.*, 1994). These mice have disease onset, initial symptoms including fine tremors in hind limb at post natal day (PND) 90, severe paralysis in hind limbs at PND 120 and death ~PND 160. However SOD1 mutant aggregates have been found in motoneurons as early as PND 30, long before initial symptoms are evident (Johnston *et al.*, 2000). Early and significant decline in muscle contractile force and loss of functional motor units in the hind limbs have been noted from PND 40 (Hegedus *et al.*, 2007). Disease phenotypes in this strain include gait and movement defects, accumulation of mutant SOD1 in the brain and spinal cord and progressive loss of spinal motoneurons, spinal interneurons and ascending/descending fibre tracks in the spinal cord. (Acevedo-Arozena *et al.*, 2011). Microarray analysis of changes in gene expression at disease stages in SOD1 mutant mice found down-regulation of genes involved in transcription and mRNA processing with disease onset (Ferraiuolo *et al.*, 2007). At presymptomatic PND 60, motoneurons showed upregulation in genes involved in transcription, carbohydrate metabolism, ATP synthesis, protein folding and protein degradation. At symptom onset PND 90, genes for transcription and translation show alteration in expression with some showing down-regulation. Ultimately at endstage PND 120, there were multiple down-regulated genes involved in transcription and metabolism, down-regulation in genes involved in cellular stress

responses and antioxidant activity and upregulation of gene for protein degradation support increasing evidence of widespread motoneuron stress in SOD1 mutant mice. Other SOD1 mutant models (G85R, G37R) are used and it is thought that these act through similar gain-of-function mechanisms in contributing to disease phenotype (Mulligan and Chakrabartty, 2013). Indeed a mouse model of C9ORF72 is currently under development with Jackson Laboratories in conjunction with John Hopkins University and may prove a vital research tool in delineating the mechanism of ALS disease progression (Cox, 2013).

1.5 Hypothesis / Aim

The hypothesis of this research study is that miR-29a expression alters apoptosis and autophagy in mouse cortical neurons through regulation with its downstream target MCL-1 and that an outcome of this research might be that neuronal cell death has a subsequent effect on neurodegenerative disorders e.g. ALS. Altered expression of miR-29a and MCL-1 has been previously demonstrated in a range of diseases characterised by altered cellular homeostasis and death.

- To investigate the relationship between miR-29a and MCL-1 in primary mouse cortical neurons undergoing ER stress

- To investigate the effects of miR-29a and MCL-1 on autophagy and apoptosis in mouse cortical neurons under conditions of ER stress

- Examine the effects of miR-29a regulation in cortical neurons

- Establish miR-29a expression patterns in SOD1 mutant mice

- Deliver miR-29a antagomirs to the CNS of SOD1 mutant mice and monitor muscle function and lifespan across disease progression

The results of this research study is intended to offer insight into a role for miR-29a in modulating ER stress-induced cell death and possible therapeutic applications of miR-29a modulation in familial ALS.

CHAPTER 2

Methods and Materials

2.1 Chemicals and general reagents

Chemical Name	Catalogue No.	Manufacturer
Hoechst 33342	H21492	Invitrogen
Propidium Iodide	P21493	Invitrogen
Lipofectamine 2000	11668-019	Invitrogen
Protease inhibitor	P2850	Sigma-Aldrich
Pentobarbitone	267543	Vetoquinol
PBS tablets	79382	Fluka
Bovine Serum Albumin	BPE9700	Fisher Scientific
Trypsin inhibitor	T6522	Sigma-Aldrich
DMSO	D8418	Sigma-Aldrich
Poly-D-lysine	81358	Fluka
Mineral Oil – embryo tested	M8410	Sigma-Aldrich
Fluorsave reagent	345789	Calbiochem
Phosphate buffered saline	17-516Q	Lonza
Jung Tissue Freezing Medium	14020108926	Leica Microsystems
Albumin Standard	23209	Thermo Scientific
Artificial cerebrospinal fluid	597316	Harvard Apparatus

Fetal calf serum (FCS), fetal bovine serum (FBS), horse serum (HS), B27 supplement, minimal essential medium (MEM), Dulbecco's modified Eagles medium (DMEM), neurobasal medium (NBM), earles balanced salt solution (EBSS), opti-MEM and Lipofectamine 2000 were from Invitrogen (Paisley, United Kingdom). Other chemicals, including penicillin/streptomycin, bovine serum albumin (BSA), phosphate buffered salts (PBS), hanks balanced salt solution, Trypsin-EDTA,

Poly-D-lysine, embryo-tested mineral oil, Hoechst 33258, propidium iodide came from Sigma-Aldrich (Dublin, Ireland). All tissue culture plastics supplied by Sarstedt.

2.2 Drugs

Compound	Solubility	Catalogue No.	Manufacturer
Tunicamycin	DMSO	T7765	Sigma-Aldrich
Rapamycin	DMSO	9904	Cell Signalling
Brefeldin A	EtOH	B7651	Sigma-Aldrich

2.3 Antagomir products

Antagomir product	Solvent	Catalogue no.	Manufacturer
I-mmu-miR-29a LNA oligonucleotide	CSF	500150	Exiqon
I-mmu-29aMMControl LNA oligonucleotide	CSF	500150	Exiqon
hsa-miR-29a LNA inhibitor	water	410173-04	Exiqon
Negative control B LNA inhibitor	water	199005-04	Exiqon
hsa-miR-29a LNA detection probe	water	38467-01	Exiqon
U6 positive control LNA detection probe	water	99002-01	Exiqon
Scrambled-miR LNA detection probe	water	99004-01	Exiqon

2.4 Kits

Kit Name	Catalogue No.	Manufacturer
Willco dish kit	79656	Qiagen
miRNeasy mini kit	217004	Qiagen
MicroBCA Assay kit	23235	Thermo Scientific

2.5 Gene targeted mice

Mouse mating pairs from the background strain C57 BL/6 were procured from Prof. Andreas Strasser at the Walter and Eliza Hall Institute of Medical Research (WEHI), Melbourne. PUMA-deficient mice were also provided from Prof. Andreas Strasser (WEHI, Melbourne, Australia) (Villunger *et al.*, 2003). Several pairs of heterozygous breeding pairs of bax-deficient mice, SOD1 wildtype and $SOD1^{G93A}$ transgenic mice were obtained from The Jackson Laboratory (Bar Harbor, Maine). All mice were maintained in-house. PUMA knockout ($puma^{-/-}$) mice were generated from ES cells that lacked PUMA exons 2 and 3 which encode the PUMA translational start site and the BH3 region respectively. $SOD1^{G93A}$ breeding pairs generated on a C57 BL/6 background were inbred for eight generations in house. $SOD1^{G93A}$ mice were housed, bred and treated in accordance with the "working with ALS mice, preclinical testing and colony management", guidelines developed by The Jackson Laboratories (Leitner, 2009). The $bax^{-/-}$ mice were originally generated on a mixed C57 BL/6x129SV genetic background, using 129SV derived ES cells, but were backcrossed for >12 generations onto the C57 BL/6 background. Wild-type, heterozygote, and gene knockout mice were generated and maintained in house, in the Biological Research Facility. The genotype of $puma^{-/-}$, $SOD1^{G93A}$ transgenic and $bax^{-/-}$ mice was confirmed by a polymerase chain reaction (PCR) with

specific primers. DNA was extracted from tail snips using High Pure PCR Template Preparation Kit (Roche, Sussex, UK) by experienced technicians in the laboratory. Genotyping was performed by an experienced animal technician in house using specific primers as follows:

5'GGACTGTCGCGGGCTAGACCCTCT3' (common)

5'AGGCTGTCCCTGGGGTCATCC3' (wildtype allele-specific)

5'ACCGCGGGCTCCGAGTAG3' (mutant allele specific) for PUMA

The presence of a single 200 bp fragment denotes *puma*$^{+/+}$ and a single 400 bp fragment denotes the deleted allele in *puma*$^{-/-}$ mice.

5' CTAGGCCACAGAATTGAAAGATCT 3'
SOD1 forward primer 0042 (SOD1 transgenic)

5' GTAGGTGGAAATTCTAGCATCATC 3'
SOD1 reverse primer 0043 (SOD1 transgenic)

5' CATCAGCCCTAATCCATCTGA 3'
SOD1 forward primer 0113 (wildtype allele-specific)

5' CGCGACTAACAATCAAAGTGA 3'
SOD1 reverse primer 0114 (wildtype allele-specific)

Transgenic SOD1 samples are identified by the presence of a 236 bp band and the wild type allele determined by the presence of a 324 bp band

5'GTTGACCAGAGTGGCGTAGG3' (common),

5'GAGCTGATCAGAACCATCATG3' (wild type allele-specific) and

5'CCGCTTCCATTGCTCAGCGG3' (mutant allele-specific) for BAX

The presence of a single 304bp fragment denotes *bax*$^{+/+}$ while a single 507bp fragment denotes the deleted allele in *bax*$^{-/-}$ mice.

2.5.1 Ethical approval and animal licence

Ethical approval was received for this project from the RCSI Research Ethics Committee. Ref: REC593bbb and REC447bbb. A licence was obtained from the Irish Government so that procedures to isolate embryonic mouse cortex could be legally carried out. This was granted under the Cruelty to Animals Act, 1976. Ref: B100/4344. A record of sacrificed animals was kept and annual reports were submitted to the Department of Health and Children.

2.6 Preparation of mouse neocortical neuron cultures

Mouse cortical neurons were isolated from C57 BL/6 embryonic day 16 pups and prepared as described previously (Concannon *et al.*, 2008). Briefly embryos (E15–17) were isolated from inbred wildtype, *bax*$^{-/-}$ and *puma*$^{-/-}$ C57 BL/6 mouse embryos by hysterectomy of the uterus. Lethal anaesthesia was applied using an abdominal injection of 40 mg/kg of pentobarbital (Dolethal) prior to hysterectomy. Pinch-reflex was used to determine anaesthesia in the mice.

The embryos were transferred to a dissection medium (1x PBS (137 mM NaCL, 2.7 mM KCL, 10mM Na_2HPO_4 and 2mM KH_2PO_4), 15mM glucose and 45mM bovine serum albumin) on ice. The embryos were decapitated and the cerebral cortices from each of the embryos were isolated, the surrounding meninges were removed and the cortical tissue was pooled in sterile dissection media on ice. Two different types of media were used during culture. Firstly, a plating media (MEM (-Glu) supplemented with 2.5% fetal bovine serum (FBS), 2.5% horse serum (HS), 100 µg/ml penicillin/streptomycin (P/S), 2 mM glutamine (Q) and 15 mM D-glucose) that contained growth factors and serum to help neurons survive following dissociation and initial plating. Secondly, a feeding medium (neurobasal media supplemented with 100 µg/ml P/S, 2 mM Q and 10% v/v B27) was used to support survival while inhibiting proliferation of glia.

The embryo was held face forward with a tweezers. A single incision was made at a 60 degree angle from the front of the embryo, cutting just behind the eyes. This incision completely removed the front portion of the head. The whole cerebrum was then isolated from the head using strokes of the tweezers along the top of the head of the embryo from the back moving forward. The cortex and midbrain were then cut away from the rest of the brain. Each cortex was cut away from the

midbrain and the meninges (three distinct connective tissue membranes that enclose and protect the CNS) were removed.The tissue from all the embryos was then pooled in a 15 mL tube containing ice-cold dissection buffer.

The tissue was incubated with trypsin (0.125 mg/ml) at 37°C for 15 min. The tube was inverted every 5 mins during incubation. Plating media (20 mL) containing serum was used to stop the reaction. The tube was then centrifuged at 1500 rpm for 3 minutes to pellet the cells. The medium was aspirated and 5 mL of fresh plating medium was added. The neurons were dissociated from tissue by gentle pipetting. The neurons were resuspended in 20–40 mL plating medium (approx. 5 mL per embryo) and the medium passed through a 40 µm filter. The cells were counted using a haemocytometer, plated 2 x 10^5 cells per cm^2 on poly-D-lysine-coated plates, and then incubated at 37°C, 5% CO_2. The following day, the cells were washed twice with DMEM to remove adherent cells. The plating medium was exchanged with 50% feeding medium, 50% plating medium supplemented with mitotic inhibitor cytosine arabinofuranoside (600 nM) added. Two days later, the medium was exchanged again for feeding medium alone. Experiments were carried out on days *in vitro* (DIV) 7 to 10. All multiwell plates and wilco dishes were precoated with poly-D-lysine matrix to aid the adhesion of neurons. Poly-D-lysine was made up in sterile water to a final concentration of 5 µg/mL. Two mL of this was added to each well of a 6 well plate, 500 µL to each well of a 24 well plate and 1 mL to each willco. These were then incubated at 37°C for 1 hour. After 1 hour, the solution was aspirated and each well washed three times with sterile water.

2.7 MEF cell culture and infection

Mcl-1$^{flox/flox}$ mouse embryonic fibroblasts (MEFs) were provided as a gift from Ruth Slack lab, Ottawa, Canada and were cultured in DMEM supplemented with 10% fetal bovine serum. Cells were plated 2.5x10^5 cells per well of 6 well plate and were passaged every 2 days. Infections with an adenoviral vector coding for myc-tagged MCL-1 were carried out as described (MOI 100) (Germain *et al.*, 2011). Briefly, media was aspirated from all wells of a 6 well plate. One mL trypsin was added per well and the plate was incubated at 37°C for 1-2 minutes. Following this incubation, 1 mL DMEM supplemented with 10% fetal bovine serum was added to each well to inhibit the trypsinisation. Cells were removed from the well by gentle pipetting. An appropriate volume of cell suspension to give 1.5 x 10^6 cells was added to a 15 mL falcon tube containing 10 mL DMEM and Cre adenovirus, MCL-1 overexpression adenovirus or LacZ control adenovirus to an MOI of 100. One mL of this solution was added to each well of a 6 well plate already containing 2 mL DMEM per well. For induction of ER stress, cells were treated with DMSO or 200 nM tunicamycin for the indicated time. Following this, cells were collected and lysed for total protein as described Pg 62 (2.12.1 Sample preparation).

Adenovirus concentration:

$$\text{MOI} = \text{viral particles/mL}$$

$$\frac{\text{Cell number} \times \text{MOI} \times 1000}{\text{Viral titre (mL)}}$$

2.8 Plasmid vector and transfection

For overexpression of MCL-1, cortical neurons were transfected with a pCMV6-MCL-1 overexpression vector (MC200829; OriGene, Maryland, USA) or pcDNA3.1 control empty vector (V790-20; Invitrogen, Paisley, United Kingdom). For inhibition of MCL-1, cells were transfected with a vector expressing shRNA targeting MCL-1 (SCHLING-Nm_008562; Sigma-Aldrich, Dublin, Ireland) or a scrambled control vector (SHC001; Sigma-Aldrich, Dublin, Ireland). A plasmid with enhanced GFP (eGFP-N1; Clontech (Unitech), Dublin, Ireland) was cotransfected to allow the identification of transfected neurons for cell death assays. For regulation of miR-29a expression LNA oligonucleotide miR-29a specific antagomir (hsa-miR29a, 410173-04, Exiqon, Vedbaek, Denmark) or scrambled miRNA control (negative control B, 199005-04, Exiqon) was used.

Table 2.1: Plasmid vector information

Vector	Backbone	Promoter	Resistance Gene	Supplier
pCMV6-MCL-1 overexpression	pCMV6	CMV	Kanamycin, Neomycin	Origene
pcDNA3.1 control empty vector	pcDNA3.1	CMV	Kanamycin, Ampicillin, Neomycin	Invitrogen
MCL-*1* shRNA	pLK0.1	hPGK	Puromycin	Sigma-Aldrich
pLK0.1 control empty vector	pLK0.1	hPGK	Puromycin	Sigma-Aldrich
pEGFP-N1	pEGFP-N1	CMV	Kanamycin Neomycin	Clontech

Primary cortical neurons were transfected using Lipofectamine 2000 (Invitrogen) according to manufacturer instructions. Cortical neuron cultures were transfected on DIV 6-8. 2.5 µg DNA or an equivalent volume of scrambled/miR29a antagomir to make 50 nM final concentration per well that was mixed with 10 µL of lipofectamine 2000 and incubated for 20 minutes in 500 µL opti-MEM. The culture media in the cortical neuron culture in 24 well plates was exchanged for 300 µL opti-MEM and in 6 well plates for 1 ml opti-MEM. Conditioned mediium was collected in tubes for replacement following transfection. Approximately 40 µL of DNA-lipofectamine solution was added to each well and the plates were incubated for 45 minutes at 37°C, 5% CO_2. Following the incubation, the opti-MEM was aspirated off and 500 µL conditioned media was replaced into each well and the plates returned to the incubator at 37°C. Tranfection period was 24 – 72 hr as stated. Neurons were treated 72 h post-transfection with tunicamycin (3 µM) or DMSO for 24 h. Cells were stained with Hoechst 33258 stain (1 µg/ml) (Sigma-Aldrich) and propidium iodide (1 µg/ml) (Sigma-Aldrich) for 20 minutes and fixed with 4% paraformaldehyde.

2.9 Cell death analysis

Hoechst 33258 staining was used to assess cell death in primary cortical neurons and MEFs. Hoechst 33258 is a *bis*-benzimide fluorescent dye that stains DNA, specifically the condensed, fragmented chromatin in apoptotic cells, more brightly that the chromatin in healthy cells. Primary cortical neurons cultured in 24 well plates were stained with Hoechst 33258 (Sigma-Aldrich) at a final concentration of 1 µg/mL. Following 20 minute incubation time at 37°C, nuclear morphology was assessed using an Eclipse TE 300 inverted microscope (Nikon Düsseldorf, Germany) with 20 x 0.43 NA phase contrast objective using the appropriate filter set for Hoechst and a charge-coupled camera (SPOT RT SE 6, Diagnostics Instruments, Sterling Heights, MI). All experiments were performed in three

separate culture wells. Images of nuclei were captured in three subfields containing ~300-400 neurons each and each result is the combination of three independent cultures. Images were processed using NIH ImageJ (Wayne Rasband, National Institute of Health, Bethesda, MD). The bright and condensed nuclei were counted as apoptotic and expressed relative to the total number of nuclei.

2.10 Microscopy

2.10.1 Dissecting microscopes

Dissecting microscopes were used in the lab in the preparation of mouse cortical neurons. The dissection microscope allows low magnification of three dimensional specimens (objects too large for the compound microscope). There are two types of illumination for these microscopes: an external light source can be used to illuminate the object by shining light directly on the object; alternatively, the microscope can have an internal light built into the base of the stage. A range of magnification for these microscopes is typically from 10 to 40 times magnification. Two dissection microscopes were used in this project: the Olympus SZ51 and the Meiji Techno EMZ.

2.10.2 Fluorescent microscopy

Fluorescent microscopy utilises the phenomenon of fluorescence and is an essential tool in biology. Fluorescent microscopy was used in this study to quantify cell death using Hoechst 33258 and propidium iodide staining of nuclear chromatin. The use of multiple fluorescent labelled molecules allows the simultaneous identification of multiple different probes. The basic function of a fluorescence microscope is to excite the sample with a desired and specific wavelength (excitation light) which is absorbed by the fluorophore, and then to emit a longer wavelength from the excitation light. The weaker emitted light should reach the eye or detector and the detection limit generally depends on the darkness of the background. The excitation for the sample is usually provided by a high energy Mercury (HBO) or Xenon (XBO) lamp which emits ultraviolet light optimally between 400-700 nm. Hoechst 33258 is excited by ultraviolet light at ~350 nm and emits blue fluorescence close to the maximum emission at 461 nm. Propidium iodide (PI) is excited at ~493 nm and emits red fluorescence at ~630 nm. Spot imaging software (Diagnostics Instruments) was used to capture images which were saved as TIFF files.

2.11 miRNA and gene expression analysis

2.11.1 Isolation of microRNA

Total RNA enriched for microRNA fractions was extracted using the miRNeasy mini kit (Qiagen). Cortical neurons seeded at 1.4 million cells/well in 6 well plates were harvested mechanically by gentle pipetting from each well and the medium containing cells for each time point/treatment was pooled and collected in a 1.5 mL eppendorf tube. The tubes were centrifuged at 2300 xg for 3 minutes and the supernatant was aspirated and discarded. Pellets were stored at –80°C until use or were treated with 700 µL QIAzol lysis reagent and incubated at room temperature for 5 minutes. Alternatively, tissue samples from mice perfused with 1X PBS were thawed on ice, lysed in 700 µL trizol as directed per kit instruction and homogenised using a tissue homogeniser (Ultra turrax t25 basic, IKA Werke, Germany) at 30000 rpm until tissue is fully homogenised. Following homogenisation of the tissue, RNA extraction was continued as per manufacturer protocols. Following incubation, 140 µL chloroform was added to each tube, the caps were replaced securely and tubes were shaken vigorously for 15 seconds. Tubes were again incubated for 2-3 minutes at room temperature and were then centrifuged for 15 minutes at 16000 xg at 4°C. Following centrifugation, the solution separates into 3 distinct phases – an upper clear phase, a middle white layer and a bottom pink layer. The clear upper aqueous phase was collected and placed in a new eppendorf. Approximately 1.5 volumes (~525 µL) of 100% ethanol was added to each tube and mixed thoroughly by pipetting. RNeasy mini spin columns were labeled and 700 µL of each sample was pitted into the spin columns. RNeasy mini columns contain a silica-membrane capable of binding 100 µg RNA using a high-salt buffer spin system. Tubes were centrifuged at 7500 xg for 15 seconds and the flow-through was discarded. This step was repeated for any remaining sample in the eppendorf. Following this, the column was

washed in buffer RWT (700 µL) and centrifuged again at 7500 xg for 15 seconds with the flow-through again discarded. Two additional washes were made with addition of 500 µL of RPE buffer to the RNeasy spin column and centrifuged for 2 minutes at 7500 xg. RNeasy column was placed in a new collection tube and centrifuged at 16000 xg for 1 minute to allow drying of the spin column membrane and to ensure no ethanol was left over during RNA elution from the column. The RNeasy mini spin column was placed in a labeled eppendorf tube and 30-50 µL of DNase RNase-free water was directly pipetted on to the centre of the column. This was spun down for 1 minute at 7500 xg. Total RNA was quantified as below and stored at -80°C.

2.11.2 Quantification of isolated microRNA enriched total RNA

RNA was quantified using NanoDrop 2000 spectrophotometer (Thermo Scientific). The upper and lower optical surfaces of the spectrophotometer were cleaned and 1 µl of sterile water was loaded onto the lower optical surface. The sampling arm was closed and blank measurement was initiated selecting the nucleic acids module in the NanoDrop software. Once the blank was complete, both optical surfaces were wiped clean with a common laboratory wipe. One µL of RNA sample was then loaded and measured. When all measurements were complete, the samples were stored at -80 °C. All measurements are automatically normalised to 340 nm. The software automatically calculates the nucleic acid concentration by choosing the appropriate constant for the measurements. The ratio of absorbance 260/absorbance 280 nm is used to assess the purity of DNA and RNA.

2.11.3 cDNA synthesis

cDNA synthesis for miRNA:

cDNA synthesis was performed using the Taqman microRNA reverse transcription kit (Applied Biosystems) and primer sets specific for the microRNAs of interest (miR-29a, miR-193a, miR-148a and miR-376a), microRNA control (RNU19) or the gene of interest (*Mcl-1, β-actin*). For taqman reverse transcription, total RNA was pipetted into PCR tubes to make 1 µg total RNA and this volume was brought up to 5 µL with DNase RNase-free water. Three µL of the appropriate primer was added to each tube. The reverse transcription master mix (per sample: 75 nM dNTP mix, 50 U multiscribe RT enzyme, 1x RT buffer, 3.8 U RNase inhibitor) was made up to 7 µL in RNase free water and added to each tube (Final total volume 15 µL).

cDNA synthesis for mRNA:

First strand cDNA synthesis was performed with 1 ug total RNA and Superscript II reverse transcriptase (invitrogen) primed with 50 pmol of random hexamers. Between step 2 and step 3 of the gene specific thermocycler program, master mix (5 x first strand buffer, 0.1 mM DTT, 10 mM dNTP, 1 µl RNAseOUT and 1 µl superscript II) was added to each sample and the cycle program was resumed. An extra sample without reverse transcriptase was made up as a control for any genomic DNA contamination

The samples were placed in a thermocycler and run as described below. Samples were stored at–20°C until use.

MicroRNA Thermocycler program	**Gene specific Thermocycler program**
1. 16°C for 30 minutes	1. 65°C for 5 minutes
2. 42°C for 30 minutes	2. 4°C for 1 minute
3. 85°C for 5 minutes	Master mix addition
4. 4°C for 1 minute	3. 25°C for 10 minutes
	4. 42°C for 50 minutes
	5. 70°C for 15 minutes

2.11.4 Real Time quantitative PCR (RT-qPCR)

Real time quantitative PCR was performed using the LightCycler 2.0 (Roche Diagnostics, Basel, Switzerland) and the Taqman Universal PCR Master mix (no AmpErase®) (Applied Biosystems, Paisley, United Kingdom) or QuantiTech SYBR green PCR kit (Qiagen, Hilden, Germany) as per manufacturers protocols. For each sample, 1.33 µL cDNA was added directly into the capillary (Roche) with 1 µL Real Time primer (Applied Biosystems), 10 µL Taqman Universal PCR mastermix and 7.76 µL DNase RNase-free water (Final volume in capillary 20 µL). SYBR green master mix was prepared and composed of 10 µl SYBR green, 7 µL RNase free water, 10 µM forward primer and 10 µM reverse primer and combined with 2 µl cDNA. Samples were repeated in triplicates. The samples were centrifuged at 3000 rpm for 15 sec to draw the entire master mix down into the capillary. Samples were run on a Lightcycler 2.0 (Roche, Basel, Switzerland).

Light Cycler Program

MicroRNA	**Gene**
1. 50°C for 2 minutes 95°C for 10 minutes (Denaturation)	1. 95°C for 15 minutes
2. 95°C for 15 seconds 60°C for 1 minute 72°C for 1 second (Amplification) 65°C for 15 seconds (Melting Curve)	2. 94°C for 15 seconds 59°C for 20 seconds 72°C for 20 seconds
3. 40°C for 30 seconds (Cooling)	3. 65°C for 15 seconds 4. 40°C for 30 seconds

Ct values were calculated using Lightcycler 4.0 software with all samples normalized to reference target RNU19, a non-coding small nuclear ribonucleic acid. miR-29a n-fold expression was calculated from ΔCt analysis in Microsoft Excel.

Table 2.2: Taqman probe (Applied Biosystems) sequence

Probe	Sequence
miR-29a	5'-UAGCACCAUCUGAAAUCGGUU-3'
miR-193a	5'-UGGGUCUUUGCGGGCGAGAUGA-3'
miR-148a	5'-UCAGUGCACUACAGAACUUUGU-3'
miR-376a	5'-AUCAUAGAGGAAAAUCCACGU-3'
U19	5'-TTGCACCTCTGAGAGTGGAATGACTC CTGTGGAGTTGATCCTAGTCTGGGTGCAAACAATT-3'

Table 2.3: Primer sequences

Gene	Sense primer	Antisense primer
Mcl-1	5'-GCTCCGGAAACTGGACATTA-3'	5'-GTCCCGTTTCGTCCTTACAA-3'
β-Actin	5'-AGCCATCCAGGCTGTGTTGT-3'	5'-CAGCTGTGGTGGTGAAGCTG-3'

2.12 Western blotting

2.12.1 Sample preparation

Cells were harvested at specific time points from 6 well plates following an appropriate treatment. Two wells of a 6 well plate plated at 1.4 million cells per well gave approximately enough protein for 4-6 western blots (30 µg per time point). Cells were harvested mechanically by gentle pipetting from each well and the media containing cells for each time point was pooled and collected in a 1.5 mL eppendorf tube. The tubes were centrifuged at 2300 xg for 3 minutes to pellet the cells. Supernatant was aspirated and discarded. The cell pellet was resuspended in 100 µL of Radio immune precipitation assay (RIPA) lysis buffer (150 mM NaCl, 1% NP40, 1% sodium deoxycholate, 0.1% SDS and 25 mM Tris-HCL, pH 7.6) containing protease and phosphatase inhibitors and samples were left on ice for 10 minutes to facilitate lysis and release of cytoplasmic contents from the cell. This was then centrifuged at 16000 xg for 10 minutes. Supernatant was collected and stored at -80°C.

2.12.2 MicroBCA method of protein quantification

To measure the total protein in each lysate, a protein quantification kit (Thermo Scientific) containing Reagent A, Reagent B, Reagent C and a 2 mg/mL BSA standard was used. The protein assay was carried out in a clear flat-bottomed 96 well plate. Samples were measured in triplicate and BSA standard curve was measured in triplicate. Reagents A, B and C were mixed in the ratio 25:25:1 (V:V:V) up to a volume required for 150 µL per sample plus standard curve, (0-5 µg BSA). One hundred and fifty microlitres of Reagent A, B, C mix and 150 µL of 0.9% NaCl was added to each well, plus 2 µL of sample or appropriate volume of standard. The plate was left in the dark for 30

min. Following this incubation, the absorbance was measured using a plate reader at 560 nm of absorbance. The average value of the blank (0 µg BSA) was subtracted from the average values of BSA standard. The resulting values were plotted and the slope of the regression line determined. The average sample absorbance was extrapolated against this curve and the concentration of the protein determined. A Microsoft Excel template was used for subsequent extrapolation and quantification of numerous samples. Protein samples for western blot were made up to 20 µg protein in "laemmli" buffer (68 mM Tris-Cl, pH 6.8, 10% SDS, 30% glycerol, 5% β-mercaptoethanol, 0.012% bromophenol blue) (6x made up to 1x with sample). The samples were boiled at 95 °C for 5-10 min before being loaded into the gel wells.

Table 2.4: Stacking gel composition

Stacking gel (3 mL)		
Gel percentage	**5%**	**Units**
H_20	2.1	mL
30% Mix-acrylamide	500	µL
1.0 M Tris-HCl (pH 6.8)	380	µL
10% SDS	30	µL
10% APS	30	µL
TEMED	7	µL

Table 2.5: Resolving Gel composition

Resolving gel (5 mL)				
Gel percentage	10%	12%	15%	Units
H_20	1.9	1.6	1.1	mL
30% *bis*-/acrylamide mix	1.7	2.0	2.5	mL
1.5 M Tris-HCl (pH 8.8)	1.3	1.3	1.3	mL
10% SDS	50	50	50	µL
10% APS	50	50	50	µL
TEMED	5	5	5	µL

A Mini-PROTEAN Tetra Electrophoresis System from BioRAD was used to prepare the gels. Glass plates, 1 mm or 1.5 mm, were washed first with water and then with 70% ethanol and assembled in the glass plate assembly kit provided. The assembly was arranged so as to cast a gel 1.5 mm in width, 8 cm x 8 cm in length and breadth. Water was added to the cast up to the top and left for 10 min to test for leakage. If leakage occurred, the plates were set again. Resolving gel (5-8 mL) was poured between the plates until the gel was approximately 2-3 cm from the top. Isopropanol was added to the top of the gel (preventing the gel from drying out). The gel was left to set until polymerized (approx 20 min). Following this, the isopropanol was removed by tipping the whole system on its side and decanting out the isopropanol. Any residual alcohol was removed using tissue or piece of Whatman filter paper. The remaining 2-4 cm gap in the gel was then filled with stacking gel and a 10 well-comb was inserted. The gel was then left to set.

2.12.3 Sodium Dodecyl Sulfate Polyacrylamide Gel Electrophoresis (SDS-PAGE)

Gels were loaded into the BioRAD electrophoresis system which comprises a mounting hold unit and two electrodes at either end. The anode (+ electrode) was connected to the bottom chamber and the cathode (- electrode) to the top chamber. The negatively-charged proteins migrate downwards toward the anode. Proteins were denatured for 10 mins at 95°C in the presence of "laemmli" buffer. SDS binds to the protein and confers a uniform negative charge across all the proteins. Electrophoresis buffer (25 mM Tris-Cl, pH 8.3, 250 mM glycine and 0.1% SDS) was added to completely fill the inner chamber of the BioRad mounting system holding the gels. The denatured protein samples (20 µg) were loaded onto the gel along with four microliters of protein marker (PageRuler, Fermentas, Germany) to the first lane to determine migration. The remaining electrophoresis buffer was added to the rig. The gels were initially run at 80 V to drive the samples through the stacking gel and then increased to 120 V through the resolving gel. Following gel electrophoresis, the proteins were blotted onto a nitrocellulose membrane using semi-dry transfer method.

2.12.4 Semi-dry transfer

Filter paper and nitrocellulose membranes (Protran™) were cut to the same size as each gel being transferred. The nitrocellulose membranes were activated for 5 mins in deionised water and then placed in transfer buffer (25 mM Tris, 192 mM Glycine, 20% methanol (v/v) and adjusted to pH 8.3). Filter paper was soaked in transfer buffer also prior to application on the BioRad transfer system. The top (cathode electrode) and bottom (anode electrode) of the transfer unit was cleaned with 70% ethanol prior to use. Filter paper was placed

directly on the anode connected plate and an activated membrane was placed on top of the filter paper. The gel was removed from the electrophoresis system and the stacking gel was discarded before placing the resolving gel on top of the nitrocellulose membrane. Caution was taken to avoid air bubbles between the gel and the membrane. This was followed by two more pieces of filter paper on top of the gel, the lid was placed back onto the rig and the transfer system was connected to a power pack. The transfer was run at a constant voltage of 18 V for ~90 minutes. Following completion of the transfer, membranes were rinsed in TBS-T (15 mM Tris-HCl, 200 mM NaCl, pH 6.8 and 0.1% Tween-20. Immersion in Ponceau Red (1% Ponceau S in 5% acetic acid), diluted 1:10 in dH_20, was used to check the success of the transfer and even protein loading across the lanes. The membranes were washed in TBS-T to remove all traces of Ponceau Red and blocked for 1-2 hours in 4% low fat milk in TBS-T.

2.12.5 Immunoblotting

The primary antibody was made up in blocking buffer according to the manufacturer instructions. Normally these were in the range of 1/200 – 1/1000 dilutions. Each membrane was incubated in primary antibody overnight at 4°C. After primary incubation overnight, the membrane was washed three times for 5 minutes with TBS-T. Each membrane was incubated for 1 hour on a rocker with its respective secondary antibody labelled with horse radish peroxidase (HRP) diluted 1/2000– 1/10000 in blocking buffer. Following secondary antibody incubation, the membrane was again washed three times for 5 minutes with TBS-T. The HRP signal was activated by rinsing the membrane with 500 µL of chemiluminescent substrate (Millipore, Massachusetts, USA) for 1 minute. The resultant signals were detected and captured with several exposure times using a Fujifilm LAS 4000 digital imaging system. An image of the protein marker was also captured with the white light.

Table 2.6: Antibody dilution

Antibody Name	Clone Information	Catalogue number	Antibody type	Manufacturer	Dilution
KDEL	10C3	ADI-SPA-827	Mouse monoclonal	Stressgen, Victoria, BC, Canada	1:500
CHOP	F-168	Sc-575	Rabbit polyclonal	Santa Cruz, California, USA	1:250
Bcl-w	n/a	AAP-050	Rabbit polyclonal	Stressgen, Victoria, BC, Canada	1:1000
LC3	n/a	NB 100-2220	Rabbit polyclonal	Novus, Oakville, ON, Canada	1:100
MCL-1	n/a	600-401-394S	Rabbit polyclonal	Rockland, Pennsylvania, USA	1:1000
MCL-1	C-2	SC-377487	Mouse monoclonal	Santa Cruz, California, USA	1:1000
Tubulin	n/a	T-3526	Mouse monoclonal	Sigma-Aldrich, Dublin, Ireland	1:10000
Actin	n/a	A2228	Mouse monoclonal	Sigma-Aldrich, Dublin, Ireland	1:10000

2.13 *In vivo* analysis

2.13.1 Perfusion in mice

Perfusion in mice was carried out with PBS to remove blood from tissues of interest or with paraformaldehyde (PFA) to fix all tissues and organs. Placing tissue directly in fixative is effective for small tissue samples but, for larger tissue samples like the brain, perfusion with fixative ensures fixation throughout the whole tissue. Mice were given an intraperitoneal (i.p) injection of sodium pentobarbitone (Dolethal®; Vetoquinol, Buckingham, United Kingdom) (40 mg/kg) and placed back in the cage while the anaesthetic took effect. When animal was unconscious, it was placed on its back on a flat surface and the pinch reflex was used to ensure complete anesthesia. An incision was made in the torso and the ribcage exposed. The ribs and diaphragm were cut away to expose the heart. A 26 gauge needle and syringe filled with 1xPBS or 4% PFA was placed into the left ventricle of the heart and the right atrium was cut at the same time as the intracardial perfusion began. 10-20 mL of PBS or PFA was used to fully perfuse each animal. Following this, the spinal cord was dissected out and then microdissected into thoracic and lumbar section by cutting at the theracolumbar junction which presents as a bulge in the spinal cord. The brain was removed from the skull and microdissected into the cortex, cerebellum and hippocampus using forceps and scalpel. Tissue for *in situ* hybridisation were post-fixed in 4% PFA for 2-3 hrs at room temperature, then transferred into 30% sucrose overnight (until the tissue sank to bottom of cryotube) and finally air dried and mounted in Jung tissue freezing medium (Leica Microsystems, Nussloch, Germany). PBS perfused tissues were snap frozen in cryotubes using liquid nitrogen and stored at -80°C.

2.13.2 *In situ* hybridisation

In situ hybridisation of labelled probes in cells and tissues allows for analysis of spatial and developmental expression of desired target genes. Recently *in situ* probes containing a modified nucleotide termed locked nucleic acid (LNA), a high affinity nucleotide analog, has made it possible to detect mature miRNAs without any loss of signal or stringency issues previously brought about when trying to shorten *in situ* probes (Obernosterer *et al.*, 2007).

Wildtype SOD1 and SOD1^{G93A} transgenic mice were perfused with 4% paraformaldehyde as previously described and lumbar spinal cord was post-fixed in PFA for 4 h and in 30% sucrose for 24 h. Spinal cords were set into Jung tissue freezing medium and fixed to the stage mount of a cryostat (Leica CM1900, Nussloch, Germany). Lumbar spinal cord tissue sections (20 µm) were cryosectioned and mounted on SuperFrost-Plus slides (VWR). Using RNase-free solutions, slides were washed with radioimmunoprecipitation assay (RIPA) buffer (150 mM NaCl, 1% IGEPAL, 0.5% sodium deoxycholate, 0.1% SDS, 1 mM EDTA and 50 mM Tris, pH 8.0), followed by treatment with 0.25% acetic anhydride in 0.1 M triethanolamine, rinsed with 0.1% Tween-20 in PBS and treated with 5 µg/ml proteinase K. Next, slides were rinsed in hybridization buffer (1× saline solution, 50% formamide and 1× Denhardt's solution) for 1 h at 56 °C. The probe to detect miR-29a was the reverse complement to the mature miRNA and was 5′-digoxigenin–labeled, 2′-O, 4′-C methylene bicyclonucleoside monomer–containing oligonucleotide (LNA-modified) (Exiqon, Vedbaek, Denmark). Sections were also labeled using a scrambled control and a U6 positive control (Exiqon, Vedbaek, Denmark). Probes were incubated at a dilution of 1:200 in hybridization buffer overnight at 58°C in a humidified chamber. The following day, sections were washed in FAM buffer (2× saline sodium citrate (SSC) buffer, 50%

formamide and 0.1% Tween 20) for 1 h at 60°C. Sections were then rinsed in B1 buffer (150 mM NaCl, 100 mM maleic acid and 0.4% IGEPAL, pH 7.5) for 1 h at room temperature and B2 buffer (2% blocking reagent and 10% goat serum in B1 buffer) for 30 min. Polyclonal antibodies to digoxigenin (1:1,000, 11093274910, Roche, Basel, Switzerland) were incubated in B2 buffer overnight at 4 °C. The next day, sections were washed in B1 buffer and incubated in B3 buffer (100 mM NaCl, 50 mM $MgCl_2$, 0.025% Tween 20 and 100 mM Trizma, pH 9.5) for 30 min. Then, 200 µl of color substrate solution (nitroblue tetrazolium (50 mg/ml) in 5-bromo-4-chloro-indolyl-phosphatase stock solution (50mg/ml) (Roche, Basel, Switzerland) diluted 1:50 in B3 buffer) was added to each slide until the signal appeared. Slides were then rinsed, mounted with fluorsave mounting medium and covered with a cover slip. Slides were imaged using an Olympus IX 51 (Olympus, Melville, NY, USA) inverted fluorescence microscope.

2.13.3 Cresyl-violet stain for motoneurons

Cresyl-violet stains neurons of the brain and spinal cord. Based on their morphology, motoneurons, large cell body and visible nucleolus, can be identified in the ventral horn of spinal cord sections. Wildtype SOD1 and $SOD1^{G93A}$ transgenic mice were perfused with 4% paraformaldehyde as previously described and lumbar spinal cord was post-fixed in PFA for 4 h and in 30% sucrose for 24 h. Spinal cords were set into Jung tissue freezing medium and fixed to the stage mount of a cryostat (Leica CM1900, Nussloch, Germany) as described previously. Lumbar spinal cord tissue sections (20 µm) were cryo-sectioned and mounted on SuperFrost®-Plus slides (VWR International, Leuven, Belgium). Cresyl-violet solution (0.1%) was prepared at time of experiment. 0.1 g of cresyl-violet acetate (Sigma-Aldrich, Dublin, Ireland) was added to 100 ml distilled water. Approximately 10 drops (0.3 mL) glacial acetic acid (Sigma-Aldrich,

Dublin, Ireland) was added, mixed thoroughly and filtered. Cresyl-violet solution was heated to 60°C for 30 mins prior to staining. Tissue sections on slides were air dried for 5 mins prior to staining. Sections were incubated in 0.1% cresyl-violet solution for 20 mins at 60°C. Following incubation, sections were rinsed in distilled water 3 times for 5 mins. Sections were then serially dehydrated in 70%, 90% and 100% ethanol respectively for 15 seconds. Sections were then incubated in Histoclear (National Diagnostics, Georgia, USA) solution twice for 1 min. Excess histoclear solution was dried off with tissue and slides were mounted in DPX mountant (Sigma-Aldrich, Dublin, Ireland) and a glass coverslip applied. Slides were left to dry overnight in a fume hood and were imaged using an Olympus IX 51 inverted microscope.

2.14 *In vivo* animal model

2.14.1 SOD1^{G93A} trangenic mouse model

As previously stated, SOD1 wildtype and SOD1^{G93A} transgenic mice were obtained from The Jackson Laboratory (Bar Harbor, Maine) and maintained in house. SOD1^{G93A} breeding pairs were generated on a C57 BL/6 background were inbred for eight generations in house. SOD1^{G93A} mice were housed, bred and treated during this study in accordance with the "working with ALS mice, preclinical testing and colony management", guidelines provided by The Jackson Laboratories (Leitner, 2009). All animals for *in vivo* ICV injection were habituated in the Molecular Research Facility (MRF) animal facility 2 days prior to surgical procedure. Animals were housed with littermates in groups no larger than 5 mice per cage. Mice had access to food and water *ad libitum*. Total mice for this study amounted to n=39 mice, n=20 transgenic and n=19 wildtype, all sex-matched and litter-matched. All mice were genotyped prior to removal to the MRF facility. Transgenic and non-transgenic SOD1^{G93A} mice were genotyped by tail snap DNA PCR. Tissue was extracted (2 millimetres) from the tails of 6 week old mice and stored at -20°C until processing. DNA was extracted from tail tissue using the High Pure PCR Template Preparation Kit (Roche) according to the manufacturer instructions by an experienced animal technician in house.

2.14.2 Antagomir preparation

miR-29a antagomir (I-mmu-miR-29a LNA oligonucleotide, 500150) or scrambled control antagomir (I-mmu-29aMMControl LNA oligonucleotide, 500150) (Exiqon) were obtained as freeze-dried samples. Antagomirs were resuspended in a volume of sterile artificial cerebrospinal fluid (CSF) (Harvard Apparatus, Massachusetts, USA) to

yield the desired 0.5 nmol concentration. This volume allowed for a 1.0 nmol dose to be delivered in the 2 µL ICV injection. Artificial CSF is produced to closely match the electrolyte concentrations found in CSF. Antagomirs were aliquoted into 3 µL aliquots to prevent repeated freeze thaw action and stored at -20°C.

2.14.3 Intracerebroventricular injection

Intracerebroventricular (ICV) injection of miR-29a antagomir (or Scrambled control) was carried out on postnatal day (PND 70) wildtype and $SOD1^{G93A}$ transgenic mice raised on a C57 BL/6 background. All animals were initially anaesthetised with 3-5% isoflurane in oxygen (O_2). Following induction, anesthesia was maintained using 1-2% isoflurane in O_2. Animals were placed face down and maintained normothermic (36-38°C) by means of a heat blanket. The head was fixed in a stereotaxic frame with guides inserted in the auditory canals for stabilisation. The skull and surrounding area was prepared with Betadine iodine solution. A midline incision of ~1 cm length was made on the skull and the skin overlying the skull was parted. Following location of bregma, the location of the right lateral ventricle was determined at coordinates: anterior-posterior: -0.3 and mediolateral: +1 compared to the point of bregma. A craniectomy was performed at this position to allow for direct injection to the ventricle. A Hamilton® syringe (Hamilton, Bonaduz, GR, Switzerland) was used to take up the 2 µL volume of scrambled or miR-29a antagomir diluted in CSF at the desired concentration and the injection needle was affixed to the frame. The needle was brought down to the surface of the brain and then brought dorsoventral -2.0 mm into the ventricle. The 2 µL dose was delivered slowly and carefully and the needle removed. The skin around the skull was then sutured closed using a curved needle. Betadine iodine solution was placed over the sutures and the mouse was placed in an incubator with food and water to recover for approx. 20-30 minutes. Following recovery, animals were returned to cages and given food and water *ad*

libitum. Injection occurred once at PND 70 and mice were monitored for a period pertaining to the experiment (10 days to 3 months).

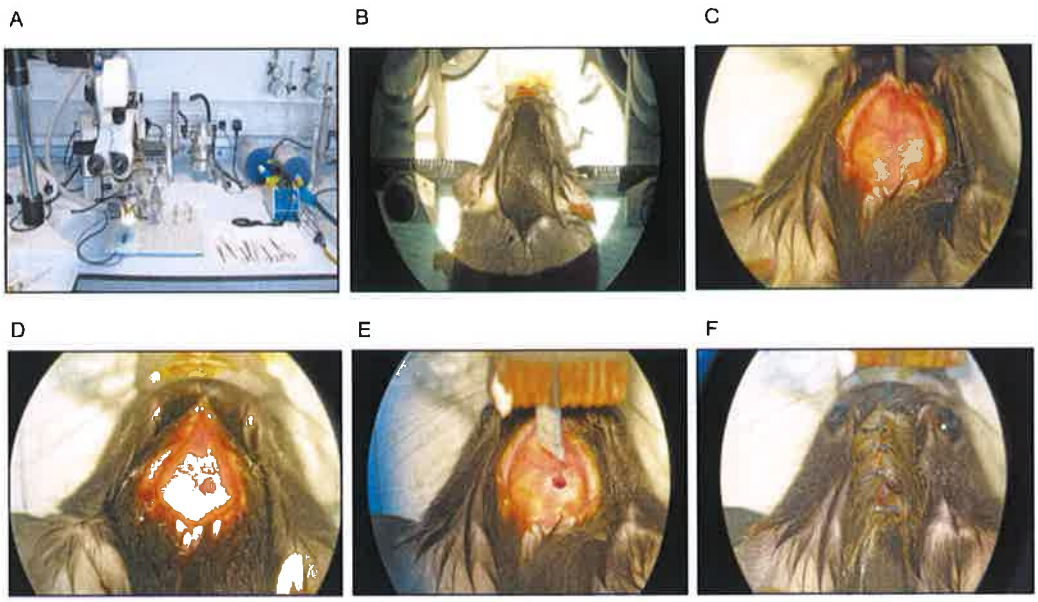

Figure 2.1: Intracerebroventricular injection of wt/SOD1 mice. (A) Working set up of stereotaxic frame, isoflurane administration and surgical utensils used for ICV injection. (B) Mouse head is fixed in the stereotaxic frame using guides in the auditory canals and isoflurane administered through nose piece. (C) Bregma is located and co-ordinates guide the needle to the position of the ventricle. (D) A hole is drilled in the skull to allow access for the needle to the brain surface. (E) The dose of antagomir is delivered through a Hamilton syringe attached to a guide needle that is inserted into the ventricle dorsoventrally. (F) The incision is sutured and swabbed with iodine solution.

2.14.4 Animal Monitoring

Mice were monitored twice daily in the week following surgery to assess any abnormalities in behaviour and to monitor wound healing. Social interactions and ability to climb for food and water were monitored also. Animals were handled as little as possible in this period to minimise stress and to prevent agitation. Povidone-iodine (Betadine®, Connecticut, USA) solution was applied to suture line if necessary.

2.15 Motorfunction analysis

In vivo work looking at ALS disease progression used a $SOD1^{G93A}$ mouse model from Jackson laboratories. $SOD1^{G93A}$ mice experience massive death of motor neurons in the ventral horn of the spinal cord and loss of myelinated axons in ventral motor roots from PND 84 until endstage. Disease onset is determined by peak body weight and characteristics of disease in these mice include hind limb tremor, hind limb paralysis and weight loss. All animals were age, sex and litter matched with n=19 wildtype mice (n=9 males and n=10 females) and n=20 $SOD1^{G93A}$ transgenic mice (n=10 males and n=10 females) used in treatment groups. Motorfunction analysis was assessed from PND 84 while mice were trained for use of motorfunction equipment between PND 77 and PND 84. Each motor function test was recorded three times, in one session, and the best performance used for analysis. Weight recordings, Paw Grip Endurance (PaGE) and stride length measurements were recorded in the same sequence twice weekly by a single observer (Brooks and Dunnett, 2009). Due to the variability of weight measurements at the later stages of disease progression in this study, the loss of righting reflex after 30 seconds was adopted as the standard end point for both the treatment and cross breeding paradigms (Ludolph *et al.*, 2010).

2.15.1 Paw Grip Endurance

Paw Grip Endurance (PaGE) is an accurate and non-invasive method of determining the initial symptoms in the $SOD1^{G93A}$ mouse model of ALS (Weydt *et al.*, 2003). Mice were placed on a mesh wire platform which was gently inverted allowing the mice to hang upside-down. The time period until a mouse released one or both hind limbs was recorded. The cut off time was 60 seconds, each mouse was given

three consecutive trials and the longest latency period was recorded. Onset of motor dysfunction, and the onset of ALS, was considered to be the first of three consecutive PaGE test days in which the mouse failed to reach the cut off time (Kieran *et al.*, 2007).

2.15.2 Weight analysis

Peak body weight analysis was used to determine disease onset in $SOD1^{G93A}$ mice in conjunction with motor dysfunction analysis (Ludolph *et al.*, 2007). Changes in weight were recorded prior to motorfunction tests using a weigh scales; weight was measured in grams (g). The weight inclusion criteria for this study were 25 g and 28 g for $SOD1^{G93A}$ female and male mice respectively. A 20% reduction in weight, the absence of motor function in one or both hind limbs and the loss of righting reflex after 30 seconds coincides with end stage ALS (Kieran *et al.*, 2007).

2.15.3 Stride lengths

Stride length measurements are a clear indicator of disease onset and progression and detect minor changes in gait and hind limb movement. Stride lengths were measured by painting the hind paws of transgenic and wild type mice with non-toxic paint and coaxing them to walk through a tube lined with graph paper. Strides were measured from the mid-stride point of consecutive right-to-right and left-to-left footprints, consisting of at least three step lengths (Knippenberg *et al.*, 2010).

2.16 Statistics

Data are given as mean ± SEM. All data sets were tested for normality using the Kolmogorov-Smirnov test. When normality could not be assumed, statistical significance was assessed using a Kruskal-Wallace test (>2 groups) or a Mann-Whitney U test (2 groups). Normally distributed data was assessed for statistical significance using ANOVA with post-hoc Tukey (>2 groups) or Independent t-tests (2 groups). Mantel-Cox (log rank) test was used to determine statistical significance in Kaplan-Meier survival analysis. P values smaller than 0.05 were considered to be statistically significant as analysed using SPSS statistical analysis software (International Business Machines (IBM)).

CHAPTER 3

Characterisation of the role of miR-29a in a cortical neuron model of ER stress

3.1 Introduction

ER stress occurs in all cellular organisms and can disrupt cellular homeostasis and affect cell survival. Signalling pathways that collectively form the UPR activate downstream mediators that reduce the cellular stress and promote cell survival (Schroder and Kaufman, 2005). Cell survival can also be maintained in part through the cellular recycling capacity of autophagy (Ogata *et al.*, 2006). Uncontrolled or increased levels of ER stress in a cell can lead to increased cell death if the stress is not alleviated. Due to the post-mitotic nature of neurons, maintaining cellular homeostasis is extremely important (Marder and Goaillard, 2006). Loss of neurons is a hallmark of almost all neurodegenerative diseases and can have devastating effects on an organism (Lindholm *et al.*, 2006). Perturbations in cellular ER stress have been implicated as a causative factor in many diseases. In neurodegeneration, unabated ER stress leads to formation of mutant protein aggregates that are seen in the pathogenesis of many neurodegenerative diseases (Matus *et al.*, 2011).

MCL-1 is a key anti-apoptotic member of the BCL-2 family which has been shown to be involved in apoptosis and cell differentiation in a variety of cells. In particular, MCL-1 has been shown to play an important role in differentiation of neuronal precursors and in mediating neurogenesis (Arbour *et al.*, 2008). MCL-1 has also been shown to be an important mediator of apoptosis downstream of ER stress. MCL-1 has been shown to interact with pro-apoptotic BAX downstream of BAX activation and prevent mitochondrial apoptosis in a model of DNA damage (Germain *et al.*, 2008). MCL-1 can also mediate apoptosis through interaction with members of the BH3-only pro-apoptotic proteins in neurons and a variety of other cell types. (Jiang *et al.*, 2008, Germain *et al.*, 2011). MCL-1-mediated antagonisation of both pro-apoptotic BH3-only proteins BIM and NOXA has been shown to mediate neuronal survival (Opferman *et al.*, 2003, Gelinas and White, 2005). Similarly

MCL-1 has been shown to interact with pro-apoptotic BH3 only protein PUMA (Willis and Adams, 2005). PUMA has previously been shown in our lab to be a potent mediator of ER stress-induced apoptosis in neurons (Reimertz *et al.*, 2003). Further work in our lab demonstrated protection of neurons during NMDA-mediated excitotoxicity in neurons overexpressing MCL-1 (Anilkumar *et al.*, 2013).

MicroRNAS have emerged in recent years as key regulators of multiple cellular systems including ER stress and mitochondrial cell death (Maurel and Chevet, 2013). Members of the miR-29 family of microRNAs have previously been implicated in both neurodegenerative diseases such as AD and ALS and in a variety of cancers (Hebert *et al.*, 2008, Shioya *et al.*, 2010). miR-29a has been shown to be involved in modulating dendritic spine morphology and synaptic plasticity (Lippi *et al.*, 2011). Previously in this lab miR-29a expression has been shown to be upregulated in response to ER stress-induced apoptosis (Concannon et al, unpublished data). While members of the miR-29a family have been shown to modulate MCL-1 expression in cells undergoing stress (Mott *et al.*, 2007), work in our lab identified miR-29a binding to the 3' UTR of MCL-1 in a neuroblastoma cell line undergoing ER stress (Concannon et al, unpublished data).

While our lab has already identified a role for miR-29a targeting MCL-1 during ER stress-induced apoptosis in a neuroblastoma cell line, the effect of miR-29a in primary cortical neurons undergoing ER stress has yet to be characterised. We aimed to investigate the differential regulation of miR-29a in cortical neurons undergoing ER stress and, furthermore, to investigate expression of miR-29a downstream target MCL-1. In addition, we aimed to identify the functional significance of miR-29a modulation in primary cortical neurons during tunicamycin-induced ER stress. The work here describes a role for miR-29a targeting MCL-1 in modulating ER stress-induced cell death in murine primary cortical neurons.

3.2 Results

3.2.1 Comparison of miRNA expression in cortical neurons undergoing ER stress

The original Taqman low density array that identified miR-29a as upregulated in SHSY5Y cells during tunicamycin-induced ER stress also identified approximately 13 other significantly regulated miRNAs (Table 1.1). Of these 13 altered miRNAs, we chose to look at comparative expression levels to miR-29a of miR-193a, -376a and -148a, as these were amongst the highest expressed miRNAs and all three had mouse homologues. Primary cortical neurons were treated with DMSO or 3 μM tunicamycin for 8 h, 16 h or 24 h respectively. Tunicamycin is a recognised paradigm for inducing ER stress in mammalian cells. Tunicamycin is an antibiotic which functions to prevent N-linked glycosylation of proteins in the ER and impedes proper protein folding (Chang and Korolev, 1996). Following treatment, cells were lysed, miRNA extracted and RT-qPCR was performed for the relevant miRNAs. We identified all miRNAs as upregulated under tunicamycin-induced cell death in the cortical neurons. However, only miR-29a upregulation reached significance. We identified miR-29a as significantly upregulated at 8 h, 16 h and 24 h tunicamycin treatment compared to DMSO-treated samples. This result and previous data in SHSY5Y neuroblastoma cells confirmed miR-29a as our main miRNA of interest in primary cortical neurons undergoing ER stress.

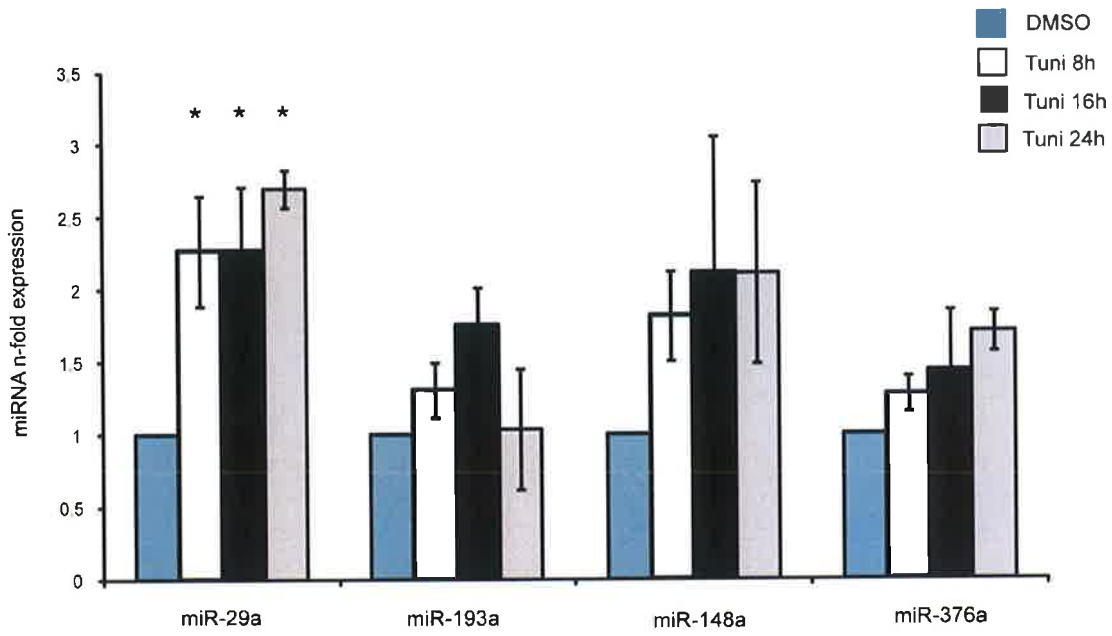

Figure 3.1: miR-29a is significantly upregulated in cortical neurons undergoing tunicamycin-induced ER stress compared to other non-significantly upregulated miRNAs of interest. miR-29a expression in mouse primary cortical neurons following DMSO or 3 μM tunicamycin treatment (8 h, 16 h and 24 h). Expression levels of individual miRNAs were analysed by RT-qPCR and samples were normalized to RNU19 controls and expressed relative to DMSO-treated cultures. Results from n= 3 cultures from three separate experiments. *P<0.05, miR-29a tunicamycin-treated samples compared to DMSO-treated samples (ANOVA, *post hoc*, Tukey).

3.2.2 Tunicamycin-induced ER stress in primary cortical neurons induces miR-29a upregulation and downregulation of anti-apoptotic MCL-1

Having identified miR-29a as significantly upregulated in primary cortical neurons undergoing ER stress, we wanted to further examine miR-29a expression during ER stress. Moreover we wished to validate ER stress induction in the cortical neurons and to examine the expression of the miR-29a proposed target MCL-1. We used tunicamycin-induced ER stress as a platform to analyse expression of miR-29a and its potential downstream target MCL-1 in cortical neurons. Primary cortical neurons were treated with 3 μM tunicamycin for 8, 16 and 24 h timepoints. Control culture received an equal volume of DMSO. Following treatment, miR-29a expression changes were examined using RT-qPCR. miR-29a was shown to be upregulated at 8 h, 16 h and significantly upregulated in cortical neurons at 24 h tunicamycin stimulation (Fig. 3.2A). Validation of ER stress was determined through Western blotting with an increased expression of ER stress markers (GRP78 and CHOP) at 16 h and 24 h respectively. GRP78, an ER chaperone that exists in a transmembrane bound state with the receptors of the UPR, is released into the cytosol during ER stress-induced UPR activation (Lee, 2005). CHOP is an ER stress-inducible protein that regulates apoptosis downstream of ER stress signaling (Ohoka *et al.*, 2007). In parallel, we showed the expression of MCL-1 to be down-regulated at 16 h and 24 h post tunicamycin treatment, time points where miR-29a was shown to be upregulated and increased levels of ER stress markers were evident (Fig. 3.2B). This result suggests a possible role for miR-29a targeting MCL-1 during ER stress in cortical neurons.

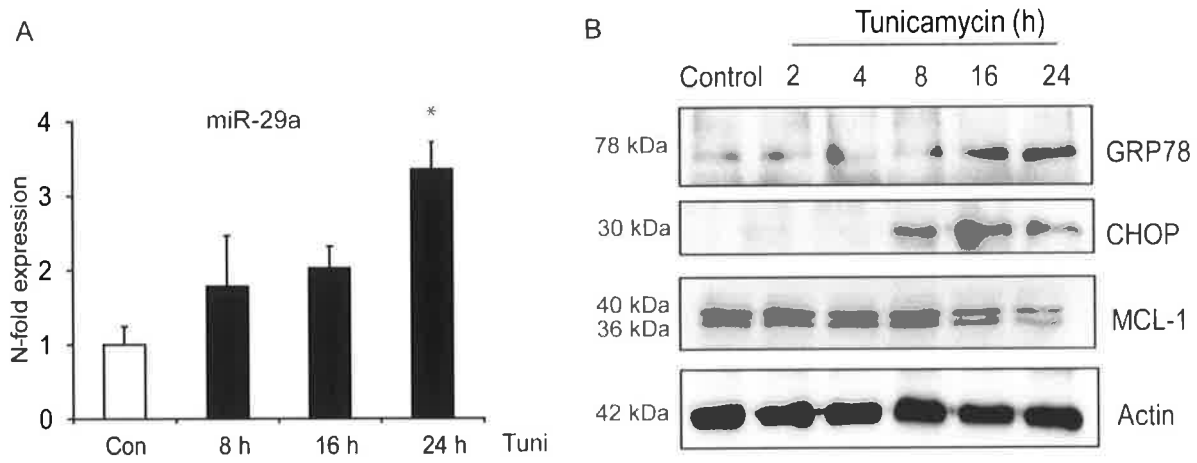

Figure 3.2: Tunicamycin regulates expression of miR-29a and MCL-1 in cortical neurons. (A) Increased expression of miR-29a in primary cortical neurons undergoing tunicamycin-induced cell death. miR-29a expression in mouse primary cortical neurons following DMSO or 3 μM tunicamycin treatment (8 h, 16 h and 24 h) assessed by RT-qPCR. Expression levels were normalized to DMSO control-treated cells and data are represented as means ± SEM from n = 9 cultures from three separate preparations. *P<0.05. (ANOVA, *post hoc*, Tukey). (B) Increased expression of ER stress markers is associated with decreased levels of MCL-1 expression. Whole cell lysates were prepared from primary cortical neurons treated with either DMSO or 3 μM tunicamycin for the indicated time periods (2-24 h). The expression levels of the ER stress markers GRP78 and CHOP and the anti-apoptotic BCL-2 family member, MCL-1 were examined by western blot analysis. Probing with β-Actin served as a loading control. Similar results were obtained in two separate experiments.

3.2.3 Effect of brefeldin A-induced ER stress on miR-29a and MCL-1 levels

We identified miR-29a expression as upregulated under tunicamycin-induced cell death. Consequently we wanted to examine miR-29a expression in another model of ER stress. We chose to look at another drug, brefeldin A, and examine its affect on ER stress in the cortical neurons. Brefeldin A is a commonly used experimental ER stress inducer and functions to inhibit protein transport from the ER to the Golgi apparatus; leading to a build-up of proteins in the ER which induces ER stress (Rao *et al.*, 2002). Primary cortical neurons were treated with 10 μM brefeldin A for 8 h, 16 h and 24 h timepoints. Following treatment, miR-29a expression changes were examined using RT-qPCR. miR-29a expression was shown to be upregulated at 8 h and 16 h brefeldin A treatment compared to EtOH control; however, this upregulation did not reach significance (Fig. 3.3A). Validation of ER stress was determined by an increase in ER stress markers expression (GRP78 and CHOP) at 16 h and 24 h respectively using western blotting. MCL-1 was shown to be down-regulated at 16 h and 24 h post ER stress induction (Fig. 3.3B). Taken together with our tunicamycin data for the cortical neurons (Fig. 3.2), we can see miR-29a upregulation occurs during ER stress-induced apoptosis in cortical neurons. Coinciding with miR-29a upregulation, we saw a decrease in MCL-1 protein level during tunicamycin- and brefeldin A-induced ER stress. This decrease in MCL-1 protein level could be due in part to miR-29a targeting the 3' UTR of MCL-1 and suggests a role for miR-29a in regulating ER stress-induced apoptosis.

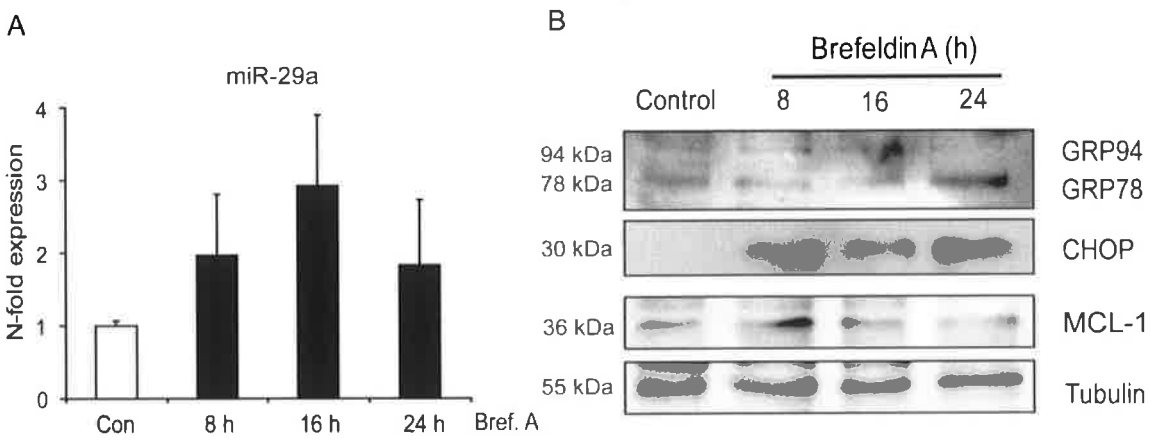

Figure 3.3: A brefeldin A-induced model of ER stress demonstrates changes in miR-29a expression and MCL-1 protein level. (A) miR-29a expression in mouse primary cortical neurons following vehicle (EtOH) or 10 μM brefeldin A treatment (8 h, 16 h and 24 h) as assessed by RT-qPCR. Expression levels were normalized to EtOH control-treated cells. Result from n=6 cultures from two separate experiments. (B) Increased expression of ER stress markers is associated with decreased levels of MCL-1 expression. Whole cell lysates were prepared from primary cortical neurons treated with either EtOH or 10 μM brefeldin A for the indicated time periods (8-24 h). The expression levels of the ER stress markers GRP78, CHOP and MCL-1 were examined by western blot analysis. Probing with β-Actin served as a loading control. Similar results were obtained in one separate experiment.

3.2.4 MCL-1 knockdown in primary cortical neurons sensitises cells to ER stress-induced cell death

Having established a change in MCL-1 expression following ER stress in neurons, we next investigated whether shRNA-mediated knockdown of MCL-1 contributed to neuronal cell death during ER stress-induced apoptosis. shRNA uptake in primary cortical neurons was analysed by fluorescent microscopy after 72 h Lipofectamine 2000 transfection with MCL-1 shRNA/scrambled control shRNA, cotransfection with EGFP plasmid and subsequent treatment with DMSO or tunicamycin (3 μM) for 24 h. Pyknotic nuclei were identified by immunofluorescence analysis of Hoechst 33358 staining and percentage cell death was calculated using ImageJ software (National Institute of Health). Increased cell death was evident in these cells with increased levels of pyknotic nuclei and loss of cells in MCL-1 shRNA transfected cells (Fig. 3.4A). MCL-1 shRNA transfected cortical neurons showed significantly increased sensitivity to cell death. MCL-1 knockdown in DMSO-treated cells was sufficient to significantly increase cell death compared to scrambled transfected cells. This demonstrated the importance of MCL-1 in mediating mitochondrial cell death and maintaining cellular homeostasis in cortical neurons. Furthermore, we identified significantly increased cell death in MCL-1 knockdown cortical neurons during DMSO and tunicamycin treatment compared to scrambled control (Fig. 3.4B). This result demonstrates that MCL-1 knockdown further increases cortical neuron sensitivity to tunicamycin treatment and shows the importance of MCL-1 in protecting cells against ER stress. Levels of pyknotic nuclei in tunicamycin-treated control shRNA was not highly increased compared to DMSO-treated control shRNA which we conclude is due to levels of pyknotic nuclei in DMSO-treated control shRNA being higher than normal and may be due to the culture and preparation of the neurons. Western blot analysis confirms shRNA-mediated knockdown of MCL-1 in NSC34, motoneuron-like cell line (Fig. 3.4C).

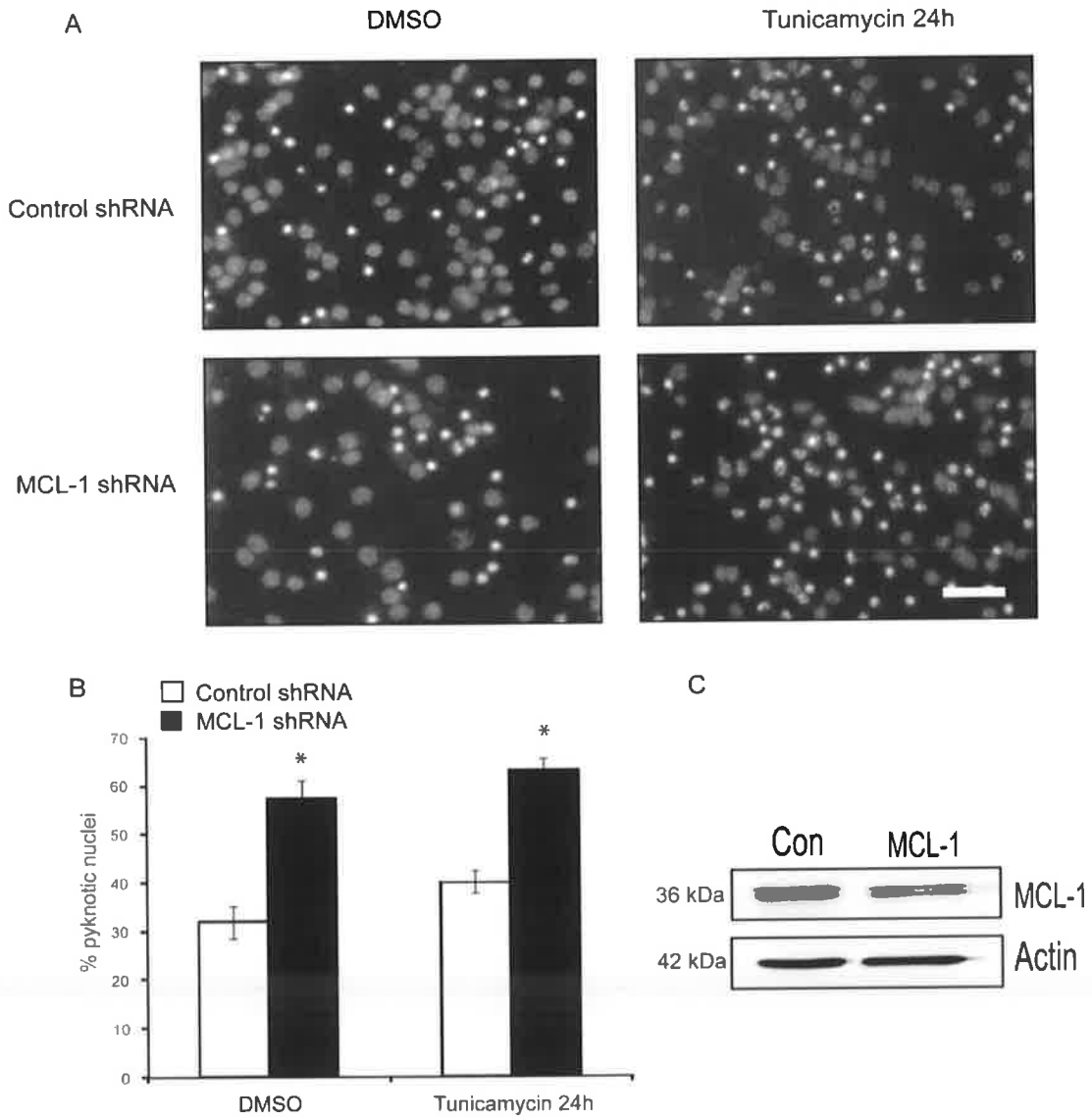

Figure 3.4: MCL-1 knockdown heightens cortical neuron response to tunicamycin-induced cell death. (A) Representative images of primary cortical neurons transfected with MCL-1 shRNA or control shRNA and treated with DMSO or 3 μM tunicamyicn for 24 h. Cells were stained with Hoechst 33358 and imaged using an inverted fluorescent microscope. (B) Effect of *Mcl-1* gene silencing in cortical neurons. ER stress-mediated cell death was analysed in cortical neurons transfected with shRNA against MCL-1 or control shRNA and subsequently treated with DMSO or 3 μM tunicamycin for 24 h. A total of n= 90-120 EGFP positive cells per treatment condition were quantified. Data represented as mean ± SEM from three wells; experiments were repeated two times from independent cultures with similar results. **P*<0.05, differences between MCL-1 shRNA and scramble control transfected neurons. (ANOVA, *post-hoc*, Tukey). (C) Western blot confirmation of MCL-1 knockdown in NSC34 cells transfected with MCL-1 shRNA/ Control shRNA. Reduced levels of MCL-1 48 h after transfection with shRNA were compared to scrambled control shRNA. Probing with β-Actin served as a loading control. Similar results were obtained in two separate experiments. Scale bar = 10 μm.

3.2.5 MCL-1 overexpression protects cortical neurons from ER stress-induced cell death

Previous studies have demonstrated ER stress-induced apoptosis to be mediated by the BH3-only protein PUMA (Reimertz *et al.*, 2003). We chose to investigate the effect of ER stress on cortical neuron apoptosis following modulation of anti-apoptotic MCL-1 and pro-apoptotic PUMA. MCL-1 overexpression was analysed in wildtype or *puma*$^{-/-}$ primary cortical neurons following 72 h Lipofectamine 2000 transfection with MCL-1 overexpression plasmid or pcDNA 3.1 control plasmid, co-transfection with EGFP plasmid and subsequent treatment with DMSO/tunicamycin (3 µM) for 24h. Cells were stained with Hoechst 33358 and percentage cell death was calculated from counts of pyknotic nuclei. *puma*$^{-/-}$ cells showed significant protection against ER stress-induced apoptosis compared to wildtype cells following 24 h tunicamycin treatment. While cell death was not completely inhibited, this result demonstrates the importance of PUMA in mediating ER stress-induced apoptosis and suggests a role for other anti-apoptotic members of the BCL-2 family in mediating ER stress and cell death. In addition, MCL-1 overexpression in *puma*$^{-/-}$ cortical neurons showed significant protection compared to control plasmid expression in *puma*$^{-/-}$ cortical neurons (Fig. 3.5). This result verifies the importance of MCL-1 in protecting cortical neurons against ER stress in the absence of pro-apoptotic PUMA. We saw that MCL-1 overexpression in *puma*$^{-/-}$ cells did not completely protect against ER stress-induced apoptosis suggesting a role for other mechanisms in mediating cell death.

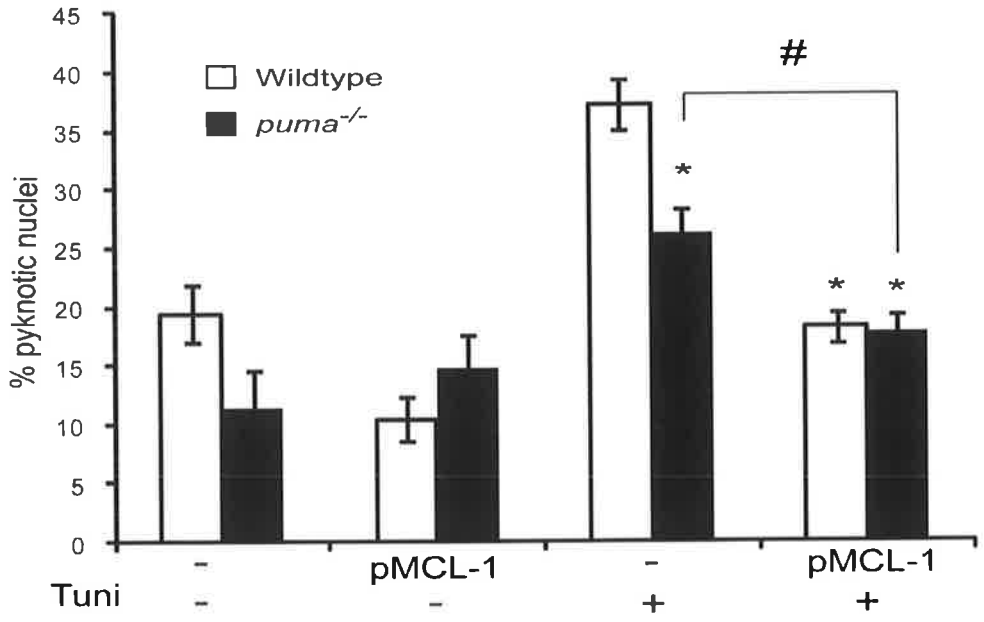

Figure 3.5: Overexpression of MCL-1 in cortical neurons protects against tunicamycin-induced cell death in a PUMA independent manner. *puma*$^{-/-}$ cortical neurons has a protective effect under tunicamycin-induced cell death which is heightened during MCL-1 overexpression. Effect of MCL-1 overexpression was analysed in wildtype and *puma*$^{-/-}$ cortical neurons transfected with MCL-1 overexpression plasmid or pcDNA3.1 control plasmid and subsequently treated with DMSO or 3 μM tunicamycin (24 h). **P*<0.05, compared with *puma*$^{-/-}$ cortical neurons and WT cortical neurons following 24 h tunicamycin treatment. #*P*<0.05, compared with MCL-1 overexpression in *puma*$^{-/-}$ neurons and control plasmids expression in *puma*$^{-/-}$ neurons. Data represented as mean ± SEM from three wells; experiments were repeated two times from independent cultures with similar results. (ANOVA, *post-hoc,* Tukey)

3.2.6 *bax*$^{-/-}$ cortical neurons undergo reduced tunicamycin-induced cell death

In an effort to explore apoptosis further in the cortical neurons, we chose a *bax*$^{-/-}$ mouse model. Wild-type and *bax*$^{-/-}$ cortical neurons were treated with DMSO or 3 µM tunicamycin for 24h. Cells were stained with Hoechst 33358 and propidium iodide to assess morphology and cell death. *bax*$^{-/-}$ cells demonstrated reduced propidium iodide staining compared to wildtype cells during DMSO and 24 h tunicamycin treatment. Propidium iodide stains the cell nucleus when the cell membrane has become permeable in dying cells (Brana *et al.*, 2002). The presence of reduced propidium iodide staining in *bax*$^{-/-}$ cells suggests a cell protective role for loss of BAX during ER stress (Fig. 3.6A). Having identified a protective role for the *bax*$^{-/-}$ model, we next looked at the effect of MCL-1 overexpression in wildtype and *bax*$^{-/-}$ cortical neurons undergoing ER stress. Cultured wildtype and *bax*$^{-/-}$ cortical neurons were transfected with MCL-1 overexpression plasmid/pcDNA3.1 control plasmid and subsequently treated with DMSO or 3 µM tunicamycin for 24h. Hoechst 33358 fluorescent images were acquired to quantify nuclear apoptosis. *bax*$^{-/-}$ cells showed significant protection against ER stress-induced apoptosis compared to wildtype cells following 24 h tunicamycin treatment. However, this protection was not enough to completely abrogate cell death and suggests a BAX-independent pathway mediating neuronal cell death in the absence of BAX. MCL-1 overexpression in *bax*$^{-/-}$ cortical neurons showed significant protection when compared to wildtype cortical neurons undergoing ER stress-induced cell death. Again there was some residual cell death that was not BAX-dependent and suggests a role for BAX-independent cell death in neurons (Fig. 3.6B).

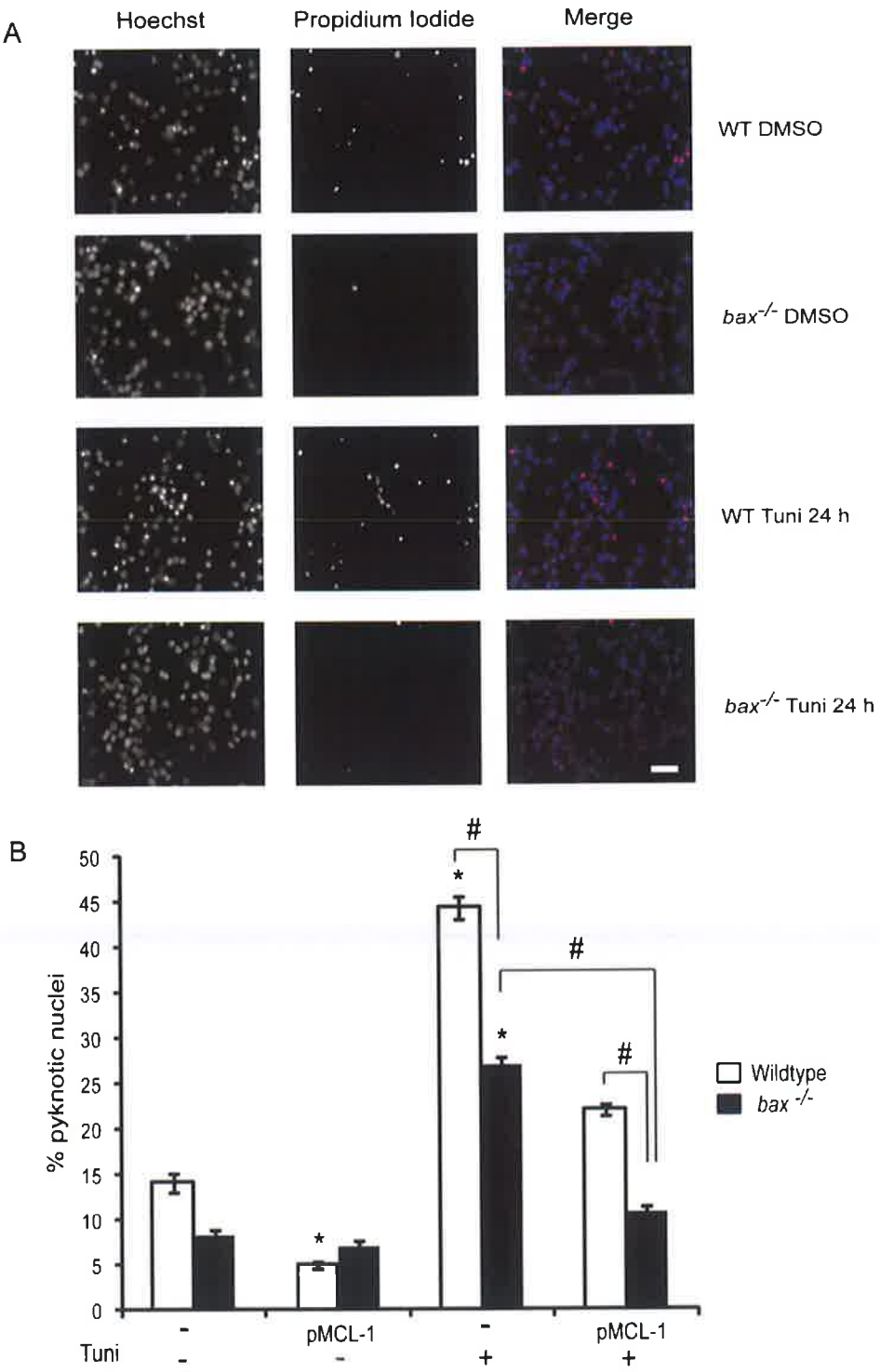

Figure 3.6: *bax*$^{-/-}$ in cortical neurons has a protective effect during tunicamycin-induced cell death. (A) Representative images of WT and *bax*$^{-/-}$ cortical neurons undergoing tunicamycin-induced cell death. Cells were stained with Hoechst 33358 and propidium iodide. Images were analysed at 40x magnification. (B) MCL-1 overexpression protects *bax*$^{-/-}$ cortical neurons from tunicamycin-induced cell death. Cortical neurons are protected from tunicamycin-induced apoptosis in the absence of proapoptotic BAX. Wildtype and *bax*$^{-/-}$ cortical neurons

transfected with MCL-1 overexpression vector or pcDNA3.1 control vector and subsequently treated with DMSO or 3 μM tunicamycin for 24 h. Cells were stained with Hoechst 33358 and propidium iodide and pyknotic nuclei were identified by immunofluorescence. Percentage cell death was calculated using ImageJ software. *P<0.05 compared to control vector DMSO-treated genotype. #P<0.05, between indicated groups. Data represented as mean ± SEM from three wells; experiments were repeated three times from independent cultures with similar results (ANOVA, *post-hoc* Tukey). Scale bar = 50 μm.

3.2.7 Overexpression of MCL-1 downregulates mediators of apoptosis and autophagy

Having identified MCL-1 overexpression as protective in the absence of two key apoptosis mediators, we advanced to look further at the effect of MCL-1 overexpression on apoptosis and another pathway linked to cell death, autophagy. A role for MCL-1 in the control of autophagy has previously been identified in mouse cortical neurons. Deletion of MCL-1 in H1299 cells and cortical neurons from transgenic mice activated a robust autophagic response following cell starvation. Increased expression of punctate LC3 in *Mcl-1*$^{-/-}$ neurons confirmed increased autophagy while increased LC3-II expression in cells infected with adenoviral vectors targeting MCL-1 demonstrates increased autophagic flux and is used as a mark of increased autophagy (Germain *et al.*, 2011).

We chose to look at autophagy induction in *Mcl-1*$^{flox/flox}$ MEFs that underwent ER stress following 200 nM tunicamycin treatment for 16 h or 24 h. The MEFs were infected with an MCL-1 overexpressing adenovirus (Agilent Technologies) or GFP control adenovirus 24 h prior to treatment. Western blot analysis identified two MCL-1 bands: a lower endogenously expressed MCL-1 band and an upper exogenously overexpressed, myc-tagged MCL-1. MCL-1 overexpression coincided with a decrease in ER stress mediators KDEL and CHOP expression following tunicamycin treatment. This suggests that MCL-1 overexpression can decrease ER stress-induced apoptosis in MEFs. To examine autophagy in the cells we also probed for LC3-II, a marker of autophagy maturation. We found LC3-II expression reduced in cells overexpressing MCL-1 compared to cells infected with a control vector. This suggests a role for MCL-1 in modulating autophagy (Fig. 3.7).

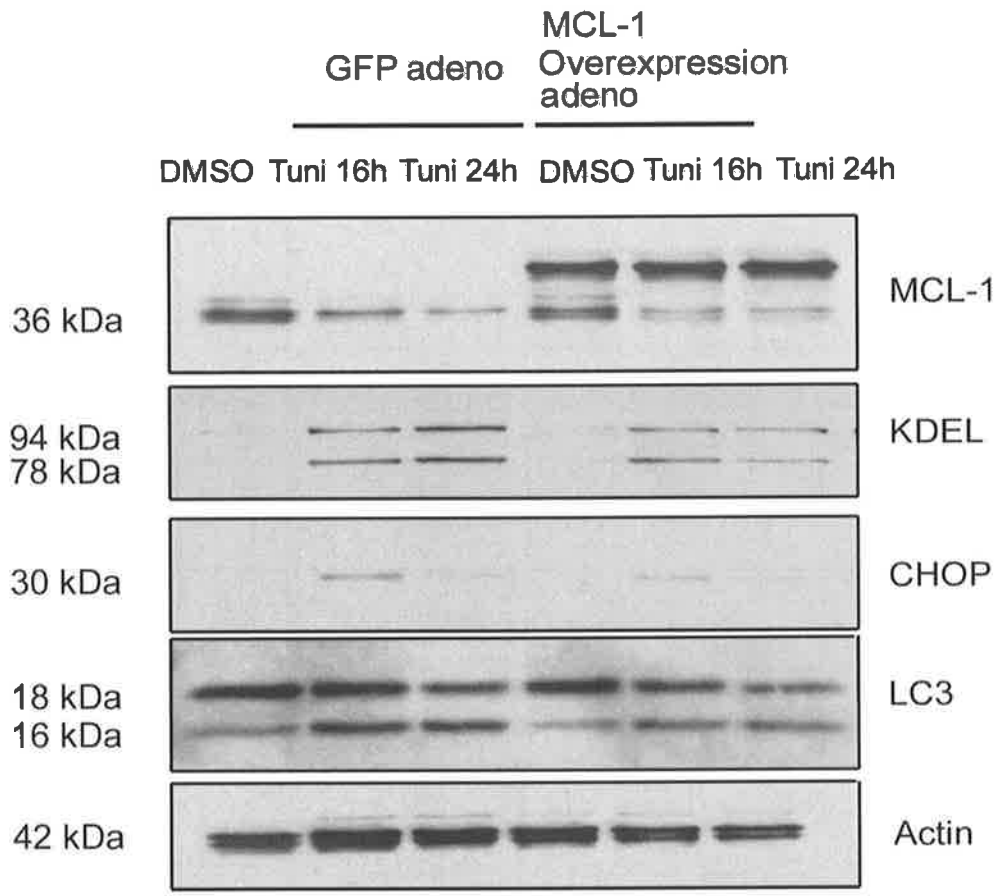

Figure 3.7: MCL-1 overexpression in *Mcl-1*$^{flox/flox}$ MEFs reduces the autophagic response to stress. Effect of MCL-1 overexpression was analysed in *Mcl-1*$^{flox/flox}$ MEFs infected with an MCL-1 overexpressing adenovirus or GFP control adenovirus (multiplicity of infection (MOI)=100) and subsequently treated with DMSO or 200 nM tunicamycin (16 h, 24 h). The experiment was repeated twice from different preparations with similar results.

3.2.8 miR-29a knockdown confirmation in primary cortical neurons undergoing tunicamycin-induced ER stress

In order to assess the function of miR-29a expression during ER stress in cortical neurons, we utilized antagomirs specific to our miRNA of interest, miR-29a. Antagomirs are single-stranded RNA molecules that can bind with perfect complementarity to their target and prevent the miRNA interacting with its target mRNA (Broderick and Zamore, 2011). The role for miRNA modulation using antagomir technology has been investigated as a possible therapeutic for a range of diseases. In our lab, antagomir-mediated silencing of miR-134 has been demonstrated as protective in a model of epilepsy (Jimenez-Mateos *et al.*, 2012). Therefore, we wanted to establish if miR-29a antagomirs could mediate the response of cortical neurons to ER stress. Antagomirs specific to miR-29a supplied the perfect platform to look at the effect of miR-29 modulation *in vitro* in primary cortical neurons. Transfection of miR-29a specific antagomir or scrambled antagomir control for 48 h in cortical neurons at DIV 6-8 was performed with Lipofectamine 2000 transfection reagent. A dose of 50 nM was found experimentally to be optimal in giving the greatest proportion of knockdown in our cells. Cells were then treated with DMSO, or 3 μM tunicamycin for 16 h or 24 h to induce stress. Samples were analysed by RT-qPCR and normalized to an RNU19 control primer (Fig. 3.8A). We identified significant knockdown of miR-29a in DMSO, tunicamyin 16 h and 24 h treated cells compared to scrambled control transfected cells. Validation of miR-29a knockdown and confirmation that PCR result was attributed solely to the antagomir effects and not to any primer annealing artifact was preformed in primary neurons incubated for 48 h with 50 nM miR-29a antagomir or scrambled control in the absence of Lipofectamine 2000 (Fig. 3.8B). miR-29a knockdown was not seen in the absence of Lipofectamine 2000 transfection reagent and confirms that transfection of miR-29a antagomir-induced knockdown during Lipofectamine 2000 transfection.

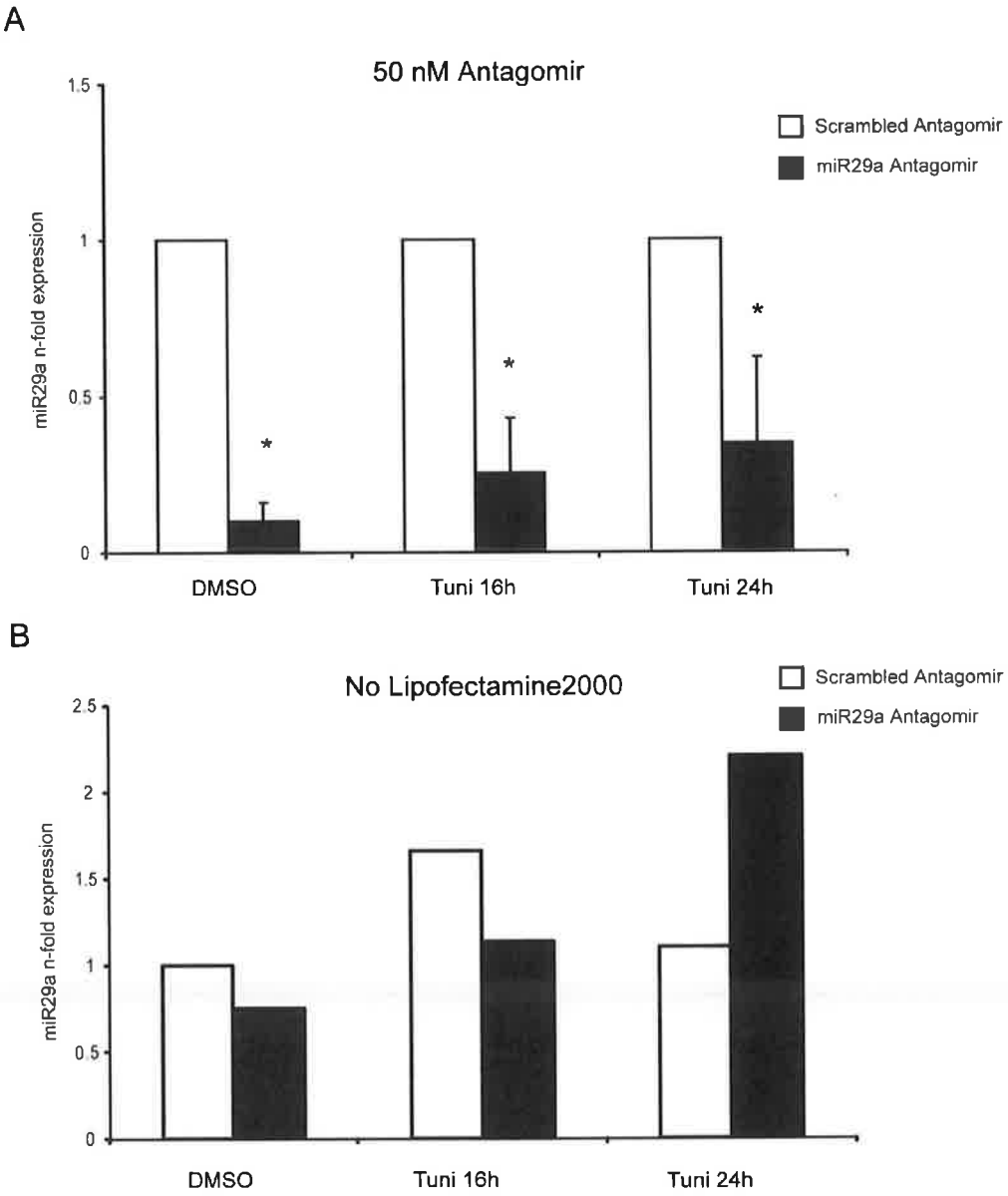

Figure 3.8: miR-29a knockdown mediated by miR-29a specific antagomirs *in vitro*. (A) miR-29a expression in mouse primary cortical neurons following Lipofectamine 2000 transfection with 50 nM scrambled control or miR-29a specific antagomir for 48 h prior to treatment with DMSO or 3 μM tunicamycin (16 h and 24 h). Data are represented as means ± SEM from n = 9 cultures from three separate preparations. *$P<0.05$, compared with scrambled antagomir treated similarly (ANOVA, *post-hoc* Tukey).(B) miR-29a expression in mouse cortical neurons incubated with control or miR-29a antagomir for 48 h in the absence of transfection reagent Lipofectamine 2000 and subsequent treatment with DMSO or tunicamycin (16 h and 24 h).Results from n=1 culture from one experiment.

3.2.9 Loss of miR-29a in cortical neurons increases *Mcl-1* expression

Having identified MCL-1 down-regulation corresponding to miR-29a upregulation in cortical neurons undergoing ER stress by western blot, we wanted to confirm that miR-29a was modulating *Mcl-1* expression in this paradigm. miR-29a has been shown previously in our lab and elsewhere to target the 3' UTR of MCL-1 and mediate translational repression (Mott *et al.*, 2007). We utilized the antagomirs to see the effect of down-regulating miR-29a in cortical neurons and any corresponding change in *Mcl-1* mRNA levels. Primary neurons were transfected as before with 50 nM miR-29a antagomir or scrambled antagomir for 48 h and subsequently treated with DMSO or 3 μM tunicamycin for 24 h. RT-qPCR was performed to analyse miR-29a and *Mcl-1* levels. miR-29a was shown to be significantly down-regulated following miR-29a antagomir transfection compared to scrambled control antagomir similarly treated (Fig. 3.9A). Correspondingly, analysis of *Mcl-1* mRNA showed upregulation in cortical neurons transfected with miR-29a antagomir prior to treatment with both DMSO and 3 μM tunicamycin (Fig. 3.9B). This result further establishes a role for miR-29a modulation in the control of *Mcl-1* expression in cortical neurons.

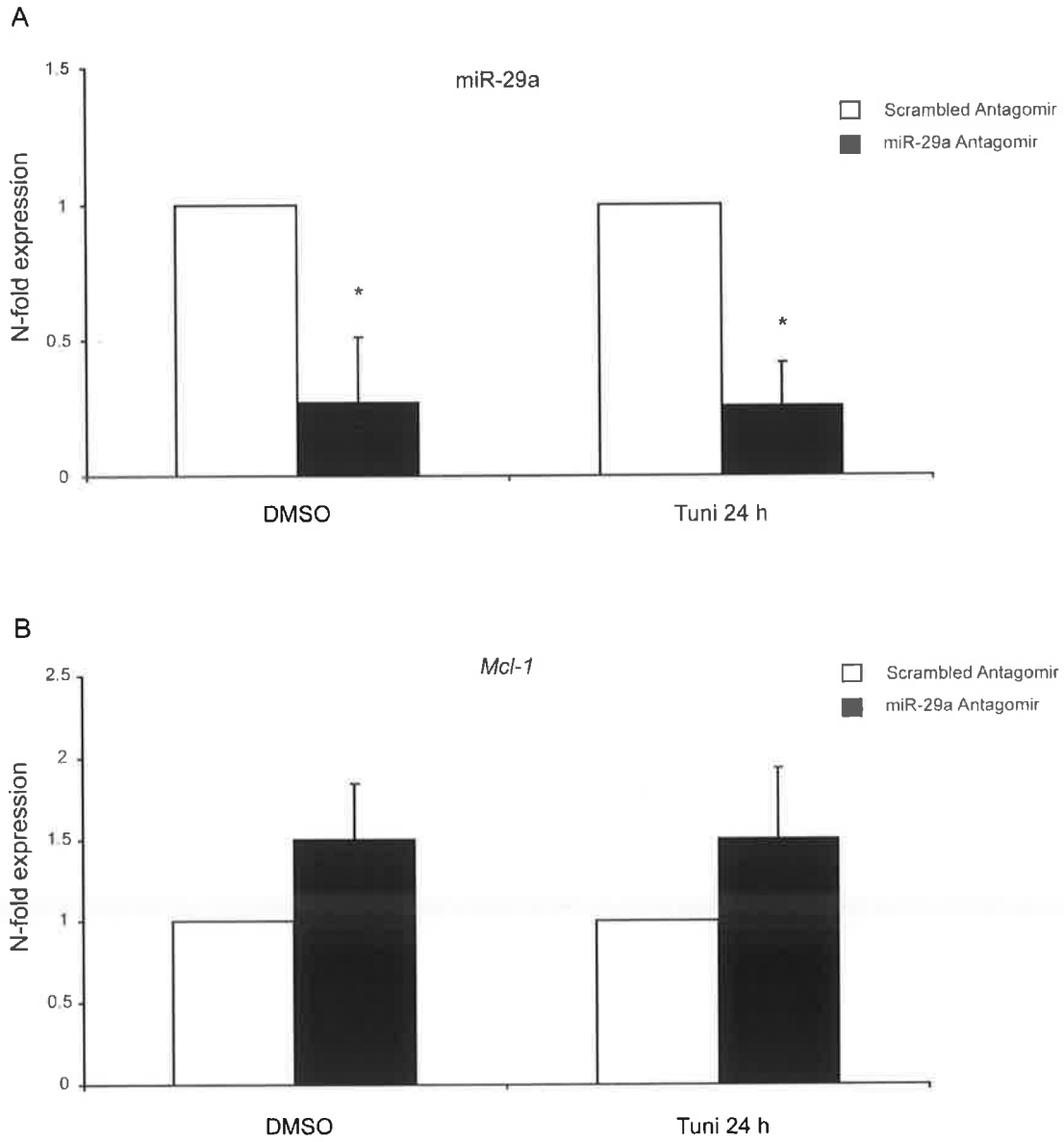

Figure 3.9: miR-29a down-regulation increases *Mcl-1* expression in cortical neurons. (A) RT-qPCR analysis of miR-29a levels following miR-29a antagomir or scrambled antagomir transfection for 48 h and subsequent treatment with DMSO or 3 µM tunicamycin for 24 h. Data are represented as means ± SEM from n = 9 cultures from three separate experiments. Expression levels were normalised to scrambled antagomir *$P<0.05$, compared to scrambled antagomir. (ANOVA, *post-hoc*, Tukey). (B) *Mcl-1* mRNA analysed by RT-qPCR in cortical neurons transfected with miR-29a antagomir or scrambled antagomir for 48 h and subsequent treatment with DMSO or 3 µM tunicamycin for 24 h. Data are represented as means ± SEM from n = 9 cultures from three separate experiments. Expression levels were normalised to control scrambled antagomir culture.

3.2.10 miR-29a knockdown in cortical neurons protects against tunicamycin-induced cell death

Following confirmation of antagomir-mediated knockdown of miR-29a in cortical neurons and having identified miR-29a targeting of MCL-1 during ER stress in cortical neurons, we wanted to assess the effect of this modulation on ER stress-induced apoptosis. Primary neurons were transfected as before with 50 nM miR-29a antagomir or scrambled antagomir for 48 h and subsequently treated with DMSO or 3 μM tunicamycin for 24 h. Cells were stained with Hoechst 33358 and imaged using an inverted microscope (Fig 3.10A). miR-29a transfected neurons undergoing tunicamycin-induced cell death demonstrated fewer visible pyknotic nuclei and greater cell density than scrambled antagomir similarly treated cells. No difference in cell density was seen for neurons treated with DMSO following tranfection with either antagomir.

To confirm and assess the protection seen in the cortical neurons, we calculated percentage cell death for each treatment assessed through nuclear morphology following Hoechst 33358 staining. Condensed or pyknotic nuclei were scored as dead and compared against intact nuclei to measure the % cell death (Fig 3.10B). We identified significant protection against tunicamycin-induced cell death in miR-29a antagomir transfected neurons compared with scrambled control. A significant increase in cell death in tunicamycin-treated cells compared to DMSO-treated cells in the absence of miR-29a confirms the presence of ER stress following tunicamycin treatment. This result suggests a protective role for miR-29a knockdown in cortical neurons undergoing tunicamycin-induced ER stress. Taking into account our previous finding miR-29a knockdown may be protective through derepression of MCL-1 translation.

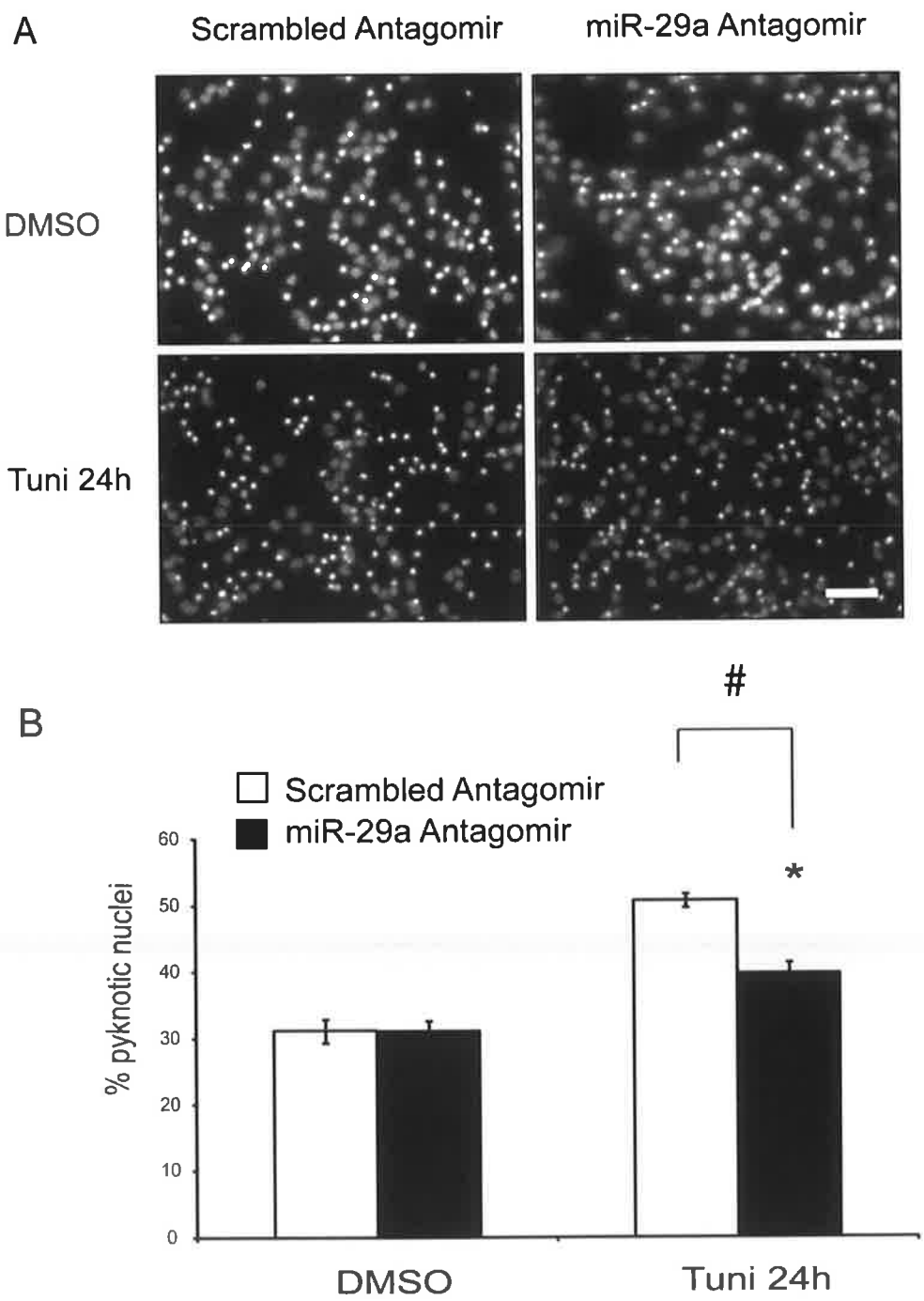

Figure 3.10: Antagomir-mediated knockdown of miR-29a protects cortical neurons during tunicamycin-induced cell death. (A) Representative images of cortical neurons transfected with control and miR-29a antagomir for 48 h. Neurons were subsequently treated with DMSO or 3 μM tunicamycin for 24 h. Hoechst 33358 fluorescence images were acquired using an inverted microscope to quantify nuclear apoptosis. (B) Cell death analysis in cortical neurons transfected with 50 nM control or miR-29a antagomir for 48 h and treated with DMSO or tunicamycin for a further 24 h. Nuclei were

stained with Hoechst 33358 and morphology of pyknotic nuclei was assessed using ImageJ software (National Institute of Health). For each timepoint images of nuclei were captured in three subfields containing 300-400 neurons each and repeated in triplicate. Data are mean ± SEM from n= 3 experiments. *P<0.05, compared with DMSO-treated cells #P<0.05, between control antagomir and miR-29a antagomir, tunicamycin-treated cells. (ANOVA, *post-hoc,* Tukey). Scale bar = 50 µm

3.3 Discussion

In this chapter we identified a role for miR-29a targeting MCL-1 during ER stress-induced apoptosis in cortical neurons. We confirmed significant miR-29a upregulation in mouse primary cortical neurons undergoing ER stress induced by both tunicamycin treatment and brefeldin A treatment. In both instances we provide evidence of MCL-1 downregulation with increasing miR-29a expression. We demonstrated the importance of MCL-1 in mediating cortical neuron survival through both knockdown and overexpression analysis of MCL-1 in the context of ER stress. We investigated the protective role of MCL-1 in the absence of both PUMA and BAX during tunicamycin-induced cell death. Confirmation of miR-29a targeting *Mcl-1* was achieved through antagomir modulation of miR-29a and suggested a role for antagomir-mediated cell survival through protection of *Mcl-1* expression. Indeed, miR-29a antagomir transfected cortical neurons were found to have significantly reduced levels of ER stress-induced cell death confirming a pro-apoptotic role for miR-29a.

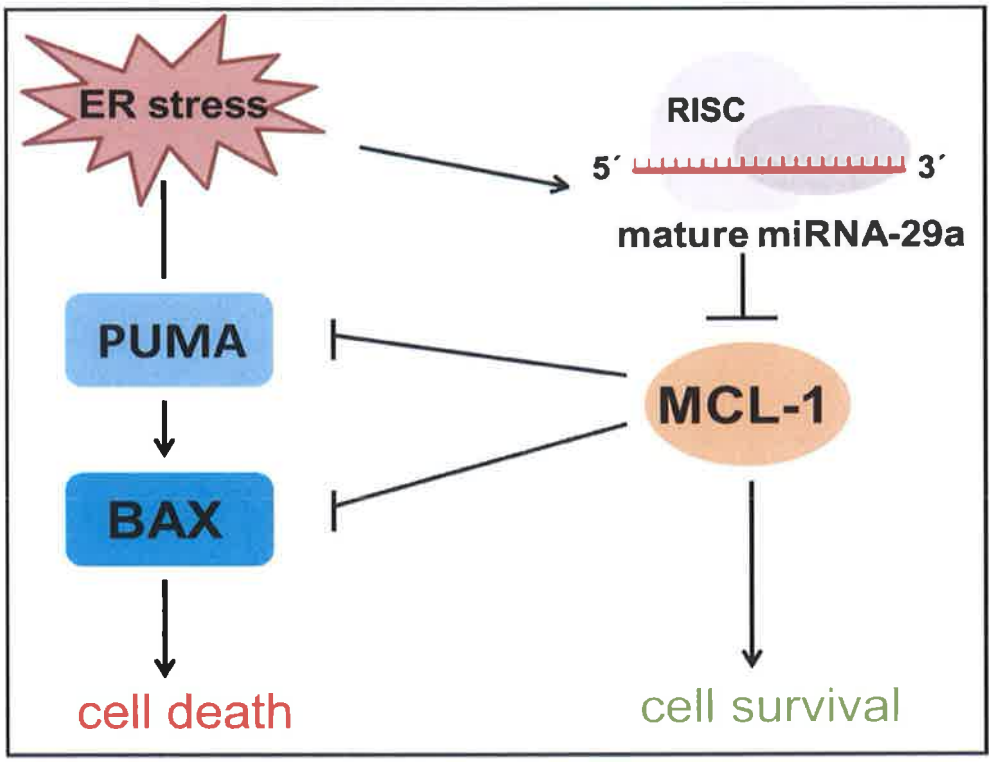

Figure 3.11: Schematic diagram of proposed miR-29a and MCL-1 interaction during ER stress-induced cell death in cortical neurons. In cortical neurons prolonged / unresolved ER stress can induce cell death through induction of BH3-only protein PUMA and activation of proapoptotic BAX. Anti-apoptotic MCL-1 can protect against PUMA- and BAX-dependent cell death and promote neuron survival. miR-29a, upregulated in neurons during ER stress, can inhibit MCL-1 protein translation and target *Mcl-1* mRNA for degradation, resulting in increased neuronal cell death.

The present study confirmed significant miR-29a upregulation at 16 h and 24 h timepoints in a model of primary cortical neurons undergoing ER stress. This result is in agreement with work previously carried out in our lab in SHSY5Y neuroblastoma cells identifying miR-29a upregulation under tunicamycin treatment (unpublished). The miR-29 family of miRNAs has been shown to target anti-apoptotic MCL-1 (Mott *et al.*, 2007). Due to altered expression of MCL-1 during ER stress (Danial and Korsmeyer, 2004), we wanted to establish a role for miR-29a targeting MCL-1 in cortical neurons during ER stress. We utilised

western blot analysis to examine the decreased expression of MCL-1 during ER stress-induced apoptosis. While it is understood that ER stress can downregulate antiapoptotic MCL-1 to induce apoptosis (Fritsch *et al.*, 2007, Allagnat *et al.*, 2011), the mechanisms underlying this are not well understood in neurons. ER-stress induced targeting of MCL-1 may occur through miR-29a upregulation and this could present a novel pathway for apoptosis induction in this setting.

We found MCL-1 to be a key regulator of ER stress-induced apoptosis in cortical neurons. Knockdown of MCL-1 in neurons subsequently treated with tunicamycin sensitised neurons to ER stress-induced cell death at 24 h post treatment. Increased cell death was also observed in DMSO-treated cells suggesting that loss of MCL-1 is detrimental to cellular homeostasis. This result is supported by work in mice with a conditional knockout of MCL-1 in the forebrain region. These mice had increasing loss of cortical neurons from the forebrain region between PND 1 and PND 30 and this coincided with deregulated autophagy in *mcl-1*$^{-/-}$ neurons (Germain *et al.*, 2011). While MCL-1 down-regulation has been shown to be sufficient to induce mitochondrial apoptosis in neurons, work in HeLa cells found that MCL-1 down-regulation sensitized cells to stress-induced apoptosis but was not sufficient to induce MOMP (Fritsch *et al.*, 2007). MCL-1 has also been shown to be targeted for degradation by NOXA (Willis *et al.*, 2005) or sequestration by BIM (Han *et al.*, 2006) to induce cell death through activation of the caspase cascade. Interestingly in neuronal precursors MCL-1 conditional deletion or overexpression was shown to increase or decrease neuronal precursor apoptosis by 2–fold respectively (Malone *et al.*, 2012).

Similarly when we examined MCL-1 overexpression in cortical neurons, we found significant protection from tunicamycin-induced cell death in neurons overexpressing MCL-1. Work by Arbour *et al.* demonstrated that MCL-1 overexpression in wildtype cortical neurons protected against cell death following DNA damage or neuronal injury

(Arbour *et al.*, 2008). Furthermore, MCL-1 overexpression in both *puma*$^{-/-}$ and *bax*$^{-/-}$ cortical neurons was shown to confer additional protection following tunicamycin treatment compared to protection conferred by PUMA or BAX knockout alone. We noted that neither MCL-1 overexpression nor *puma*$^{-/-}$/*bax*$^{-/-}$ was sufficient to abrogate cell death and that other mediators or pathways must be mediating apoptosis in the cortical neurons. Similar results were seen by Concannon *et al.* in which *puma*$^{-/-}$neurons were significantly protected following tunicamycin treatment. However, cell death was not halted completely (Concannon *et al.*, 2008). This could be due to activation of other BH3-only proteins or down-regulation of anti-apoptotic members of the BCL-2 family. BIM, PUMA and NOXA have all been shown to interact with MCL-1 and have been implicated in driving ER stress-induced cell death. PUMA interaction with MCL-1 has been shown to stabilise MCL-1 and prevent PUMA-induced cell death (Mei *et al.*, 2005). On the other hand, NOXA has been implicated in assisting BIM-mediated cell death during ER stress through NOXA-mediated sequestration of MCL-1 and release of "free" BIM (Zhang *et al.*, 2011). PUMA activation, not NOXA or BIM, has been shown to be sufficient to drive neuronal apoptosis through p53 activation (Cregan *et al.*, 2004) suggesting an important role for PUMA in mediating neuronal apoptosis. In MEFs we found that exogenously overexpressed MCL-1 decreased ER stress and apoptotic mediators (GRP78 and CHOP respectively) while also decreasing autophagy protein LC3. MCL-1 knockout neurons have been shown to undergo a robust autophagic response while MCL-1 overexpression was shown to decrease LC3 expression and therefore autophagy in cortical neurons following starvation induced stress (Germain *et al.*, 2011). This demonstrates a dual role for MCL-1 in modulating cellular homeostasis through either apoptotic cell death or cellular recycling and adaptation to stress. Our results taken in context with previous finding suggest multiple levels of regulation of MCL-1 in cells undergoing ER stress-induced cell death but emphasise the importance of MCL-1 in mediating the cellular response to stress.

Having identified the importance of MCL-1 in the cortical neuron response to ER stress-induced cell death, we wanted to confirm miR-29a targeting MCL-1 in the control of neuronal apoptosis. We utilised antagomir-mediated knockdown of miR-29a in cortical neurons and identified *Mcl-1* mRNA upregulation in response to loss of miR-29a. miR-29a has been shown to target MCL-1 for degradation in carcinoma tissue (Xiong *et al.*, 2010) and in lymphoma tissue (Desjobert *et al.*, 2011). *In vitro* analysis of cell death identified significant survival conferred to neurons undergoing tunicamycin-induced cell death following antagomir- mediated miR-29a knockdown. Previous work in our lab demonstrated miR-29a targeting the 3' UTR of MCL-1 in a neuroblastoma cell line (Concannon et al, unpublished). Complementing these results, we found that miR-29a knockdown was protective against tunicamycin-induced cell death. Taking this into account, we are confident that miR-29a plays a role in targeting MCL-1 for degradation in cortical neurons and that loss of MCL-1 may contribute to ER stress-induced cell death in cortical neurons.

Our lab previously elucidated the relationship between miR-29a, MCL-1 and ER stress in cell lines. Work here has described and characterised a similar model in cortical neurons with ER stress modulating miR-29a and MCL-1 and subsequently mediating neuronal survival in culture. The next step was to examine this relationship *in vivo*.

CHAPTER 4

Characterisation of miR-29a expression in the mouse central nervous system

4.1 Introduction

Having identified a role for miR-29a during ER stress in cortical neurons, we wanted to investigate expression of miR-29a in a chronic neurodegenerative model associated with increased levels of ER stress. The $SOD1^{G93A}$ mutant mouse model is a widely used experimental model of ALS and neurodegeneration. These SOD1 mutant mice display the hallmark muscle wasting and loss of spinal motoneurons seen in familial amyotrophic lateral sclerosis (ALS). ER stress has previously been implicated in the pathogenesis of ALS (Lindholm *et al.*, 2006) and specifically $SOD1^{G93A}$ mice have previously been shown to have higher expression of ER stress markers in neurons of the spinal cord (Saxena *et al.*, 2009) . Downstream mediators of ER stress have been shown to enhance ER stress-induced apoptosis in motoneurons (Kieran *et al.*, 2007). Furthermore ER stress induction of the UPR machinery has been shown to exacerbate motoneuron loss in mouse models of familial ALS (Saxena *et al.*, 2009, Kikuchi *et al.*, 2006). Mutant SOD1 has also been shown to induce ERAD dysfunction in $SOD1^{G93A}$ mice and lead to motoneuron death through activation of apoptosis signal-regulating kinase 1 (ASK1) cell death pathway (Nishitoh *et al.*, 2008).

The $SOD1^{G93A}$ mouse model has become the benchmark model for familial ALS since its first publication by (Gurney *et al.*, 1994). $SOD1^{G93A}$ mice live approximately 5-6 months with progressive disease onset evident from 3-4 months. Symptoms include hind limb weakness, hind limb tremor and a thin appearance along their flanks. $SOD1^{G93A}$ mice exhibit massive loss of lower motoneurons from the ventral horn of the lumbar spinal cord and loss of myelinated axons from the ventral motor roots which gives these mice their characteristic paralysis and muscle atrophy (Acevedo-Arozena *et al.*, 2011). These disease characteristics are thought to be at least in part caused by

aggregation of mutant SOD1 protein in the ER of spinal cord motoneurons (Kikuchi *et al.*, 2006). These aggregates compound ER stress and inflammation in these mice and further aggravate motoneuron apoptosis.

SOD1 transgenic mice were designed with a mutant SOD1 gene injected into fertilised B6SJLF1 mouse eggs. Congenic-transgenic SOD1 mice were generated by transferring the SOD1 mutation from the transgenic mouse background to a specific inbred background (C57 BL/6) through repeated backcrossing. In this case 10+ generations of backcrossing is required after which a strain is considered completely congenic (designated Black6 (B6). Cg-Tg(SOD1^{*G93A})1Gur/J). Congenic mice are mice bred to contain a desired mutation and are almost genetically identical which gives increased uniformity of phenotype between each animal. Uniformity of phenotype across a colony of mice has two advantages. Firstly, any differences in phenotype between two mice are more likely to be caused by non-genetic factors or exogenous factors. This serves to make congenic animals more susceptible to environmental influences and experimental treatments. Secondly, increased phenotypic uniformity decreases the number of animals necessary to achieve statistical significance (Working with ALS mice: Guidelines for preclinical testing and colony management, guidelines provided by The Jackson Laboratories (Leitner, 2009).

Due to the established role of ER stress in ALS disease pathology (Nishitoh *et al.*, 2008) and having identified a role for miR-29a in mediating neuronal cell death *in vitro*, we hypothesised that miR-29a could play a role in modulating ER stress-induced apoptosis of motoneurons. Before we could examine miR-29a modulation in SOD1^{G93A} mice *in vivo*, we initially had to characterise miR-29a levels in wildtype inbred C57 BL/6 mice which are the background onto which all the SOD1 mice are bred. C57 BL/6 mice are the most commonly used inbred strain for generating transgenic mice (Mekada *et al.*,

2009). C57 BL is the parent strain while 6 denotes a substrain. C57 BL/6 mice live long, have a low susceptibility to tumours and their use has been well documented in neurodegenerative research. Following identification of miR-29a expression levels in the organs of the CNS, we could examine region-specific expression of miR-29a in the lumbar spinal cord from $SOD1^{G93A}$ mice. We aimed to identify miR-29a localisation within the lumbar spinal cord from wildtype and SOD1G93A mice. Motoneuron specific expression of miR-29a would identify a potential role for miR-29a in $SOD1^{G93A}$ disease progression and ALS neurodegeneration.

4.2 Results

4.2.1 Characterisation of miR-29a and *Mcl-1* expression in the C57 BL/6 mouse

miR-29a has been shown to be highly conserved in both humans and mice with expression in a wide variety of cell types (Kriegel *et al.*, 2012). Having identified a role for miR-29a and miR-29a targeting MCL-1 in primary cortical neurons from C57 BL/6 mice, we wanted to measure miR-29a levels in some of the major mouse organs from C57 BL/6 mice. We also wanted to compare miR-29a levels to *Mcl-1* mRNA levels in these tissues. We screened 5 major organs to identify key areas of miR-29a expression in a C57 BL/6 wild-type mouse model. RT-qPCR was performed on organs harvested from PND 90 wild-type C57 BL/6 mice following PBS perfusion, tissue microdissection and microRNA isolation. miR-29a expression was shown to be significantly stronger in the CNS, especially the cortex, the hippocampus and the lumbar spinal cord compared with the organs such as the heart, the liver or the spleen (Fig. 4.1A). *Mcl-1* expression was higher in the liver, heart and spleen while having lower expression in the cortex, the hippocampus and the lumbar spinal cord (Fig. 4.1B). Spearman rank correlation analysis for miR-29a and *Mcl-1* expression identified significant inverse correlation between expression levels for each organ (Fig. 4.1C). This result further confirms a relationship between miR-29a abundance and *Mcl-1* expression *in vivo* in C57 BL/6 mice. Furthermore the abundance of miR-29a in the CNS suggests a possible role for miR-29a in neuronal homeostasis and cell death.

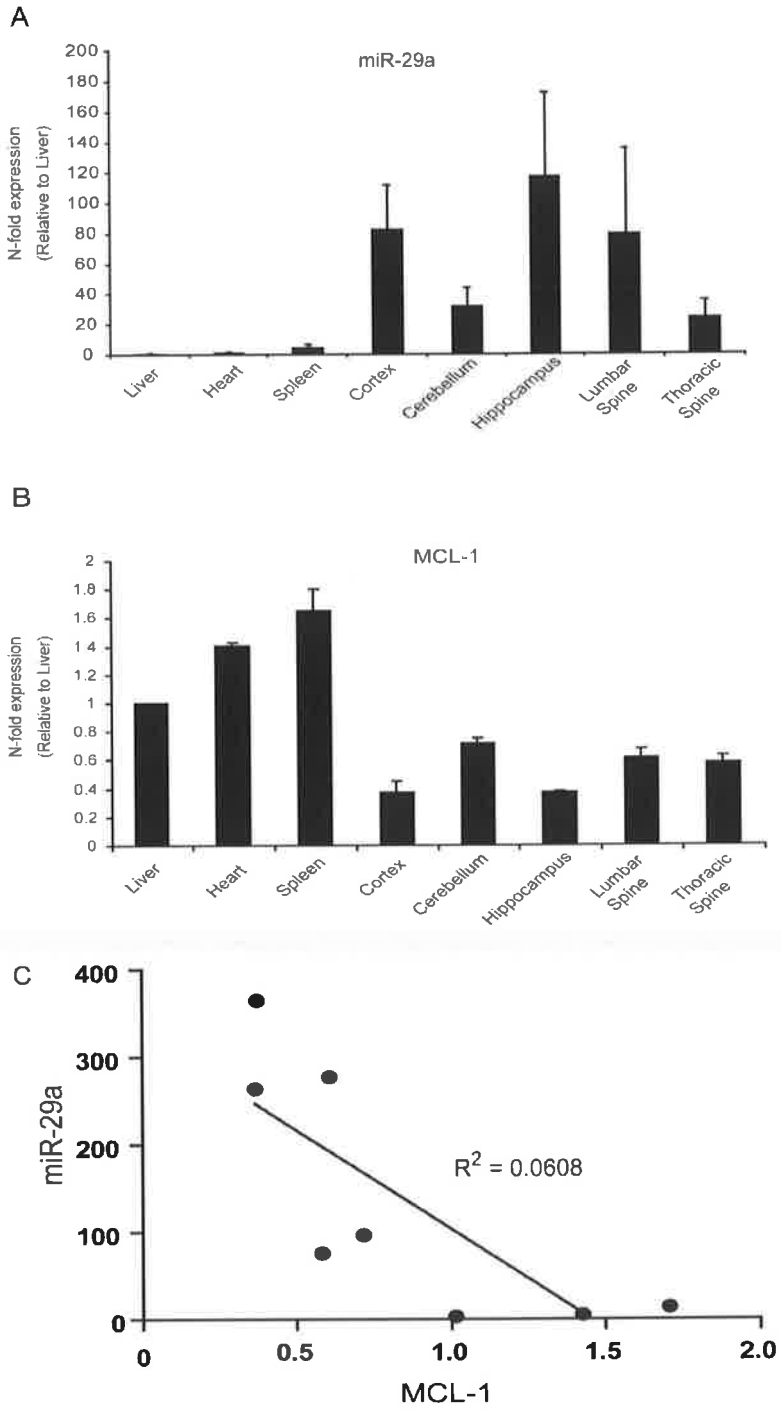

Figure 4.1: miR-29a is abundant in the mouse CNS while *Mcl-1* expression is more abundant in the internal organs. (A) Increased expression of miR-29a in organs of the CNS. miR-29a expression in organs from C57 BL/6 mice was assessed by RT-qPCR. Expression levels were normalised to RNU19 control and expressed relative to the liver sample. Data are represented as mean ± SEM from n=4 C57 BL/6 mice. (B) Increased expression of *Mcl-1* in internal organs compared to

CNS organs. *Mcl-1* expression in organs from C57 BL/6 mice was assessed by RT-qPCR. Expression levels were normalised to β-actin control and expressed relative to the liver sample. Data are represented as mean ± SEM from n=4 C57 BL/6 mice. (C) Spearman rank correlation analysis of *Mcl-1* and miR-29a expression for each organ from C57 BL/6 mice. *P<0.05, comparing miR-29a expression and *Mcl-1* expression for individual organs. Data are average expression levels from n=4 C57 BL/6 mice

4.2.2. Comparative miRNA expression in C57 BL/6 mouse CNS

Following from the work on cortical neurons, we wanted to look at expression of other miRNAs in regions of the mouse CNS where miR-29a was most abundantly expressed. We chose to look at the lumbar spine, the cortex and the hippocampus as this was where we saw the highest expression of miR-29a in the C57 BL/6 mice. We conducted RT-qPCR and compared miR-29a Ct value to that of miR-193a, -148a and -376a for the same samples. The cycle threshold (Ct) value is a measure of the time when the fluorescence intensity of a sample exceeds the background fluorescence. Ct values are inversely proportional to the amount of target nucleic acid present in the sample (Wong and Medrano, 2005); the lower the Ct value, the more abundant the miRNA is in each tissue sample. We found that miR-29a was more abundantly expressed than miR-193a and miR-148a across all three tissues (Fig. 4.2). miR-376a had similar expression levels to miR-29a in the cortex and the hippocampus. Individual expression of each miRNA was found to be uniform across the three tissues. Having identified miR-29a as abundantly expressed in cortical neurons during ER stress and abundantly expressed *in vivo* compared to other ER stress-induced miRNAs during non-stress conditions, we can hypothesise that miR-29a relative abundance may be of importance in the CNS whether during disease modulation or growth.

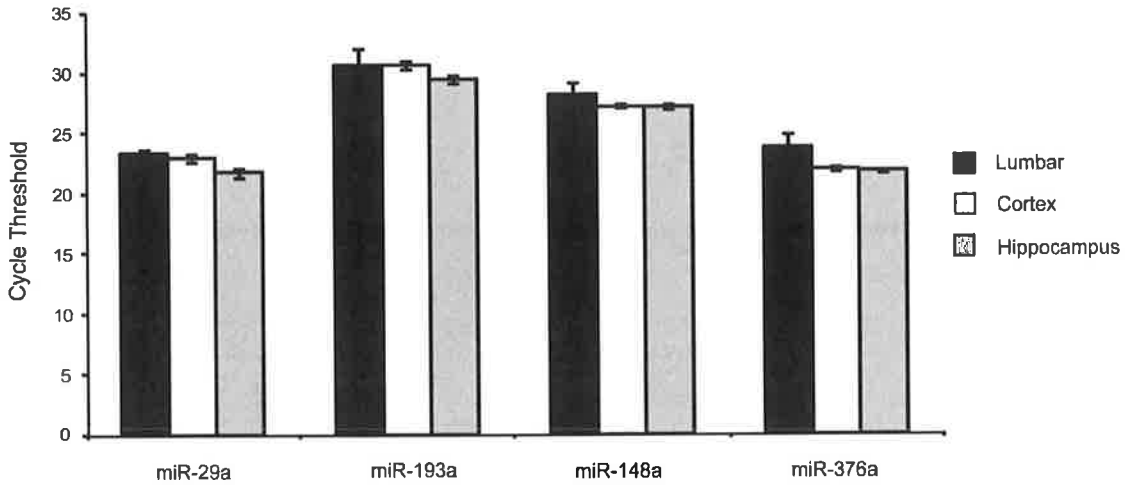

Figure 4.2: miR-29a is present in the mouse lumbar spine in greater abundance than miR-193a, -148a and -376a. miRNA expression in lumbar spine, cortex and hippocampus from wildtype C57 BL/6 mice. miRNA expression of miR-29a, miR-193a, miR-148a and miR-376a were measured by RT-qPCR and data was displayed as the average Ct value for each sample. Data are from n=4 C57 BL/6 mice.

4.2.3 miR-29a expression is induced in transgenic SOD1^{G93A} mice earlier than wildtype mice

Having identified increased miR-29a expression in the lumbar spine of C57 BL/6 mice, we wanted to investigate miR-29a expression in SOD1^{G93A} lumbar spinal cord. Previous work in this lab by Simone Poeschel had identified miR-29a as upregulated in SOD1^{G93A} mice at PND 70 and PND 90 compared to wildtype mice (Fig 4.3.1). We conducted *in situ* hybridisation with DIG-labelled probes for miR-29a, scrambled negative control and small nuclear RNA U6 positive control to confirm miR-29a expression changes and elucidate the localisation of miR-29a in the lumbar spinal cord. *In situ* hybridisation involves detection of specific nuclei acid sequences in cells and tissues and offers information on specific cell location and expression levels (Nielsen, 2012). Dioxygenin-labelled riboprobes are non-radioactive detection probes that can be detected by high affinity anti-DIG antibodies. We utilised DIG-labelled probes conjugated to alkaline phosphatase which can be visualised by colorimetric (NBT and BCIP) alkaline phosphatase substrate. Colorimetric analysis confirmed miR-29a expression in lumbar spinal cord tissue sections. miR-29a expression was observed as circular purple staining throughout the grey matter of the spinal cord sections and was identified as intra-cell staining at 60x magnification. The grey matter is the inner "butterfly shaped" matter of the spinal cord and contains all the cell bodies of neurons in the spinal cord as well as astrocytes and microglial cells (Sherwood, 2012). Strong miR-29a expression was identified in PND 70, 90 and 120 spinal sections, above background, from SOD1^{G93A} mutant mice while miR-29a expression was only identified in PND 90 and 120 spinal sections from wildtype mice. Weak staining for miR-29a was seen in the PND 70 spinal cord in the wildtype mice. ER stress is an early event in the pathogenesis of ALS (Matus *et al.*, 2013). Increased expression of ER stress-mediated miR-29a in transgenic SOD1 mice at PND 70 suggests that there is exacerbated ER stress in the spinal cords of these mice compared to wildtype mice. This increased ER stress may contribute to motoneuron loss characteristic of ALS in a miR-29a dependent manner.

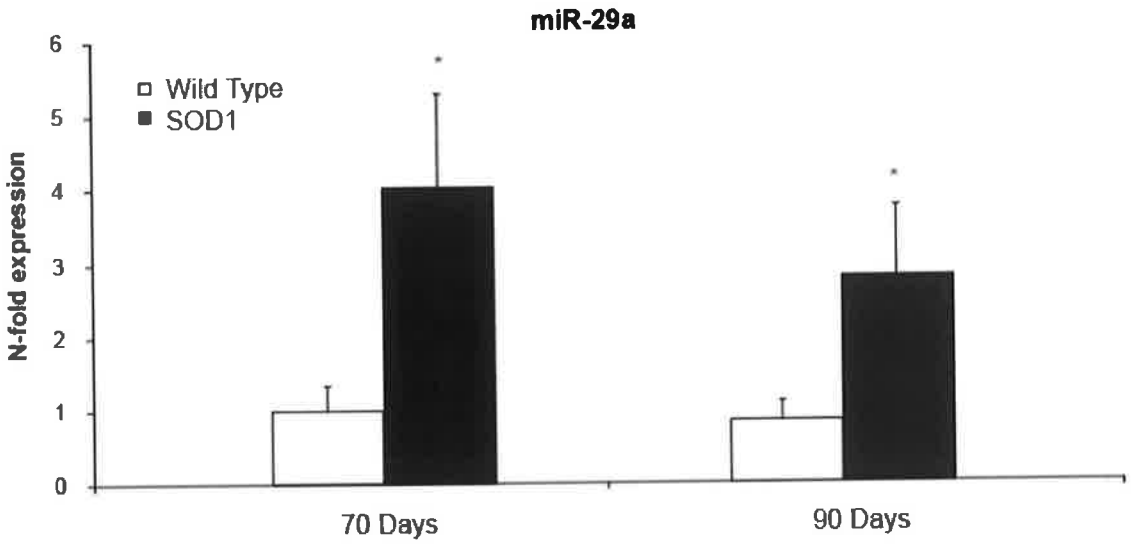

Figure 4.3.1: miR-29a expression is increased in presymptomatic and symptomatic SOD1^{G93A} spinal cord. miR-29a expression in spinal cord from wildtype and transgenic SOD1^{G93A} mice were assessed by RT-qPCR. Expression levels were normalised to RNU19 control and expressed relative to wildtype spinal cord. Data are represented as mean ± SEM from n=4 mice. *P<0.05 compared with wildtype mice (Independent t-test). This work was conducted previously in this lab by Simone Poeschel and adapted here.

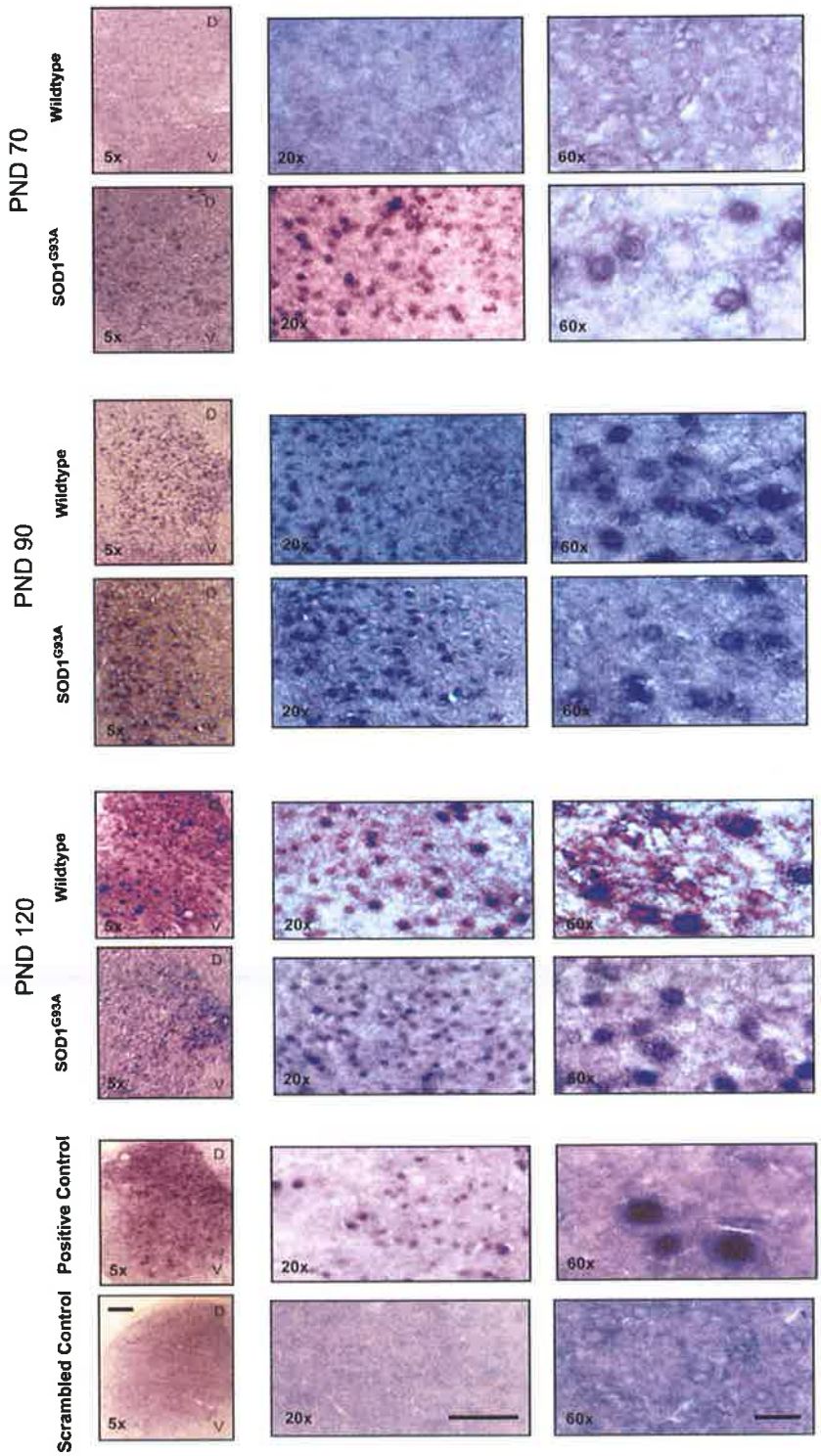

Figure 4.3.2: miR-29a expression is increased in SOD1^{G93A} mice at PND 70 compared to wildtype SOD1 mice. miR-29a expression in lumbar spinal cord sections from wildtype and SOD1^{G93A} mice was analysed by *in situ* hybridisation. miR-29a DIG-labelled probe, U6 positive control or scrambled negative control were incubated with tissue sections for 24 h and signal developed over 4-7 days. Images were acquired using an Olympus IX51 inverted microscope. A positive

control probe was used to confirm the success of the *in situ* protocol. A scrambled control probe gave no expression and confirmed specificity of our miR-29a specific probe. Similar results were obtained in two separate experiments utilising n=2 SOD1G93A and n=2 wildtype mice PND 70, n=1 SOD1G93A and n=1 wildtype mice PND 90 and n=2 SOD1G93A and n=1 wildtype mice PND 120. Scale bar: 5x image = 500 µm, 20x image = 50 µm, 60x image = 100 µm.

4.2.4 miR-29a expression localised to motoneurons in PND 70 lumbar tissue sections in SOD1^{G93A} mice

Having identified miR-29a expression in the spinal cord grey matter, we next looked at whether miR-29a expression was present in motoneurons. Loss of lower motoneurons from the ventral horn of the lumbar spinal cord is characteristic of SOD1^{G93A} mice and leads to muscle atrophy and paralysis during disease progression (Gurney *et al.*, 1994). Nissl staining with 0.1 % cresyl-violet stain was performed on spinal sections consecutive to those used for the *in situ* hybridisation study. Cresyl-violet is a dye that stains the Nissl bodies/ rough endoplasmic reticulum of neurons (Pilati *et al.*, 2008). The cresyl-violet stains DNA and RNA a blue/purple colour and is an efficient way to stain all neurons in tissue sections. Nissl-stained motoneurons were identified based on size, large cell body > 40 µm and a visible nucleolus. miR-29a expression can clearly be seen in the ventral horn regions of the spinal cord from SOD1^{G93A} mutant mice as well as throughout the grey matter. miR-29a expression is weak in wildtype mouse sections (Fig. 4.4A). Studying the images at 5x and 20x magnification, it is possible to identify possible overlap between miR-29a expressing cells and Nissl-stained motoneurons in both wildtype and SOD1^{G93A} mutant mouse sections. Smirnova *et al.* identified miR-29 as expressed in neurons and specifically astrocytes in large abundance in the adult mouse brain (Smirnova *et al.*, 2005). miR-29a expression was also identified in other neuronal and non-neuronal cell types within the grey matter. However this was not investigated further as we chose to focus on miR-29a expression in motoneurons. Motoneuron counts of individual PND 70 lumbar spinal sections from both wildtype and SOD1^{G93A} mice show no significant difference in motoneuron number from section to section (Fig. 4.4B). These sections were consecutive to sections used in the *in situ* hybridisation and demonstrated some overlap in motoneuron staining.

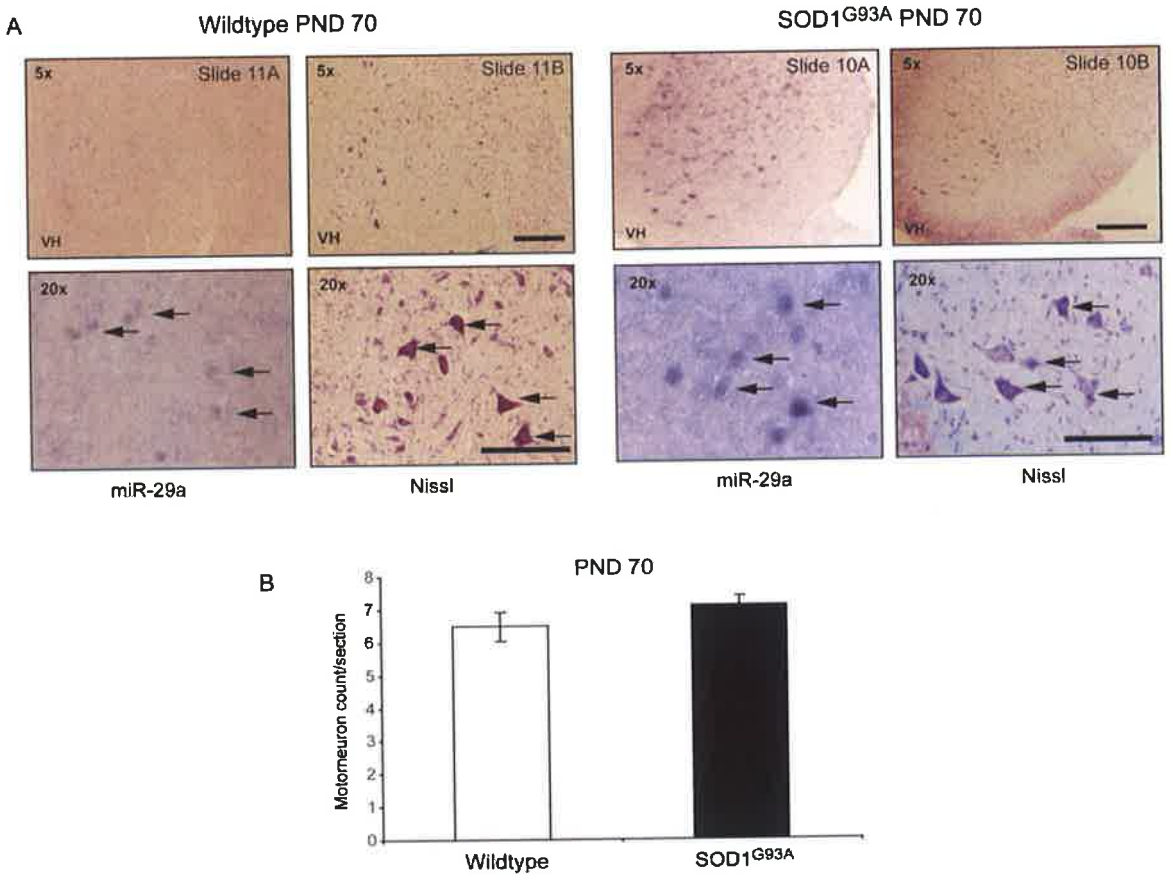

Figure 4.4: miR-29a expression is increased in the grey matter of lumbar spinal cord from SOG1^{G93A} mice. (A) *In situ* hybridisation and Nissl stain was analysed in consecutive lumbar tissue sections from PND 70 SOD1^{G93A} mice or wildtype SOD1 mice. Hybridisation was conducted using DIG-labelled miR-29a, U6 positive control and scrambled negative control (controls not shown) for 24 h and alkaline phosphatase substrate for 4-7 days. Nissl stain was conducted using 0.1 % cresyl-violet dye. Mounted sections were imaged using an Olympus IX51 inverted microscope and images were analysed using ImageJ (National Institute of Health). Similar results were obtained in two separate experiments utilising two mice per group. (B) Motoneuron counts were analysed in Nissl-stained sections from wildtype and SOD1^{G93A} PND 70 mice. Motoneurons were identified in the ventral horn based on size criteria and the presence of a clear and distinct nucleolus using an Olympus IX51 inverted microscope. The average motoneuron count for the left and right ventral horn was calculated. Data is representative of n=15 sections from n=2 spines per group. Scale bar: 5x = 500 µm, 20x = 50 µm

4.2.5 Decrease in miR-29a expression in SOD1^{G93A} lumbar spine sections due to loss of motoneurons during disease onset

miR-29a expression was also analysed at PND 90, the experimental point of disease onset and PND 120, during disease progression. *In situ* hybridisation with DIG-labelled probes specific for miR-29a identified miR-29a expression in the grey matter of lumbar spinal sections from PND 90 and PND 120 wildtype and SOD1^{G93A} mice. Nissl staining of consecutive sections identified motoneurons in the ventral horn of lumbar spine sections. Image analysis using ImageJ software allowed for identification of overlap between miR-29a stained cells and Nissl stained motoneurons in both PND 90 and PND 120 sections. Strong miR-29a signal was identified in wildtype sections for both PND 90 and PND 120 timepoints. Unlike PND 70 sections, miR-29a signal was comparable if not reduced in SOD1^{G93A} mouse sections compared to wildtype (Fig. 4.5.1A and Fig. 4.5.2A). The reduction in miR-29a staining in transgenic spinal sections could be due to motoneuron loss during disease progression in these mice. Indeed, motoneuron counts of Nissl stained lumbar sections from PND 90 and PND 120 timepoints identified significant loss of motoneurons in these sections compared to wildtype mice (Fig. 4.5.1B and Fig. 4.5.2B). miR-29a staining was seen in both neuronal and non-neuronal cells, with our emphasis on miR-29a staining in the motoneurons of the ventral horn. Loss of motoneurons expressing miR-29a could explain the diminished miR-29a signal at PND 90 and PND 120. Due to the role miR-29a plays in sensitising cortical neurons to ER stress-induced cell death, motoneuron loss could be intensified due to miR-29a expression.

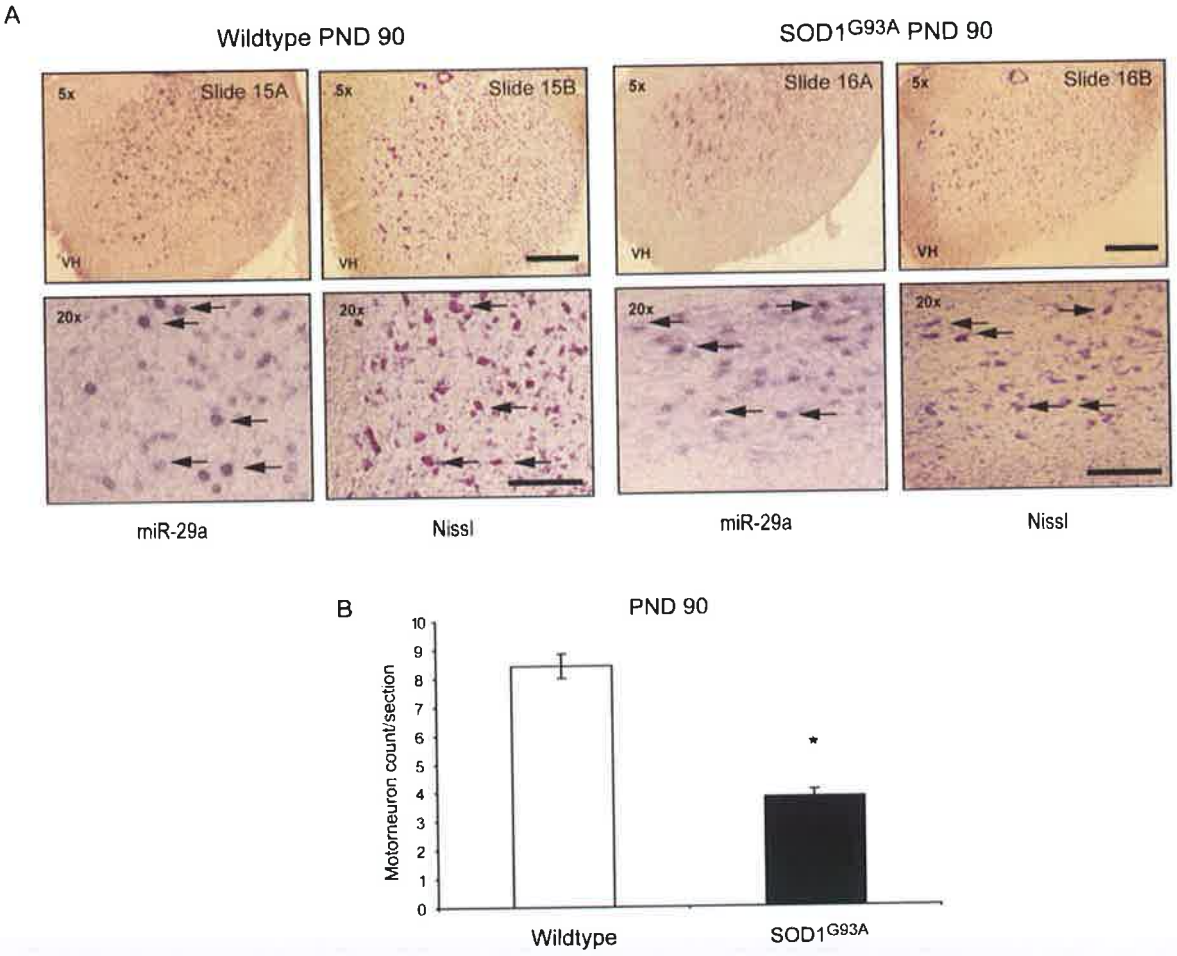

Figure 4.5.1: miR-29a expression is decreased in SOD1^{G93A} PND 90 lumbar spinal sections due to loss of motoneurons. (A) *In situ* hybridisation and Nissl stain was analysed in consecutive lumbar tissue sections from PND 90 SOD1^{G93A} mice or wildtype SOD1 mice using DIG-labelled miR-29a, U6 positive control and scrambled negative control (controls not shown) for 24 h and alkaline phosphatase substrate for 4-7 days. Nissl stain was conducted using 0.1 % cresyl-violet dye. Mounted sections were imaged using an Olympus IX51 inverted microscope and images were analysed using ImageJ (National Institute of Health). Results were obtained from n=1 mice per group. (B) Motoneuron counts were analysed in Nissl stained sections from wildtype and SOD1^{G93A} PND 90 mice. Motoneurons were identified in the ventral horn using an Olympus IX51 inverted microscope and images were analysed using ImageJ software (National Institute of Health).*P<0.05, compared to wildtype motoneuron count/section (ANOVA, *post hoc*, Tukey). Data is representative of n=15 sections from n=2 spines per group. Scale bar: 5x = 500 µm, 20x = 50 µm.

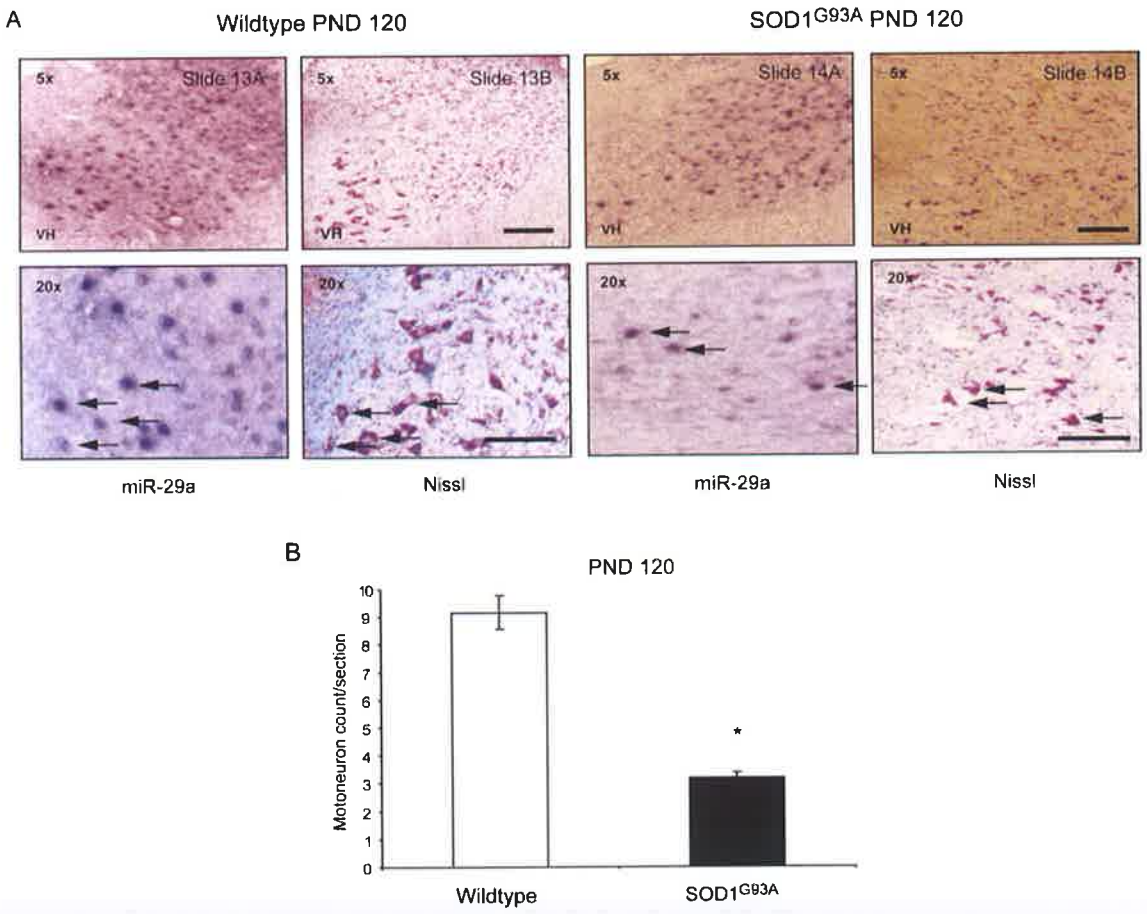

Figure 4.5.2: Decreased miR-29a expression in SOD1^{G93A} PND 120 lumbar spinal sections is comparable to loss of motoneurons. (A) *In situ* hybridisation and Nissl stain was analysed in adjacent lumbar tissue sections from PND 120 SOD1^{G93A} mice or wildtype SOD1 mice using DIG-labelled miR-29a, U6 positive control and scrambled negative control (controls not shown) for 24 h and alkaline phosphatase substrate for 4-7 days. Nissl stain was conducted using 0.1 % cresyl-violet dye. Mounted sections were imaged using an Olympus IX51 inverted microscope and images were analysed using ImageJ (National Institute of Health). Similar results were obtained in two separate experiments utilising two transgenic and one wildtype mouse per group. (B) Motoneuron counts were analysed in Nissl stained sections from wildtype and SOD1^{G93A} PND 120 mice. Motoneurons were identified in the ventral horn using an Olympus IX51 inverted microscope and images were analysed using ImageJ software (National Institute of Health).*P<0.05, compared to wildtype motoneuron count/section (ANOVA, *post hoc*, Tukey). Data is representative of n=15 sections from n=2 spines per group. Scale bar: 5x = 500 µm, 20x = 50 µm.

4.2.6 *Mcl-1* mRNA is not differentially expressed in wildtype and SOD1^{G93A} mice across disease progression

Having identified early induction of miR-29a expression in SOD1^{G93A} lumbar spinal cord and having localised miR-29a expression to motoneurons of the ventral horn of the lumbar spine, we chose to examine *Mcl-1* mRNA levels in lumbar spinal cord from PND 70, PND 90 and PND 120. RT-qPCR analysis of lumbar spinal cord samples from wildtype and SOD1^{G93A} mice identified comparable levels of *Mcl-1* mRNA between wildtype and SOD1^{G93A} mice. Furthermore we identified no differential expression of *Mcl-1* mRNA across disease progression (Fig. 4.6). *Mcl-1* expression was expressed relative to wildtype mice for each timepoint and results show very little change in expression for any of the three disease progression timepoints.

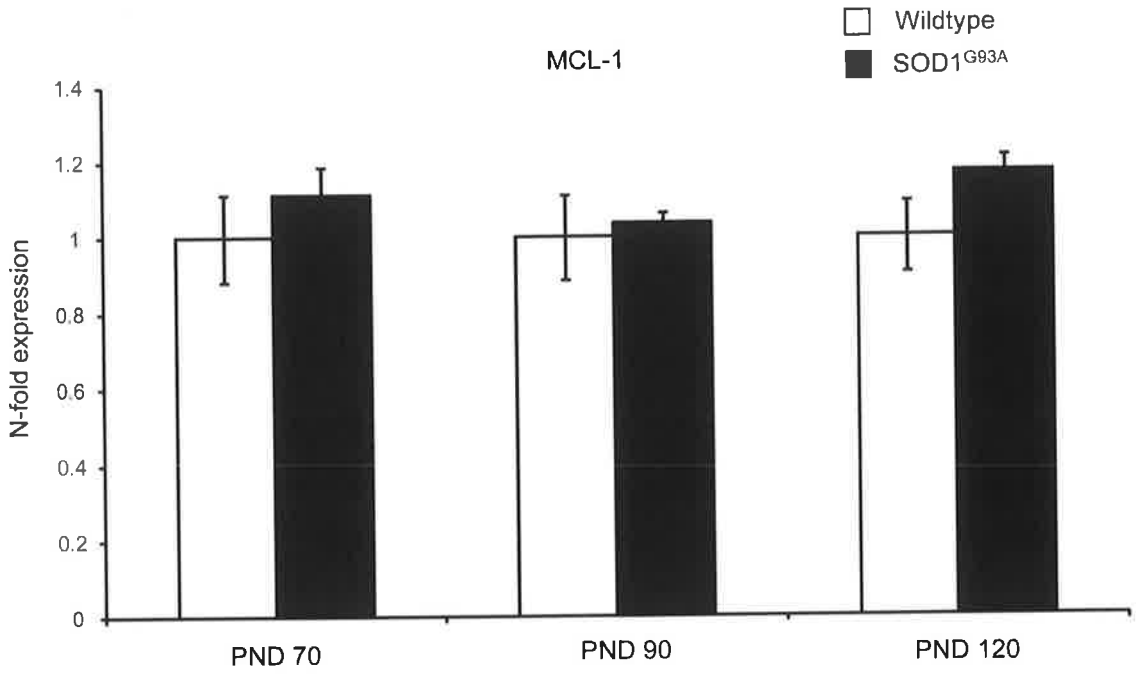

Figure 4.6: *Mcl-1* mRNA is not differentially regulated during disease progression in SOD1^{G93A} mice. *Mcl-1* mRNA expression levels were analysed in lumbar spinal cord samples from wildtype and SOD1^{G93A} mice at PND 70, PND 90 and PND 120 using RT-qPCR. Expression levels were normalised to β-actin control and expressed relative to wildtype mice at each time point. Data are represented as mean ± SEM from n=5 mice per group

4.3 Discussion

Our previous results have demonstrated a role for miR-29a and MCL-1 in the control of ER stress-induced cell death in primary cortical neurons. Whether or not miR-29a acts to sensitise neurons to ER stress-induced insults through targeting of MCL-1, as we can hypothesise from our results in cortical neurons, or some as-of-yet unknown target, is still a topic of investigation. Knowing that miR-29a targets MCL-1 (Mott *et al.*, 2007) and due to the importance of MCL-1 in the context of neuronal cell death (Germain *et al.*, 2011), we wanted to identify what miR-29a targeting MCL-1 could mean in the context of disease. ALS is a neurodegenerative disease where neuron loss is due to a combination of cytotoxic cellular insults including inflammation, oxidative stress and ER stress (Cheah *et al.*, 2010). Although the area of research into microRNAs in ALS is currently small and largely unexplored, miR-29a has been identified as potentially up-regulated in the brains of ALS patients (Shioya *et al.*, 2010). While ER stress and activation of the UPR have been identified as early events in motoneuron degeneration in SOD1 mutant mice (Walker and Atkin, 2011), it is possible that increased miR-29a expression following ER stress induction propagates motoneuron degeneration and ALS disease progression. We aimed to locate and identify changes in miR-29a expression during disease progression in a SOD1 mouse model.

Before advancing to an *in vivo* model of ALS, it was important to ascertain miR-29a and MCL-1 expression levels in our $SOD1^{G93A}$ mouse system and to analyse if this was similar to our work in cortical neurons. Our $SOD1^{G93A}$ mice are ideal for looking at possible therapeutics for familial ALS but due to constraints of availability and cost, we chose to do some preliminary work in C57 BL/6 mice, the genetic background onto which all $SOD1^{G93A}$ mice in our colony are bred. In C57 BL/6 mice we identified increased miR-29a expression in organs of the CNS, most notably the cortex, lumbar spinal cord and the

hippocampus compared to the liver. ALS is characterised by increased neuronal apoptosis in the lumbar spinal cord and motorcortex (Bains and Shaw, 1997) and increased levels of miR-29a could be a causative factor through mediating apoptosis. Interestingly we found *Mcl-1* mRNA levels to be higher in the heart, the liver and the spleen while being comparatively lower in organs of the CNS. MCL-1 distribution in human tissue similarly identified MCL-1 abundance in epithelial tissue and muscle tissue but little or no MCL-1 expression in the brain and spinal cord (Krajewski *et al.*, 1995). Correlation analysis of miR-29a and MCL-1 expression levels for all organs identified a significant correlation between miR-29a upregulation in certain organs and Mcl-1 downregulation in the same organs. This strengthens the hypothesis of an antagonistic relationship for miR-29a and MCL-1. Further analysis of miRNA expression in some organs of the CNS of these mice also identified miR-29a as more highly expressed than miR-193a and miR-148a. Binding sites for members of both the miR-29 and miR-193 families have been previously identified for MCL-1 (Mott *et al.*, 2007). However, due to the increased abundance of miR-29a in the mouse CNS, it is possible to deduce that miR-29a is modulating MCL-1 in the CNS.

ALS is a disease of motoneurons and $SOD1^{G93A}$ mice lose motoneurons from the ventral horn of the lumbar spine (Gurney *et al.*, 2004). Using *in situ* hybridization, we localized miR-29a expression to the grey matter of lumbar spinal cord tissue sections from $SOD1^{G93A}$ mice. In the spinal cord, the outer ring of white matter contains myelinated/non-myelinated nerve fibers, oligodendrocytes, astrocytes and microglial cells (Sherwood, 2012). The axons of the neurons run in tracts through the white matter. The inner butterfly-shaped grey matter contains the cell bodies of the neurons as well as astrocytes and microglial cells. miR-29a has been identified as specifically enriched in the dendritic spines of neurons where it targeted Arpc3 and affected actin cytoskeleton remodeling in hippocampal neurons (Lippi *et al.*, 2011). Dendrites are specifically found in the grey matter of both the

brain and spinal cord (Skibo and Pogorelaia, 1978) and support the miR-29a localisation we see *in situ.*

For $SOD1^{G93A}$ mice, disease progression is defined as PND 70, presymptom onset, PND 90 represents symptom onset and PND 120 is a disease progression paradigm (Vinsant, 2013a). We identified strong miR-29a expression in the grey matter of the lumbar spinal section in PND 70, PND 90 and PND 120 $SOD1^{G93A}$ samples while strong expression was only seen for PND 90 and PND 120 wildtype section with very weak signal was identified for PND 70 sections. This result suggests that miR-29a expression is induced or upregulated earlier in $SOD1^{G93A}$ mice compared to wildtype mice and may play a role in the increased ER stress that has been identified in ALS disease pathology (Lindholm *et al.*, 2006). Indeed ER stress has been identified as an early pathological event in motoneuron degeneration in SOD1 mice (Saxena *et al.*, 2009) and supports our finding of increased miR-29a expression in PND 70 spinal cord from transgenic mice compared to wildtype mice. ER stress has been identified in age-related cellular degeneration due to decreased expression of ER molecular chaperones such as GRP78 (Macario and Conway de Macario, 2002). This failure of the protein-folding capacity can present as neurodegeneration accompanied by the presence of protein aggregates, as seen in diseases such as AD (Salminen *et al.*, 2009b). The presence of insoluble mutant SOD1 protein complexes in the spinal cord during early ALS disease progression (Johnston *et al.*, 2000) suggest that ER stress is an early event in SOD1 mutant mice and propagates ER stress-induced apoptosis during disease progression.

Comparative image analysis of miR-29a stained sections and Nissl-stained consecutive sections confirmed miR-29a expression in ventral horn motoneurons from $SOD1^{G93A}$ mice for all timepoints. Wei *et al.* identified miR-29a expression in rat motoneuron although this expression was low compared to other neural cells (Wei *et al.*, 2010).

While PND 70 sections from SOD1^{G93A} mice had higher miR-29a expression than PND 70 wildtype, miR-29a expression in PND 90 and PND 120 SOD1^{G93A} mice was slightly lower than wildtype. We hypothesised that this shift in expression could be due to loss of motoneurons during disease progression in SOD1^{G93A} mice. Motoneuron counts in each section analysed from PND 70, PND 90 and PND 120 identified little difference in motoneuron density for PND 70 sections from wildtype and SOD1^{G93A} mice while PND 90 and PND 120 motoneuron counts showed significant loss of motoneurons in SOD1^{G93A} mice compared to wildtype mice. Mutant SOD1 aggregation has been shown to induce early motoneuron damage (Bruijn and Cudkowicz, 2006) while mutant SOD1 expressed in astrocytes and microglia has been shown to propagate loss of motoneurons later in disease stage (Nagai *et al.*, 2007, Boillee *et al.*, 2006b). While PND 90 is classed as symptom onset (Garbuzova-Davis *et al.*, 2007), the variable nature of the disease and the loss of motoneurons needed to initiate visible symptoms can account for the level of motoneuron loss seen in our sectioned spines.

Examining *Mcl-1* mRNA expression in lumbar sections we identified similar expression levels of *Mcl-1* mRNA between SOD1^{G93A} mice and wildtype mice. Furthermore *Mcl-1* expression levels did not alter significantly across SOD1^{G93A} disease progression. It is understood that miRNAs target mRNA for translational repression and mRNA sequestration or degradation (Esau and Monia, 2007, Soifer *et al.*, 2007). miR-29a may be targeting *Mcl-1* mRNA for sequestration and may not induce *Mcl-1* degradation and a subsequent decrease in *Mcl-1* mRNA levels. The absence of altered *Mcl-1* mRNA levels could also indicate that miR-29a is targeting *Mcl-1* mRNA for translation inhibition thereby decreasing MCL-1 protein levels as opposed to targeting *Mcl-1* mRNA for degradation. It could also indicate miR-29a targeting other mediators of ER stress-induced apoptosis in the SOD1^{G93A} spinal cord. Furthermore, it is important to note that the RT-qPCR was conducted on whole lumbar sections that consist of a mixed population

of cells and do not reflect solely the expression of MCL-1 in motoneurons. This could mask the effect of miR-29a modulating MCL-1 in motoneuron populations or indeed other neuronal populations. Furthermore, in melanoma cell lines, ER stress-induction with tunicamycin or thapsigargin was shown to increase *Mcl-1* mRNA levels (Jiang *et al.*, 2008). A subsequent decrease in MCL-1 protein level could lead to a transcriptional feedback loop to increase *Mcl-1* mRNA induced during ER stress to promote cell survival. Since we see downregulation of MCL-1 during ER stress in our cortical neuron model and the lack of change in *Mcl-1* mRNA expression in transgenic mice demonstrated here suggests a role for other targets of miR-29a in mediating ER stress in SOD1^{G93A} mice.

Our work here further characterizes miR-29a and its proposed target MCL-1 in a C57 BL/6 mouse model. This was an important starting point for further *in vivo* exploration. Having identified miR-29a in the lumbar spinal cord we could confidently assess miR-29a localization in the lumbar spine from SOD1^{G93A} mice. We identified miR-29a expression induced in SOD1^{G93A} mice at an earlier timepoint than wildtype mice suggesting a role for ER stress early in ALS disease onset and progression. We identified miR-29a expression in motoneurons of the ventral horn of the lumbar spine and identified loss of motoneurons at PND 90 and PND 120 in SOD1^{G93A} mice. Furthermore we identified no change in *Mcl-1* mRNA levels in SOD1 lumbar spine compared to wildtype across disease progression, suggesting a role for other targets of miR-29a in mediating ER stress-induced apoptosis. The results here identify a potential role for miR-29a in motoneuron loss and lumbar degeneration in a SOD1^{G93A} model of ALS and suggest that modulation of miR-29a expression in the CNS of transgenic mice may be of therapeutic benefit.

CHAPTER 5

A role for miR-29a in modulating motoneuron loss and lifespan in a SOD1^{G93A} mouse model of ALS

5.1 Introduction

In the previous chapter we established the baseline miR-29a expression levels in organs from a C57 BL/6 mouse. From these studies, it was apparent that the expression levels of miR-29a were higher in organs of the CNS, most notably the lumbar spine, cortex and hippocampus compared to the heart, the liver and the spleen. Furthermore, utilising *in situ* hybridisation we confirmed miR-29a expression in the grey matter of lumbar spinal sections from PND 70, PND 90 and PND 120 $SOD1^{G93A}$ mice. Differential expression of miR-29a was identified at PND 70 with increased miR-29a staining in $SOD1^{G93A}$ mouse lumbar spinal sections compared to wildtype mice. Nissl staining of adjacent sections had identified that at least some of the miR-29a positive cells were motoneurons in the ventral horn of these mice suggesting a role for miR-29a during motoneuron loss in ALS mice.

The $SOD1^{G93A}$ ALS disease model is an example of a chronic neurodegenerative disease model associated with increased expression of ER stress markers (Nagata *et al.*, 2007, Nishitoh *et al.*, 2008). We identified increased miR-29a expression during ER stress in cortical neurons and, furthermore, demonstrated that loss of miR-29a protected neurons from ER stress-induced cell death. Indeed, work in our lab previously identified upregulation of GRP78 and CHOP during disease progression and demonstrated that loss of PUMA, involved in ER stress-induced neuronal apoptosis, was protective against ER stress-induced apoptosis of motoneurons in a $SOD1^{G93A}$ model of ALS (Kieran *et al*, 2007). Given that we found miR-29a knockdown to be protective during ER stress *in vitro* and having established a link between both miR-29a and the $SOD1^{G93A}$ disease model, it was imperative to examine miRNA modulation *in vivo*. As previously discussed, our $SOD1^{G93A}$ mouse model (Gurney *et al.*, 1994) is the

benchmark for research in familial ALS and is a long-studied system in our lab. All therapeutic agent studies in ALS have been performed in $SOD1^{G93A}$ mice to date (Jackson *et al.*, 2002), with the results and efficacy of previous therapeutic studies closely matching the results for human ALS clinical trials with the same therapy; riluzole is a prime example of this (Miller *et al.*, 1996). The $SOD1^{G93A}$ transgenic mice demonstrate progressive loss of motoneurons and the $SOD1^{G93A}$ mutation has been shown to be pathogenic due to a toxic gain of function (Acevedo-Arozena *et al.*, 2011).

Functional therapies for ALS are very few. Many therapies focus on maintaining a patient's comfort and managing complications as the disease progresses rather than acting as a cure for the disease (Miller *et al.*, 2009a). The three most common palliative therapies for patients include non-invasive ventilation (NIV), percutaneous endoscopic gastronomy (PEG) and the drug riluzole. Riluzole blocks tetrodotoxin-sensitive sodium channels in neurons and prevents downstream activation of glutamate receptors. Riluzole, the only available drug therapeutic for ALS patients, prolongs life by maximum 2-3 months but does not abrogate symptoms (Miller *et al.*, 2009b). The variability of phenotypes and lack of understanding surrounding fundamental mechanisms of the disease have made finding functional therapies difficult (Ravits and La Spada, 2009). MicroRNA-based therapeutics have been a novel and much anticipated therapeutic prospect since their discovery (Burnett and Rossi, 2012). While animal studies have proved highly effective, the translation to humans is still being investigated with clinical trials for certain miRNAs already underway (Bouchie, 2013). The work presented by this research project *in vitro* thus far suggests a possible role for miR-29a in an ALS paradigm and a potential therapeutic role for miR-29a modulation in $SOD1^{G93A}$ ALS mice *in vivo*.

Due to phenotypic variation and inter-individual variations in patients, there are strict guidelines referring to ALS disease models. Studies in

SOD1^{G93A} mice have strict design parameters set in place (Scott *et al.*, 2008). Treatment groups should be sex-matched (equal numbers of males and females in each group) and litter-matched (litter mates have similar ages of disease onset and progression) while high treatment group numbers reduce noise (Ludolph *et al.*, 2007). Previous in-depth analysis of the SOD1^{G93A} mouse model of ALS found a clear difference in male and female disease onset and lifespan with female lifespan averaging 4 days more than males and an overall average lifespan of 134±10days (Gurney *et al.*, 1994, Scott *et al.*, 2008, Veldink *et al.*, 2003). Disease onset is defined from peak bodyweight measurements for all animals and from decreasing neurological score which can include assessment through motorfunction analysis, including paw grip endurance (PaGE) testing and gait analysis, both of which are assessed in this study (Ludolph *et al.*, 2010). Endstage is defined as "the inability of an animal to right itself within 15-30 seconds if laid on either side" and occurs at approximately PND 160 (Leitner, 2009).

Following these guidelines, we sought to investigate the effect of downregulating miR-29a in the CNS of wildtype and SOD1^{G93A} mice. We aimed to administer an experimentally-derived dose of miR-29a antagomir *in vivo* to the brain and spinal cord of 39 mice (approximately n=4-6 per sex-matched treatment group) through intracerebroventricular injection. We ICV-injected our scrambled or miR-29a antagomir into wildtype mice to conduct preliminary analysis of our miR-29a antagomir which allowed us to choose an optimum experimental dose and measure efficacy of our delivery system. Once the efficacy of the antagomir-mediated knockdown was established in wildtype mice, we conducted a full study of scrambled antagomir and miR-29a antagomir ICV-injected wildtype and SOD1^{G93A} mice and investigated the effects on motorfunction and lifespan through disease progression.

5.2 Results

5.2.1 Antagomir-mediated knockdown of miR-29a delivered through ICV injection *in vivo*

To confirm surgical accuracy, a representative mouse had haematoxylin and eosin (H&E) stain injected directly into the cerebral ventricles to demonstrate accuracy of surgical technique. The brain was sectioned post-mortem and H&E stain was visualised and confirmed present in the cerebral ventricle (Fig 5.1.1). This results confirmed accuracy of stereotaxic coordinates in delineating the position of the ICV injection.

The first step in designing our *in vivo* animal study was to determine the optimal dose of miR-29a antagomir needed to induce miR-29a knockdown following ICV administration. Previous work on antagomir-modulation in our lab had looked at 3 doses in mice – 0.12 nmol, 0.5 nmol and 1.0 nmol (Jimenez-Mateos *et al.*, 2012). Although the antagomirs used in that study target different miRNAs, the manufacturer was the same, antagomirs were LNA-modified and contained a cholesterol tag in both instances and we chose to use these three doses for our dose-response study. miR-29a antagomir, scrambled antagomir or a CSF control were delivered by ICV injection directly to the cerebral ventricles and mice were monitored for 72 h before being sacrificed. Spinal cord was separated into lumbar and thoracic portions and the brain was micro-dissected into the cortex and hippocampus. RT-qPCR was used to assess miR-29a expression levels for each dose of antagomir. The 0.12 nmol and 0.5 nmol doses did not show consistent miR-29a knockdown with the miR-29a antagomir across all three organs (Fig. 5.1.2C, Fig. 5.1.2B) while the 1.0 nmol miR-29a antagomir dose demonstrated knockdown in the lumbar, the cortex and the hippocampus tissue (Fig. 5.1.2A) compared to scrambled control. Statistical significance could not be obtained due to low sample size; however effect of miR-29a antagomir in all three tissues was apparent and made it a viable choice for our *in vivo* model.

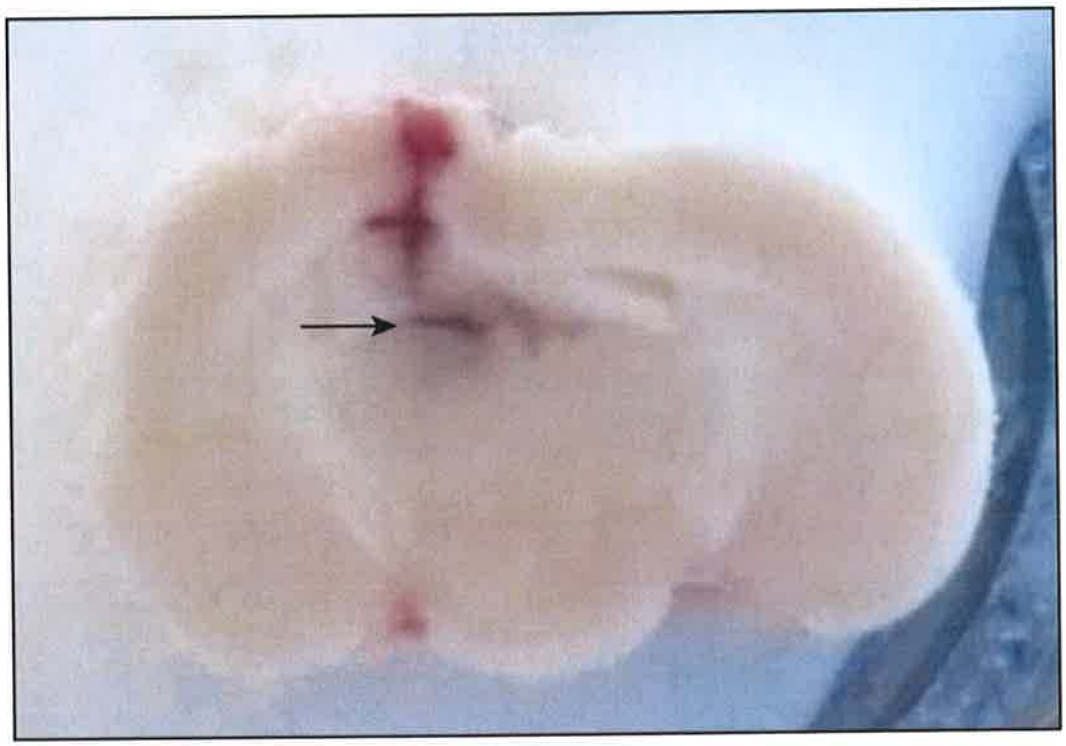

Figure 5.1.1: Visualisation of ICV injection to the right lateral cerebral ventricle. Wildtype C57 BL/6 mouse ICV injected with haematoxylin and eosin (H&E) stain and sacrificed immediately afterwards. Brain was dissected post-mortem and sectioned on the cryostat. Stain was confirmed by eye and imaged by digital camera. Image was analysed using ImageJ software.

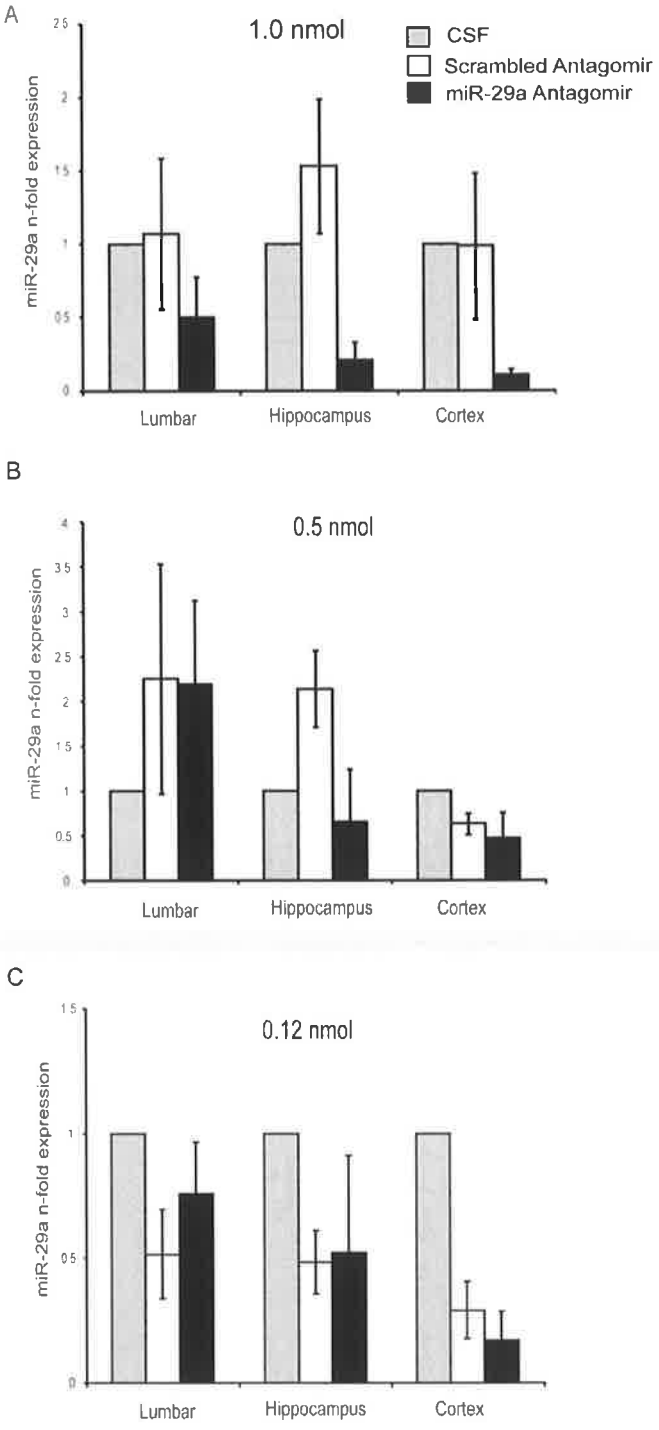

Figure 5.1.2: Antagomir mediated knockdown of miR-29a through ICV injection *in vivo*. PND 90 C57 BL/6 mice were ICV injected with 1.0 nmol (A), 0.5 nmol (B) or 0.12 nmol (C) scrambled or miR-29a antagomir diluted in CSF (2 µl) and sacrificed after 72 h. A non-treatment control group were given an ICV injection of CSF fluid alone and incubated for 72 h. Mice were perfused with PBS and organs were

harvested. RT-qPCR analysis of miR-29a expression was conducted. Expression levels were normalized to RNU19 control and expressed relative to CSF control-treated mice. No significance, ANOVA (*post-hoc*, Tukey) was used to assess statistical significance. Data are represented as means ± SEM from n = 3 mice per treatment group.

5.2.2 miR-29a antagomir 1.0 nmol dose does not have miRNA-associated off target effects in C57 BL/6 mice

Having chosen our optimum dose for miR-29a antagomir-mediated knockdown, it was important to assess any off-target effects our dose might have on other miRNAs in our tissues of interest. Using RNA from our 1.0 nmol scrambled- or miR-29a antagomir-dosed mice, we analysed expression levels for other miRNAs of interest: miR-193a, -148a, -376a. RT-qPCR analysis did not show any significant change in expression of the three miRNAs in any of our CNS tissue samples. The cortex showed some variability for miR-193a (A), miR-148a (B) and miR-376a (C) but as this is the principal site of injection it is likely that the trauma of surgery or inflammation at the site of injection could increase variability of results from this tissue sample. It was not possible to control for small changes brought about by surgical trauma although all efforts were made to minimise any trauma and to keep mice as uniform as possible. LNA-modifications to antagomirs such as our LNA-modified miR-29a antagomir, increases stability *in vitro* and *in vivo* and increase antagomir specificity for its target miRNA (van Rooij, 2011). We were confident that the 1.0 nmol dose of miR-29a antagomir was not mediating a change in our mouse model through off-targeting of other miRNAs and that any changes we saw in our mice were likely mediated in part by the modulation of miR-29a expression.

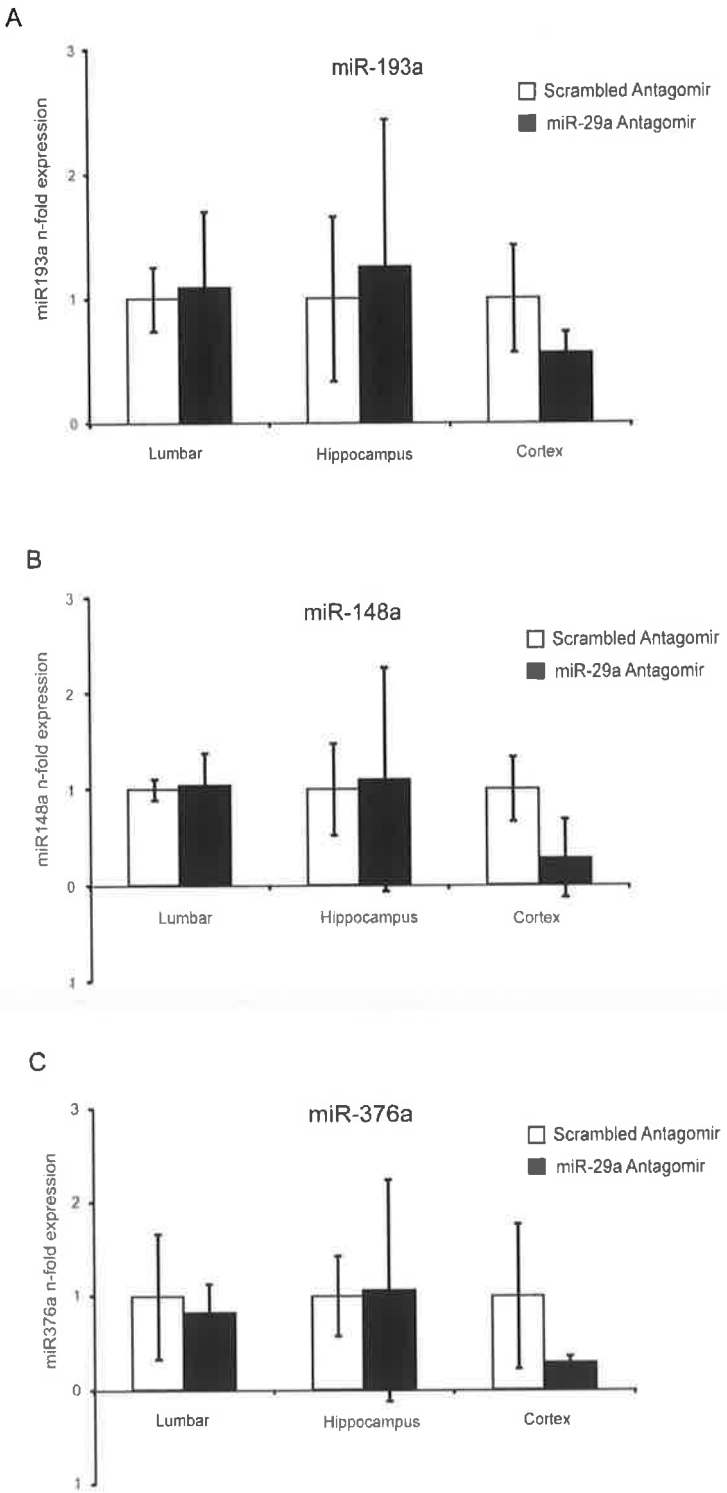

Figure 5.2: miR-29a antagomir does not mediate off-target effects at 1.0 nmol dose in organs of the CNS. PND 90 C57 BL/6 mice were ICV injected with 1.0 nmol scrambled or miR-29a antagomir diluted in artificialCSF (2 µl) and sacrificed after 72 h. RT-qPCR analysis of miR-193a (A) , miR-148a (B) and miR-376a (C) expression levels were conducted. Expression levels were normalized to RNU19 control and

expressed relative to scrambled antagomir-treated mice. No significance, independent t-test was used to assess statistical significance. Data are represented as means ± SEM from n = 3 mice per treatment group.

5.2.3 Antagomir-mediated miR-29a knockdown detectable 30 days post-injection

We had established a suitable dose of miR-29a antagomir for our system, a dose that induced knockdown in our three primary CNS tissues but did not significantly modulate other miRNAs in these tissues. Next it was necessary to look at the duration in which knockdown could be sustained. In our transgenic animals, surgery and ICV antagomir administration would occur at PND 70, a presymptom onset timepoint, and motorfunction analysis would be carried out from PND 84 until endstage. The antagomir was administered in a single dose to minimise trauma to the animals and to ensure that a repeat procedure did not interfere with the motorfunction analysis. Due to the length of time of disease progression and the need for a single administration of antagomir, it was important to establish that the effect of our antagomir remained for a lengthy period of time following injection. We chose to check knockdown at 10 days and 30 days post-injection. We found significant levels of miR-29a knockdown in the cortex and hippocampus of C57 BL/6 wildtype mice at 10 days post-injection (Fig. 5.3A). This significant knockdown was maintained in the cortex at 30 days post injection. Knockdown of miR-29a was still seen in the lumbar spine and hippocampus at 30 days post injection but efficacy was reduced (Fig. 5.3B). The presence of continued knockdown up to 30 days post-antagomir administration suggested that miR-29a knockdown using antagomirs *in vivo* could modulate miR-29a and miR-29a target expression in a therapeutic manner, possibly through modulation of ER stress *in vivo*.

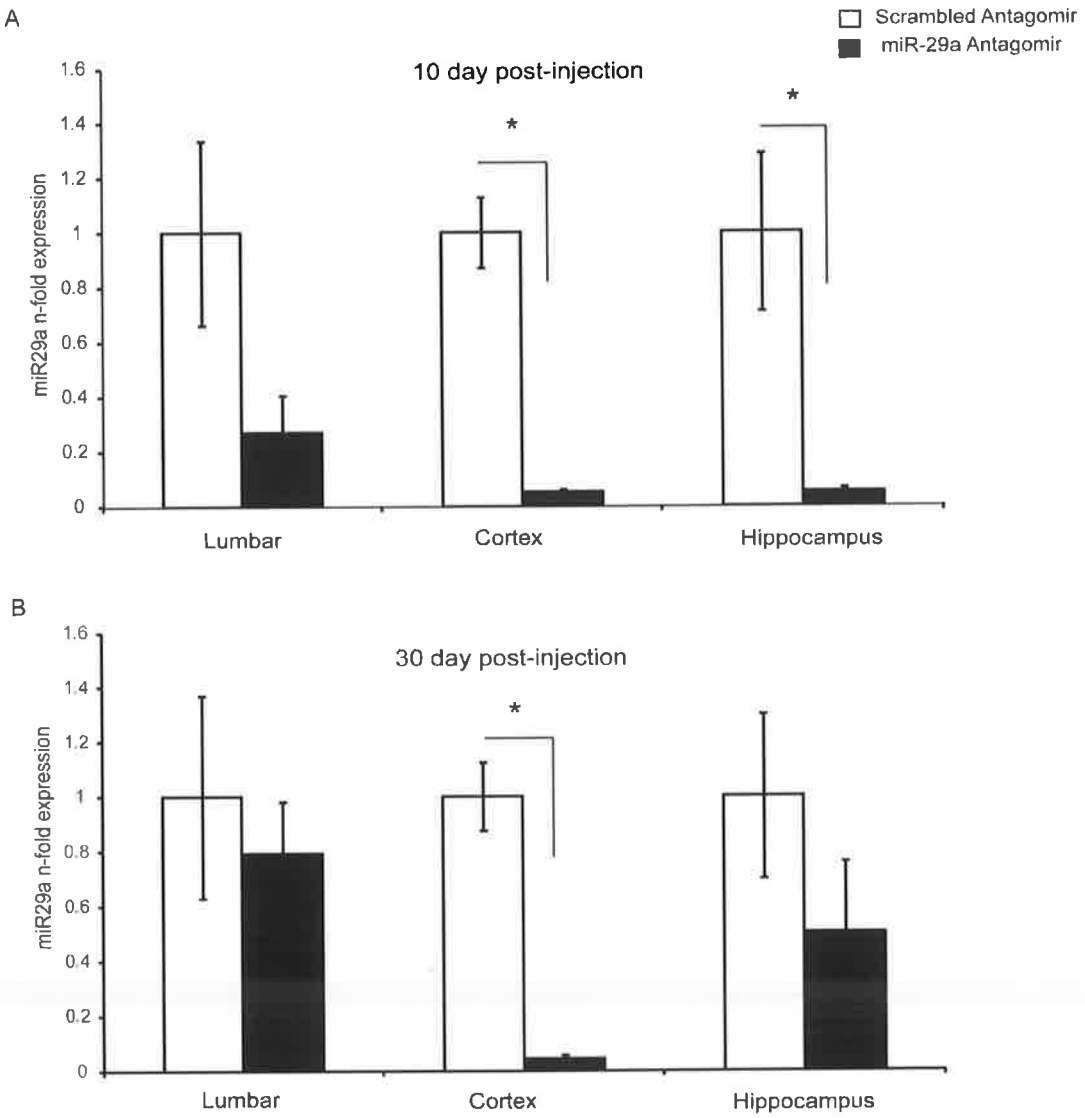

Figure 5.3: Significant and detectable miR-29a knockdown at 10 days and 30 days post-antagomir injection. PND 90 C57 BL/6 mice were ICV injected with 1.0 nmol scrambled or miR-29a antagomir diluted in CSF (2 µl) and sacrificed after 10 days (A) or 30 days (B) post-injection. RT-qPCR analysis of miR-29a expression levels was conducted. Expression levels were normalized to RNU19 control and expressed relative to scrambled antagomir-treated mice. Data are represented as means ± SEM from n = 4 mice per treatment group. *P<0.05 compared to scrambled antagomir-treated mice. (Mann-Whitney U test)

5.2.4 Antagomir-mediated miR-29a knockdown modulates *Mcl-1* expression *in vivo*

We previously identified a role for miR-29a antagomir knockdown in cortical neurons modulating *Mcl-1* expression *in vitro.* Having identified miR-29a knockdown *in vivo* using specific miRNA antagomirs, it was important to look at changes in expression of the identified miR-29a target, MCL-1. Firstly we looked at *Mcl-1* expression levels 72 h post injection with 1.0 nmol scrambled, miR-29a antagomir or CSF control. In the lumbar and cortex miR-29a antagomir-treated samples, we saw a marginal increase compared to scrambled treated samples (Fig. 5.4A). The hippocampus showed little change in expression for these samples. We also looked at *Mcl-1* levels in 10 day post-injection samples. We chose the 10 days samples as these had maintained significant levels of miR-29a knockdown in all three CNS tissues compared to 30 day samples. Again in these samples, a slight increase in *Mcl-1* mRNA could be seen in lumbar and hippocampus samples; however these changes were not significant (Fig. 5.4B). We previously demonstrated *Mcl-1* as expressed in low levels in the CNS relative to other organs from C57 BL/6 mice. The relatively low abundance of *Mcl-1* in the lumbar, cortex and hippocampus may account for the small increase in *Mcl-1* levels that we see with miR-29a knockdown.

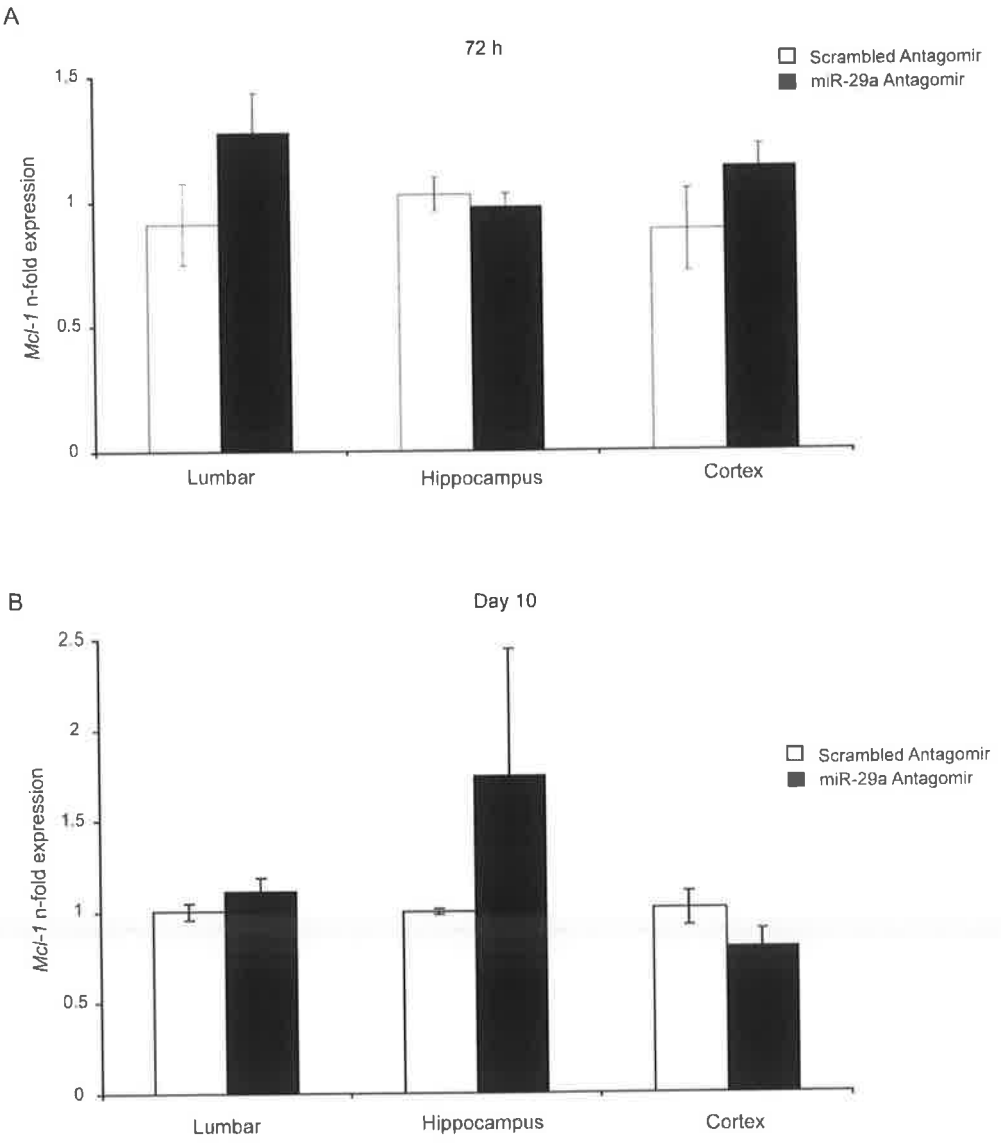

Figure 5.4: Modulation of miR-29a mediates change in *Mcl-1* mRNA expression *in vivo*. (A) PND 90 C57 BL/6 mice were ICV injected with 0.12 nmol, 0.5 nmol or 1.0 nmol scrambled or miR-29a antagomir diluted in CSF (2 µl) and sacrificed after 72 h. A non-treatment control group were given an ICV injection of 2 µl CSF fluid and incubated for 72 h. RT-qPCR analysis of *Mcl-1* expression levels were conducted. Expression levels were normalized to β-actin control and expressed relative to CSF control treated mice. Data are represented as means ± SEM from n = 3 mice per treatment group. (B) PND 90 C57 BL/6 mice were ICV injected with 1.0 nmol scrambled or miR-29a antagomir and sacrificed 10 days post-injection. RT-qPCR analysis of *Mcl-1* expression levels was conducted. Expression levels were normalized to β-actin control and expressed relative to scrambled antagomir-treated mice. Data are represented as means ± SEM from n = 4 mice per treatment group.

5.2.5 SOD1^{G93A} model of miR-29a knockdown *in vivo* – examination of changes in motorfunction and lifespan

We conducted surgery on 39 mice at PND 70. This consisted of n=19 wildtype SOD1 mice (n=8 scrambled antagomir-treated and n=11 miR-29a antagomir-treated) and n=20 SOD1^{G93A} mutant mice (n=10 scrambled antagomir-treated and n=10 miR-29a antagomir-treated). In the case of males, nine were injected with scrambled antagomir and ten were injected with miR-29a antagomir. In females, nine were injected with scrambled antagomir and eleven were injected with miR-29a antagomir. Males and females were evenly numbered and litter-matched where possible. Following surgery, which took approximately 20 minutes per mouse, animals were left to recover for up to a week with water and food available *ad libitum*. Following the recovery period, each mouse was trained for motorfunction analysis for one week, sessions on Tuesday, Wednesday and Thursday (PND 77). The following week, approximately PND 84, measurements were recorded including weight (g), PaGE (s) and stride length (mm). Each test was designed to measure changes in disease progression through monitoring of weight loss or hind limb weakness, an indication of motoneuron loss (Kong and Xu, 1998). Every effort was made to conduct a blind test for each mouse so as to remove treatment-based bias from the analysis. Recordings were made in the same environment and at the same time of day each week. Mice were scored for each test and their average score for each week was plotted.

5.2.5.1 Scrambled- and miR-29a antagomir-treated SOD1^{G93A} mouse body weight decline is induced at the same time and rate

Peak body weight analysis was used to determine disease onset in SOD1^{G93A} mice (Ludolph *et al.*, 2007). Body weight has also been used to measure endstage with a loss of 20% bodyweight from maximum adult weight signalling experimental endstage (Banerjee *et al.*, 2008). Body weight, measured in grams, was assessed twice a week with the average of the two weights recorded for each week. Body mass is lost due to muscle wasting as motoneurons are lost with disease progression and due to an inability to access food as freely. Studies in mice and rat SOD1^{G93A} models indicate loss of motoneuron onset at PND 90 with subsequent loss of motorfunction and body weight to follow (Acevedo-Arozena *et al.*, 2011, Nagai *et al.*, 2001). While each mouse increased in body weight over the first 30 – 40 days, the wildtype and SOD1^{G93A} transgenic animals soon deviated from each other. While wildtype animals continued to steadily increase in weight, reaching approximately 25-30 grams for females and 30-35 grams for males, the transgenic animals began to steadily lose weight at approximately 119 days for both males (Fig. 5.5.1B) and females (Fig. 5.5.1A). The decline in body weight was the same for both scrambled- and miR-29a antagomir-treated male and female mice with no significant protection in body weight detected. We can assume that motoneuron loss occurred between approximately PND 112 and PND 119 and continued at a steady rate until endstage. There was no indication that miR-29a antagomir treatment in the transgenic mice affected loss of body weight or disease progression when all animals were analysed together (Fig. 5.5.1C).

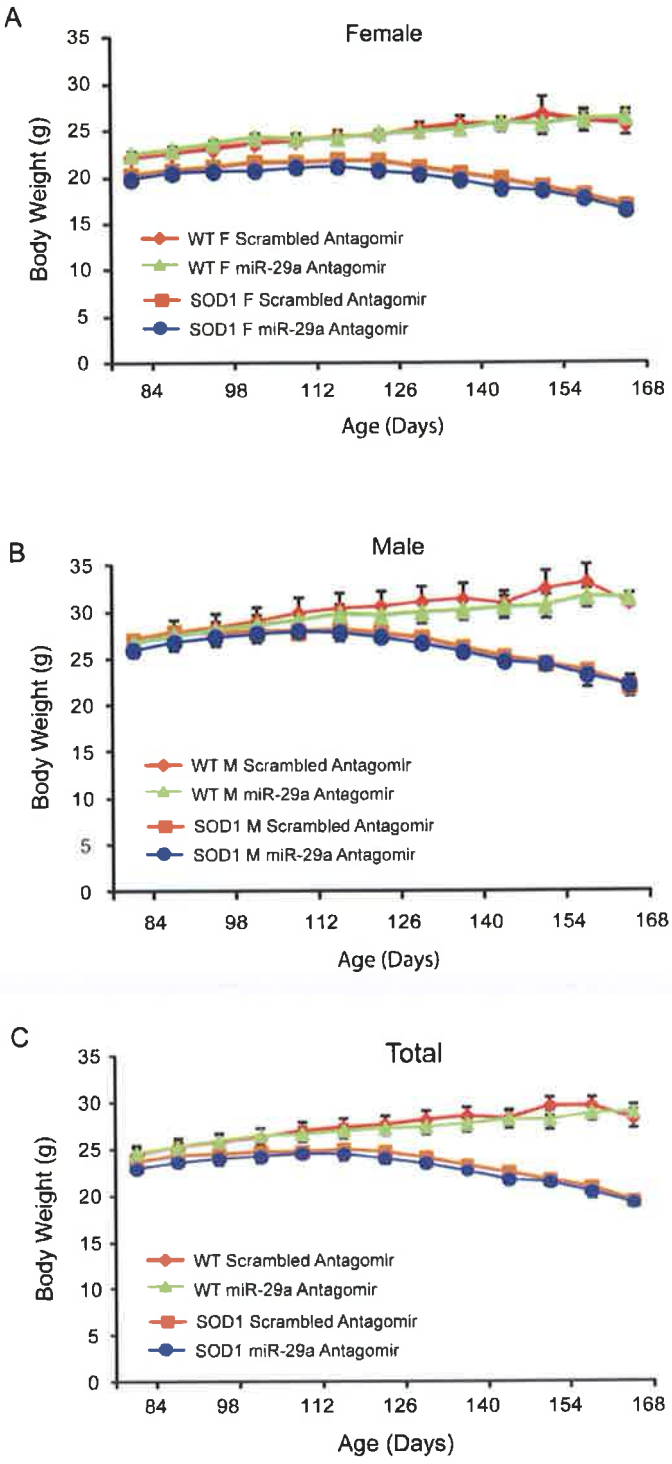

Figure 5.5.1: miR-29a antagomir-treatment does not maintain body weight in SOD1^{G93A} mice. Scrambled or miR-29a antagomir was administered through ICV injection at PND 70 and body weight was recorded from PND 84 onwards. Body weight was assessed twice weekly and the average weekly bodyweight was recorded for each mouse. Weight was measured on a laboratory scales and recorded in

grams. (A) Female mice: (Wildtype/Scrambled: PND 84-147; 4/ 154-161; 3/ 168; 2) (Wildtype/miR-29a Antagomir: PND 84-161; 6/ 168; 4) (SOD1 Transgenic/Scrambled: PND 84-168; 5) (SOD1 Transgenic/miR-29a Antagomir: PND 84-147; 5/ 154-168; 4) (B) Male mice: (Wildtype/Scrambled: PND 84-161; 4/ 168; 2) (Wildtype/miR-29a Antagomir: PND 84-154; 5/ 161; 4/ 168; 3) (SOD1 Transgenic/Scrambled: PND 84-133; 5/ 140-147; 4/ 154; 3/ 161; 2/ 168; 1) (SOD1 Transgenic/miR-29a Antagomir: PND 84-147; 5/ 154; 3/ 161-168; 2). (C) Total = combined female and male mouse numbers. No significance, ANOVA (*post-hoc*, Tukey) was used to assess statistical significance. Data are mean ± SEM n= 4-6 mice per sex-matched treatment group.

5.2.5.2 Paw Grip Endurance (PaGE) analysis identified loss of hind limb strength in SOD1^{G93A} mice irrespective of treatment

PaGE analysis measures hind limb strength and endurance over a 60 sec period for each mouse, in which they are suspended upsidedown on a mesh cage. PaGE was measured twice weekly and two values were recorded for each session, allowing the mouse to fall once and be replaced on the cage. The better of these two attempts was taken for that day and the average best latency period was recorded for each mouse for that week. All mice could maintain 60 sec on the training week (PND 77) and at commencement of motorfunction (PND 84). While females maintained grip endurance until approximately PND 98 (Fig. 5.5.2A), males began to decrease in grip from PND 91 onwards (Fig. 5.5.2B). We saw a trend towards miR-29a antagomir-treated males and females maintaining grip for slightly longer time periods than scrambled-treated animals; however this diminished over time and did not reach significance (Fig. 5.5.2C). Whilst males began to drop off consistently from PND 98 reaching complete loss of grip at PND 147, females maintained grip strength until PND 112 and then began to slowly decline until they could no longer maintain grip at PND 154.

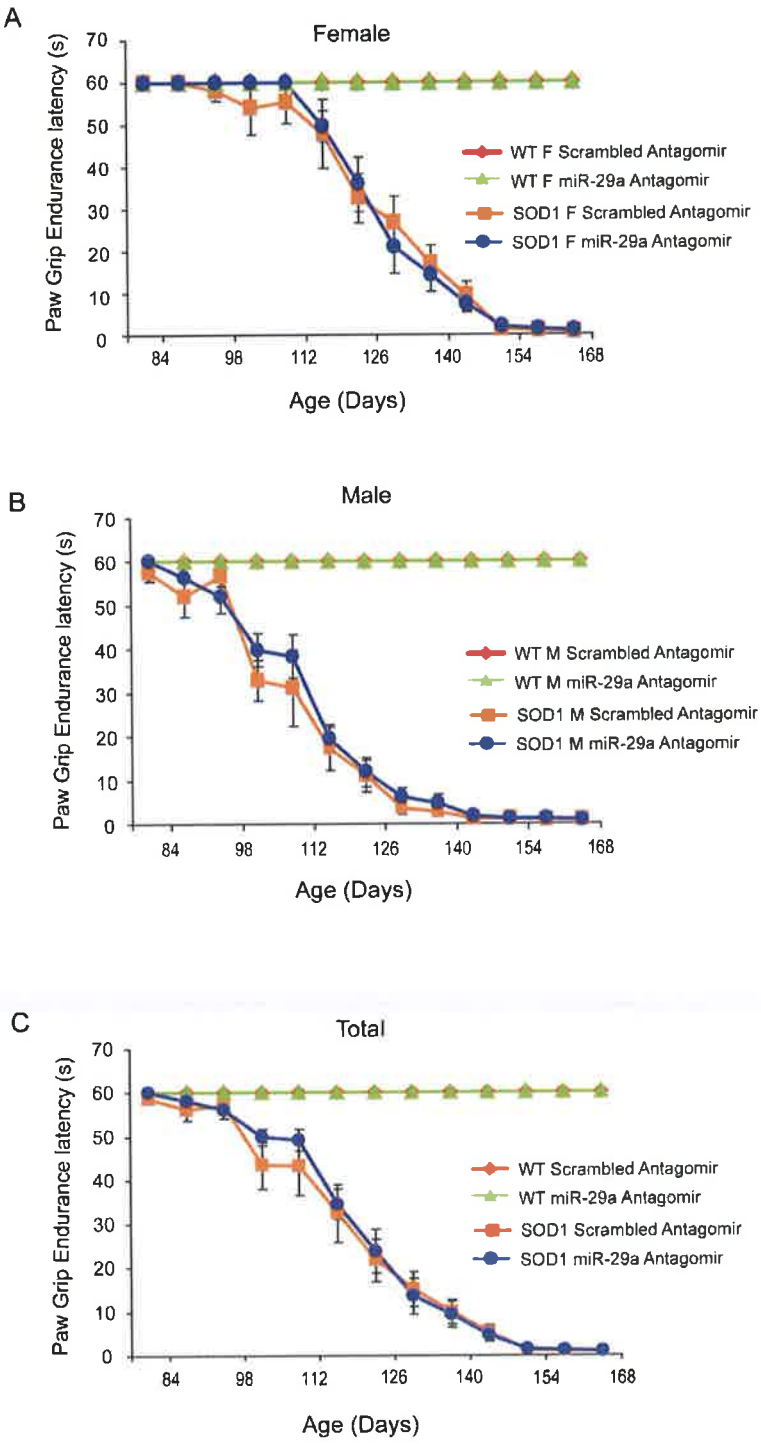

Figure 5.5.2: miR-29a antagomir knockdown does not protect muscle endurance across ALS disease progression in SOD1^{G93A} mice. Scrambled or miR-29a antagomir was administered through ICV injection at PND 70 and PaGE was recorded from PND 84 onwards. Mice were suspended on a mesh cage for up to 60 sec and latency to fall was recorded for each mouse. Two sessions were performed weekly with the average of the two recorded latencies recorded for each mouse at the end of each week. PaGE was measured in seconds

(s) and 60 sec was the maximum time achievable for each mouse. (A) Female mice: (Wildtype/Scrambled: PND 84-147; 4/ 154-161; 3/ 168; 2) (Wildtype/miR-29a Antagomir: PND 84-161; 6/ 168; 4) (SOD1 Transgenic/Scrambled: PND 84-168; 5) (SOD1 Transgenic/miR-29a Antagomir: PND 84-147; 5/ 154-168; 4). (B) Male mice: (Wildtype/Scrambled: PND 84-161 ; 4/ 168; 2) (Wildtype/miR-29a Antagomir: PND 84-154; 5/ 161; 4/ 168; 3) (SOD1 Transgenic/Scrambled: PND 84-133; 5/ 140-147; 4/ 154; 3/ 161; 2) (SOD1 Transgenic/miR-29a Antagomir: PND 84-147; 5/ 154; 3/ 161-168; 2). (C) Total = combined female and male mouse numbers. No significance, Mann-Whitney U test was used to assess statistical significance. Data are mean ± SEM n= 4-6 mice per sex-matched treatment group.

5.2.5.3 Decline in stride length is unabated by miR-29a knockdown in SOD1^{G93A} mice during disease progression

Stride lengths assessed the average width of each mouse's gait and indicated loss of hind limb strength and control. Stride length for each mouse was measured once a week. Each mouse had its hind feet painted with non-toxic paint and was made to walk along a sheet of paper. Four measurements were taken in millimetres (mm) from the centre of one paw to the next, for two consecutive strides and for both right and left limbs. The average of these four strides per mouse was recorded for each week. Measurements were taken in mid-stride across the sheet of paper to ensure it was a natural, uninterrupted stride.

Wildtype mice could maintain a stride of 60-70 mm irrespective of treatment across PND 84-168 (Fig. 5.5.3C). While scrambled-treated female mice maintained a slightly longer stride that miR-29a antagomir-treated female mice, both treatment groups had declining stride length from PND 119 onwards (Fig. 5.5.3A). Males began a steady decline in stride length from PND 98 onwards with a sharper decline than females for both treatment groups (Fig. 5.5.3B). Scrambled-treated males had the same stride length decline as miR-29a antagomir-treated males. Gait differences between males and females have been shown in SOD1 mice although differences in size and weight were not deemed contributing factors (Wooley *et al.*, 2005). As previously discussed, the sharper decline in stride length in males is likely due to the earlier disease onset seen in males compared to females (Suzuki *et al.*, 2007).

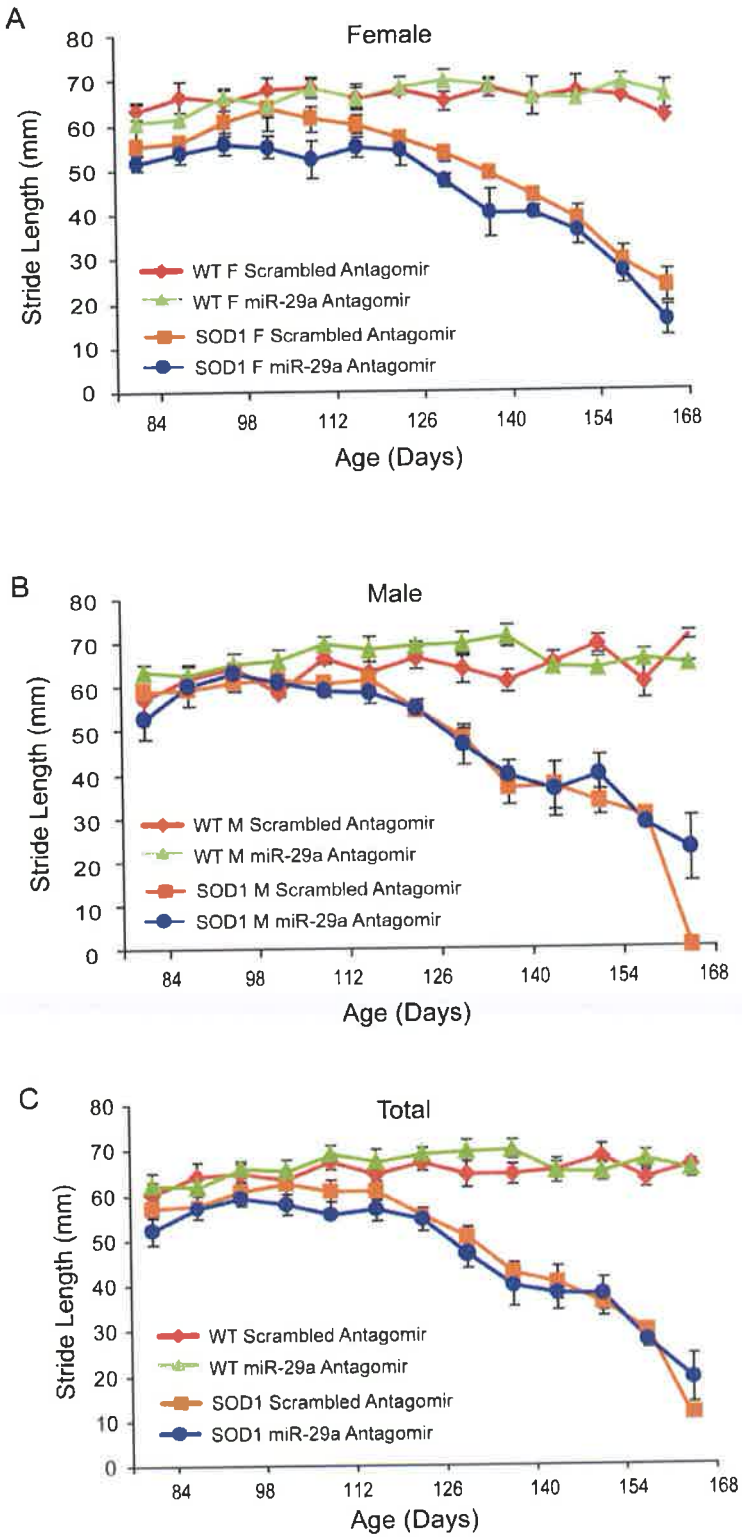

Figure 5.5.3: Loss of miR-29a has no affect on hind limb motility in SOD1^{G93A} mice across disease progression. Scrambled or miR-29a antagomir was administered through ICV injection at PND 70 and stride length was recorded from PND 84 onwards. The hind limbs of each mouse were painted with non-toxic paint and the mouse was

made to walk in a straight line along a sheet of paper. The distance from the mid-paw to the next mid-paw was measured in millimetres (mm) for two consecutive strides on the right and left feet. The average of the four stride lengths was recorded for each week and plotted against wildtype mice. (A) Female mice: (Wildtype/Scrambled: PND 84-147; 4/ 154; 3/ 161; 2/ 168; 1) (Wildtype/miR-29a Antagomir: PND 94-161; 6/ 168; 4) (SOD1 Transgenic/Scrambled: PND 84-154; 5/ 161-168; 4) (SOD1 Transgenic/miR-29a Antagomir: PND 84-140; 5/147-161; 4/ 168; 3). (B) Male mice: Wildtype/Scrambled: PND 84-161; 4/ 168; 2) Wildtype/miR-29a Antagomir: PND 84-154; 5/ 161; 3/ 168; 2) (SOD1 Transgenic/Scrambled: PND 84-126; 5/ 133-140; 4/ 147; 3/ 154; 2/ 161; 1) (Transgenic/miR-29a Antagomir: PND 84-140; 5/ 147; 4/ 154-168; 2). (C) Total = combined female and male mouse numbers. No significance, ANOVA (*post-hoc*, Tukey) was used to assess statistical significance. Data are mean ± SEM n= 4-6 mice per sex-matched treatment group.

5.2.6 Altering miR-29a expression prior to symptom onset in SOD1^{G93A} mice does not affect disease duration or survival

SOD1^{G93A} mice are endstage when they can no longer right themselves in under 30 seconds when placed on either side (Ludolph *et al.*, 2010). This criteria was used to assess when SOD1^{G93A} had reached endstage and were to be culled. Lifespan was calculated for each mouse from date of birth up to/and including the day they were culled. All mice were assessed equally and all attempts were made to remain unbiased in our approach. A total of 20 transgenic SOD1^{G93A} animals was analysed in this research project. A Kaplan-Meier survival plot was created showing the survival between transgenic scrambled-treated and transgenic miR-29a antagomir-treated mice. For each transgenic culled, a littermate wildtype was culled where appropriate. The wildtype mice had no disease symptoms or limb defects and are represented by red (miR-29a antagomir) and green (scrambled antagomir) continuous lines.

Female mice had no change in lifespan irrespective of treatment with scrambled antagomir or miR-29a antagomir (Fig. 5.6A). Male mice treated with miR-29a antagomir showed a trend towards a longer lifespan; however this did not reach significance (Fig. 5.6B). Overall, the total miR-29a antagomir-treated SOD1^{G93A} mice had a trend towards elongated lifespan in a subset of mice; however this was not significant (Fig. 5.6C).

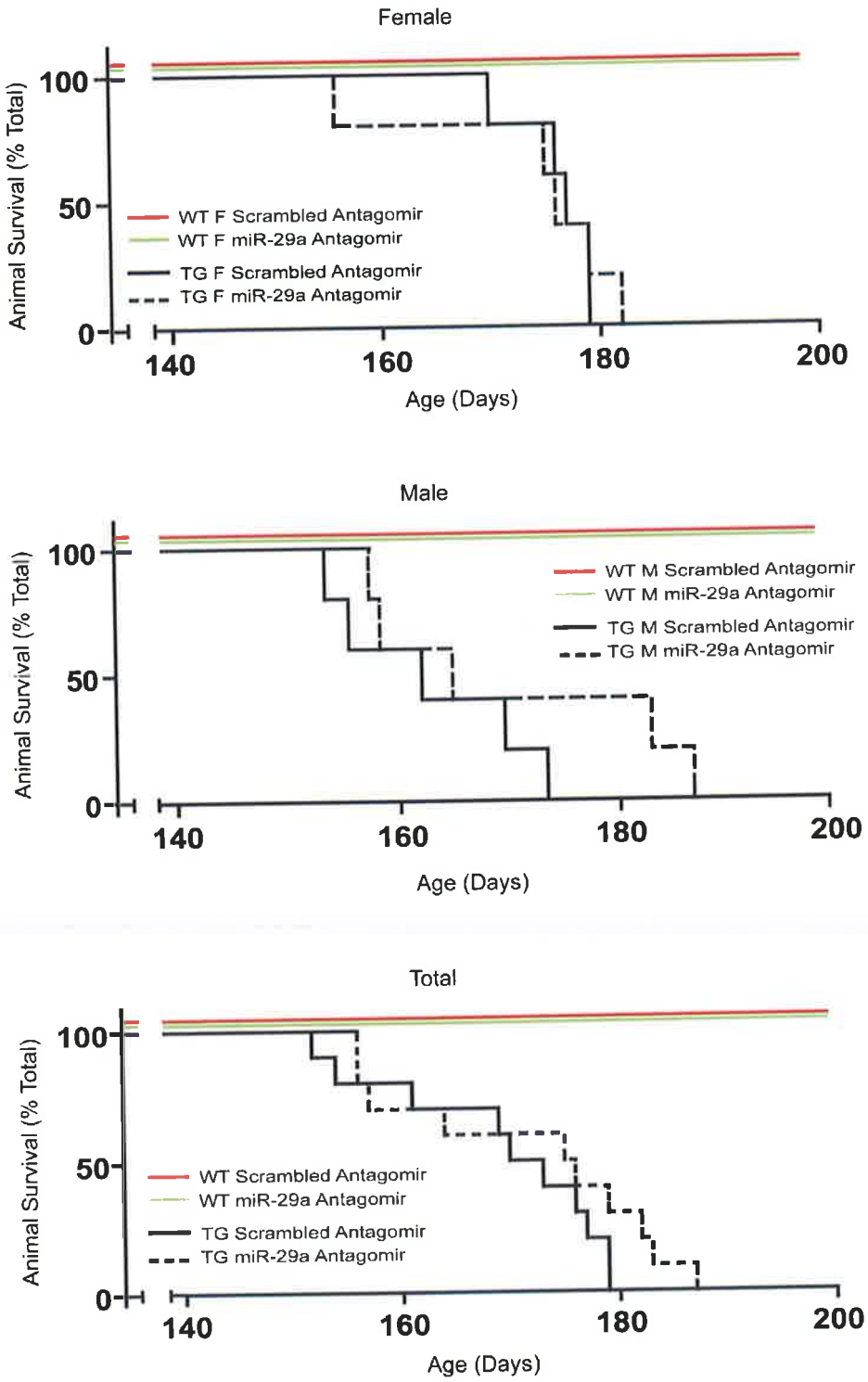

Figure 5.6: Loss of miR-29a demonstrated a trend towards elongated lifespan in a subset of SOD1^{G93A} mice. Scrambled or miR-29a antagomir was administered through ICV injection at PND 70 and mice were monitored throughout disease progression. Endstage was assessed through an inability for any one mouse to right itself within 30 sec when placed on either side. Endstage mice were culled

by intra-cardial perfusion. Lifespan was calculated from their date of birth up to/and including the day they were culled. Kaplan-Meier analysis was assessed using SPSS statistical analysis software. No significance, Mantel-Cox test was used to assess statistical significance. Data represent n= 20 $SOD1^{G93A}$ transgenic mice (n=10 males and n=10 females) and n=19 wildtype mice (n=9 males and n=10 females).

5.3 Discussion

While miR-29a has been identified in a subset of ALS patient samples (Shioya *et al.*, 2010), further research examining miR-29a modulation *in vivo* has yet to be established. Having identified a protective role for miR-29a antagomirs in neurons undergoing ER stress *in vitro* and with evidence to suggest that ER stress is an early pathogenic feature of ALS (Kieran *et al.*, 2007, Nishitoh *et al.*, 2008), we wanted to see the effects of examining miR-29a modulation in wildtype and $SOD1^{G93A}$ transgenic mice, focusing on motorfunction and lifespan analysis. We designed a method of antagomir delivery directly to the intracerebroventricular system that can by-pass the blood-brain barrier and allow the antagomir direct access to the spinal cord through the CSF. The blood-brain barrier and blood-cerebrospinal fluid barrier both hinder effective drug delivery to the CNS and prevent efficient dosing (Begley, 2004). Direct ICV injection of target-specific antagomirs can by-pass these barriers and has become popular in recent years with miRNA knockdown being shown to be protective in models of epilepsy (Jimenez-Mateos *et al.*, 2012) and ischemic stroke (Selvamani *et al.*, 2012).

Before a full study could be carried out, some crucial questions needed answering. A dose-response study using 0.12 nmol, 0.5 nmol and 1.0 nmol scrambled or miR-29a antagomir tested the efficacy of our antagomir *in vivo* and also allowed us to establish an optimum dose. We found no knockdown in the 0.12 nmol dose and variable knockdown in the 0.5 nmol dose; however the 1.0 nmol dose showed good knockdown of miR-29a in our three tissues of interest. Previous work in our lab had identified 0.5 nmol antagomir as optimum for knockdown of their chosen antagomir (Jimenez-Mateos *et al.*, 2012). While the mechanisms of antagomir-mediated knockdown are still unknown, studies have shown that antagomirs mediate target miRNA

degradation through some as-of-yet unknown mechanism (Krutzfeldt *et al.*, 2005).

Due to the potential of antagomir-based therapeutics, the specificity of our chosen antagomir needed to be assessed. While LNA-modified antagomirs are sensitive to single mismatched nucleotides in miRNA sequences (Kloosterman *et al.*, 2006, Krutzfeldt *et al.*, 2007), it was important to assess effects, if any, of our antagomir on some other miRNAs of interest. Furthermore, due to the high concentration of antagomir we proposed to use we had to examine any off-target effects of the antagomir. We examined levels of miR-193a, miR-148a and miR-376a in 1.0 nmol scrambled or miR-29a antagomir-treated samples and found no significant changes in the levels of the three miRNAs in the CNS tissue. While we did not identify other miRNA levels being altered in response to miR-29a knockdown, it is important to note that a single miRNA can have multiple target mRNA and that "off-target" effects could be mediated downstream of miR-29a regulation (Lim *et al.*, 2005).

While other studies have maintained successful miRNA knockdown through continued dosing from osmotic pumps (Pandi *et al.*, 2013, Care *et al.*, 2007), our study required a one-time injection followed by a rigorous course of motorfunction analysis. While we could not utilise osmotic pumps as they might interfere with motorfunction analysis, a time course study identified miR-29a knockdown at both 10 days and 30 days post-injection following administration of 1.0 nmol scrambled or miR-29a antagomir. We identified significant knockdown in the cortex and hippocampus at 10 days post injection. The cortex still had significant down-regulation of miR-29a at 30 days; however other miRNAs also showed reduction in the cortex. As this is the site of injection, the local effects in the cortex could be expected to be higher due to increased dosing, changes in intracranial pressure and surgery trauma (Misra *et al.*, 2003). Since we still saw some knockdown in all three tissues at 30 days post injection, it was plausible to think that *in*

vivo the antagomir could affect disease progression in wildtype versus SOD1^{G93A} mice.

We examined miR-29a target *Mcl-1* in both the 72 h and 10 day post-injection 1.0 nmol miR-29a antagomir-treated samples. There was an increase in *Mcl-1* expression in the lumbar and cortex samples at 72 h, while at 10 days there was an increase in *Mcl-1* expression in the hippocampus and lumbar samples. This change in *Mcl-1* mRNA expression did not reach significance, possibly due to low n numbers. The heterogeneity of tissue samples must also be considered here. As we demonstrated previously *Mcl-1* mRNA is endogenously expressed at low levels in the mouse CNS (Fig. 4.1) and this could also be the explanation / reason for the absence of a significant increase in *Mcl-1* expression even following miR-29a knockdown. The modest increase in *Mcl-1* expression following miR-29a knockdown *in vivo* suggests that *Mcl-1* expression changes are unlikely to mediate a strong cytoprotective role in our disease model. This result could also suggest that miR-29a is preferentially targeting another gene in these tissue samples and therefore the change in *Mcl-1* expression is reduced. Indeed miR-29a has been shown to modulate apoptosis in neurodegenerative disease through a variety of target genes including interferon-γ in multiple sclerosis (Smith *et al.*, 2012) and BACE1 in Alzheimer's disease (Hebert *et al.*, 2008).

To assess the effect of miR-29a knockdown in SOD1^{G93A} mice across disease progression, we monitored motorfunction changes and lifespan in n=19 wildtype and n=20 transgenic mice treated with scrambled or miR-29a antagomir at PND 70. We could see no protection of motorfunction in SOD1^{G93A} mice compared to wildtype in PaGE or stride length tests compared to wildtype mice. Similarly male and female transgenic mice lost body mass at a steady rate during disease progression irrespective of treatment. We saw some differences in disease progression and motorfunction performance in male and females. It is well recorded that male SOD1 mice experience

disease onset earlier than female mice (Veldink et al., 2003, McCombe and Henderson, 2010). Indeed in human ALS patients both age and sex have been established as risk factors in disease progression with males developing disease at earlier stages in life (Traynor *et al.*, 1999). Research has shown that this difference is mediated by sex hormones with oestrogen proving protective in females (Choi *et al.*, 2008, Li *et al.*, 2012). We did see a trend towards lifespan protection in a subset of miR-29a antagomir-treated mice; however this did not reach significance. Since miR-29 has been suggested to play a role in mediating apoptosis (Mott *et al.*, 2007) as well as synaptogenesis in the CNS (Lippi *et al.*, 2011) we conclude that a more robust and stringent dosing protocol in conjunction with higher animal numbers could demonstrate a delay in disease progression and protection of lifespan. Interindividual variation in SOD1 animals means large numbers are needed to reach significance (Ludolph *et al.*, 2007). Indeed studies that provide extended lifespan in SOD1 mouse models have more prolonged dosing paradigms and higher transgenic mouse numbers (Mancuso *et al.*, 2012).

Our surgery model was guided by work conducted in our lab using antagomirs in a model of epilepsy (Jimenez-Mateos *et al.*, 2012). While they demonstrated significant knockdown of miR-134 using ICV-injected antagomirs up to one month post-injection, their disease model was assessed over shorter time periods than an ALS model requires. Indeed in a model of ischemia, a high dose (25 μM) of Let-7 antagomir administered to the ICV in a continual infusion over an 8 minute time period afforded neuroprotection to female rats (Selvamani *et al.*, 2012). Let-7 targets IGF-1, shown to prevent oestrogen-mediated neurotoxicity following stroke, for translational repression and antagomirs specific for Let-7 were shown to induce IGF-like neuroprotection. However, as with the epilepsy study, mice were sacrificed 5 days post-injection and infarct volume assessed. Given the high volume of dose used and the short time period, it can be assumed that any effects mediated by Let-7 knockdown would be evident.

In ALS knockdown studies the dosing is also much more consistent across disease progression. Administration of a Sigma-1 receptor agonist to $SOD1^{G93A}$ mice was shown to extend survival in transgenic mice by 15% and demonstrated reduced microglial reactivity (Mancuso *et al.*, 2012). Sigma-1 receptor has been shown to be important for mediating protection following stroke and traumatic brain injury and mutations of the Sigma-1 receptor have also been described in ALS patients (Al-Saif *et al.*, 2011). Mancuso *et al.* described consistent administration of the agonist by i.p. injections from week 8 (56 days) until endstage at 16 weeks (112 days). They also used n=19 transgenic animals in their Sigma-1 receptor agonist treatment group. Another study looking at a small molecule, SUN N8075, an upregulator of VGF nerve growth factor inducible protein (VGF) during cellular stress, found that subcutaneous administration of the molecule in $SOD1^{G93A}$ mice could delay disease onset and prolong lifespan (Shimazawa *et al.*, 2010). VGF has been reported to be reduced in CSF from ALS patients (Zhao *et al.*, 2008) and was shown to be protective in SHSY5Y cells undergoing ER stress. As in the stroke model, the agonist was administered to the mice daily from week 10 until endstage. The analysis of other therapies in ALS models suggests that prolonged and consistent dosing is needed to maintain therapeutic benefit during disease progression. While it was outside the scope of this study to have such a stringent dosing regime, the trend towards increased lifespan in miR-29a antagomir-treated mice could be much enhanced with continued dosing. Indeed recent work using an antagomir specific for miR-155 administered continually by osmotic pump allowed for continual dosing through the ICV with daily i.p. injections to bolster the systemic dosing (Koval *et al.*, 2013). They found significant delay in disease onset and increased lifespan in transgenic antagomir-treated mice. It would be interesting to see the effect of continued administration of miR-29a antagomir on disease progression given its cell protective effects *in vitro.*

CHAPTER 6

General Discussion

ER stress has been identified in mediating the pathogenesis of multiple diseases (Nakatani *et al.*, 2005, Greene *et al.*, 2013, Hoozemans *et al.*, 2005). Our lab has focused on a role for ER stress in mediating cell death and neurodegeneration with an emphasis on the BCL-2 family of proteins. BCL-2 family members have been shown to control a variety of prosurvival and proapoptotic mechanisms in almost all cell types. The emerging evidence that miRNAs can further regulate ER stress-mediated apoptosis through targeting of the BCL-2 family proteins has indicated a new level of cellular regulation (Gupta *et al.*, 2012). miRNAs have been of keen interest in recent years owing to their abundance in cells and their ability to regulate gene expression in a variety of cell systems (Gurtan and Sharp, 2013). Work in our lab preceding this research project identified miR-29a as upregulated under tunicamycin-induced ER stress in a neuroblastoma cell line. Through further miRNA based analysis, MCL-1 was confirmed as a target of miR-29a. This research project aimed to further explore miR-29a modulation in a neuronal model of ER stress. We aimed to corroborate previous findings in a SHSY5Y neuroblastoma cell line and to examine miR-29a modulation of its putative target MCL-1 in cortical neurons. Furthermore, we aimed to examine miR-29a modulation in a chronic neurodegenerative model in which increased ER stress has been implicated in the progression of the disease. *In vivo* modulation of miR-29a in the CNS of $SOD1^{G93A}$ mice was expected to identify a role for miR-29a in the pathogenesis of familial ALS. This could set the basis for a possible therapeutic strategy for ALS patients.

6.1 ER stress-mediated neuronal apoptosis

BIM, PUMA and NOXA are all members of the BH3-only family of proapoptotic proteins that have been implicated in mediating ER stress-induced apoptosis. The first stress-induced BH3-only protein that was found to be regulated during ER stress was PUMA (Reimertz *et al.*, 2003). Although PUMA is a p53 inducible protein that has been implicated in mediating apoptosis in numerous cell types (Nakano and Vousden, 2001), its induction during ER stress has been demonstrated to occur independently of p53 expression in several studies (Ghosh *et al.*, 2012, Li *et al.*, 2006, Reimertz *et al.*, 2003). Indeed, 6-hydroxydopamine treatment, which has been demonstrated to induce ER stress (Deng *et al.*, 2012), also increased PUMA mRNA and protein expression in SHSY5Y neuroblastoma cells in a p53-independent manner (Gomez-Lazaro *et al.*, 2008). ER stress-mediated activation of BIM has been shown to be mediated by the stress-induced transcription factor, CHOP, in several cell lines and this activated BIM dependent cellular apoptosis (Puthalakath *et al.*, 2007). Similarly NOXA induction has been shown to be mediated by ER stress-induced upregulation of p53 in MEFs (Li *et al.*, 2006). However, work in this lab in SHSY5Y neuroblastoma cells showed that tunicamycin-induced ER stress did not alter BIM levels during ER stress-induced apoptosis (Reimertz *et al.*, 2003).

Specifically in the case of neurons, PUMA has been shown to be a key mediator of apoptosis. In cortical neurons PUMA was shown to induce apoptosis following proteasome inhibition, with knockdown of PUMA expression providing incomplete protection from apoptosis (Tuffy *et al.*, 2010). PUMA has also been shown to be induced during ER stress-induced apoptosis in neurons (Galehdar *et al.*, 2010). p53-independent PUMA activation in neurons following ER stress has been shown to be directed by ATF4-mediated induction of CHOP

which can in turn activate PUMA induction. BIM and NOXA were not significantly induced in this study and cortical neurons deficient in the expression of BIM were not protected from tunicamycin or thapsigargin treatment. In the context of neurodegeneration, PUMA deletion was shown to be cytoprotective to motoneurons undergoing ER stress-induced apoptosis (Kieran *et al.*, 2007). Indeed we identified PUMA knockdown as protective in cortical neurons undergoing tunicamycin-induced cell death although, as seen in other research, this protection was not complete. We demonstrated further protection against tunicamycin-induced cell death in PUMA deficient cortical neurons which overexpressed MCL-1. The BH3-only proteins BIM, NOXA and PUMA as well as BID, BIK and BAK have all been shown to bind to and interact with proapoptotic MCL-1 (Chen *et al.*, 2005, Cuconati *et al.*, 2003). Our work suggests that MCL-1 can elicit a cell protective effect, even in the absence of PUMA expression, in cortical neurons and indicates a cytoprotective role for MCL-1 in neurons undergoing ER stress-mediated apoptosis. Furthermore the presence of apoptosis in cortical neurons in which PUMA knockdown and MCL-1 overexpression is induced suggests roles for other apoptotic mediators in ER stress-induced neuronal cell death.

Maintaining the balance of both pro- and anti-apoptotic signals has been shown to be critical in maintaining cell survival. Other factors that can mediate members of the BCL-2 family or exert their effects downstream can help maintain this balance. miRNAs regulate gene expression in a vast array of targets and have been shown to regulate the pathways of ER stress through mediating the ER stress response or by themselves being regulated by ER stress (Logue *et al.*, 2013, Chitnis *et al.*, 2013). This suggests a role for other potential mediators of ER stress-induced neuronal apoptosis.

6.2 miRNAs during ER stress

The far reaching effects of miRNAs in multiple cellular systems and disease paradigms have been of key research interest in previous years. The downstream effects of ER stress on protein translation and protein degradation make it a promising context for miRNA involvement. Indeed, the effect of a number of miRNAs induced by members of the UPR have been found in cells undergoing ER stress (Maurel and Chevet, 2013).

The PERK arm of the UPR has demonstrated involvement in mediating miRNA expression in response to stress. PERK was shown to transcriptionally induce miR-30c-2-3p, a regulator of XBP1 expression, in a variety of cells through activation of NF-κB and promote the cellular adaptive response to ER stress (Byrd *et al.*, 2012). Similarly, PERK was shown to induce miR-211 expression through eIF2α-mediated expression of ATF4. The increased expression of miR-211 was shown to target CHOP for transcriptional repression under conditions of ER stress (Chitnis *et al.*, 2012). Downstream targets of the UPR have also been shown to regulate miRNA expression, with CHOP mediating expression of miR-708 in a model of the developing eye. miR-708, found encoded on the CHOP-regulated *odz4* gene, controls rhodopsin synthesis and prevents ER stress through misfolding (Behrman *et al.*, 2011). Work on a miRNA cluster mediated by PERK was shown to target BH3-only proapoptotic BIM. The miR-106b-25 cluster, comprising miR-106b, miR-25 and miR-93, was downregulated by PERK in an ATF4-dependent manner during tunicamycin-induced ER stress. Having confirmed expression of miR-106b-25 attenuated ER stress-induced upregulation of BIM, they further identified BIM upregulation and miR-106b-25 downregulation in post-symptomatic $SOD1^{G86R}$ ALS mice (Gupta *et al.*, 2012). This research identifies the interplay between miRNAs, apoptotic mediators

and neurodegenerative diseases further enhancing our understanding of the importance of miRNAs.

As stated previously, miR-29a and other members of the miR-29 family of miRNAs have been implicated in mediating ER stress (Kole *et al.*, 2011) and mediating cell survival (Mott *et al.*, 2007) through targeting of BCL-2 family members. Furthermore miR-29a and miR-29b have previously been identified as downregulated in a model of sporadic AD (Hebert *et al.*, 2008). AD, a disease characterised by aberrant protein aggregation, has been shown to downregulate the unfolded protein response and implement ER stress-induced apoptosis (Katayama *et al.*, 2004).

6.3 Characterising miR-29a expression in cortical neurons

The miR-29 family of microRNAs has shown increasing roles for its members in various neurodegenerative diseases and in neuronal development (Hebert *et al.*, 2008, Lippi *et al.*, 2011). ER stress has long been deemed an instigator and protagonist of the cell death characteristic of many neurodegenerative diseases. Using an unbiased approach to identify differentially regulated miRNAs in neural cells, our lab identified miR-29a as up-regulated in SHSY5Y neuroblastoma cells undergoing tunicamycin-induced cell death. It was the aim of this body of work to characterise miR-29a expression in primary cortical neurons from C57 BL/6 embryonic mice undergoing ER stress and to examine these results in an *in vivo* animal model of neurodegeneration.

We identified increased ER stress *in vitro* following tunicamycin treatment in both MEFs and in cortical neurons and this coincided with significant upregulation of miR-29a. Similarly, brefeldin A-induced ER stress was confirmed in cortical neurons; however, miR-29a induction was not as robust as seen with tunicamycin treatment. Interestingly ER stress-induced upregulation of miR-29a coincided with a decrease in MCL-1 protein level. This result was similar to that seen previously in our lab in SHSY5Y cells (unpublished). Similar results were seen in cancer cell lines, with enforced miR-29a expression leading to a reduction in MCL-1 protein levels (Mott *et al.*, 2007).

Having established a role for miR-29a during ER stress in cortical neurons, we wanted to look further at the role of miR-29a modulation in mediating neuronal cell death. Antagomirs, a new breed of miRNA specific inhibitors, have allowed for modulation of miRNA in multiple cell and tissue types and have helped our understanding of the roles of miRNAs in disease systems (Krutzfeldt *et al.*, 2005). We utilised antagomirs both *in vitro* and *in vivo* to knockdown miR-29a expression.

In cortical neurons we found miR-29a knockdown could protect against ER stress-induced cell death, which we hypothesised could be due in part to regulation of miR-29a target protein, MCL-1. We found that our miR-29a antagomir reduced miR-29a levels significantly while protecting *Mcl-1* mRNA levels even under conditions of ER stress. The protective effect of miR-29a knockdown on *Mcl-1* levels and the reproducibility of the results achieved made the prospect of an *in vivo* miR-29a antagomir desirable.

Although it has been shown in various experimental models that miR-29a has the ability to target the 3' UTR of MCL-1 and while we found evidence to suggest that miR-29a downregulates MCL-1 in a model of ER stress-induced apoptosis, the nature of miRNAs and their ability to target multiple genes means that miR-29a targeted regulation of another apoptotic mediator cannot be ruled out. Indeed new evidence suggests that multiple miRNAs may act together in order to regulate multiple targets at once, thus widening the scope for miRNA-directed gene regulation even further (Hashimoto *et al.*, 2013). In the case of our our research, it must be considered that miR-29a could be modulating expression of several targets during ER stress.

miR-29b, a closely linked member of the miR-29 family, has been shown to target the 3' UTR of various BH3-only protein mRNA transcripts. miR-29b was shown to bind to the 3' UTR of BIM, PUMA, BMF and N-BAK in neurons with reduced levels of each protein found in mature neurons which expressed high levels of miR-29b (Kole *et al.*, 2011). It was suggested that miR-29b could block endogenous expression of these proteins during cellular stress and therefore promote survival. Due to the close homology of members of the miR-29 family, it is possible that miR-29a could also control apoptosis through modulation of members of the BH3-only proteins.

Members of the miR-29 family have also been shown to upregulate p53 indirectly with all three members identified as negative regulators

of p85 and CDC42, both of which target p53 and suppress its expression. This upregulation of p53 induced apoptosis in a p53-dependent manner (Park *et al.*, 2009). Since p53 has been shown to direct mitochondrial apoptosis through induction of BH3-only members PUMA (Nakano and Vousden, 2001) and NOXA (Cregan *et al.*, 2004, Li *et al.*, 2006) in several cell lines, this also demonstrates the multiple roles of miRNAs through mediating similar processes in a number of different ways. While miR-29 is known to target MCL-1, this suggests an indirect role for miR-29 in mediating BH3-only protein expression.

Research identifying a role for miR-29 in sporadic AD found β site APP-cleaving enzyme (BACE) as a target of miR-29. BACE levels have been found to be elevated in sporadic AD where BACE generates free β-amyloid. Loss of miR-29 therefore could increase BACE levels and β-amyloid plaques leading to sporadic AD (Hebert *et al.*, 2008). The suggested role for miR-29 in the control of BH3-only-mediated apoptosis explains why loss of miR-29 has been associated with increased cell death.

Furthermore, miRNA screens in HEK293T cells identified voltage-dependent anion channel 1 and 2 (VDAC) as differentially regulated following overexpression of miR-29a (Bargaje *et al.*, 2012). VDAC is an ion channel present in abundance on the mitochondrial outer membrane with roles in mediating cytochrome c release and apoptosis. BAX has been shown to interact with VDAC and induce release of cytochrome c and apoptosis with this effect being antagonised by BCL-XL (Shimizu *et al.*, 1999). If miR-29a overexpression targets the 3' UTR of VDAC reducing VDAC protein expression, and with miR-29a targeting other members of the apoptotic pathway including MCL-1, as suggested by our research findings, coordinated regulation of these apoptosis regulators by miR-29a could be mediating cell death.

6.4 A role for MCL-1 in protecting cortical neurons from ER stress-induced apoptosis

Anti-apoptotic MCL-1 has been shown to be a key mediator of cellular development during embryogenesis (Rinkenberger *et al.*, 2000) and in maintaining cellular homeostasis and survival following cytotoxic insult (Jiang *et al.*, 2008, Nijhawan *et al.*, 2003). Furthermore MCL-1 has been identified as a key mediator of apoptosis in the CNS and in neuronal cell types (Arbour *et al.*, 2008). The apoptotic pathway must be inhibited following development to ensure survival of mature neurons and it was expected that MCL-1 would play an important role in mediating this survival.

We identified MCL-1 as downregulated under both tunicamycin- and brefeldin A-induced ER stress in our cortical neurons suggesting that MCL-1 expression can be decreased by ER stress. Furthermore loss of MCL-1 sensitised cortical neurons to ER stress-induced apoptosis, further indicating the importance of MCL-1 in mediating ER stress in cortical neurons. Loss of MCL-1 has previously been shown to sensitise neurons to DNA damage-induced cell death (Arbour *et al.*, 2008) and to sensitise HeLa cells to ultraviolet irradiation-induced cell death (Nijhawan *et al.*, 2003). By contrast, MCL-1 overexpression, which has been associated with oncogenesis (Konopleva *et al.*, 2006, Wei *et al.*, 2001), has also been shown to protect neurons against mitochondrial dysfunction (Arbour *et al.*, 2008). Coinciding with this, we demonstrated that MCL-1 overexpression in wildtype, *puma*$^{-/-}$ *and* *bax*$^{-/-}$ neurons significantly protected cortical neurons during tunicamycin-induced cell death. Both *puma*$^{-/-}$ and *bax*$^{-/-}$ conferred increased protection against tunicamycin-induced cell death compared to wildtypes, which is consistent with other studies (Smith and Deshmukh, 2007, Ren *et al.*, 2010). This demonstrates the strength of MCL-1 role in protecting against cell death. Indeed, MCL-1 overexpression has been characterised in cancer cells where it

protects against ER stress-mediated apoptosis and increases malignancy (Koshikawa *et al.*, 2006, Jiang *et al.*, 2008). In MEFs, adenovirus-mediated overexpression of MCL-1 was shown to decrease expression of ER stress mediators following tunicamycin treatment. Western blot analysis revealed a decrease in endogenous MCL-1 during ER stress while exogenous MCL-1 expressed by the adenovirus was not affected by ER stress. Our explanation for this change is that the MCL-1 expressed by the adenovirus does not contain a 3' UTR while endogenous MCL-1 does have a 3'UTR region which can be targeted by miR-29a. This further implicates miR-29a targeting of MCL-1 during ER stress. Since miRNAs bind to mRNA at the 3' UTR and direct translational arrest, if MCL-1 downregulation was merely to do with degradation of MCL-1 then exogenously expressed MCL-1 would also be downregulated.

MCL-1 overexpression also decreased expression of the autophagy marker LC3. BCL-2 homologues, including MCL-1, have been implicated in mediating autophagy in the control of cell survival and apoptosis (Pattingre *et al.*, 2005, Martin *et al.*, 2009). MCL-1 overexpression was shown previously to decrease autophagosome formation and reduce autophagy induction following serum starvation (Germain *et al.*, 2011). This suggests a further mechanism by which MCL-1 mediates cell survival. As an antiapoptotic member of the BCL-2 family, the importance of MCL-1 in mediating apoptosis during development and following injury has been published previously (Arbour *et al.*, 2008, Germain *et al.*, 2011). Our work describes a further paradigm in which MCL-1 mediates ER stress-induced apoptosis in neurons. Our results could have implications for other neurodegenerative diseases characterised by ER stress.

6.5 Characterising miR-29a expression during ALS disease progression *in vivo*

ALS is a chronic neurodegenerative disorder associated with increased levels of ER stress due to aggregation of misfolded proteins such as SOD1 (Kikuchi *et al.*, 2006), FUS (Farg *et al.*, 2012), TDP43 (Ayala *et al.*, 2011) and the newly identified C9ORF72 (Mori *et al.*, 2013) during disease progression. While the pathological characteristic of ALS are well defined, the point of initiation and a specific mechanism of degeneration remains unclear (Turner *et al.*, 2013). Loss of 20% of motoneurons at PND 60 in $SOD1^{G93A}$ mice suggests a role for early initiating factors such as ER stress that potentiate disease progression (Vinsant, 2013b). ER stress signalling may mediate motoneuron death (Suzuki *et al.*, 2009) or may be a result of increased cellular stress due to aggregation of misfolded proteins and subsequent motoneuron degeneration (Nagata *et al.*, 2007)

Having identified miR-29a as of importance to ER stress-induced neuronal cell death and, furthermore, having identified a role for miR-29a mediating MCL-1 expression in primary cortical neurons, we wanted to look at miR-29a modulation *in vivo*. Increased expression of miR-29a in the forebrain of patients with ALS has been previously identified (Shioya *et al.*, 2010) and implicates a family of miRNAs with reported effects in other neurodegenerative diseases (Shioya *et al.*, 2010) in the pathogenesis of ALS. Since there is no known cause of ALS and multiple proposed mediators of the disease (Goodall and Morrison, 2006), we wanted to investigate if ER stress-induced upregulation of miR-29a could play a role in enhancing motoneuron susceptibility to cell death and whether this may be related to its ability to target MCL-1.

Our lab has a well-characterised colony of SOD1^{G93A} mice which are the benchmark research model for familial ALS models (Gurney *et al.*, 1994). These mice have a clear disease start point and a consistent timeline of symptoms due to loss of lower motoneurons and subsequent muscle atrophy which allows for marked disease progression (Acevedo-Arozena *et al.*, 2011).

We identified miR-29a as upregulated in organs of the CNS, specifically the lumbar spine, the cortex and the hippocampus. The ventral horn of the lumbar spine is the site of lower motoneurons that control movement in the hind limbs of the mice. In SOD1^{G93A} mice, it is these motoneurons that are lost and result in muscle wasting and atrophy. We identified miR-29a expression in the spinal cord of wildtype and SOD1 transgenic mice. More specifically, we localised miR-29a expression to the grey matter of the lumbar spinal cord. *In situ* hybridisation of LNA-modified miRNA probes using alkaline phosphatase substrate (Obernosterer *et al.*, 2007) highlighted cells expressing miR-29a in diffuse purple "dots" throughout the grey matter. Nissl staining of semi-adjacent sections allowed us to localise miR-29a staining in motoneurons in the ventral horn of each spinal section. Interestingly, we found that miR-29a expression was induced in SOD1^{G93A} spinal sections earlier than wildtype sections. SOD1^{G93A} mice exhibit miR-29a expression at PND 70, pre-symptom onset while wildtype PND 70 had very weak signal at the same timepoint. This suggests that SOD1^{G93A} mice undergo more ER stress in the spinal cord prior to symptom onset and may predispose these neurons to undergo degeneration. Muscle denervation has been identified at PND 30 with identification of motoneurons that are committed to undergo apoptosis as early as PND 60 suggesting that early stress events prime motoneurons for apoptosis and culminate in motoneurons death and symptom onset at later timepoints in SOD1^{G93A} mice (Vinsant, 2013b, Gould *et al.*, 2006). SOD1^{G93A} mice have been reported to have mutant SOD1 aggregates that accumulate in the spinal cord (Bruijn *et al.*, 1998) and we speculate that these protein aggregates

could induce ER stress in these mice and elevate miR-29a levels. miR-29a levels were slightly less at PND 90 and PND 120 in our transgenic mice compared to wildtype mice; however, we suggest this decreased expression is most likely due to loss of neurons. Indeed motoneuron counts in these sections reveal substantial loss of motoneurons from the ventral horn region of transgenic mouse sections at PND 90 and PND 120. This high motoneuron degeneracy at PND 90 has been shown in other studies of $SOD1^{G93A}$ mice (Garbuzova-Davis *et al.*, 2007).

Interestingly dysregulation of miR-29a has also been implicated in other diseases and injuries associated with the spinal cord. Members of the miR-29 family have been shown to be expressed in the rat spinal cord and downregulated following spinal injury (Yunta *et al.*, 2012). The miR-29a/b1 cluster has also been found to be increased in T-cells from multiple sclerosis mice and patient samples suggesting a role for miR-29 in mediating neuronal loss through modulation of inflammatory mediators (Smith *et al.*, 2012). Whether miR-29a mediates motoneuron loss through ER stress-induced apoptosis, as we have seen here in cortical neurons, or through modulation of neuronal inflammation, we have been able to identify a correlation between levels of miR-29 expression and neuronal cell death.

6.6 Designing an *in vivo* animal study for miR-29a modulation

In vivo models of disease are the closest experimental tool to a clinical trial. Animal studies form the basis of drug development. Success in an animal model of disease can give researchers some idea of effects in humans, although there can be a lot of variation (Gillespie, 2005). The success of our antagomirs *in vitro* at protecting against ER stress-induced cell death made this a desirable model for analysis of miR-29a modulation *in vivo*. We designed a cannula-free ICV injection model of miR-29a antagomir administered directly to the cerebral ventricles in $SOD1^{G93A}$ mice. Transport of the antagomir to the spinal cord occurs through trafficking in the cerebrospinal fluid which is produced in the cerebral ventricles and circulates throughout the spinal cord and the ventricles of the brain (Sherwood, 2012). A single dose was administered to all mice at PND 70, a pre-symptom onset stage for these mice. Delivering the antagomir prior to symptom onset would give us a pre-conditioning effect. We were hopeful that it would decrease disease symptoms in these mice at later ages. A huge disadvantage to patients with ALS is that they are diagnosed following onset of symptoms and so early treatments are less effective. Characteristically familial ALS is defined as two or more blood relatives in a family who have developed ALS (Brooks *et al.*, 2000). Pre-symptomatic treatments would be of benefit to those with direct family affected by the disease, who stand a high chance of developing the same disease. If modulating miR-29a could reduce motoneuron cell death in a mouse model of cell death as it did *in vitro* for cortical neurons undergoing ER stress-induced cell death, then there could be a good argument made for miRNA-based therapeutics for ALS patients.

Motorfunction analysis in wildtype and $SOD1^{G93A}$ treated mice from PND 84 until approximately PND 168 identified no significant effect on weight gain, stride length or paw grip endurance analysis following miR-29a antagonisation. Peak body weight was used to assess disease onset. Transgenic males and females lost body weight at a comparable level with weight loss beginning to be evident from PND 119 onward in scrambled- and transgenic-treated animals. Strength analysis revealed that hind limb weakness due to loss of motoneurons was not abrogated by miR-29a downregulation. Paw grip endurance analysis identified deficiencies in males' ability to maintain a 60 sec grip with their hind limbs at PND 91 and this steady drop in ability was seen in both scrambled and antagomir-treated males at a similar rate of decline. Female antagomir-treated mice maintained a 60 sec grip until PND 98 while scrambled-treated transgenic females were just short within the 50 sec range at this date. Transgenic females began a steady decline in paw grip endurance at PND 112. This progression in females occurred later than transgenic males and has been attributed to gender-mediated affects on disease progression (Traynor *et al.*, 1999). Stride length analysis identified a steady decline in transgenic stride length for females from PND 119 onwards while males began to decline earlier at PND 98. Loss of miR-29a did not show any protective effect on stride length.

Endstage for all mice was determined by an inability to right themselves within 30 sec when placed on either side. Lifespan data collected from each mouse identified a trend towards prolonged lifespan in miR-29a antagomir-treated mice compared to scrambled-treated mice. Kaplan Meier analysis confirmed that this prolonged lifespan in miR-29a antagomir-treated mice was not significant compared to scrambled antagomir treatment. Prolonged survival with no change in disease progression or duration has been seen previously in studies of ALS (Kostic *et al.*, 1997). Having identified miR-29a knockdown present at 10 and 30 days post-injection with miR-29a antagomir, we could hypothesise miR-29a knockdown at PND

70 would have a preconditioning effect in asymptomatic mice and could reduce ER stress in early stage ALS. While miR-29a knockdown had little effect on overall motorfunction and hind limb strength in both male and female transgenic mice, miR-29a antagomir-treated mice displayed a trend towards maintaining grip strength for longer time periods than scrambled antagomir-treated mice in early PaGE anaylsis. A trend towards prolonged lifespan in the absence of miR-29a suggests that miR-29a may be targeting mediators of apoptosis outside of motoneurons, the effect of which promotes motoneuron loss downstream. While we saw no change in disease onset in scrambled or antagomir-treated mice, as assessed by peak bodyweight or onset of hind limb weakness, prolonged survival seen in a subset of miR-29a antagomir-treated mice suggests that a more robust dosing regime might induce significant survival. However, it remains possible that miR-29a inhibition may not have any effect on motoneuron degeneration and ALS disease progression.

While we hypothesised that miR-29a could be mediating ER stress-induced cell death in motoneurons, possibly through targeting of MCL-1, we did not see a change in motorfunction ability in miR-29a antagomir-treated mice during disease progression. Indeed both males and females progressed with similar levels of motor decline regardless of scrambled or miR-29a antagomir administration. If, as we saw in cortical neurons, miR-29a could reduce motoneuron cell death during ER stress then we would expect a protection in motorfunction in any of the tests. This could be for one of a number of reasons. Firstly, if motoneuron cell death is not mediated by ER stress but by some other mechanism than this, unlike the cortical neurons undergoing tunicamycin-induced cell death, would not be as protected by knockdown of miR-29a. Roles for astrocyte-mediated neurotoxicity (Nagai *et al.*, 2007) and glutamate-induced excitotoxicity (Tolosa *et al.*, 2008) have also been implicated in mediating spinal motoneuron loss in SOD1 ALS models. In our model, while PND 70 is pre-disease onset, *in situ* analysis showed miR-29a expression increased in

transgenic mice. If endogenous levels of circulating miR-29a are high in transgenic animals, then knockdown of miR-29a at PND 70 may be too late to act as a preconditioning effect to protect motoneurons. An earlier timepoint for antagomir administration could have a bigger effect on disease progression or provide a more robust preconditioning effect. Indeed, the need for a longer and more complete dosing paradigm has been demonstrated previously in $SOD1^{G93A}$ mice treated with a miR-155 antagomir (Koval *et al.*, 2013). Mice were administered a miR-155 inhibitor daily through an osmotic pump and intraperitoneal injections for up to 42 days from PND 60 onwards. This study found prolonged survival as well as a delay in disease duration of 38 %.This suggests a need for a more prolonged dosing strategy for miR-29a in our SOD1 mice and perhaps a review of the timing of administration to further prolong survival and delay disease onset in our experimental model.

Looking at a role for MCL-1, we could hypothesise that miR-29a could be modulating MCL-1 levels in cells other than motoneurons. As we saw in our model, the presence of a righting reflex up to endstage in SOD1 mice suggests some prolonged motorfunction even if stringent motor assessment could not be attained. MCL-1 protection, through miR-29a antagonisation in cells of the motorcortex or in supporting cells and neurons of the spinal cord, could prolong survival even in the presence of hind limb dysfunction. While no direct role for MCL-1 has been established for ALS, the BH3-only member BIM has previously been shown to be an important mediator of motoneuron loss in SOD1-mediated ALS (Hetz *et al.*, 2007, Soo *et al.*, 2012). BIM is a potent member of the BH3-only family and can bind MCL-1 and mediate its release from BAK and thereby induce apoptosis (Willis and Adams, 2005). If BIM can induce cell death through removal of MCL-1, then protecting MCL-1 levels could help reduce cell death and protect motoneuron integrity. In addition, while a definitive role for MCL-1 in mediating astrocyte and microglia function has not been established in ALS, microglia have been shown to increase TNFα expression which

in turn increases neuronal precursor cell apoptosis through activation of proapoptotic PUMA. miR-29 has been shown to induce expression of p53 which can upregulate mediators of apoptosis including PUMA and drive apoptosis (Park *et al.*, 2009). Deletion of PUMA in motoneurons has previously been shown to prevent motoneuron apoptosis in a SOD1 mouse model (Kieran *et al.*, 2007). Although miR-29a knockdown may not protect motoneuron loss, the ability to prolong the lifespan of a subset of treated animals compared to scrambled-treated animals suggests that miR-29a targeting MCL-1 may affect apoptosis in cells other than motoneurons or that miR-29a may target another mediator of apoptosis in SOD1 mutant mice.

As previously stated, miR-29a can activate p53 (Park *et al.*, 2009, Ugalde *et al.*, 2011). Increased p53 has been identified in spinal motoneurons undergoing apoptosis (LJ Martin, 2002) and in reactive astrocytes (Cho *et al.*, 1999). This suggests a potential role for miR-29a modulation in protecting motoneuron viability through repression of p53 expression. Voltage-dependent anion channel 1 and 2 (VDAC) are both miR-29a targets that have been shown to play a role in mediating apoptosis (Bargaje *et al.*, 2012). VDAC1 has been shown to play a role in neuronal apoptosis mediated by excitotoxicity during ischemia (Park *et al.*, 2010) and in ER stress-mediated apoptosis (Deniaud *et al.*, 2008). In ALS, mutant SOD1 was shown to bind BCL-2 and induce a conformation change in BCL-2 that allowed it to bind VDAC with greater affinity. VDAC/BCL-2 were shown to prevent mitochondrial ADP permeability and induce motoneuron cell death (Tan *et al.*, 2013). If miR-29a downregulated VDAC, it could have wide ranging effects in multiple cell types and could impact on a number of diseases characterised by increased apoptosis.

While a role for miR-29a in apoptosis has been established, members of the miR-29 family have also been shown to regulate synaptogenesis. In hippocampal neurons, work has demonstrated a role for members of the miR-29 family, specifically miR-29a and miR-

29b, in modulating dendritic spine morphology and synaptic plasticity (Lippi *et al.*, 2011). Screens performed on mouse brains stimulated with psychoactive drugs to induce adaptations in the brain led to identification of miR29a/b as regulators of synaptogenesis. Confocal microscopy and luciferase assay analysis identified ARPC3, a subunit of ARP2/3 actin nucleation complex as a target of miR29a/b. It is through this targeting of ARPC3 that miR29a/b was shown to reduce mushroom-shaped dendritic spines and increase filopodial-like outgrowths in hippocampal neuron cultures. In ALS, modulation of dendritic spine growth and synaptogenesis could facilitate neuromuscular signalling and delay muscle atrophy.

A role for miR-29 in mediating muscle cell differentiation suggests a further mechanism by which miR-29 could modulate disease progression in ALS. Furthermore, miR-29 has been shown to inhibit HDAC4, an inhibitor of myogenic differentiation (Winbanks *et al.*, 2011). TGF-β-mediated upregulation of HDAC4 can be attenuated by both miR-29 and miR-206, a skeletal muscle specific miRNA implicated in delaying ALS disease progression (Williams *et al.*, 2009). This suggests a further mechanism by which miR-29 can mediate apoptosis and delay disease progression in an ALS model through indirect targeting of motoneurons.

6.7 miRNA therapeutics

The realisation that loss or overexpression of various miRNAs can lead to disease has sparked interest in miRNA-based therapeutics. While still in its infancy, and with current emphasis on experimentally-controlled delivery and modulation of miRNAs, a role for modulating miRNAs in the treatment of disease has already proved promising. miRNA-based therapeutics have been a novel idea since their discovery and the wide variety of miRNAs and their vast list of targets make them desirable therapeutic options. Although modulation of a single miRNA can affect multiple targets and incur unexpected changes in a disease model, the first trials of miRNA therapeutics *in vivo* have proved successful.

Let-7, one of the first miRNAs discovered, has been shown to repress oncogenic proteins Ras and HMGA-2 and low levels of Let-7 have been described in various tumour types (Yu *et al.*, 2007). Introduction of Let-7 using a transfected vector expressing Let-7 induced lung cancer cell death *in vitro*. Furthermore, intra-tumour injection of Let-7 into mice reduced tumorigenesis through targeting of mutant K-Ras *in vivo* (Kumar *et al.*, 2008). While most cancers are found to have reduced levels of miRNAs, which supports the role of miRNAs as tumour suppressors (Broderick and Zamore, 2011); in some instances, miRNA inhibition has been shown to be therapeutic.

miR-21 has been shown to increase glioblastoma invasiveness and malignancy through targeting of RECK and TIMP3, both suppressors of tumour malignancy. Anti-sense oligonucleotide-mediated suppression of miR-21 reduced tumour invasiveness through reduction in matrix metalloprotease activation *in vitro* and *in vivo* (Gabriely *et al.*, 2008). In a model of neurodegeneration, antagomir-mediated inhibition of miR-134 was shown to be protective in temporal lobe epilepsy

following ICV injection of LNA modified antagomirs (Jimenez-Mateos *et al.*, 2012). As with work in this research project, while delivery to the CNS was achieved *in vivo*, it is not yet clear how delivery of antagomirs or miRNAs to the CNS would be feasible. Safety of administration and dosing concerns are at the forefront of all clinical trials for new therapies. However, systemic administration of miRNAs has already moved into clinical trial phase. miR-122, a liver specific miRNA has been shown to reduce hepatitis C virus (HCV) replication in chimpanzees following intravenous injection of LNA-modified miR-122 anti-sense oligonucleotide (Elmen *et al.*, 2008). Currently phase 2 clinical trials are underway by Santaris Pharma for the miR-122 inhibitor, named miraversin, which has been shown to substantially reduce HCV following four week subcutaneous administration (SPC3649/miraversin).

2013 also sees the first clinical trial of a miRNA mimic get underway. MRX34 is a synthetic mimic of miR-34. miR-34 has been shown to have tumour suppressor capacity in certain cancer types. MRX34 was shown to restore functioning apoptosis in tumour cells from *in vitro* and *in vivo* mouse models. MRX34 can regulate oncogenes by restoring the tumour suppressor function of endogenous miR-34 (Bouchie, 2013). A breakthrough with this type of therapy could prove vital in the treatment of a wide variety of the most prevalent diseases. Although our work could not significantly alter ALS disease progression in SOD1 mice, we identified a successful delivery system for miRNA modulation in the CNS and have indicated a therapeutic paradigm that could prove successful with more rigorous analysis. While therapeutic dosing of the CNS is far more problematical than subcutaneous or intravenous administration, the promise of miRNA-based therapeutics in treating a multitude of diseases is becoming an evermore possible reality.

6.8 Conclusion

In conclusion, our study has contributed to our understanding of miR-29a and its role in ER stress-induced apoptosis in neuronal cells. We were able to identify miR-29a as significantly upregulated compared to other miRNAs in cortical neurons undergoing tunicamycin-induced cell death. We could identify a role for miR-29a in mediating decreased MCL-1 expression during ER stress through antagomir-mediated modulation of miR-29a expression. Furthermore, we established a cytoprotective role for MCL-1 in neuronal cells undergoing ER stress-induced apoptosis, where loss of MCL-1 sensitises cortical neurons to tunicamycin-induced cell death while MCL-1 overexpression was deemed cytoprotective. We also demonstrated that many pro- and anti-apoptotic proteins including PUMA, BAX and MCL-1 can mediate the balance of cellular apoptosis. Loss of key pro-apoptotic proteins did not completely protect against ER stress-induced cell death. Similarly, protection of MCL-1 expression through downregulation of miR-29a did not abrogate tunicamycin-induced cell death. Identification of reduced expression of key autophagic mediators following MCL-1 overexpression also suggests that many pathways converge to maintain neuronal homeostasis following cellular stress.

Furthermore we demonstrated high levels of miR-29a expression in organs of the CNS from mice. We could further localise miR-29a expression to the spinal cord of wildtype and $SOD1^{G93A}$ transgenic mice. We identified low expression of MCL-1 in organs of the mouse CNS and identified minor changes in MCL-1 expression following miR-29a modulation in the brain and spinal cord from wildtype mice. In addition, we were able to induce prolonged miR-29a knockdown *in vivo* through ICV antagomir administration in a mouse model of ALS. Comprehensive analysis of disease progression and motorfunction could not identify a significant alteration in ALS disease manifestations

when miR-29a knockdown was induced at a presymptomatic timepoint. We concluded that, while miR-29a knockdown is cytoprotective, possibly through modulation of MCL-1 expression in neurons, this effect was not strong enough in spinal cord of $SOD1^{G93A}$ mice to mediate a protective effect in living animals. In summary, we suggest that, while miR-29a can target MCL-1 for translational repression, there may be other target genes or proteins that mediate its effect in neurons. Furthermore while miR-29a knockdown is cytoprotective in neurons of the CNS, other mediators or apoptotic mechanisms may compensate for the loss of miR-29a and prevent cessation of apoptosis.

Future prospects

Our present study has contributed to our understanding of miR-29a and MCL-1 in cortical neurons. However, several questions have been raised from the results of this work:

- To conduct a robust *in situ* co-staining study between miR-29a, neuronal marker NeuN, motoneuron marker SMI-32 and astrocyte marker GFAP to further delineate miR-29a expression in the mouse spinal cord.

- To identify miR-29a in the motorcortex from mice following ICV injection and furthermore to analyse changes in target expression.

- To assess motorfunction and perform lifespan analysis following a more robust dosing paradigm of miR-29a antagomir in an ALS mouse model.

BIBLIOGRAPHY

ACEVEDO-AROZENA, A., KALMAR, B., ESSA, S., RICKETTS, T., JOYCE, P., KENT, R., ROWE, C., PARKER, A., GRAY, A., HAFEZPARAST, M., THORPE, J. R., GREENSMITH, L. & FISHER, E. M. 2011. A comprehensive assessment of the SOD1G93A low-copy transgenic mouse, which models human amyotrophic lateral sclerosis. *Dis Model Mech,* 4, 686-700.

AKGUL, C. 2009. Mcl-1 is a potential therapeutic target in multiple types of cancer. *Cell Mol Life Sci,* 66, 1326-36.

AL-SAIF, A., AL-MOHANNA, F. & BOHLEGA, S. 2011. A mutation in sigma-1 receptor causes juvenile amyotrophic lateral sclerosis. *Ann Neurol,* 70, 913-9.

ALLAGNAT, F., CUNHA, D., MOORE, F., VANDERWINDEN, J. M., EIZIRIK, D. L. & CARDOZO, A. K. 2011. Mcl-1 downregulation by pro-inflammatory cytokines and palmitate is an early event contributing to beta-cell apoptosis. *Cell Death Differ,* 18, 328-37.

AMODIO, N., DI MARTINO, M. T., FORESTA, U., LEONE, E., LIONETTI, M., LEOTTA, M., GULLA, A. M., PITARI, M. R., CONFORTI, F., ROSSI, M., AGOSTI, V., FULCINITI, M., MISSO, G., MORABITO, F., FERRARINI, M., NERI, A., CARAGLIA, M., MUNSHI, N. C., ANDERSON, K. C., TAGLIAFERRI, P. & TASSONE, P. 2012. miR-29b sensitizes multiple myeloma cells to bortezomib-induced apoptosis through the activation of a feedback loop with the transcription factor Sp1. *Cell Death Dis,* 3, e436.

ANILKUMAR, U., WEISOVA, P., DUSSMANN, H., CONCANNON, C. G., KONIG, H. G. & PREHN, J. H. 2013. AMP-activated protein kinase (AMPK)-induced preconditioning in primary cortical neurons involves activation of MCL-1. *J Neurochem,* 124, 721-34.

AOUACHERIA, A., RECH DE LAVAL, V., COMBET, C. & HARDWICK, J. M. 2013. Evolution of Bcl-2 homology motifs: homology versus homoplasy. *Trends Cell Biol,* 23, 103-11.

APPEL, S. H., ZHAO, W., BEERS, D. R. & HENKEL, J. S. 2011. The microglial-motoneuron dialogue in ALS. *Acta Myol,* 30, 4-8.

ARBOUR, N., VANDERLUIT, J. L., LE GRAND, J. N., JAHANI-ASL, A., RUZHYNSKY, V. A., CHEUNG, E. C., KELLY, M. A., MACKENZIE, A. E., PARK, D. S., OPFERMAN, J. T. & SLACK, R. S. 2008. Mcl-1 is a key regulator of apoptosis during CNS development and after DNA damage. *J Neurosci,* 28, 6068-78.

AYALA, V., GRANADO-SERRANO, A. B., CACABELOS, D., NAUDI, A., ILIEVA, E. V., BOADA, J., CARABALLO-MIRALLES, V., LLADO, J., FERRER, I., PAMPLONA, R. & PORTERO-OTIN, M. 2011. Cell stress induces TDP-43 pathological changes associated with ERK1/2 dysfunction: implications in ALS. *Acta Neuropathol,* 122, 259-70.

BAINS, J. S. & SHAW, C. A. 1997. Neurodegenerative disorders in humans: the role of glutathione in oxidative stress-mediated neuronal death. *Brain Res Brain Res Rev,* 25, 335-58.

BANERJEE, R., MOSLEY, R. L., REYNOLDS, A. D., DHAR, A., JACKSON-LEWIS, V., GORDON, P. H., PRZEDBORSKI, S. & GENDELMAN, H. E. 2008. Adaptive immune neuroprotection in G93A-SOD1 amyotrophic lateral sclerosis mice. *PLoS One,* 3, e2740.

BARGAJE, R., GUPTA, S., SARKESHIK, A., PARK, R., XU, T., SARKAR, M., HALIMANI, M., ROY, S. S., YATES, J. & PILLAI, B. 2012. Identification of novel targets for miR-29a using miRNA proteomics. *PLoS One,* 7, e43243.

BAULCOMBE, D. 2002. DNA events. An RNA microcosm. *Science,* 297, 2002-3.

BEGLEY, D. J. 2004. Delivery of therapeutic agents to the central nervous system: the problems and the possibilities. *Pharmacol Ther,* 104, 29-45.

BEHRMAN, S., ACOSTA-ALVEAR, D. & WALTER, P. 2011. A CHOP-regulated microRNA controls rhodopsin expression. *J Cell Biol,* 192, 919-27.

BINGLE, C. D., CRAIG, R. W., SWALES, B. M., SINGLETON, V., ZHOU, P. & WHYTE, M. K. 2000. Exon skipping in Mcl-1 results in a bcl-2 homology domain 3 only gene product that promotes cell death. *J Biol Chem,* 275, 22136-46.

BOILLEE, S., VANDE VELDE, C. & CLEVELAND, D. W. 2006a. ALS: a disease of motor neurons and their nonneuronal neighbors. *Neuron,* 52, 39-59.

BOILLEE, S., YAMANAKA, K., LOBSIGER, C. S., COPELAND, N. G., JENKINS, N. A., KASSIOTIS, G., KOLLIAS, G. & CLEVELAND, D. W. 2006b. Onset and progression in inherited ALS determined by motor neurons and microglia. *Science,* 312, 1389-92.

BOUCHIE, A. 2013. First microRNA mimic enters clinic. *Nat Biotechnol,* 31, 577.

BOYA, P., GONZALEZ-POLO, R. A., CASARES, N., PERFETTINI, J. L., DESSEN, P., LAROCHETTE, N., METIVIER, D., MELEY, D., SOUQUERE, S., YOSHIMORI, T., PIERRON, G., CODOGNO, P. & KROEMER, G. 2005. Inhibition of macroautophagy triggers apoptosis. *Mol Cell Biol,* 25, 1025-40.

BRANA, C., BENHAM, C. & SUNDSTROM, L. 2002. A method for characterising cell death *in vitro* by combining propidium iodide staining with immunohistochemistry. *Brain Res Brain Res Protoc,* 10, 109-14.

BRENNER, D. & MAK, T. W. 2009. Mitochondrial cell death effectors. *Curr Opin Cell Biol,* 21, 871-7.

BRODERICK, J. A. & ZAMORE, P. D. 2011. MicroRNA therapeutics. *Gene Ther,* 18, 1104-10.

BROOKS, B. R., MILLER, R. G., SWASH, M. & MUNSAT, T. L. 2000. El Escorial revisited: revised criteria for the diagnosis of amyotrophic lateral sclerosis. *Amyotroph Lateral Scler Other Motor Neuron Disord,* 1, 293-9.

BROOKS, S. P. & DUNNETT, S. B. 2009. Tests to assess motor phenotype in mice: a user's guide. *Nat Rev Neurosci,* 10, 519-29.

BRUIJN, L. I. & CUDKOWICZ, M. 2006. Therapeutic targets for amyotrophic lateral sclerosis: current treatments and prospects for more effective therapies. *Expert Rev Neurother,* 6, 417-28.

BRUIJN, L. I., HOUSEWEART, M. K., KATO, S., ANDERSON, K. L., ANDERSON, S. D., OHAMA, E., REAUME, A. G., SCOTT, R. W. & CLEVELAND, D. W. 1998. Aggregation and motor neuron toxicity of an ALS-linked SOD1 mutant independent from wild-type SOD1. *Science,* 281, 1851-4.

BURNETT, J. C. & ROSSI, J. J. 2012. RNA-based therapeutics: current progress and future prospects. *Chem Biol,* 19, 60-71.

BUTOVSKY, O., SIDDIQUI, S., GABRIELY, G., LANSER, A. J., DAKE, B., MURUGAIYAN, G., DOYKAN, C. E., WU, P. M., GALI, R. R., IYER, L. K., LAWSON, R., BERRY, J., KRICHEVSKY, A. M., CUDKOWICZ, M. E. & WEINER, H. L. 2012. Modulating inflammatory monocytes with a unique microRNA gene signature ameliorates murine ALS. *J Clin Invest,* 122, 3063-87.

BYRD, A. E., ARAGON, I. V. & BREWER, J. W. 2012. MicroRNA-30c-2* limits expression of proadaptive factor XBP1 in the unfolded protein response. *J Cell Biol,* 196, 689-98.

BYRNE, S., WALSH, C., LYNCH, C., BEDE, P., ELAMIN, M., KENNA, K., MCLAUGHLIN, R. & HARDIMAN, O. 2011. Rate of familial amyotrophic lateral sclerosis: a systematic review and meta-analysis. *J Neurol Neurosurg Psychiatry,* 82, 623-7.

CALIN, G. A., DUMITRU, C. D., SHIMIZU, M., BICHI, R., ZUPO, S., NOCH, E., ALDLER, H., RATTAN, S., KEATING, M., RAI, K., RASSENTI, L., KIPPS, T., NEGRINI, M., BULLRICH, F. & CROCE, C. M. 2002. Frequent deletions and down-regulation of micro- RNA genes miR15 and miR16 at 13q14 in chronic lymphocytic leukemia. *Proc Natl Acad Sci U S A,* 99, 15524-9.

CARE, A., CATALUCCI, D., FELICETTI, F., BONCI, D., ADDARIO, A., GALLO, P., BANG, M. L., SEGNALINI, P., GU, Y., DALTON, N. D., ELIA, L., LATRONICO, M. V., HOYDAL, M., AUTORE, C., RUSSO, M. A., DORN, G. W., 2ND, ELLINGSEN, O., RUIZ-LOZANO, P., PETERSON, K. L., CROCE, C. M., PESCHLE, C. & CONDORELLI, G. 2007. MicroRNA-133 controls cardiac hypertrophy. *Nat Med,* 13, 613-8.

CARTRON, P. F., OLIVER, L., MAYAT, E., MEFLAH, K. & VALLETTE, F. M. 2004. Impact of pH on Bax alpha conformation, oligomerisation and mitochondrial integration. *FEBS Lett,* 578, 41-6.

CHAABANE, W., USER, S. D., EL-GAZZAH, M., JAKSIK, R., SAJJADI, E., RZESZOWSKA-WOLNY, J. & LOS, M. J. 2013. Autophagy, apoptosis, mitoptosis and necrosis: interdependence between those pathways and effects on cancer. *Arch Immunol Ther Exp (Warsz),* 61, 43-58.

CHANG, J. Y. & KOROLEV, V. V. 1996. Specific toxicity of tunicamycin in induction of programmed cell death of sympathetic neurons. *Exp Neurol,* 137, 201-11.

CHEAH, B. C., VUCIC, S., KRISHNAN, A. V. & KIERNAN, M. C. 2010. Riluzole, neuroprotection and amyotrophic lateral sclerosis. *Curr Med Chem,* 17, 1942-199.

CHEN, B., ZHANG, B., LUO, H., YUAN, J., SKOGERBO, G. & CHEN, R. 2012. Distinct MicroRNA Subcellular Size and Expression Patterns in Human Cancer Cells. *Int J Cell Biol,* 2012, 672462.

CHEN, L., WILLIS, S. N., WEI, A., SMITH, B. J., FLETCHER, J. I., HINDS, M. G., COLMAN, P. M., DAY, C. L., ADAMS, J. M. & HUANG, D. C. 2005. Differential targeting of prosurvival Bcl-2 proteins by their BH3-only ligands allows complementary apoptotic function. *Mol Cell,* 17, 393-403.

CHENDRIMADA, T. P., GREGORY, R. I., KUMARASWAMY, E., NORMAN, J., COOCH, N., NISHIKURA, K. & SHIEKHATTAR, R. 2005. TRBP recruits the Dicer complex to Ago2 for microRNA processing and gene silencing. *Nature,* 436, 740-4.

CHENG, E. H., WEI, M. C., WEILER, S., FLAVELL, R. A., MAK, T. W., LINDSTEN, T. & KORSMEYER, S. J. 2001. BCL-2, BCL-X(L) sequester BH3 domain-only molecules preventing BAX- and BAK-mediated mitochondrial apoptosis. *Mol Cell,* 8, 705-11.

CHIPUK, J. E. & GREEN, D. R. 2008. How do BCL-2 proteins induce mitochondrial outer membrane permeabilization? *Trends Cell Biol,* 18, 157-64.

CHITNIS, N., PYTEL, D. & DIEHL, J. A. 2013. UPR-inducible miRNAs contribute to stressful situations. *Trends Biochem Sci.*

CHITNIS, N. S., PYTEL, D., BOBROVNIKOVA-MARJON, E., PANT, D., ZHENG, H., MAAS, N. L., FREDERICK, B., KUSHNER, J. A., CHODOSH, L. A., KOUMENIS, C., FUCHS, S. Y. & DIEHL, J. A. 2012. miR-211 is a prosurvival microRNA that regulates chop expression in a PERK-dependent manner. *Mol Cell,* 48, 353-64.

CHO, K. J., CHUNG, Y. H., SHIN, C., SHIN, D. H., KIM, Y. S., GURNEY, M. E., LEE, K. W. & CHA, C. I. 1999. Reactive astrocytes express p53 in the spinal cord of transgenic mice expressing a human Cu/Zn SOD mutation. *Neuroreport,* 10, 3939-43.

CHOI, C. I., LEE, Y. D., GWAG, B. J., CHO, S. I., KIM, S. S. & SUH-KIM, H. 2008. Effects of estrogen on lifespan and motor functions in female hSOD1 G93A transgenic mice. *J Neurol Sci,* 268, 40-7.

CLEVELAND, D. W. & ROTHSTEIN, J. D. 2001. From Charcot to Lou Gehrig: deciphering selective motor neuron death in ALS. *Nat Rev Neurosci,* 2, 806-19.

CONCANNON, C. G., WARD, M. W., BONNER, H. P., KUROKI, K., TUFFY, L. P., BONNER, C. T., WOODS, I., ENGEL, T., HENSHALL, D. C. & PREHN, J. H. 2008. NMDA receptor-mediated excitotoxic neuronal apoptosis *in vitro* and *in vivo* occurs in an ER stress and PUMA independent manner. *J Neurochem,* 105, 891-903.

COSTA, R. O., FERREIRO, E., CARDOSO, S. M., OLIVEIRA, C. R. & PEREIRA, C. M. 2010. ER stress-mediated apoptotic pathway induced by Abeta peptide requires the presence of functional mitochondria. *J Alzheimers Dis,* 20, 625-36.

COX, G. 2013. *National ALS mouse resource is key component in effort to uncover root causes of ALS* [Online]. The Jackson Laboratory. Available: http://research.jax.org/highlight/als-partnership.html 2013].

CRAWFORD, M., BATTE, K., YU, L., WU, X., NUOVO, G. J., MARSH, C. B., OTTERSON, G. A. & NANA-SINKAM, S. P. 2009. MicroRNA

133B targets pro-survival molecules MCL-1 and BCL2L2 in lung cancer. *Biochem Biophys Res Commun,* 388, 483-9.
CREGAN, S. P., ARBOUR, N. A., MACLAURIN, J. G., CALLAGHAN, S. M., FORTIN, A., CHEUNG, E. C., GUBERMAN, D. S., PARK, D. S. & SLACK, R. S. 2004. p53 activation domain 1 is essential for PUMA upregulation and p53-mediated neuronal cell death. *J Neurosci,* 24, 10003-12.
CRUTS, M., GIJSELINCK, I., VAN LANGENHOVE, T., VAN DER ZEE, J. & VAN BROECKHOVEN, C. 2013. Current insights into the C9orf72 repeat expansion diseases of the FTLD/ALS spectrum. *Trends Neurosci,* 36, 450-9.
CUCONATI, A., MUKHERJEE, C., PEREZ, D. & WHITE, E. 2003. DNA damage response and MCL-1 destruction initiate apoptosis in adenovirus-infected cells. *Genes Dev,* 17, 2922-32.
DANIAL, N. N. 2007. BCL-2 family proteins: critical checkpoints of apoptotic cell death. *Clin Cancer Res,* 13, 7254-63.
DANIAL, N. N. & KORSMEYER, S. J. 2004. Cell death: critical control points. *Cell,* 116, 205-19.
DAVIS, T. H., CUELLAR, T. L., KOCH, S. M., BARKER, A. J., HARFE, B. D., MCMANUS, M. T. & ULLIAN, E. M. 2008. Conditional loss of Dicer disrupts cellular and tissue morphogenesis in the cortex and hippocampus. *J Neurosci,* 28, 4322-30.
DENG, C., TAO, R., YU, S. Z. & JIN, H. 2012. Inhibition of 6-hydroxydopamine-induced endoplasmic reticulum stress by sulforaphane through the activation of Nrf2 nuclear translocation. *Mol Med Rep,* 6, 215-9.
DENIAUD, A., SHARAF EL DEIN, O., MAILLIER, E., PONCET, D., KROEMER, G., LEMAIRE, C. & BRENNER, C. 2008. Endoplasmic reticulum stress induces calcium-dependent permeability transition, mitochondrial outer membrane permeabilization and apoptosis. *Oncogene,* 27, 285-99.
DESJOBERT, C., RENALIER, M. H., BERGALET, J., DEJEAN, E., JOSEPH, N., KRUCZYNSKI, A., SOULIER, J., ESPINOS, E., MEGGETTO, F., CAVAILLE, J., DELSOL, G. & LAMANT, L. 2011. MiR-29a down-regulation in ALK-positive anaplastic large cell lymphomas contributes to apoptosis blockade through MCL-1 overexpression. *Blood,* 117, 6627-37.
DU, H., WOLF, J., SCHAFER, B., MOLDOVEANU, T., CHIPUK, J. E. & KUWANA, T. 2011. BH3 domains other than Bim and Bid can directly activate Bax/Bak. *J Biol Chem,* 286, 491-501.
EDINGER, A. L. & THOMPSON, C. B. 2004. Death by design: apoptosis, necrosis and autophagy. *Curr Opin Cell Biol,* 16, 663-9.
ELMEN, J., LINDOW, M., SILAHTAROGLU, A., BAK, M., CHRISTENSEN, M., LIND-THOMSEN, A., HEDTJARN, M., HANSEN, J. B., HANSEN, H. F., STRAARUP, E. M., MCCULLAGH, K., KEARNEY, P. & KAUPPINEN, S. 2008. Antagonism of microRNA-122 in mice by systemically administered LNA-antimiR leads to up-regulation of a large set of predicted target mRNAs in the liver. *Nucleic Acids Res,* 36, 1153-62.

ELMORE, S. 2007. Apoptosis: a review of programmed cell death. *Toxicol Pathol,* 35, 495-516.

ERLICH, S., MIZRACHY, L., SEGEV, O., LINDENBOIM, L., ZMIRA, O., ADI-HAREL, S., HIRSCH, J. A., STEIN, R. & PINKAS-KRAMARSKI, R. 2007. Differential interactions between Beclin 1 and Bcl-2 family members. *Autophagy,* 3, 561-8.

ESAU, C. C. & MONIA, B. P. 2007. Therapeutic potential for microRNAs. *Adv Drug Deliv Rev,* 59, 101-14.

FARG, M. A., SOO, K. Y., WALKER, A. K., PHAM, H., ORIAN, J., HORNE, M. K., WARRAICH, S. T., WILLIAMS, K. L., BLAIR, I. P. & ATKIN, J. D. 2012. Mutant FUS induces endoplasmic reticulum stress in amyotrophic lateral sclerosis and interacts with protein disulfide-isomerase. *Neurobiol Aging,* 33, 2855-68.

FERRAIUOLO, L., HEATH, P. R., HOLDEN, H., KASHER, P., KIRBY, J. & SHAW, P. J. 2007. Microarray analysis of the cellular pathways involved in the adaptation to and progression of motor neuron injury in the SOD1 G93A mouse model of familial ALS. *J Neurosci,* 27, 9201-19.

FILIPOWICZ, W., BHATTACHARYYA, S. N. & SONENBERG, N. 2008. Mechanisms of post-transcriptional regulation by microRNAs: are the answers in sight? *Nat Rev Genet,* 9, 102-14.

FRICKER, M., PAPADIA, S., HARDINGHAM, G. E. & TOLKOVSKY, A. M. 2010. Implication of TAp73 in the p53-independent pathway of Puma induction and Puma-dependent apoptosis in primary cortical neurons. *J Neurochem,* 114, 772-83.

FRIEDMAN, R. C., FARH, K. K., BURGE, C. B. & BARTEL, D. P. 2009. Most mammalian mRNAs are conserved targets of microRNAs. *Genome Res,* 19, 92-105.

FRITSCH, R. M., SCHNEIDER, G., SAUR, D., SCHEIBEL, M. & SCHMID, R. M. 2007. Translational repression of MCL-1 couples stress-induced eIF2 alpha phosphorylation to mitochondrial apoptosis initiation. *J Biol Chem,* 282, 22551-62.

GABRIELY, G., WURDINGER, T., KESARI, S., ESAU, C. C., BURCHARD, J., LINSLEY, P. S. & KRICHEVSKY, A. M. 2008. MicroRNA 21 promotes glioma invasion by targeting matrix metalloproteinase regulators. *Mol Cell Biol,* 28, 5369-80.

GALEHDAR, Z., SWAN, P., FUERTH, B., CALLAGHAN, S. M., PARK, D. S. & CREGAN, S. P. 2010. Neuronal apoptosis induced by endoplasmic reticulum stress is regulated by ATF4-CHOP-mediated induction of the Bcl-2 homology 3-only member PUMA. *J Neurosci,* 30, 16938-48.

GARBUZOVA-DAVIS, S., SAPORTA, S., HALLER, E., KOLOMEY, I., BENNETT, S. P., POTTER, H. & SANBERG, P. R. 2007. Evidence of compromised blood-spinal cord barrier in early and late symptomatic SOD1 mice modeling ALS. *PLoS One,* 2, e1205.

GELINAS, C. & WHITE, E. 2005. BH3-only proteins in control: specificity regulates MCL-1 and BAK-mediated apoptosis. *Genes Dev,* 19, 1263-8.

GERMAIN, M., MILBURN, J. & DURONIO, V. 2008. MCL-1 inhibits BAX in the absence of MCL-1/BAX Interaction. *J Biol Chem,* 283, 6384-92.

GERMAIN, M., NGUYEN, A. P., LE GRAND, J. N., ARBOUR, N., VANDERLUIT, J. L., PARK, D. S., OPFERMAN, J. T. & SLACK, R. S. 2011. MCL-1 is a stress sensor that regulates autophagy in a developmentally regulated manner. *EMBO J,* 30, 395-407.

GHOSH, A. P., KLOCKE, B. J., BALLESTAS, M. E. & ROTH, K. A. 2012. CHOP potentially co-operates with FOXO3a in neuronal cells to regulate PUMA and BIM expression in response to ER stress. *PLoS One,* 7, e39586.

GILLESPIE, J. I. 2005. A developing view of the origins of urgency: the importance of animal models. *BJU Int,* 96 Suppl 1, 22-8.

GITCHO, M. A., BALOH, R. H., CHAKRAVERTY, S., MAYO, K., NORTON, J. B., LEVITCH, D., HATANPAA, K. J., WHITE, C. L., 3RD, BIGIO, E. H., CASELLI, R., BAKER, M., AL-LOZI, M. T., MORRIS, J. C., PESTRONK, A., RADEMAKERS, R., GOATE, A. M. & CAIRNS, N. J. 2008. TDP-43 A315T mutation in familial motor neuron disease. *Ann Neurol,* 63, 535-8.

GOMEZ-LAZARO, M., GALINDO, M. F., CONCANNON, C. G., SEGURA, M. F., FERNANDEZ-GOMEZ, F. J., LLECHA, N., COMELLA, J. X., PREHN, J. H. & JORDAN, J. 2008. 6-Hydroxydopamine activates the mitochondrial apoptosis pathway through p38 MAPK-mediated, p53-independent activation of Bax and PUMA. *J Neurochem,* 104, 1599-612.

GOODALL, E. F. & MORRISON, K. E. 2006. Amyotrophic lateral sclerosis (motor neuron disease): proposed mechanisms and pathways to treatment. *Expert Rev Mol Med,* 8, 1-22.

GOULD, T. W., BUSS, R. R., VINSANT, S., PREVETTE, D., SUN, W., KNUDSON, C. M., MILLIGAN, C. E. & OPPENHEIM, R. W. 2006. Complete dissociation of motor neuron death from motor dysfunction by Bax deletion in a mouse model of ALS. *J Neurosci,* 26, 8774-86.

GREENE, C. M., CHHABRA, R. & MCELVANEY, N. G. 2013. Is there a therapeutic role for selenium in alpha-1 antitrypsin deficiency? *Nutrients,* 5, 758-70.

GUO, H., INGOLIA, N. T., WEISSMAN, J. S. & BARTEL, D. P. 2010. Mammalian microRNAs predominantly act to decrease target mRNA levels. *Nature,* 466, 835-40.

GUPTA, S., READ, D. E., DEEPTI, A., CAWLEY, K., GUPTA, A., OOMMEN, D., VERFAILLIE, T., MATUS, S., SMITH, M. A., MOTT, J. L., AGOSTINIS, P., HETZ, C. & SAMALI, A. 2012. Perk-dependent repression of miR-106b-25 cluster is required for ER stress-induced apoptosis. *Cell Death Dis,* 3, e333.

GURNEY, M. E., PU, H., CHIU, A. Y., DAL CANTO, M. C., POLCHOW, C. Y., ALEXANDER, D. D., CALIENDO, J., HENTATI, A., KWON, Y. W., DENG, H. X. & ET AL. 1994. Motor neuron degeneration in mice that express a human Cu,Zn superoxide dismutase mutation. *Science,* 264, 1772-5.

GURTAN, A. M. & SHARP, P. A. 2013. The Role of miRNAs in Regulating Gene Expression Networks. *J Mol Biol.*

HAN, J., GOLDSTEIN, L. A., GASTMAN, B. R. & RABINOWICH, H. 2006. Interrelated roles for Mcl-1 and BIM in regulation of TRAIL-mediated mitochondrial apoptosis. *J Biol Chem,* 281, 10153-63.

HARAMATI, S., CHAPNIK, E., SZTAINBERG, Y., EILAM, R., ZWANG, R., GERSHONI, N., MCGLINN, E., HEISER, P. W., WILLS, A. M., WIRGUIN, I., RUBIN, L. L., MISAWA, H., TABIN, C. J., BROWN, R., JR., CHEN, A. & HORNSTEIN, E. 2010. miRNA malfunction causes spinal motor neuron disease. *Proc Natl Acad Sci U S A,* 107, 13111-6.

HARDING, H. P., ZHANG, Y., BERTOLOTTI, A., ZENG, H. & RON, D. 2000. Perk is essential for translational regulation and cell survival during the unfolded protein response. *Mol Cell,* 5, 897-904.

HASHIMOTO, Y., AKIYAMA, Y. & YUASA, Y. 2013. Multiple-to-multiple relationships between microRNAs and target genes in gastric cancer. *PLoS One,* 8, e62589.

HEBERT, S. S., HORRE, K., NICOLAI, L., PAPADOPOULOU, A. S., MANDEMAKERS, W., SILAHTAROGLU, A. N., KAUPPINEN, S., DELACOURTE, A. & DE STROOPER, B. 2008. Loss of microRNA cluster miR-29a/b-1 in sporadic Alzheimer's disease correlates with increased BACE1/beta-secretase expression. *Proc Natl Acad Sci U S A,* 105, 6415-20.

HEGEDUS, J., PUTMAN, C. T. & GORDON, T. 2007. Time course of preferential motor unit loss in the SOD1 G93A mouse model of amyotrophic lateral sclerosis. *Neurobiol Dis,* 28, 154-64.

HERRANT, M., JACQUEL, A., MARCHETTI, S., BELHACENE, N., COLOSETTI, P., LUCIANO, F. & AUBERGER, P. 2004. Cleavage of Mcl-1 by caspases impaired its ability to counteract Bim-induced apoptosis. *Oncogene,* 23, 7863-73.

HETZ, C., THIELEN, P., FISHER, J., PASINELLI, P., BROWN, R. H., KORSMEYER, S. & GLIMCHER, L. 2007. The proapoptotic BCL-2 family member BIM mediates motoneuron loss in a model of amyotrophic lateral sclerosis. *Cell Death Differ,* 14, 1386-9.

HIBIO, N., HINO, K., SHIMIZU, E., NAGATA, Y. & UI-TEI, K. 2012. Stability of miRNA 5'terminal and seed regions is correlated with experimentally observed miRNA-mediated silencing efficacy. *Sci Rep,* 2, 996.

HOOZEMANS, J. J., VEERHUIS, R., VAN HAASTERT, E. S., ROZEMULLER, J. M., BAAS, F., EIKELENBOOM, P. & SCHEPER, W. 2005. The unfolded protein response is activated in Alzheimer's disease. *Acta Neuropathol,* 110, 165-72.

HWANG, H. W., WENTZEL, E. A. & MENDELL, J. T. 2007. A hexanucleotide element directs microRNA nuclear import. *Science,* 315, 97-100.

ILIEVA, E. V., AYALA, V., JOVE, M., DALFO, E., CACABELOS, D., POVEDANO, M., BELLMUNT, M. J., FERRER, I., PAMPLONA, R. & PORTERO-OTIN, M. 2007. Oxidative and endoplasmic reticulum stress interplay in sporadic amyotrophic lateral sclerosis. *Brain,* 130, 3111-23.

JACKSON, M., GANEL, R. & ROTHSTEIN, J. D. 2002. Models of amyotrophic lateral sclerosis. *Curr Protoc Neurosci,* Chapter 9, Unit 9 13.

JAROSCH, E., TAXIS, C., VOLKWEIN, C., BORDALLO, J., FINLEY, D., WOLF, D. H. & SOMMER, T. 2002. Protein dislocation from the ER requires polyubiquitination and the AAA-ATPase Cdc48. *Nat Cell Biol,* 4, 134-9.

JIANG, C. C., LUCAS, K., AVERY-KIEJDA, K. A., WADE, M., DEBOCK, C. E., THORNE, R. F., ALLEN, J., HERSEY, P. & ZHANG, X. D. 2008. Up-regulation of Mcl-1 is critical for survival of human melanoma cells upon endoplasmic reticulum stress. *Cancer Res,* 68, 6708-17.

JIMENEZ-MATEOS, E. M., ENGEL, T., MERINO-SERRAIS, P., MCKIERNAN, R. C., TANAKA, K., MOURI, G., SANO, T., O'TUATHAIGH, C., WADDINGTON, J. L., PRENTER, S., DELANTY, N., FARRELL, M. A., O'BRIEN, D. F., CONROY, R. M., STALLINGS, R. L., DEFELIPE, J. & HENSHALL, D. C. 2012. Silencing microRNA-134 produces neuroprotective and prolonged seizure-suppressive effects. *Nat Med,* 18, 1087-94.

JOHNSON, R., ZUCCATO, C., BELYAEV, N. D., GUEST, D. J., CATTANEO, E. & BUCKLEY, N. J. 2008. A microRNA-based gene dysregulation pathway in Huntington's disease. *Neurobiol Dis,* 29, 438-45.

JOHNSTON, J. A., DALTON, M. J., GURNEY, M. E. & KOPITO, R. R. 2000. Formation of high molecular weight complexes of mutant Cu, Zn-superoxide dismutase in a mouse model for familial amyotrophic lateral sclerosis. *Proc Natl Acad Sci U S A,* 97, 12571-6.

JULIEN, J. P. 2007. ALS: astrocytes move in as deadly neighbors. *Nat Neurosci,* 10, 535-7.

JUNN, E. & MOURADIAN, M. M. 2012. MicroRNAs in neurodegenerative diseases and their therapeutic potential. *Pharmacol Ther,* 133, 142-50.

KACZMAREK, A., VANDENABEELE, P. & KRYSKO, D. V. 2013. Necroptosis: the release of damage-associated molecular patterns and its physiological relevance. *Immunity,* 38, 209-23.

KANEKURA, K., SUZUKI, H., AISO, S. & MATSUOKA, M. 2009. ER stress and unfolded protein response in amyotrophic lateral sclerosis. *Mol Neurobiol,* 39, 81-9.

KANG, R., ZEH, H. J., LOTZE, M. T. & TANG, D. 2011. The Beclin 1 network regulates autophagy and apoptosis. *Cell Death Differ,* 18, 571-80.

KATAYAMA, T., IMAIZUMI, K., MANABE, T., HITOMI, J., KUDO, T. & TOHYAMA, M. 2004. Induction of neuronal death by ER stress in Alzheimer's disease. *J Chem Neuroanat,* 28, 67-78.

KIERAN, D., WOODS, I., VILLUNGER, A., STRASSER, A. & PREHN, J. H. 2007. Deletion of the BH3-only protein puma protects motoneurons from ER stress-induced apoptosis and delays motoneuron loss in ALS mice. *Proc Natl Acad Sci U S A,* 104, 20606-11.

KIKUCHI, H., ALMER, G., YAMASHITA, S., GUEGAN, C., NAGAI, M., XU, Z., SOSUNOV, A. A., MCKHANN, G. M., 2ND & PRZEDBORSKI, S. 2006. Spinal cord endoplasmic reticulum stress

associated with a microsomal accumulation of mutant superoxide dismutase-1 in an ALS model. *Proc Natl Acad Sci U S A,* 103, 6025-30.

KIM, J., INOUE, K., ISHII, J., VANTI, W. B., VORONOV, S. V., MURCHISON, E., HANNON, G. & ABELIOVICH, A. 2007. A MicroRNA feedback circuit in midbrain dopamine neurons. *Science,* 317, 1220-4.

KLOOSTERMAN, W. P. & PLASTERK, R. H. 2006. The diverse functions of microRNAs in animal development and disease. *Dev Cell,* 11, 441-50.

KLOOSTERMAN, W. P., WIENHOLDS, E., DE BRUIJN, E., KAUPPINEN, S. & PLASTERK, R. H. 2006. *In situ* detection of miRNAs in animal embryos using LNA-modified oligonucleotide probes. *Nat Methods,* 3, 27-9.

KNIPPENBERG, S., THAU, N., DENGLER, R. & PETRI, S. 2010. Significance of behavioural tests in a transgenic mouse model of amyotrophic lateral sclerosis (ALS). *Behav Brain Res,* 213, 82-7.

KOLE, A. J., SWAHARI, V., HAMMOND, S. M. & DESHMUKH, M. 2011. miR-29b is activated during neuronal maturation and targets BH3-only genes to restrict apoptosis. *Genes Dev,* 25, 125-30.

KONG, J. & XU, Z. 1998. Massive mitochondrial degeneration in motor neurons triggers the onset of amyotrophic lateral sclerosis in mice expressing a mutant SOD1. *J Neurosci,* 18, 3241-50.

KONOPLEVA, M., CONTRACTOR, R., TSAO, T., SAMUDIO, I., RUVOLO, P. P., KITADA, S., DENG, X., ZHAI, D., SHI, Y. X., SNEED, T., VERHAEGEN, M., SOENGAS, M., RUVOLO, V. R., MCQUEEN, T., SCHOBER, W. D., WATT, J. C., JIFFAR, T., LING, X., MARINI, F. C., HARRIS, D., DIETRICH, M., ESTROV, Z., MCCUBREY, J., MAY, W. S., REED, J. C. & ANDREEFF, M. 2006. Mechanisms of apoptosis sensitivity and resistance to the BH3 mimetic ABT-737 in acute myeloid leukemia. *Cancer Cell,* 10, 375-88.

KOSHIKAWA, N., MAEJIMA, C., MIYAZAKI, K., NAKAGAWARA, A. & TAKENAGA, K. 2006. Hypoxia selects for high-metastatic Lewis lung carcinoma cells overexpressing Mcl-1 and exhibiting reduced apoptotic potential in solid tumors. *Oncogene,* 25, 917-28.

KOSTIC, V., JACKSON-LEWIS, V., DE BILBAO, F., DUBOIS-DAUPHIN, M. & PRZEDBORSKI, S. 1997. Bcl-2: prolonging life in a transgenic mouse model of familial amyotrophic lateral sclerosis. *Science,* 277, 559-62.

KOVAL, E. D., SHANER, C., ZHANG, P., DU MAINE, X., FISCHER, K., TAY, J., CHAU, B. N., WU, G. F. & MILLER, T. M. 2013. Method for widespread microRNA-155 inhibition prolongs survival in ALS-model mice. *Hum Mol Genet.*

KOZOPAS, K. M., YANG, T., BUCHAN, H. L., ZHOU, P. & CRAIG, R. W. 1993. MCL1, a gene expressed in programmed myeloid cell differentiation, has sequence similarity to BCL2. *Proc Natl Acad Sci U S A,* 90, 3516-20.

KRAJEWSKI, S., BODRUG, S., KRAJEWSKA, M., SHABAIK, A., GASCOYNE, R., BEREAN, K. & REED, J. C. 1995.

Immunohistochemical analysis of Mcl-1 protein in human tissues. Differential regulation of Mcl-1 and Bcl-2 protein production suggests a unique role for Mcl-1 in control of programmed cell death *in vivo*. *Am J Pathol,* 146, 1309-19.

KRIEGEL, A. J., LIU, Y., FANG, Y., DING, X. & LIANG, M. 2012. The miR-29 family: genomics, cell biology, and relevance to renal and cardiovascular injury. *Physiol Genomics,* 44, 237-44.

KROEMER, G. & LEVINE, B. 2008. Autophagic cell death: the story of a misnomer. *Nat Rev Mol Cell Biol,* 9, 1004-10.

KROEMER, G. & MARTIN, S. J. 2005. Caspase-independent cell death. *Nat Med,* 11, 725-30.

KROL, J., SOBCZAK, K., WILCZYNSKA, U., DRATH, M., JASINSKA, A., KACZYNSKA, D. & KRZYZOSIAK, W. J. 2004. Structural features of microRNA (miRNA) precursors and their relevance to miRNA biogenesis and small interfering RNA/short hairpin RNA design. *J Biol Chem,* 279, 42230-9.

KRUTZFELDT, J., KUWAJIMA, S., BRAICH, R., RAJEEV, K. G., PENA, J., TUSCHL, T., MANOHARAN, M. & STOFFEL, M. 2007. Specificity, duplex degradation and subcellular localization of antagomirs. *Nucleic Acids Res,* 35, 2885-92.

KRUTZFELDT, J., RAJEWSKY, N., BRAICH, R., RAJEEV, K. G., TUSCHL, T., MANOHARAN, M. & STOFFEL, M. 2005. Silencing of microRNAs *in vivo* with 'antagomirs'. *Nature,* 438, 685-9.

KUMAR, M. S., ERKELAND, S. J., PESTER, R. E., CHEN, C. Y., EBERT, M. S., SHARP, P. A. & JACKS, T. 2008. Suppression of non-small cell lung tumor development by the let-7 microRNA family. *Proc Natl Acad Sci U S A,* 105, 3903-8.

KUNDU, M. & THOMPSON, C. B. 2008. Autophagy: basic principles and relevance to disease. *Annu Rev Pathol,* 3, 427-55.

KUWANA, T., BOUCHIER-HAYES, L., CHIPUK, J. E., BONZON, C., SULLIVAN, B. A., GREEN, D. R. & NEWMEYER, D. D. 2005. BH3 domains of BH3-only proteins differentially regulate Bax-mediated mitochondrial membrane permeabilization both directly and indirectly. *Mol Cell,* 17, 525-35.

KUWANA, T. & NEWMEYER, D. D. 2003. Bcl-2-family proteins and the role of mitochondria in apoptosis. *Curr Opin Cell Biol,* 15, 691-9.

LAGIER-TOURENNE, C. & CLEVELAND, D. W. 2009. Rethinking ALS: the FUS about TDP-43. *Cell,* 136, 1001-4.

LAM, L. T., LU, X., ZHANG, H., LESNIEWSKI, R., ROSENBERG, S. & SEMIZAROV, D. 2010. A microRNA screen to identify modulators of sensitivity to BCL2 inhibitor ABT-263 (navitoclax). *Mol Cancer Ther,* 9, 2943-50.

LEE, A. S. 2005. The ER chaperone and signaling regulator GRP78/BiP as a monitor of endoplasmic reticulum stress. *Methods,* 35, 373-81.

LEE, K., TIRASOPHON, W., SHEN, X., MICHALAK, M., PRYWES, R., OKADA, T., YOSHIDA, H., MORI, K. & KAUFMAN, R. J. 2002. IRE1-mediated unconventional mRNA splicing and S2P-mediated ATF6 cleavage merge to regulate XBP1 in signaling the unfolded protein response. *Genes Dev,* 16, 452-66.

LEE, Y., AHN, C., HAN, J., CHOI, H., KIM, J., YIM, J., LEE, J., PROVOST, P., RADMARK, O., KIM, S. & KIM, V. N. 2003. The nuclear RNase III Drosha initiates microRNA processing. *Nature,* 425, 415-9.

LEIGH, P. N. & RAY-CHAUDHURI, K. 1994. Motor neuron disease. *J Neurol Neurosurg Psychiatry,* 57, 886-96.

LEITNER, M. 2009. Working with ALS mice: Guidelines for preclinical testing and colony management. *In:* LABORATORY, T. J. (ed.). The Jackson Laboratory.

LI, J., LEE, B. & LEE, A. S. 2006. Endoplasmic reticulum stress-induced apoptosis: multiple pathways and activation of p53-up-regulated modulator of apoptosis (PUMA) and NOXA by p53. *J Biol Chem,* 281, 7260-70.

LI, K., LI, Y., SHELTON, J. M., RICHARDSON, J. A., SPENCER, E., CHEN, Z. J., WANG, X. & WILLIAMS, R. S. 2000. Cytochrome c deficiency causes embryonic lethality and attenuates stress-induced apoptosis. *Cell,* 101, 389-99.

LI, R., STRYKOWSKI, R., MEYER, M., MULCRONE, P., KRAKORA, D. & SUZUKI, M. 2012. Male-specific differences in proliferation, neurogenesis, and sensitivity to oxidative stress in neural progenitor cells derived from a rat model of ALS. *PLoS One,* 7, e48581.

LI, S., ZHAO, Y., HE, X., KIM, T. H., KUHARSKY, D. K., RABINOWICH, H., CHEN, J., DU, C. & YIN, X. M. 2002. Relief of extrinsic pathway inhibition by the Bid-dependent mitochondrial release of Smac in Fas-mediated hepatocyte apoptosis. *J Biol Chem,* 277, 26912-20.

LIM, L. P., LAU, N. C., GARRETT-ENGELE, P., GRIMSON, A., SCHELTER, J. M., CASTLE, J., BARTEL, D. P., LINSLEY, P. S. & JOHNSON, J. M. 2005. Microarray analysis shows that some microRNAs downregulate large numbers of target mRNAs. *Nature,* 433, 769-73.

LIN, J. H., WALTER, P. & YEN, T. S. 2008. Endoplasmic reticulum stress in disease pathogenesis. *Annu Rev Pathol,* 3, 399-425.

LINDHOLM, D., WOOTZ, H. & KORHONEN, L. 2006. ER stress and neurodegenerative diseases. *Cell Death Differ,* 13, 385-92.

LINDSTEN, T., GOLDEN, J. A., ZONG, W. X., MINARCIK, J., HARRIS, M. H. & THOMPSON, C. B. 2003. The proapoptotic activities of Bax and Bak limit the size of the neural stem cell pool. *J Neurosci,* 23, 11112-9.

LIPPI, G., STEINERT, J. R., MARCZYLO, E. L., D'ORO, S., FIORE, R., FORSYTHE, I. D., SCHRATT, G., ZOLI, M., NICOTERA, P. & YOUNG, K. W. 2011. Targeting of the Arpc3 actin nucleation factor by miR-29a/b regulates dendritic spine morphology. *J Cell Biol,* 194, 889-904.

LIPSON, C., ALALOUF, G., BAJOREK, M., RABINOVICH, E., ATIR-LANDE, A., GLICKMAN, M. & BAR-NUN, S. 2008. A proteasomal ATPase contributes to dislocation of endoplasmic reticulum-associated degradation (ERAD) substrates. *J Biol Chem,* 283, 7166-75.

LISCIC, R. M., GRINBERG, L. T., ZIDAR, J., GITCHO, M. A. & CAIRNS, N. J. 2008. ALS and FTLD: two faces of TDP-43 proteinopathy. *Eur J Neurol,* 15, 772-80.

LODISH, H., BERK, A., KAISER, C.A., KREIGER, M., SCOTT, M.P., BRETSCHER, A., PLOEGH, H., MATSUDAIRA, P. 2008. *Molecular Cell Biology*.

LOGUE, S. E., CLEARY, P., SAVELJEVA, S. & SAMALI, A. 2013. New directions in ER stress-induced cell death. *Apoptosis,* 18, 537-46.

LUDOLPH, A. C., BENDOTTI, C., BLAUGRUND, E., CHIO, A., GREENSMITH, L., LOEFFLER, J. P., MEAD, R., NIESSEN, H. G., PETRI, S., PRADAT, P. F., ROBBERECHT, W., RUEGG, M., SCHWALENSTOCKER, B., STILLER, D., VAN DEN BERG, L., VIEIRA, F. & VON HORSTEN, S. 2010. Guidelines for preclinical animal research in ALS/MND: A consensus meeting. *Amyotroph Lateral Scler,* 11, 38-45.

LUDOLPH, A. C., BENDOTTI, C., BLAUGRUND, E., HENGERER, B., LOFFLER, J. P., MARTIN, J., MEININGER, V., MEYER, T., MOUSSAOUI, S., ROBBERECHT, W., SCOTT, S., SILANI, V. & VAN DEN BERG, L. H. 2007. Guidelines for the preclinical *in vivo* evaluation of pharmacological active drugs for ALS/MND: report on the 142nd ENMC international workshop. *Amyotroph Lateral Scler,* 8, 217-23.

MACARIO, A. J. & CONWAY DE MACARIO, E. 2002. Sick chaperones and ageing: a perspective. *Ageing Res Rev,* 1, 295-311.

MAGIERA, M. M., MORA, S., MOJSA, B., ROBBINS, I., LASSOT, I. & DESAGHER, S. 2013. Trim17-mediated ubiquitination and degradation of Mcl-1 initiate apoptosis in neurons. *Cell Death Differ,* 20, 281-92.

MAIURI, M. C., ZALCKVAR, E., KIMCHI, A. & KROEMER, G. 2007. Self-eating and self-killing: crosstalk between autophagy and apoptosis. *Nat Rev Mol Cell Biol,* 8, 741-52.

MALONE, C. D., HASAN, S. M., ROOME, R. B., XIONG, J., FURLONG, M., OPFERMAN, J. T. & VANDERLUIT, J. L. 2012. Mcl-1 regulates the survival of adult neural precursor cells. *Mol Cell Neurosci,* 49, 439-47.

MANCUSO, R., OLIVAN, S., RANDO, A., CASAS, C., OSTA, R. & NAVARRO, X. 2012. Sigma-1R agonist improves motor function and motoneuron survival in ALS mice. *Neurotherapeutics,* 9, 814-26.

MARDER, E. & GOAILLARD, J. M. 2006. Variability, compensation and homeostasis in neuron and network function. *Nat Rev Neurosci,* 7, 563-74.

MARTIN, A. P., MITCHELL, C., RAHMANI, M., NEPHEW, K. P., GRANT, S. & DENT, P. 2009. Inhibition of MCL-1 enhances lapatinib toxicity and overcomes lapatinib resistance via BAK-dependent autophagy. *Cancer Biol Ther,* 8, 2084-96.

MARTIN, L. J. 2010. Mitochondrial and Cell Death Mechanisms in Neurodegenerative Diseases. *Pharmaceuticals (Basel),* 3, 839-915.

MARTIN, L. J., AL-ABDULLA, N. A., BRAMBRINK, A. M., KIRSCH, J. R., SIEBER, F. E. & PORTERA-CAILLIAU, C. 1998. Neurodegeneration in excitotoxicity, global cerebral ischemia, and target deprivation: A perspective on the contributions of apoptosis and necrosis. *Brain Res Bull,* 46, 281-309.

MATTSON, M. P. 2000. Apoptosis in neurodegenerative disorders. *Nat Rev Mol Cell Biol,* 1, 120-9.
MATUS, S., GLIMCHER, L. H. & HETZ, C. 2011. Protein folding stress in neurodegenerative diseases: a glimpse into the ER. *Curr Opin Cell Biol,* 23, 239-52.
MATUS, S., LOPEZ, E., VALENZUELA, V., NASSIF, M. & HETZ, C. 2013. Functional Contribution of the Transcription Factor ATF4 to the Pathogenesis of Amyotrophic Lateral Sclerosis. *PLoS One,* 8, e66672.
MAUREL, M. & CHEVET, E. 2013. Endoplasmic reticulum stress signaling: the microRNA connection. *Am J Physiol Cell Physiol,* 304, C1117-26.
MCCOMBE, P. A. & HENDERSON, R. D. 2010. Effects of gender in amyotrophic lateral sclerosis. *Gend Med,* 7, 557-70.
MCILWAIN, D. R., BERGER, T. & MAK, T. W. 2013. Caspase functions in cell death and disease. *Cold Spring Harb Perspect Med,* 3, a008656.
MEI, Y., DU, W., YANG, Y. & WU, M. 2005. Puma(*)Mcl-1 interaction is not sufficient to prevent rapid degradation of Mcl-1. *Oncogene,* 24, 7224-37.
MEKADA, K., ABE, K., MURAKAMI, A., NAKAMURA, S., NAKATA, H., MORIWAKI, K., OBATA, Y. & YOSHIKI, A. 2009. Genetic differences among C57BL/6 substrains. *Exp Anim,* 58, 141-9.
MEUSSER, B., HIRSCH, C., JAROSCH, E. & SOMMER, T. 2005. ERAD: the long road to destruction. *Nat Cell Biol,* 7, 766-72.
MILLER, R. G., BOUCHARD, J. P., DUQUETTE, P., EISEN, A., GELINAS, D., HARATI, Y., MUNSAT, T. L., POWE, L., ROTHSTEIN, J., SALZMAN, P. & SUFIT, R. L. 1996. Clinical trials of riluzole in patients with ALS. ALS/Riluzole Study Group-II. *Neurology,* 47, S86-90; discussion S90-2.
MILLER, R. G., JACKSON, C. E., KASARSKIS, E. J., ENGLAND, J. D., FORSHEW, D., JOHNSTON, W., KALRA, S., KATZ, J. S., MITSUMOTO, H., ROSENFELD, J., SHOESMITH, C., STRONG, M. J. & WOOLLEY, S. C. 2009a. Practice parameter update: the care of the patient with amyotrophic lateral sclerosis: drug, nutritional, and respiratory therapies (an evidence-based review): report of the Quality Standards Subcommittee of the American Academy of Neurology. *Neurology,* 73, 1218-26.
MILLER, R. G., JACKSON, C. E., KASARSKIS, E. J., ENGLAND, J. D., FORSHEW, D., JOHNSTON, W., KALRA, S., KATZ, J. S., MITSUMOTO, H., ROSENFELD, J., SHOESMITH, C., STRONG, M. J. & WOOLLEY, S. C. 2009b. Practice parameter update: the care of the patient with amyotrophic lateral sclerosis: multidisciplinary care, symptom management, and cognitive/behavioral impairment (an evidence-based review): report of the Quality Standards Subcommittee of the American Academy of Neurology. *Neurology,* 73, 1227-33.
MISRA, A., GANESH, S., SHAHIWALA, A. & SHAH, S. P. 2003. Drug delivery to the central nervous system: a review. *J Pharm Pharm Sci,* 6, 252-73.
MIURA, M. 2011. Active participation of cell death in development and organismal homeostasis. *Dev Growth Differ,* 53, 125-36.
MORI, K., WENG, S. M., ARZBERGER, T., MAY, S., RENTZSCH, K., KREMMER, E., SCHMID, B., KRETZSCHMAR, H. A., CRUTS, M.,

VAN BROECKHOVEN, C., HAASS, C. & EDBAUER, D. 2013. The C9orf72 GGGGCC repeat is translated into aggregating dipeptide-repeat proteins in FTLD/ALS. *Science,* 339, 1335-8.
MORIWAKI, K. & CHAN, F. K. 2013. RIP3: a molecular switch for necrosis and inflammation. *Genes Dev,* 27, 1640-9.
MOTT, J. L., KOBAYASHI, S., BRONK, S. F. & GORES, G. J. 2007. mir-29 regulates Mcl-1 protein expression and apoptosis. *Oncogene,* 26, 6133-40.
MOTT, J. L., KURITA, S., CAZANAVE, S. C., BRONK, S. F., WERNEBURG, N. W. & FERNANDEZ-ZAPICO, M. E. 2010. Transcriptional suppression of mir-29b-1/mir-29a promoter by c-Myc, hedgehog, and NF-kappaB. *J Cell Biochem,* 110, 1155-64.
MULLIGAN, V. K. & CHAKRABARTTY, A. 2013. Protein misfolding in the late-onset neurodegenerative diseases: Common themes and the unique case of amyotrophic lateral sclerosis. *Proteins,* 81, 1285-303.
NAGAI, M., AOKI, M., MIYOSHI, I., KATO, M., PASINELLI, P., KASAI, N., BROWN, R. H., JR. & ITOYAMA, Y. 2001. Rats expressing human cytosolic copper-zinc superoxide dismutase transgenes with amyotrophic lateral sclerosis: associated mutations develop motor neuron disease. *J Neurosci,* 21, 9246-54.
NAGAI, M., RE, D. B., NAGATA, T., CHALAZONITIS, A., JESSELL, T. M., WICHTERLE, H. & PRZEDBORSKI, S. 2007. Astrocytes expressing ALS-linked mutated SOD1 release factors selectively toxic to motor neurons. *Nat Neurosci,* 10, 615-22.
NAGATA, T., ILIEVA, H., MURAKAMI, T., SHIOTE, M., NARAI, H., OHTA, Y., HAYASHI, T., SHOJI, M. & ABE, K. 2007. Increased ER stress during motor neuron degeneration in a transgenic mouse model of amyotrophic lateral sclerosis. *Neurol Res,* 29, 767-71.
NAKANO, K. & VOUSDEN, K. H. 2001. PUMA, a novel proapoptotic gene, is induced by p53. *Mol Cell,* 7, 683-94.
NAKATANI, Y., KANETO, H., KAWAMORI, D., YOSHIUCHI, K., HATAZAKI, M., MATSUOKA, T. A., OZAWA, K., OGAWA, S., HORI, M., YAMASAKI, Y. & MATSUHISA, M. 2005. Involvement of endoplasmic reticulum stress in insulin resistance and diabetes. *J Biol Chem,* 280, 847-51.
NAWA, M., KANEKURA, K., HASHIMOTO, Y., AISO, S. & MATSUOKA, M. 2008. A novel Akt/PKB-interacting protein promotes cell adhesion and inhibits familial amyotrophic lateral sclerosis-linked mutant SOD1-induced neuronal death via inhibition of PP2A-mediated dephosphorylation of Akt/PKB. *Cell Signal,* 20, 493-505.
NAZIO, F., STRAPPAZZON, F., ANTONIOLI, M., BIELLI, P., CIANFANELLI, V., BORDI, M., GRETZMEIER, C., DENGJEL, J., PIACENTINI, M., FIMIA, G. M. & CECCONI, F. 2013. mTOR inhibits autophagy by controlling ULK1 ubiquitylation, self-association and function through AMBRA1 and TRAF6. *Nat Cell Biol,* 15, 406-16.
NEEDHAM, P. G. & BRODSKY, J. L. 2013. How early studies on secreted and membrane protein quality control gave rise to the ER associated

degradation (ERAD) pathway: The early history of ERAD. *Biochim Biophys Acta,* 1833, 2447-57.
NICCHITTA, C. V., CARRICK, D. M. & BAKER-LEPAIN, J. C. 2004. The messenger and the message: gp96 (GRP94)-peptide interactions in cellular immunity. *Cell Stress Chaperones,* 9, 325-31.
NIELSEN, B. S. 2012. MicroRNA *in situ* hybridization. *Methods Mol Biol,* 822, 67-84.
NIEMINEN, A. L. 2003. Apoptosis and necrosis in health and disease: role of mitochondria. *Int Rev Cytol,* 224, 29-55.
NIJHAWAN, D., FANG, M., TRAER, E., ZHONG, Q., GAO, W., DU, F. & WANG, X. 2003. Elimination of Mcl-1 is required for the initiation of apoptosis following ultraviolet irradiation. *Genes Dev,* 17, 1475-86.
NISHIKAWA, S., BRODSKY, J. L. & NAKATSUKASA, K. 2005. Roles of molecular chaperones in endoplasmic reticulum (ER) quality control and ER-associated degradation (ERAD). *J Biochem,* 137, 551-5.
NISHITOH, H., KADOWAKI, H., NAGAI, A., MARUYAMA, T., YOKOTA, T., FUKUTOMI, H., NOGUCHI, T., MATSUZAWA, A., TAKEDA, K. & ICHIJO, H. 2008. ALS-linked mutant SOD1 induces ER stress- and ASK1-dependent motor neuron death by targeting Derlin-1. *Genes Dev,* 22, 1451-64.
OBERNOSTERER, G., MARTINEZ, J. & ALENIUS, M. 2007. Locked nucleic acid-based *in situ* detection of microRNAs in mouse tissue sections. *Nat Protoc,* 2, 1508-14.
OGATA, M., HINO, S., SAITO, A., MORIKAWA, K., KONDO, S., KANEMOTO, S., MURAKAMI, T., TANIGUCHI, M., TANII, I., YOSHINAGA, K., SHIOSAKA, S., HAMMARBACK, J. A., URANO, F. & IMAIZUMI, K. 2006. Autophagy is activated for cell survival after endoplasmic reticulum stress. *Mol Cell Biol,* 26, 9220-31.
OHOKA, N., HATTORI, T., KITAGAWA, M., ONOZAKI, K. & HAYASHI, H. 2007. Critical and functional regulation of CHOP (C/EBP homologous protein) through the N-terminal portion. *J Biol Chem,* 282, 35687-94.
OLIVE, V., JIANG, I. & HE, L. 2010. mir-17-92, a cluster of miRNAs in the midst of the cancer network. *Int J Biochem Cell Biol,* 42, 1348-54.
OMURA, T., KANEKO, M., OKUMA, Y., MATSUBARA, K. & NOMURA, Y. 2013. Endoplasmic reticulum stress and Parkinson's disease: the role of HRD1 in averting apoptosis in neurodegenerative disease. *Oxid Med Cell Longev,* 2013, 239854.
OPFERMAN, J. T., LETAI, A., BEARD, C., SORCINELLI, M. D., ONG, C. C. & KORSMEYER, S. J. 2003. Development and maintenance of B and T lymphocytes requires antiapoptotic MCL-1. *Nature,* 426, 671-6.
OYADOMARI, S. & MORI, M. 2004. Roles of CHOP/GADD153 in endoplasmic reticulum stress. *Cell Death Differ,* 11, 381-9.
PANDI, G., NAKKA, V. P., DHARAP, A., ROOPRA, A. & VEMUGANTI, R. 2013. MicroRNA miR-29c down-regulation leading to de-repression of its target DNA methyltransferase 3a promotes ischemic brain damage. *PLoS One,* 8, e58039.
PARK, E., LEE, G. J., CHOI, S., CHOI, S. K., CHAE, S. J., KANG, S. W., PAK, Y. K. & PARK, H. K. 2010. The role of glutamate release on

voltage-dependent anion channels (VDAC)-mediated apoptosis in an eleven vessel occlusion model in rats. *PLoS One,* 5, e15192.
PARK, S. Y., LEE, J. H., HA, M., NAM, J. W. & KIM, V. N. 2009. miR-29 miRNAs activate p53 by targeting p85 alpha and CDC42. *Nat Struct Mol Biol,* 16, 23-9.
PASINELLI, P. & BROWN, R. H. 2006. Molecular biology of amyotrophic lateral sclerosis: insights from genetics. *Nat Rev Neurosci,* 7, 710-23.
PATTINGRE, S., TASSA, A., QU, X., GARUTI, R., LIANG, X. H., MIZUSHIMA, N., PACKER, M., SCHNEIDER, M. D. & LEVINE, B. 2005. Bcl-2 antiapoptotic proteins inhibit Beclin 1-dependent autophagy. *Cell,* 122, 927-39.
PEI, J. J. & HUGON, J. 2008. mTOR-dependent signalling in Alzheimer's disease. *J Cell Mol Med,* 12, 2525-32.
PENG, Z., XUE, B., KURGAN, L. & UVERSKY, V. N. 2013. Resilience of death: intrinsic disorder in proteins involved in the programmed cell death. *Cell Death Differ,* 20, 1257-67.
PILATI, N., BARKER, M., PANTELEIMONITIS, S., DONGA, R. & HAMANN, M. 2008. A rapid method combining Golgi and Nissl staining to study neuronal morphology and cytoarchitecture. *J Histochem Cytochem,* 56, 539-50.
PORTERA-CAILLIAU, C., PRICE, D. L. & MARTIN, L. J. 1997. Non-NMDA and NMDA receptor-mediated excitotoxic neuronal deaths in adult brain are morphologically distinct: further evidence for an apoptosis-necrosis continuum. *J Comp Neurol,* 378, 88-104.
PUTHALAKATH, H., O'REILLY, L. A., GUNN, P., LEE, L., KELLY, P. N., HUNTINGTON, N. D., HUGHES, P. D., MICHALAK, E. M., MCKIMM-BRESCHKIN, J., MOTOYAMA, N., GOTOH, T., AKIRA, S., BOUILLET, P. & STRASSER, A. 2007. ER stress triggers apoptosis by activating BH3-only protein Bim. *Cell,* 129, 1337-49.
RABINOVICH, E., KEREM, A., FROHLICH, K. U., DIAMANT, N. & BAR-NUN, S. 2002. AAA-ATPase p97/Cdc48p, a cytosolic chaperone required for endoplasmic reticulum-associated protein degradation. *Mol Cell Biol,* 22, 626-34.
RAMAKRISHNAN, M., SCHONTHAL, A. H. & LEE, A. S. 1997. Endoplasmic reticulum stress-inducible protein GRP94 is associated with an Mg2+-dependent serine kinase activity modulated by Ca2+ and GRP78/BiP. *J Cell Physiol,* 170, 115-29.
RAO, R. V., CASTRO-OBREGON, S., FRANKOWSKI, H., SCHULER, M., STOKA, V., DEL RIO, G., BREDESEN, D. E. & ELLERBY, H. M. 2002. Coupling endoplasmic reticulum stress to the cell death program. An Apaf-1-independent intrinsic pathway. *J Biol Chem,* 277, 21836-42.
RAVITS, J. M. & LA SPADA, A. R. 2009. ALS motor phenotype heterogeneity, focality, and spread: deconstructing motor neuron degeneration. *Neurology,* 73, 805-11.
REIMERTZ, C., KOGEL, D., RAMI, A., CHITTENDEN, T. & PREHN, J. H. 2003. Gene expression during ER stress-induced apoptosis in neurons: induction of the BH3-only protein Bbc3/PUMA and activation of the mitochondrial apoptosis pathway. *J Cell Biol,* 162, 587-97.

REN, D., TU, H. C., KIM, H., WANG, G. X., BEAN, G. R., TAKEUCHI, O., JEFFERS, J. R., ZAMBETTI, G. P., HSIEH, J. J. & CHENG, E. H. 2010. BID, BIM, and PUMA are essential for activation of the BAX- and BAK-dependent cell death program. *Science,* 330, 1390-3.

RENTON, A. E., MAJOUNIE, E., WAITE, A., SIMON-SANCHEZ, J., ROLLINSON, S., GIBBS, J. R., SCHYMICK, J. C., LAAKSOVIRTA, H., VAN SWIETEN, J. C., MYLLYKANGAS, L., KALIMO, H., PAETAU, A., ABRAMZON, Y., REMES, A. M., KAGANOVICH, A., SCHOLZ, S. W., DUCKWORTH, J., DING, J., HARMER, D. W., HERNANDEZ, D. G., JOHNSON, J. O., MOK, K., RYTEN, M., TRABZUNI, D., GUERREIRO, R. J., ORRELL, R. W., NEAL, J., MURRAY, A., PEARSON, J., JANSEN, I. E., SONDERVAN, D., SEELAAR, H., BLAKE, D., YOUNG, K., HALLIWELL, N., CALLISTER, J. B., TOULSON, G., RICHARDSON, A., GERHARD, A., SNOWDEN, J., MANN, D., NEARY, D., NALLS, M. A., PEURALINNA, T., JANSSON, L., ISOVIITA, V. M., KAIVORINNE, A. L., HOLTTA-VUORI, M., IKONEN, E., SULKAVA, R., BENATAR, M., WUU, J., CHIO, A., RESTAGNO, G., BORGHERO, G., SABATELLI, M., HECKERMAN, D., ROGAEVA, E., ZINMAN, L., ROTHSTEIN, J. D., SENDTNER, M., DREPPER, C., EICHLER, E. E., ALKAN, C., ABDULLAEV, Z., PACK, S. D., DUTRA, A., PAK, E., HARDY, J., SINGLETON, A., WILLIAMS, N. M., HEUTINK, P., PICKERING-BROWN, S., MORRIS, H. R., TIENARI, P. J. & TRAYNOR, B. J. 2011. A hexanucleotide repeat expansion in C9ORF72 is the cause of chromosome 9p21-linked ALS-FTD. *Neuron,* 72, 257-68.

REYES, N. A., FISHER, J. K., AUSTGEN, K., VANDENBERG, S., HUANG, E. J. & OAKES, S. A. 2010. Blocking the mitochondrial apoptotic pathway preserves motor neuron viability and function in a mouse model of amyotrophic lateral sclerosis. *J Clin Invest,* 120, 3673-9.

RINKENBERGER, J. L., HORNING, S., KLOCKE, B., ROTH, K. & KORSMEYER, S. J. 2000. Mcl-1 deficiency results in peri-implantation embryonic lethality. *Genes Dev,* 14, 23-7.

ROGERS, S., WELLS, R. & RECHSTEINER, M. 1986. Amino acid sequences common to rapidly degraded proteins: the PEST hypothesis. *Science,* 234, 364-8.

ROSEN, D. R. 1993. Mutations in Cu/Zn superoxide dismutase gene are associated with familial amyotrophic lateral sclerosis. *Nature,* 364, 362.

ROSEN, D. R., SIDDIQUE, T., PATTERSON, D., FIGLEWICZ, D. A., SAPP, P., HENTATI, A., DONALDSON, D., GOTO, J., O'REGAN, J. P., DENG, H. X. & ET AL. 1993. Mutations in Cu/Zn superoxide dismutase gene are associated with familial amyotrophic lateral sclerosis. *Nature,* 362, 59-62.

ROUSSEL, B. D., KRUPPA, A. J., MIRANDA, E., CROWTHER, D. C., LOMAS, D. A. & MARCINIAK, S. J. 2013. Endoplasmic reticulum dysfunction in neurological disease. *Lancet Neurol,* 12, 105-18.

SAITO, Y., SUZUKI, H., TSUGAWA, H., NAKAGAWA, I., MATSUZAKI, J., KANAI, Y. & HIBI, T. 2009. Chromatin remodeling at Alu repeats

by epigenetic treatment activates silenced microRNA-512-5p with downregulation of Mcl-1 in human gastric cancer cells. *Oncogene,* 28, 2738-44.

SALMINEN, A., KAUPPINEN, A., SUURONEN, T., KAARNIRANTA, K. & OJALA, J. 2009a. ER stress in Alzheimer's disease: a novel neuronal trigger for inflammation and Alzheimer's pathology. *J Neuroinflammation,* 6, 41.

SALMINEN, A., OJALA, J., KAUPPINEN, A., KAARNIRANTA, K. & SUURONEN, T. 2009b. Inflammation in Alzheimer's disease: amyloid-beta oligomers trigger innate immunity defence via pattern recognition receptors. *Prog Neurobiol,* 87, 181-94.

SARKAR, S. & RUBINSZTEIN, D. C. 2008. Huntington's disease: degradation of mutant huntingtin by autophagy. *FEBS J,* 275, 4263-70.

SATHASIVAM, S., INCE, P. G. & SHAW, P. J. 2001. Apoptosis in amyotrophic lateral sclerosis: a review of the evidence. *Neuropathol Appl Neurobiol,* 27, 257-74.

SAXENA, S., CABUY, E. & CARONI, P. 2009. A role for motoneuron subtype-selective ER stress in disease manifestations of FALS mice. *Nat Neurosci,* 12, 627-36.

SCHRODER, M. & KAUFMAN, R. J. 2005. ER stress and the unfolded protein response. *Mutat Res,* 569, 29-63.

SCHYMICK, J. C., TALBOT, K. & TRAYNOR, B. J. 2007. Genetics of sporadic amyotrophic lateral sclerosis. *Hum Mol Genet,* 16 Spec No. 2, R233-42.

SCOTT, S., KRANZ, J. E., COLE, J., LINCECUM, J. M., THOMPSON, K., KELLY, N., BOSTROM, A., THEODOSS, J., AL-NAKHALA, B. M., VIEIRA, F. G., RAMASUBBU, J. & HEYWOOD, J. A. 2008. Design, power, and interpretation of studies in the standard murine model of ALS. *Amyotroph Lateral Scler,* 9, 4-15.

SELVAMANI, A., SATHYAN, P., MIRANDA, R. C. & SOHRABJI, F. 2012. An antagomir to microRNA Let7f promotes neuroprotection in an ischemic stroke model. *PLoS One,* 7, e32662.

SENGUPTA, S., DEN BOON, J. A., CHEN, I. H., NEWTON, M. A., STANHOPE, S. A., CHENG, Y. J., CHEN, C. J., HILDESHEIM, A., SUGDEN, B. & AHLQUIST, P. 2008. MicroRNA 29c is down-regulated in nasopharyngeal carcinomas, up-regulating mRNAs encoding extracellular matrix proteins. *Proc Natl Acad Sci U S A,* 105, 5874-8.

SHERWOOD, L. 2012. *Essentials of Physiology,* United States of America, Brooks/Cole Cengage Learning.

SHIMAZAWA, M., TANAKA, H., ITO, Y., MORIMOTO, N., TSURUMA, K., KADOKURA, M., TAMURA, S., INOUE, T., YAMADA, M., TAKAHASHI, H., WARITA, H., AOKI, M. & HARA, H. 2010. An inducer of VGF protects cells against ER stress-induced cell death and prolongs survival in the mutant SOD1 animal models of familial ALS. *PLoS One,* 5, e15307.

SHIMIZU, S., NARITA, M. & TSUJIMOTO, Y. 1999. Bcl-2 family proteins regulate the release of apoptogenic cytochrome c by the mitochondrial channel VDAC. *Nature,* 399, 483-7.

SHIOYA, M., OBAYASHI, S., TABUNOKI, H., ARIMA, K., SAITO, Y., ISHIDA, T. & SATOH, J. 2010. Aberrant microRNA expression in the brains of neurodegenerative diseases: miR-29a decreased in Alzheimer disease brains targets neurone navigator 3. *Neuropathol Appl Neurobiol,* 36, 320-30.

SKIBO, G. G. & POGORELAIA, N. 1978. [Ultrastructural characteristics of the dendrites of spinal neurons]. *Neirofiziologiia,* 10, 271-7.

SMIRNOVA, L., GRAFE, A., SEILER, A., SCHUMACHER, S., NITSCH, R. & WULCZYN, F. G. 2005. Regulation of miRNA expression during neural cell specification. *Eur J Neurosci,* 21, 1469-77.

SMITH, K. M., GUERAU-DE-ARELLANO, M., COSTINEAN, S., WILLIAMS, J. L., BOTTONI, A., MAVRIKIS COX, G., SATOSKAR, A. R., CROCE, C. M., RACKE, M. K., LOVETT-RACKE, A. E. & WHITACRE, C. C. 2012. miR-29ab1 deficiency identifies a negative feedback loop controlling Th1 bias that is dysregulated in multiple sclerosis. *J Immunol,* 189, 1567-76.

SMITH, M. I. & DESHMUKH, M. 2007. Endoplasmic reticulum stress-induced apoptosis requires bax for commitment and Apaf-1 for execution in primary neurons. *Cell Death Differ,* 14, 1011-9.

SOIFER, H. S., ROSSI, J. J. & SAETROM, P. 2007. MicroRNAs in disease and potential therapeutic applications. *Mol Ther,* 15, 2070-9.

SONG, S., LEE, H., KAM, T. I., TAI, M. L., LEE, J. Y., NOH, J. Y., SHIM, S. M., SEO, S. J., KONG, Y. Y., NAKAGAWA, T., CHUNG, C. W., CHOI, D. Y., OUBRAHIM, H. & JUNG, Y. K. 2008. E2-25K/Hip-2 regulates caspase-12 in ER stress-mediated Abeta neurotoxicity. *J Cell Biol,* 182, 675-84.

SOO, K. Y., ATKIN, J. D., FARG, M., WALKER, A. K., HORNE, M. K. & NAGLEY, P. 2012. Bim links ER stress and apoptosis in cells expressing mutant SOD1 associated with amyotrophic lateral sclerosis. *PLoS One,* 7, e35413.

SRINIVASULA, S. M., HEGDE, R., SALEH, A., DATTA, P., SHIOZAKI, E., CHAI, J., LEE, R. A., ROBBINS, P. D., FERNANDES-ALNEMRI, T., SHI, Y. & ALNEMRI, E. S. 2001. A conserved XIAP-interaction motif in caspase-9 and Smac/DIABLO regulates caspase activity and apoptosis. *Nature,* 410, 112-6.

STEELE, R., MOTT, J. L. & RAY, R. B. 2010. MBP-1 upregulates miR-29b that represses Mcl-1, collagens, and matrix-metalloproteinase-2 in prostate cancer cells. *Genes Cancer,* 1, 381-387.

STENVANG, J., PETRI, A., LINDOW, M., OBAD, S. & KAUPPINEN, S. 2012. Inhibition of microRNA function by antimiR oligonucleotides. *Silence,* 3, 1.

STONELEY, M. & WILLIS, A. E. 2004. Cellular internal ribosome entry segments: structures, trans-acting factors and regulation of gene expression. *Oncogene,* 23, 3200-7.

SUZUKI, H., KANEKURA, K., LEVINE, T. P., KOHNO, K., OLKKONEN, V. M., AISO, S. & MATSUOKA, M. 2009. ALS-linked P56S-VAPB, an aggregated loss-of-function mutant of VAPB, predisposes motor neurons to ER stress-related death by inducing aggregation of co-expressed wild-type VAPB. *J Neurochem,* 108, 973-985.

SUZUKI, M., TORK, C., SHELLEY, B., MCHUGH, J., WALLACE, K., KLEIN, S. M., LINDSTROM, M. J. & SVENDSEN, C. N. 2007. Sexual dimorphism in disease onset and progression of a rat model of ALS. *Amyotroph Lateral Scler,* 8, 20-5.

SZEGEZDI, E., LOGUE, S. E., GORMAN, A. M. & SAMALI, A. 2006. Mediators of endoplasmic reticulum stress-induced apoptosis. *EMBO Rep,* 7, 880-5.

TAIT, S. W. & GREEN, D. R. 2010. Cell survival in tough times: The mitochondrial recovery plan. *Cell Cycle,* 9, 4254-5.

TAN, W., NANICHE, N., BOGUSH, A., PEDRINI, S., TROTTI, D. & PASINELLI, P. 2013. Small Peptides against the Mutant SOD1/Bcl-2 Toxic Mitochondrial Complex Restore Mitochondrial Function and Cell Viability in Mutant SOD1-Mediated ALS. *J Neurosci,* 33, 11588-98.

THAKOR, N. & HOLCIK, M. 2012. IRES-mediated translation of cellular messenger RNA operates in eIF2alpha- independent manner during stress. *Nucleic Acids Res,* 40, 541-52.

TOLOSA, L., MIR, M., ASENSIO, V. J., OLMOS, G. & LLADO, J. 2008. Vascular endothelial growth factor protects spinal cord motoneurons against glutamate-induced excitotoxicity via phosphatidylinositol 3-kinase. *J Neurochem,* 105, 1080-90.

TRAYNOR, B. J., CODD, M. B., CORR, B., FORDE, C., FROST, E. & HARDIMAN, O. 1999. Incidence and prevalence of ALS in Ireland, 1995-1997: a population-based study. *Neurology,* 52, 504-9.

TSVETKOV, A. S., MILLER, J., ARRASATE, M., WONG, J. S., PLEISS, M. A. & FINKBEINER, S. 2010. A small-molecule scaffold induces autophagy in primary neurons and protects against toxicity in a Huntington disease model. *Proc Natl Acad Sci U S A,* 107, 16982-7.

TUFFY, L. P., CONCANNON, C. G., D'ORSI, B., KING, M. A., WOODS, I., HUBER, H. J., WARD, M. W. & PREHN, J. H. 2010. Characterization of Puma-dependent and Puma-independent neuronal cell death pathways following prolonged proteasomal inhibition. *Mol Cell Biol,* 30, 5484-501.

TURNER, M. R., BOWSER, R., BRUIJN, L., DUPUIS, L., LUDOLPH, A., MCGRATH, M., MANFREDI, G., MARAGAKIS, N., MILLER, R. G., PULLMAN, S. L., RUTKOVE, S. B., SHAW, P. J., SHEFNER, J. & FISCHBECK, K. H. 2013. Mechanisms, models and biomarkers in amyotrophic lateral sclerosis. *Amyotroph Lateral Scler Frontotemporal Degener,* 14 Suppl 1, 19-32.

UGALDE, A. P., RAMSAY, A. J., DE LA ROSA, J., VARELA, I., MARINO, G., CADINANOS, J., LU, J., FREIJE, J. M. & LOPEZ-OTIN, C. 2011. Aging and chronic DNA damage response activate a regulatory pathway involving miR-29 and p53. *EMBO J,* 30, 2219-32.

ULLMAN, E., FAN, Y., STAWOWCZYK, M., CHEN, H. M., YUE, Z. & ZONG, W. X. 2008. Autophagy promotes necrosis in apoptosis-deficient cells in response to ER stress. *Cell Death Differ,* 15, 422-5.

UPTON, J. P., WANG, L., HAN, D., WANG, E. S., HUSKEY, N. E., LIM, L., TRUITT, M., MCMANUS, M. T., RUGGERO, D., GOGA, A., PAPA, F. R. & OAKES, S. A. 2012. IRE1alpha cleaves select

microRNAs during ER stress to derepress translation of proapoptotic Caspase-2. *Science,* 338, 818-22.
VAN ROOIJ, E. 2011. The art of microRNA research. *Circ Res,* 108, 219-34.
VELDINK, J. H., BAR, P. R., JOOSTEN, E. A., OTTEN, M., WOKKE, J. H. & VAN DEN BERG, L. H. 2003. Sexual differences in onset of disease and response to exercise in a transgenic model of ALS. *Neuromuscul Disord,* 13, 737-43.
VEMBAR, S. S. & BRODSKY, J. L. 2008. One step at a time: endoplasmic reticulum-associated degradation. *Nat Rev Mol Cell Biol,* 9, 944-57.
VIDAL, R., CABALLERO, B., COUVE, A. & HETZ, C. 2011. Converging pathways in the occurrence of endoplasmic reticulum (ER) stress in Huntington's disease. *Curr Mol Med,* 11, 1-12.
VILLUNGER, A., MICHALAK, E. M., COULTAS, L., MULLAUER, F., BOCK, G., AUSSERLECHNER, M. J., ADAMS, J. M. & STRASSER, A. 2003. p53- and drug-induced apoptotic responses mediated by BH3-only proteins puma and noxa. *Science,* 302, 1036-8.
VINSANT, S. 2013a. Characterization of early pathogenesis in the SOD1G93A mouse model of ALS: part 1, background and methods. *Brain and behaviour,* 3, 335-350.
VINSANT, S., MANSFIELD, C., JIMENEZ-MORENO, R., DEL GAIZO MOORE, V., YOSHIKAWA, M., HAMPTON, T.G., PREVETTE, D., CARESS, J., OPPENHEIM, R.W. AND C.MILLIGAN 2013b. Characterisation of early pathogenesis in the SODG93A mouse model of ALS: part II, results and discussion. *Brain and behaviour,* 3, 431-457.
VUKOSAVIC, S., STEFANIS, L., JACKSON-LEWIS, V., GUEGAN, C., ROMERO, N., CHEN, C., DUBOIS-DAUPHIN, M. & PRZEDBORSKI, S. 2000. Delaying caspase activation by Bcl-2: A clue to disease retardation in a transgenic mouse model of amyotrophic lateral sclerosis. *J Neurosci,* 20, 9119-25.
WALKER, A. K. & ATKIN, J. D. 2011. Stress signaling from the endoplasmic reticulum: A central player in the pathogenesis of amyotrophic lateral sclerosis. *IUBMB Life,* 63, 754-63.
WALTER, P. & RON, D. 2011. The unfolded protein response: from stress pathway to homeostatic regulation. *Science,* 334, 1081-6.
WANG, S. & EL-DEIRY, W. S. 2003. TRAIL and apoptosis induction by TNF-family death receptors. *Oncogene,* 22, 8628-33.
WARD, M. W., KOGEL, D. & PREHN, J. H. 2004. Neuronal apoptosis: BH3-only proteins the real killers? *J Bioenerg Biomembr,* 36, 295-8.
WEI, H., WANG, C., ZHANG, C., LI, P., WANG, F. & ZHANG, Z. 2010. Comparative profiling of microRNA expression between neural stem cells and motor neurons in embryonic spinal cord in rat. *Int J Dev Neurosci,* 28, 545-51.
WEI, L. H., KUO, M. L., CHEN, C. A., CHOU, C. H., CHENG, W. F., CHANG, M. C., SU, J. L. & HSIEH, C. Y. 2001. The anti-apoptotic role of interleukin-6 in human cervical cancer is mediated by up-regulation of Mcl-1 through a PI 3-K/Akt pathway. *Oncogene,* 20, 5799-809.

WEYDT, P., HONG, S. Y., KLIOT, M. & MOLLER, T. 2003. Assessing disease onset and progression in the SOD1 mouse model of ALS. *Neuroreport,* 14, 1051-4.

WILLIAMS, A. H., VALDEZ, G., MORESI, V., QI, X., MCANALLY, J., ELLIOTT, J. L., BASSEL-DUBY, R., SANES, J. R. & OLSON, E. N. 2009. MicroRNA-206 delays ALS progression and promotes regeneration of neuromuscular synapses in mice. *Science,* 326, 1549-54.

WILLIS, S. N. & ADAMS, J. M. 2005. Life in the balance: how BH3-only proteins induce apoptosis. *Curr Opin Cell Biol,* 17, 617-25.

WILLIS, S. N., CHEN, L., DEWSON, G., WEI, A., NAIK, E., FLETCHER, J. I., ADAMS, J. M. & HUANG, D. C. 2005. Proapoptotic Bak is sequestered by Mcl-1 and Bcl-xL, but not Bcl-2, until displaced by BH3-only proteins. *Genes Dev,* 19, 1294-305.

WINBANKS, C. E., WANG, B., BEYER, C., KOH, P., WHITE, L., KANTHARIDIS, P. & GREGOREVIC, P. 2011. TGF-beta regulates miR-206 and miR-29 to control myogenic differentiation through regulation of HDAC4. *J Biol Chem,* 286, 13805-14.

WINTER, J., JUNG, S., KELLER, S., GREGORY, R. I. & DIEDERICHS, S. 2009. Many roads to maturity: microRNA biogenesis pathways and their regulation. *Nat Cell Biol,* 11, 228-34.

WIRAWAN, E., VANDE WALLE, L., KERSSE, K., CORNELIS, S., CLAERHOUT, S., VANOVERBERGHE, I., ROELANDT, R., DE RYCKE, R., VERSPURTEN, J., DECLERCQ, W., AGOSTINIS, P., VANDEN BERGHE, T., LIPPENS, S. & VANDENABEELE, P. 2010. Caspase-mediated cleavage of Beclin-1 inactivates Beclin-1-induced autophagy and enhances apoptosis by promoting the release of proapoptotic factors from mitochondria. *Cell Death Dis,* 1, e18.

WONG, M. L. & MEDRANO, J. F. 2005. Real-time PCR for mRNA quantitation. *Biotechniques,* 39, 75-85.

WOOLEY, C. M., SHER, R. B., KALE, A., FRANKEL, W. N., COX, G. A. & SEBURN, K. L. 2005. Gait analysis detects early changes in transgenic SOD1(G93A) mice. *Muscle Nerve,* 32, 43-50.

XIONG, Y., FANG, J. H., YUN, J. P., YANG, J., ZHANG, Y., JIA, W. H. & ZHUANG, S. M. 2010. Effects of microRNA-29 on apoptosis, tumorigenicity, and prognosis of hepatocellular carcinoma. *Hepatology,* 51, 836-45.

YAMASAKI, S. & ANDERSON, P. 2008. Reprogramming mRNA translation during stress. *Curr Opin Cell Biol,* 20, 222-6.

YANG, T., BUCHAN, H. L., TOWNSEND, K. J. & CRAIG, R. W. 1996. MCL-1, a member of the BLC-2 family, is induced rapidly in response to signals for cell differentiation or death, but not to signals for cell proliferation. *J Cell Physiol,* 166, 523-36.

YE, Y., HU, Z., LIN, Y., ZHANG, C. & PEREZ-POLO, J. R. 2010. Downregulation of microRNA-29 by antisense inhibitors and a PPAR-gamma agonist protects against myocardial ischaemia-reperfusion injury. *Cardiovasc Res,* 87, 535-44.

YE, Y., SHIBATA, Y., KIKKERT, M., VAN VOORDEN, S., WIERTZ, E. & RAPOPORT, T. A. 2005. Recruitment of the p97 ATPase and

ubiquitin ligases to the site of retrotranslocation at the endoplasmic reticulum membrane. *Proc Natl Acad Sci U S A,* 102, 14132-8.

YIP, K. W. & REED, J. C. 2008. Bcl-2 family proteins and cancer. *Oncogene,* 27, 6398-406.

YOULE, R. J. & STRASSER, A. 2008. The BCL-2 protein family: opposing activities that mediate cell death. *Nat Rev Mol Cell Biol,* 9, 47-59.

YU, F., YAO, H., ZHU, P., ZHANG, X., PAN, Q., GONG, C., HUANG, Y., HU, X., SU, F., LIEBERMAN, J. & SONG, E. 2007. let-7 regulates self renewal and tumorigenicity of breast cancer cells. *Cell,* 131, 1109-23.

YU, L., LENARDO, M. J. & BAEHRECKE, E. H. 2004. Autophagy and caspases: a new cell death program. *Cell Cycle,* 3, 1124-6.

YUAN, J. & YANKNER, B. A. 2000. Apoptosis in the nervous system. *Nature,* 407, 802-9.

YUNTA, M., NIETO-DIAZ, M., ESTEBAN, F. J., CABALLERO-LOPEZ, M., NAVARRO-RUIZ, R., REIGADA, D., PITA-THOMAS, D. W., DEL AGUILA, A., MUNOZ-GALDEANO, T. & MAZA, R. M. 2012. MicroRNA dysregulation in the spinal cord following traumatic injury. *PLoS One,* 7, e34534.

ZHANG, L., LOPEZ, H., GEORGE, N. M., LIU, X., PANG, X. & LUO, X. 2011. Selective involvement of BH3-only proteins and differential targets of Noxa in diverse apoptotic pathways. *Cell Death Differ,* 18, 864-73.

ZHAO, L. & ACKERMAN, S. L. 2006. Endoplasmic reticulum stress in health and disease. *Curr Opin Cell Biol,* 18, 444-52.

ZHAO, Z., LANGE, D. J., HO, L., BONINI, S., SHAO, B., SALTON, S. R., THOMAS, S. & PASINETTI, G. M. 2008. Vgf is a novel biomarker associated with muscle weakness in amyotrophic lateral sclerosis (ALS), with a potential role in disease pathogenesis. *Int J Med Sci,* 5, 92-9.

ZHONG, Q., GAO, W., DU, F. & WANG, X. 2005. Mule/ARF-BP1, a BH3-only E3 ubiquitin ligase, catalyzes the polyubiquitination of Mcl-1 and regulates apoptosis. *Cell,* 121, 1085-95.

ZHUANG, J. & BRADY, H. J. 2006. Emerging role of Mcl-1 in actively counteracting BH3-only proteins in apoptosis. *Cell Death Differ,* 13, 1263-7.

ZONG, W. X., LINDSTEN, T., ROSS, A. J., MACGREGOR, G. R. & THOMPSON, C. B. 2001. BH3-only proteins that bind pro-survival Bcl-2 family members fail to induce apoptosis in the absence of Bax and Bak. *Genes Dev,* 15, 1481-6.

RESEARCH OUTPUTS

ER Stress-Mediated Upregulation of miR-29a Enhances Sensitivity to Apoptosis in a Mcl-1 Dependent Manner

Caoimhín G. Concannon, **Katie Nolan**, Isabella Bray, Simone Poeschel, Ross Gallagher, Liam P. Tuffy, Raymond L. Stallings and Jochen H. M. Prehn

(Currently in preparation for publication)

MicroRNA-29a targeting Mcl-1 controls ER stress-induced apoptosis **Katie Nolan**, Ross Gallagher, Caoimhín G Concannon and Jochen H Prehn

Poster presented at Cell Death meeting, Cold Spring Harbour, 2011

MicroRNA-29a targeting Mcl-1 controls ER stress-induced apoptosis and autophagy

Katie Nolan, Ross Gallagher, Marc Germain, Ruth Slack, Caoimhín G Concannon and Jochen H Prehn

Poster presented at Society for Neuroscience meeting 2012